INTERNATIONAL DOCTORAL
SCHOOL OF THE USC

Leticia
Montes Martínez

PhD Thesis

Rheology and Digestibility of Gluten-Free Starchy Systems with Different Biopolymers from *Ascophyllum nodosum* Brown Seaweeds

Santiago de Compostela, 2024

Doctoral Programme in Chemical and Environmental Engineering

ESCOLA DE DOUTORAMENTO INTERNACIONAL DA USC

DOCTORAL THESIS

Rheology and Digestibility of Gluten-Free Starchy Systems with Different Biopolymers from *Ascophyllum nodosum* Brown Seaweeds

Author

Leticia Montes Martínez

Supervisor/s: Ramón F. Moreira Martínez and Jorge Sineiro Torres

Tutor: Ramón F. Moreira Martínez

PHD PROGRAMME IN CHEMICAL AND ENVIRONMENTAL ENGINEERING

SANTIAGO DE COMPOSTELA

Aos meus avós,

Porque sei que se estivésedes aquí estaríades moi orgullosos de min

Agradecementos

En primeiro lugar quero agradecerlle aos meus directores de Tese, Ramón Moreira (**Moncho**) e Jorge Sineiro (**Xurxo**) pola tan boa acollida no grupo de investigación. Gracias por toda a axuda recibida durante estes cinco anos, pero sobre todo gracias por toda a aprendizaxe que gañei. En especial, gracias a Moncho por todo o que me ensinou de reoloxía, sen dúbida comezar e rematar esta Tese foi a mellor decisión que puiden tomar para poder aprender todo que sei agora sobre a reoloxía. E gracias a Xurxo por toda a información sobre o mundo das algas e, sobre todo, polo apoio informático.

Tamén me gustaría agradecer a preocupación e apoio por parte das novas incorporacións ao grupo, **Amaya Franco** e Daniel Franco (**Dani**). Sobre todo a ti, Dani, todos sabemos que sen ti esta Tese non se acabaría escribindo, moitas gracias. En definitiva, gracias a todo o Departamento de Enxeñaría Química por acollerme tan ben.

Ao persoal da ETSE co que tanto nos cruzamos polos pasillos: **Agus**, **Noelia**, **Helena**, **Montse**, **Susan** e **Vanesa,** polos bos momentos vividos.

Gracias ao **Ministerio de Ciencia e Innovación de España**, ao **Fondo Europeo de Desarrollo Regional** (FEDER) da Unión Europea polo proxecto de investigación (RTI2018–095919–B–C2) e a **Xunta de Galicia** (Proxecto de Consolidación ED431B 2019/01) axudas sen as cales esta Tese non podería ter sido levada a cabo.

Ao Lab-109, especialmente a **Cristina M. Rosell** e a **María Santamaría**, ese laboratorio na outra punta de España onde me acolleron cos brazos abertos e me ensinaron todo o que sei sobre a dixestión dos amidóns, gracias por todo o aprendido. María, gracias por coidarme tan ben a primeira vez que estiven por alí, fixeches que Valencia me parecese incluso máis bonita do que é. Moltes gràcies! Gracias tamén a **Eva**, **María Ruíz**, **Raquel** e **Rita** pola axuda e hospitalidade.

A **Mauro Gisbert**, o que foi o meu compañeiro de Tese durante os tres primeiros anos, a verdade é que estes dous últimos anos foron máis aburridos no laboratorio sen as nosas extensas charlas, partidas de cartas e piques co trivial. Aínda que teño que mencionar que me acordo de ti case tódolos días ao ver os armarios do laboratorio, ti xa me entendes.

A tódolos TFGs e TFMs e compañeiros que pasaron polo noso laboratorio e me fixeron máis levadeiro o meu día a día: **Manu**, **Ignacio**, **Antón**, **Maylee**, **David**, **Mario**, **Claudia**, **Sofi**, **Ale**, **Carlos**, **Alonso** e **Álvaro**. Gracias a todos polos bos momentos compartidos! Sobre todo a ti Sofi, que ademais de compañeira de laboratorio te fuches convertendo día a día nunha boa amiga (a clave foi o momento no que me invitaches a comer arepas), gracias por levar tan ben os últimos momentos de escritura e deposito da Tese.

Aos da primeira planta da ETSE polo apoio recibido durante estes anos, pola compañía durante tantas horas de cafés e comidas e polas conversacións sobre *skin care*, inversións, viaxes ou o que se nos pasase pola cabeza: **Alexandra**, **Bochra**, **Catarina**, **Fede**, **Isa**, **Jose**, **Joselu**, **Lidia**, **René** e **Vahid**, pero sobre todo quero darlle as gracias aos que ademais de compañeiros se converteron en amigos: **Andrea**, **Carlos** e **Cris**.

A **Alba Somoza**, que xa non está na ESTE, pero é unha desas persoas que ademais de compañeira se converteu en amiga. Gracias por toda a axuda recibida nestes últimos meses, pero sobre todo polas charlas, polas comidas e polas aventuras vividas xuntas.

Aos meus mellores amigos: **Mile** e **Saúl**. Ás de sempre: **Alba Amigo**, **Jenny** e **Iri**. Ás miñas amigas de tenis: **Gloria** e **Ened**. A **Javi** e a **Noe**, que foron o mellor que me levei do máster. Aos que apareceron durante estes cinco anos e viñeron para

quedarse: **Dani**, **Lara** e **Mónica**. Moitas gracias a todos polo apoio e polos bos momentos compartidos.

A miña familia, sen eles non podería chegar a onde estou agora. Gracias **mamá** e **papá** por todo o apoio emocional e económico recibido. Gracias a meu irmán (**Jose**) e a miña cuñada (**Adela**) por todos os bos momentos durante estes cinco anos, levouse mellor gracias a vos, pero sobre todo gracias polo mellor regalo que me puidéchedes en toda a vida, a **Iria**, de verdade que un sorriso dela cura calquera día malo.

A **Marisa** e **Alberto** polos bos ánimos e consellos que me déchedes baseados na vosa experiencia.

E por último, gracias a miña parella (**Óscar**), o pilar fundamental da miña vida, gracias por animarme a rematar a Tese sempre que estaba un pouco desanimada, pero sobre todo gracias por ensinarme a desafogarme no ximnasio, "**JN Entrenamiento Personal**" foi clave nesta Tese. Gracias por ser o mellor adestrador que se pode ter e o mellor compañeiro de vida.

Moitísimas gracias a todos os que tivéchedes algo que ver neste longo camiño!

Leti

Resumo

Hoxe en día o aumento de persoas con enfermidade celíaca está aumentando drasticamente. En termos de incidencia global, aumentou de maneira significativa na segunda metade do século XX e no século XXI en todo o mundo industrializado occidental. De feito, a enfermidade celíaca é un dos trastornos crónicos máis comúns a nivel mundial, cun predominio que oscila maioritariamente entre o 0,7 e o 2,9% na poboación xeral. Curiosamente, a enfermidade celíaca diagnostícase 1,5 veces máis frecuentemente en mulleres que en homes e é aproximadamente dúas veces máis común en nenos que en adultos. Debido a isto, o mercado global de produtos sen glute está a crecer rapidamente debido á maior demanda de alimentos saudables sen glute. Para 2023, este mercado alcanzou un valor aproximado de 7.500 millóns de dólares e prevese que supere os 14.000 millóns de dólares para 2032. Este crecemento vén impulsado pola diversificación de produtos como pans e pastas, que agora están amplamente distribuídos a través de supermercados e ventas online. Ademais, rexións como Asia-Pacífico están a mostrar un rápido crecemento e os produtos sen glute adoitan ter un prezo superior, o que os converte nunha opción atractiva e rendible para os fabricantes.

A enfermidade celíaca considérase unha enfermidade autoinmune, é un proceso crónico que dana o intestino e pode danar calquera órgano e tecido. Cando as persoas con enfermidade celíaca comen glute o seu sistema inmunitario responde danando o revestimento do intestino delgado. Isto pode levar a varios problemas dixestivos, deficiencias de nutrientes e outras complicacións. Ademais, a enfermidade celíaca está asociada a un maior risco de problemas psicosociais, como depresión, ansiedade e trastornos alimentarios. Actualmente, a única solución dispoñible para mellorar a calidade de vida dunha persoa que padece enfermidade celíaca é manter o cumprimento estrito dunha dieta sen glute. Polo xeral, o pan sen glute considérase apto para toda a poboación xa que o seu consumo está relacionado coa alimentación saudable. O aumento do consumo de produtos sen glute non só estivo ligado á crecente incidencia de trastornos relacionados co glute, senón á demanda dos

consumidores de alimentos sen glute para controlar o peso e a saúde dixestiva. Non obstante, os produtos sen glute adoitan ter unha menor cantidade de proteína e fibra en comparación co pan convencional, xa que adoita conter un maior contido de graxa e hidratos de carbono. Esta característica débese á necesidade de utilizar ingredientes alternativos para substituír o glute. Existen diferentes tipos de enfermidade celíaca segundo diferentes criterios, a enfermidade celíaca potencial, que se refire á presenza de marcadores da enfermidade, como anticorpos, pero sen evidencia de dano intestinal (as persoas con enfermidade celíaca potencial teñen un maior risco de desenvolver a enfermidade no futuro) e a enfermidade celíaca refractaria, que é unha complicación rara pero grave da enfermidade celíaca. Caracterízase pola persistencia dos síntomas e danos no revestimento do intestino delgado, a pesar de seguir unha dieta estrita sen glute durante un período prolongado, normalmente durante polo menos 12 meses.

Como mencionamos anteriormente, a única solución que existe para mellorar a calidade de vida das persoas que padecen a enfermidade celíaca é o cumprimento estrito dunha dieta sen glute. Non obstante, desde unha perspectiva nutricional, os produtos sen glute tenden a ser ricos en graxas e hidratos de carbono, pero baixos en proteínas, o que pode provocar picos no índice glicémico durante a dixestión. Este problema podería levar ao desenvolvemento de diabetes en persoas que antes non padecían esta condición debido á maior inxestión de hidratos de carbono. Entre as varias enfermidades autoinmunes relacionadas coa enfermidade celíaca está a diabetes mellitus. Este é un trastorno crónico no que o corpo non pode regular adecuadamente os niveis de azucre no sangue. Pode deberse a unha produción inadecuada de insulina ou á resistencia a esta hormona. O principal resultado é o alto nivel de glicosa no sangue, que pode causar complicacións graves. O tratamento da diabetes xeralmente implica manter unha dieta saudable, controlar os niveis de azucre no sangue e realizar actividade física regular. En resumo, observouse que as persoas con enfermidade celíaca teñen un maior risco de desenvolver diabetes.

Tendo isto en conta, o estudo desta Tese de Doutoramento céntrase na investigación de potenciais substitutos do glute, que poidan mellorar tanto as propiedades

nutricionais como estruturais destes produtos, centrándose na procura de aditivos naturais que reduzan tamén o seu índice glicémico. Un modo de reducir o índice glicémico é a adición de compostos con inhibición da actividade da amilasa e/ou amiloglucosidasa, como é o caso dos polifenois. Ademais, a obtención tanto do axente modificador da textura como das moléculas inhibidoras de encimas a partir da mesma materia prima resulta notablemente interesante. Por este motivo, o estudo comezou centrándose nun composto natural obtido a partir dunha alga parda (*Ascophyllum nodosum*) rica en polifenois. Os polifenois teñen unha alta capacidade antioxidante, son metabolitos secundarios lixeiramente hidrófobos e son un dos grupos máis abundantes no reino vexetal.

Nunha primeira fase, a nosa investigación tivo como obxectivo coñecer como interactúan os polifenois co amidón de millo nativo e o amidón de millo xelatinizado. Para iso, ás disolucións de polifenois, de diferentes concentracións, engadíuselle unha cantidade constante de amidón (1,95 e 5,00% p/p) para analizar en equilibrio a fracción de polifenois adsorbida polo amidón. Calculouse a cantidade de polifenois adsorbidos por masa de amidón a partir dos valores de concentración de cada experimento no equilibrio. Observouse que a cantidade de polifenois necesaria para saturar a superficie do amidón aumenta coa cantidade de amidón. En ambos sistemas (1,95 e 5,00%) a forma da curva correspondeuse cunha isoterma de Langmuir (R^2 > 0,98) que indica que a adsorción de polifenois na superficie do amidón está fisicamente limitada. Por outra parte, o amidón xelatinizado analizouse dun modo similar ao dos experimentos anteriores co amidón nativo e mantendo a mesma relación polifenois/masa de amidón. Polo tanto, estes estudos realizáronse tanto para o 1,95% como para o 5,00% p/p de almidón en xel. A adsorción do amidón xelatinizado non só é maior senón que tamén é moito máis rápida. Neste caso observouse unha relación lineal (R^2 > 0,99) entre a concentración de polifenois en equilibrio da solución e os polifenois adsorbidos. A adsorción de polifenois en xeles de amidón está lonxe da saturación; porén, aplicouse un modelo diferente, a isoterma de Henry. En resumo, a adsorción de polifenois aumentou de maneira significativa (case 7 veces) con xeles de amidón en comparación co amidón nativo, indicando que

o amidón xelificado aumentou notablemente a superficie dispoñible e melloraron as interaccións entre o amidón e os polifenois.

Os ensaios realizados para caracterizar o amidón e a súa dixestión en presenza de polifenois baseáronse en probas previas de adsorción sobre amidón nativo. Esta decisión tomouse coa intención de simular a produción de pan tradicional e industrial. Porén, tamén se estudou o efecto da adsorción de polifenois sobre o xel de amidón sobre a estrutura e a dixestión dos xeles formados. Ademais, este procedemento xustifícase polo proceso de elaboración de pan sen glute que finalmente contou cunha fase de prexelatinización, xa que tras diversas probas era a vía para obter masas con características adecuadas.

Despois de estudar a interacción entre polifenois e amidón, realizáronse estudos con xeles de amidón para investigar como a presenza de polifenois pode afectar tanto ás características viscoelásticas dos xeles de amidón de millo como á súa dixestión. Para acadar este obxectivo, estudáronse os sistemas de 1,95 e 5,00% p/p de amidón de millo (*AM*) con diferentes concentracións de polifenois (*PP*). Para as mostras do 1,95% p/p, as relacións nominais *PP/AM* (gPP/gAM) foron 0,0, 0,5, 2,5 e 5,0; mentres que para os xeles ao 5,00% p/p as relacións foron 0,0, 0,2, 0,9 e 1,9, engadindo diferentes cantidades de solucións de *PP* de 0,0, 0,1, 0,5 e 1,0 g/L. A presenza de polifenois aumentou a temperatura máxima de xelatinización (T_p), que corresponde ao valor máis alto do módulo elástico ($G´$) durante a rampa de quecemento. Nos xeles sen polifenois, estes valores foron de 11,1 ± 0,3 Pa e 78,3 ± 5,9 Pa para o 1,95 e 5,00% p/p de contido de amidón, respectivamente, mentres que coa presenza de polifenois os valores máximos obtidos foron de 15,1 ± 0,4 Pa e 125,4 ± 4,1 Pa, para 1,95 e 5,00% p/p, respectivamente. Este resultado pode estar relacionado coa diminución da auga dispoñible para a xelatinización do amidón pola natureza hidrófila dos polifenois. Durante o barrido de temperatura a 90ºC, observouse unha diminución relevante do valor de $G´$ para os sistemas con polifenois engadidos; esta observación pode estar relacionada coa reticulación formada entre os polifenois e o amidón durante a xelatinización, polo que se incrementa o carácter elástico a alta temperatura. No barrido de arrefriamento, os xeles con polifenois

presentaron valores de *G´* máis altos que os sistemas sen polifenois desde o principio (90ºC), pero as mostras con polifenois mostraron valores de *G´* inferiores aos sistemas sen polifenois ao final (25ºC). Este resultado parece indicar que a presenza de polifenois interfire na formación da estrutura tridimensional final do xel de amidón. Durante a etapa de maduración do xel a 25ºC durante 30 min, observouse que a presenza de polifenois aumentaba notablemente a estabilidade dos xeles, xa que o cambio dos valores de *G´* durante este período foi moito maior para sistemas sen polifenois. Finalmente, realizouse un barrido de frecuencia en xeles madurados, e observouse que as mostras tiñan un comportamento típico dos xeles de amidón que mostraban valores do módulo elástico (*G´*) superiores aos do módulo viscoso (*G´´*). Para os xeles de amidón menos concentrados, 1,95% p/p, observouse un claro efecto dos polifenois sobre as características finais do xel, dando como resultado valores de *G´* significativamente máis baixos. Ademais, non se observaron diferenzas significativas co aumento da concentración de polifenois engadidos, o que confirma que era necesaria unha concentración baixa para interferir coa estrutura do xel e debilitala. Para xeles cun contido de amidón do 5,00% p/p, observouse un comportamento similar entre xeles sen polifenois engadidos e con baixo contido en polifenois (por debaixo de 0,9 *PP/CS* (g*PP*/g*CS*)), pero os xeles cun alto ratio *PP*/*CS* mostrou unha diminución significativa dos valores *G´*.

Unha vez analizadas as características reolóxicas, estudouse a dixestión destes xeles. Para estudar a dixestión realizouse a cinética química ademais dun método rápido para a hidrólise do amidón medido mediante a caída de viscosidade no reómetro. En primeiro lugar, analizouse a cinética química da dixestión do amidón. Os valores das constantes cinéticas da dixestión (*k*) foron similares en ambos valores de concentración, os valores obtidos foron 0,149 ± 0,002 e 0,136 ± 0,005 min^{-1}, para 1,95 e 5,00% p/p, respectivamente. Este resultado pódese explicar porque os xeles son tan débiles que a estrutura non influíu na acción encimática. Independentemente do contido de amidón en xel, a adición de polifenois diminuíu tanto a constante cinética da dixestión como a concentración final de amidón dixerido. Ademais, canto maior sexa a cantidade de polifenois engadidos, maior será a diminución do valor *k*.

Probablemente, a estrutura do amidón cambiou en presenza de polifenois, xa que poderían estar formando un complexo de "amilosa de tipo V inclusiva" ao longo das cadeas glicosídicas α (1→4) coa amilosa. Os valores de amidón de dixestión rápida corroboraron esta teoría, xa que se dixería rapidamente menos amidón cando se engadían polifenois aos xeles. Non obstante, observouse que os valores de amidón de dixestión lenta aumentaron significativamente coa adición de polifenois. En calquera caso, a cantidade de amidón hidrolizado diminuíu considerablemente cos polifenois engadidos aos xeles. Por outra banda, o estudo da hidrólise do amidón por reometría desenvolvido nesta Tese baseouse na diminución da viscosidade aparente co tempo. O xel formouse no reómetro e o encima engadiuse ao xel diluído en tampón maleato. Inmediatamente, os datos de viscosidade aparente medíronse nun barrido de tempo ata que se conseguiu unha meseta de viscosidade, o que significa o final da dixestión do amidón. Os resultados obtidos pola reoloxía sobre o efecto dos polifenois na dixestión coincidiron cos informados pola dixestión bioquímica e confirmaron que a constante cinética por viscosimetría era menor en presenza de polifenois.

Despois de estudar sistemas sinxelos de amidón en presenza de polifenois e de obter diferenzas significativas elaboráronse formulacións simples de pan sen glute. Observouse que a incorporación de polifenois influíu nas características e na formación final dos pans sen glute. O índice de luminosidade diminuíu mentres que as coordenadas de vermello/verde e amarelo/azul aumentaron. En canto á estrutura, o volume de pan e o tamaño medio de poro reduciuse coa adición de polifenois mentres que tanto o numero poros como a porosidade aumentaron. Os parámetros de textura dos pans foron medidos e observouse que a adición de polifenois aumentou a dureza e a mastigación do pan fresco. O endurecemento diminuíu considerablemente, o que indica que os polifenois retrasaron a retrogradación do amidón por interaccións (formando enlaces de hidróxeno) coas moléculas de amidón.

Despois de obter e analizar o efecto da adición de polifenois a materiais amiláceos, decidiuse utilizar o residuo sólido de algas obtidos da extracción de polifenois para

obter e caracterizar alxinatos para ser utilizados como aditivo que poida modificar as propiedades reolóxicas e texturais das masas e pans sen glute. Deste xeito, poderíase conseguir unha mellor explotación das algas como materia prima. Os alxinatos secáronse ao aire nun secadoiro convectivo a dúas temperaturas diferentes: 50°C (*50D*) e 90°C (*90D*). A terceira mostra foi secada estaticamente sobre unha superficie plana en condicións ambientais (*ND*: "non secado por convección forzada"). Así mesmo, utilizouse como referencia o alxinato comercial de Sigma Aldrich (*S*) para comparar os resultados cos alxinatos obtidos no laboratorio.

Os alxinatos secados a diferentes temperaturas foron estudados nesta Tese porque previamente se confirmou no noso laboratorio que o tamaño do polímero dos alxinatos extraídos estaba afectado polas condicións do secado. Este achado levou a realizar un estudo exhaustivo mediante viscosimetría capilar, non só obtendo o peso molecular viscométrico medio ($\overline{M}_v$), senón tamén analizando as curvas completas de viscosidade específica en función da concentración para varios réximes de concentración: diluído, semidiluído e concentrado. Observando os resultados, pódense distinguir dous réximes diferentes para os alxinatos elaborados no laboratorio e tres zonas para os alxinatos comerciais. Ao identificar os puntos de intersección das rectas de regresión lineal determináronse as concentracións críticas de solapamento (*C**), que se corresponden coa transición do réxime diluído ao semidiluído. Despois de identificar os réximes para unha medición de viscosidade adecuada, determinouse a viscosidade intrínseca ($[\mu]$) mediante as ecuacións de Huggins e Kraemer e Fedors. Posteriormente, calculouse o peso molecular viscosimétrico medio ($\overline{M}_v$) mediante a ecuación de Mark-Houwink. En canto a ambos métodos, reportáronse valores similares de $\overline{M}_v$. Atopouse un amplo intervalo no valor do peso molecular viscométrico medio dos alxinatos extraídos no laboratorio dende 133,3 KDa (*90D*) a 427,8 KDa (*ND*). Estes resultados indicaron que o tamaño molecular dos alxinatos extraídos pode verse fortemente influenciado polos métodos e condicións empregados durante o secado. Curiosamente, non se atoparon diferenzas significativas entre os valores de peso molecular viscosimétrico obtidos para *90D* e *S*, a pesar das diferenzas na orixe das algas e outros factores; esta

similitude poderíase atribuír posiblemente ás severas condicións industriais empregadas durante o proceso de extracción para obter alxinatos comerciais. É importante destacar que os pesos moleculares obtidos estaban dentro dos intervalos típicos dos alxinatos comerciais.

Para unha análise máis detallada dos alxinatos realizáronse probas reolóxicas. Empregáronse tres valores de concentración para cada alxinato ensaiado, correspondentes a 2*C**, 4*C** e 6*C**, onde *C** representa a concentración de solapamento do réxime diluído ao semidiluído. As curvas de fluxo de velocidade de cizalla ascendente e descendente coincidiron en todos os casos, o que indica que dentro do intervalo de concentración de polímero probado, as solucións de alxinato non mostraron un comportamento dependente do tempo, como o comportamento tixotrópico ou reopéxico. As curvas de fluxo revelaron dúas tendencias relativas á velocidade de cizalla. A baixa velocidade de cizalla a viscosidade aparente mantívose constante mentres que ao superar unha velocidade de cizalla crítica a viscosidade aparente diminúe. O rango da meseta tendía a aumentar coa diminución do peso molecular viscométrico medio ou coa concentración de alxinato, afectando a determinación da velocidade de cizalla crítica. A viscosidade aparente das solucións aumentou notablemente coa concentración de alxinato, dando lugar á formación de solucións viscosas, que se considera unha das propiedades máis cruciais para que os alxinatos se usen en numerosas aplicacións industriais. Para modelar matematicamente as curvas de fluxo, empregouse o modelo de Cross-Williamson. O modelo reproduciu satisfactoriamente a viscosidade aparente dentro do intervalo probado de concentración de alxinato e temperatura de secado, mostrando un erro relativo medio do 16% e $R^2 > 0,95$.

O valor de concentración sinalado como 6*C** utilizouse para determinar as características viscoelásticas das solucións mediante probas de cizallamento oscilatorio de pequena amplitude (*SAOS*). Comprobouse que tanto os módulos elásticos (*G´*) como viscosos (*G´´*) aumentaron coa frecuencia en todos os ensaios e, de forma consistente, *G´´* superou a *G´*, indicando así un comportamento similar ao líquido. Ambos módulos diminuíron coa temperatura ao aumentar de 25 a 45ºC para

as solucións de alxinato *50D* e *90D*. Non obstante, o alxinato *ND* mostrou un comportamento diferente a 45ºC, onde *G´* se mantivo constante co aumento da temperatura, e *G´´* aumentou notablemente a baixas frecuencias (por debaixo de 1 Hz). Esta observación indica que unha temperatura máis alta pode levar potencialmente á consecución do punto de xel para esta solución de alxinato. Este comportamento é típico das solucións de polímeros semidiluídos que presentan un alto grao de enredo. Este resultado suxire que as solucións que conteñen alxinatos de alto peso molecular teñen temperaturas de xelación máis baixas. A relación entre o fluxo de corte constante e a reoloxía de corte dinámico examinouse mediante a regra de Cox-Merz, onde a viscosidade aparente obtida dos ensaios rotacionais coincidía coa viscosidade complexa (μ^*) obtida dos ensaios oscilatorios. En xeral, a regra de Cox-Merz cumpriuse satisfactoriamente para as solucións *50D* e *90D*, demostrando unha superposición de ambas curvas de viscosidade independentemente do intervalo de velocidade de cizallamento. Non obstante, para a disolución de alxinato *ND*, a superposición observouse só a altas velocidades de cizalla ($> 10\ s^{-1}$), mentres que a baixas velocidades de cizalla ($< 10\ s^{-1}$), a viscosidade dinámica era notablemente maior que a viscosidade complexa.

Como se pode deducir dos resultados mostrados ata o momento, os alxinatos poden presentar características diferentes dependendo da orixe das algas ou das condicións térmicas empregadas durante o procesado. Por estes achados, decidiuse realizar un estudo máis profundo da estrutura e composición química dos alxinatos e tamén sobre as relacións de composición co carácter hidrófilo dos alxinatos. Esta última propiedade é clave para comprender a interacción da auga nas matrices de amidón en presenza de alxinatos como aditivo. Para este fin, determináronse isotermas de absorción de auga de diferentes alxinatos con diferentes características estruturais a diferentes temperaturas (25, 37 e 50ºC). Para este estudo, seleccionáronse dous alxinatos comerciais, un de Panreac (*P*) e outro de Sigma (*S*) ademais dun dos obtidos no noso laboratorio, o *50D*. Dado que o alxinato é un biopolímero formado por unidades de monosacáridos D-manurónico e L-gulurónico, e a distribución destas unidades é a responsable da solubilidade, a viscosidade en solución líquida e

as propiedades xelificantes, é importante analizar a relación manurónico-gulurónico (*M/G*), xa que nos proporciona información sobre a súa composición. Neste caso, os valores das relacións *M/G* foron 1,15, 0,91 e 1,21 para *P*, *S* e *50D*, respectivamente. Para modelar os datos da isoterma de sorción de auga utilizouse o modelo de Halsey que se centra na relación entre a cantidade de adsorbato e presión parcial do adsorbato no equilibrio. En xeral, non se atoparon diferenzas significativas entre os dous alxinatos comerciais, a diferenza do alxinato obtido no noso laboratorio o *50D*, que foi o alxinato máis higroscópico.

Tras a extensa caracterización dos alxinatos, continuamos coa incorporación destes aos sistemas de amidón. Realizáronse varios ensaios con xeles de amidón de millo 1:4 p:p coa adición de ata un 2% p/p de alxinato sódico, en base ao amidón. Para estes ensaios utilizáronse os cinco alxinatos analizados previamente (*S*, *P*, *ND*, *50D* e *90D*). Neste caso, analizouse a capacidade de retención de auga (*WRC*) para os sistemas de amidón con e sen alxinatos. O valor de *WRC* para o amidón de millo foi de 0,97 ± 0,04 (g de auga/g d.b.). Mentres que os valores de *WRC* dos alxinatos comerciais foron 12,09 ± 1,08 e 10,16 ± 2,37 (g auga/g d.b.) para *P* e *S*, respectivamente. Para os alxinatos obtidos no laboratorio, os valores de *WRC* foron 7,31 ± 0,61, 5,26 ± 0,88 e 3,77 ± 0,18 (g auga/g d.b.) para *ND*, *50D* e *90D*, respectivamente. Para estes alxinatos, observouse unha relación lineal ($R^2 > 0,99$) entre o *WRC* e o $\bar{M}_v$, o que suxire que a capacidade de retención de auga aumenta coa lonxitude dos polímeros de alxinato. Non obstante, esta relación non se observou para os alxinatos comerciais, o que indica que factores como a fonte do alxinato, outras características do polímero e o método de extracción poden afectar significativamente ás propiedades fisicoquímicas do alxinatos. Realizáronse probas reolóxicas para o estudo da xelatinización do amidón, no que se xelatinizaba amidón de millo, só ou en presenza de alxinatos. Como resultado principal, comprobouse que a adición de alxinatos de sodio provocou cambios importantes no comportamento viscoelástico.

En xeral, as características reolóxicas dos xeles formados con alxinatos dunha mesma alga e con diferente $\bar{M}_v$ (mostras *ND*, *50D* e *90D*) non mostraron diferenzas

significativas entre eles. Estes resultados indicaron que o $\bar{M}_v$ do alxinato non era crítico para as características reolóxicas dos xeles de amidón cando os alxinatos tiñan natureza e procedementos de extracción similares. Non obstante, atopáronse diferenzas significativas cando se utilizaron diferentes concentracións e alxinatos de diferentes fontes. Observouse que o módulo elástico ($G´$) diminuíu e o módulo viscoso ($G´´$) aumentou debido á adición de alxinatos. Este resultado é diferente dos resultados obtidos anteriormente con polifenois, xa que a presenza de polifenois diminuíu tanto os módulos $G´$ como $G´´$. Polo tanto, a característica viscoelástica dos xeles de amidón pódese cambiar engadindo alxinato ou polifenois. En ambos casos fórmanse xeles máis débiles, pero pódense utilizar alxinatos cando se precisa un xel con comportamento máis viscoso, mentres que o uso de polifenois permite obter un xel menos viscoso.

Tamén se analizou a microestrutura de xeles de amidón con e sen alxinatos mediante microscopía electrónica de varrido (SEM). Como resultado principal da microestructura, comprobouse que a presenza de alxinatos creou estruturas de xel con cavidades alongadas e desiguais ademais da formación de muros de división lineais, formando así unha rede espacial anisotrópica, independentemente do alxinato utilizado.

Finalmente, tras analizar os resultados da dixestión *in vitro* dos sistemas ensaiados determinouse que a presenza de alxinatos no sistema deu como resultado unha diminución da constante cinética de hidrólise experimental (k). Non obstante, a adición de alxinatos deu lugar a un aumento do grao máximo de hidrólise (C_∞), atribuído principalmente ao aumento observado da fracción de amidón de dixestión lenta (*SDS*). Se se compara o efecto dos alxinatos co observado coa adición de polifenois nos sistemas de amidón de millo, observouse que ambos tipos de compostos diminuían a constante de velocidade de dixestión. Non obstante, os valores da fracción de amidón de dixestión rápida (*RDS*) víronse influenciados pola presenza de polifenois, mentres que este valor non mostrou diferenzas significativas co control (amidón sen alxinatos) cos sistemas de amidón en presenza de alxinatos. Non obstante, como vimos anteriormente, a presenza de polifenois provocou unha

diminución significativa do *RDS*. Por outra banda, o *SDS* aumentou coa presenza tanto de alxinatos como de polifenois. En canto aos resultados, pódese concluír que a adición de polifenois é máis adecuada para o noso obxectivo principal de reducir a constante de velocidade de dixestión e a cantidade de *RDS*, para evitar picos de glicosa no sangue.

Finalmente, engadiuse ao amidón un aditivo común como a hidroxipropilmetilcelulosa (HPMC) que se usa nas manufacturas de alimentos derivados do amidón a escala industrial para comparar o seu efecto cos mostrados anteriormente para xeles de amidón con aditivos de orixe mariña. Tendo en conta que se revelou previamente a importancia do tamaño molecular dos alxinatos, decidiuse estudar tres HPMC con diferentes pesos moleculares (caracterizadas polo rango de valores de viscosidade desenvolvido en solución acuosa ao 2% a 20ºC: 40-60 (*L*), 80-120 (*M*) e 2600-5600 (*H*) mPa s). Polo tanto, a primeira determinación realizada foi o peso molecular viscométrico medio ($\overline{M}_v$), empregando o mesmo procedemento descrito anteriormente para os alxinatos. Como os valores de Huggins e Kraemer e Fedors obtidos para os alxinatos eran coincidentes, só se utilizou neste caso o método de Huggins e Kraemer. Os valores obtidos foron 27,2 ± 1,8, 32,7 ± 1,0 e 82,7 ± 1,8 para *L*, *M* e *H*, respectivamente. Tamén se analizou a capacidade de retención de auga (*WRC*) do mesmo xeito que se realizou nos alxinatos. O valor obtido para o amidón de millo foi de 0,95 ± 0,01 (g de auga/g d.b.), mentres que os valores obtidos para as diferentes HPMCs aumentaron co peso molecular de 8,54 ± 0,28 ata 12,97 ± 0,45 (g de auga/g d.b.). A mesma tendencia atopouse entre o *WRC* e o peso molecular viscosimétrico medio dos alxinatos probados desde 3,77 ± 0,18 ata 12,09 ± 1,08 (g de auga/g d.b.). De feito, obtivéronse relacións lineais respectivas entre $\overline{M}_v$ e *WRC* ($R^2 > 0,99$) tanto para alxinatos como para HPMC. En todos os casos, a adición de HPMC aumentou as temperaturas de xelatinización inicial e final. O atraso no proceso de xelatinización podería ser atribuído á absorción de auga polos hidrocoloides engadidos, que compite co amidón pola auga dispoñible. Esta relación está apoiada polos resultados do *WRC* obtidos anteriormente, que indicaban que as mesturas de amidón e HPMC retiñan máis auga que o amidón de millo. Nos barridos

de frecuencia de xeles madurados, observouse que *G´* aumentaba coa frecuencia, o que indica que as mostras, con ou sen HPMC, son xeles débiles típicos. A adición de HPMC de viscosidade baixa e media (*L* e *M*) diminuíu os valores de *G´*; este mesmo comportamento observouse previamente coa adición de alxinatos e polifenois ao amidón. Non obstante, a adición de HPMC de alta viscosidade (*H*) por riba do 1,0% p/p aumentou os valores de *G´*.

Para a comparación de xeles de amidón con polifenois, alxinatos e HPMC, os datos normalizáronse con respecto ao control de amidón e á cantidade de biopolímero engadido. En primeiro lugar, comparouse a reoloxía dos xeles centrándose na proba de barrido de frecuencia, xa que se realizou para todos os sistemas de amidón que conteñen os biopolímeros de estudo. Ademais, esta proba considerouse a máis interesante para relacionar os valores obtidos de cada sistema, xa que é o punto onde se obtén o xel final. Dado que o carácter elástico é predominante nos nosos sistemas, escolléronse os valores de *G´* a 1 Hz para a comparación dos resultados. Na maioría dos casos, a adición de biopolímeros reduciu o módulo elástico (con algunhas excepcións), o que indica a formación dun xel máis débil. Isto explícase polo feito de que a presenza do biopolímero engadido interfire coa estrutura do xel na reticulación das moléculas de amidón e na formación dunha estrutura de rede completa dentro do xel. Ademais, en xeral, os valores de G´ obtidos para cada mostra mostraron unha tendencia segundo a cal canto máis biopolímero se engade, maior será o cambio. O valor G´ normalizado representa a porcentaxe de cambio do valor G´ por relación biopolímero/masa de amidón. Observouse que, nunha dobre gráfica logarítmica, os datos experimentais seguían unha función lineal ($R^2 > 0,90$). Polo tanto, pódese concluír que a elasticidade dos xeles de amidón, dada polo parámetro G´, non dependía da natureza do biopolímero utilizado (dos avaliados nesta Tese), senón que dependía da concentración de biopolímero empregado.

Con respecto a dixestión do amidón observousse que a adición de polifenois aumentou a proporción de amidón de dixestión lenta e diminuíu o amidón de dixestión rápida, así como a constante de velocidade, o que provocou unha redución do grao máximo de hidrólise. Pola contra, a presenza de alxinato non deu lugar a

diferenzas significativas no amidón de dixestión rápida entre o control e os sistemas que conteñen alxinato. Non obstante, observouse un aumento do amidón de dixestión lenta e do grao máximo de hidrólise, xunto cunha diminución da constante de velocidade de dixestión do amidón resistente (nalgúns sistemas). Dado que só hai resultados da dixestión de polifenois e alxinatos o estudo para a normalización dos datos, centrouse no rango común de concentracións destes biopolímeros que se engadiron. Polo tanto, o intervalo avaliado para ambos polímeros foi do 1 ao 2% p/p en base ao amidón. En ambos os casos, ao aumentar a concentración de biopolímero, a eficiencia enzimática diminuíu, xa que a constante de velocidade de dixestión é menor, aumentando a concentración de biopolímero. Analizando conxuntamente os resultados normalizados atopados da reoloxía e da dixestión do amidón, pódese concluír que a inhibición da dixestión con polifenois ou alxinatos é puramente química. Por outra banda, observáronse diferenzas significativas na constante de velocidade de dixestión co uso de polifenois ou alxinatos, xa que cun 1% de biopolímero o efecto inhibidor dos polifenois foi 6,3 veces maior no que respecta ao efecto dos alxinatos e para o 2% de concentración é un 6,0 maior. En conclusión, o uso de alxinatos ou polifenois modificou o comportamento elástico do amidón dun modo similar, pero a inhibición da hidrólise enzimática do amidón en presenza de polifenois é significativamente maior.

Abstract

Gluten-free products are in high demand either due to related pathologies or consumers' choices. However, a high relationship between type 1 diabetes and celiac disease exists because gluten-free diet is richer in carbohydrates and poorer in protein, fiber and trace-elements. Because of that, there is a growing interest in modulating starch digestion, particularly in gluten-free starch-based foods.

Polyphenols are secondary metabolites with many benefits associated to their antioxidant power but also, they have been targeted as great inhibitors of the starch hydrolysis. In this PhD Thesis the interaction of polyphenols extracted from *Ascophyllum nodosum* brown seaweeds with native and gelled starch was studied. Particularly, rheological features of starch gels were measured and elastic character decreased with increasing polyphenols content. Starch digestion with alpha-amylase enzyme was monitored employing a biochemical method and by rheology (monitoring the apparent viscosity with digestion time) and good agreement between both methods was found by analysis of respective digestion rate constants and the final concentrations of digested starch. In these studies, it was found a strong polyphenols action as inhibitors of starch digestibility was determined. Some simplified breads with polyphenols were baked and they showed greater hardness and chewiness and lower cohesiveness and resilience in relation breads without polyphenols. Nonetheless, the crumb hardening during storage was less noticeable, suggesting the potential integration of polyphenols into gluten-free bread formulations to delay the bread aging.

Alginates are other biopolymers present in brown seaweeds. A sequential extraction operation including drying stage to obtain polyphenols and alginates was analysed. It was found that the average molecular weights of alginates (measured by capillary viscosimetry) can be modulated by drying conditions, mainly drying temperature. The hygroscopic character (water sorption isotherms) of extracted and commercial alginates was experimentally determined and related with the structural characteristics of biopolymers at low water activities. Rheology of alginates

solutions was also experimentally determined by means of the corresponding flow curves and viscoelastic behaviour in a wide range of biopolymer concentrations and temperatures. Weak starch gels were obtained with the presence of alginates, and the microstructure of gels was hardly modified depending on alginates size. In alginate-corn gels with similar structure the increase of the viscoelastic characteristics decreased the hydrolysis rate of starch. Consequently, the hydrolysis rate depended on rheology and structure of gel. Measured enzyme inhibitions of alginates were less than those measured with polyphenols at the same biopolymer concentration.

Cellulosic derivates, particularly hydroxypropyl methylcellulose (HPMC), are common additives, together with other natural gums, employed in formulations to obtain gluten-free starchy products with better quality. In this PhD Thesis, HPMC with different average molecular weights were tested. Rheological and viscoelastic characteristics were experimentally determined of aqueous solutions with HPMC at different concentrations. The effect on the elastic character and stiffness of starch gels was also studied when different HPMC were added, and results were conveniently compared to those found with polyphenols and alginates addition.

In brief, this research tries to contribute the current knowledge about the effect of some alternative additives to enhance the functional properties of gluten free starchy products, particularly, in the physical, rheological, textural and digestion features to can formulate new commercial products for coeliac and diabetic people.

Contents

Agradecementos ii

Resumo v

Abstract xix

1. Introduction 1

1.1. Celiac disease 2

1.2. Diabetes disease 4

1.2.1. Type 1 diabetes 4

1.2.2. Type 2 diabetes 5

1.3. Gluten-free products 5

1.4. Food biopolymers 7

1.4.1. Xanthan gum 7

1.4.2. Guar gum 8

1.4.3. Hydroxypropylmethylcelluose (HPMC) 9

1.4.4. Alginates: characteristic carbohydrates in brown seaweeds 10

1.4.5. Polyphenols 11

1.4.6. Phlorotannins: characteristic polyphenols of brown seaweeds 12

1.5. *Ascophyllum nodosum* seaweed 13

1.6. Rheology 14

1.6.1. Capillary viscometry 15

1.6.1.1. Dynamic and kinematic viscosities 15

1.6.1.2. Kinematic viscosity and capillary viscosimetry 16

1.6.1.3. Relative, specific and intrinsic viscosities 17

1.6.1.4. Models for viscosity estimation 17

1.6.2. Stress-controlled rheology 19

1.6.2.1. Elastic behaviour 19

1.6.2.2. Viscous behaviour 21

1.6.2.3. Viscoelastic behaviour 22

1.6.2.4. Small amplitude oscillatory shear rheological analysis 24

1.7. Rheology of starchy systems 29

1.7.1. Starchy behaviour with temperature 29

1.7.1.1. Gelatinization and pasting 29

1.7.1.2. Retrogradation 30

1.8. Starch digestibility 31

2. Objectives 36

3. Methodology 39

3.1. Materials 40

3.2. Extraction and determination of polyphenols 40

3.2.1. Extraction of polyphenols 40

3.2.2. Determination of the concentration of total polyphenols in the extract of Ascophyllum nodosum seaweed 41

3.3. Characterization of alginates and hydroxypropyl methylcellulose (HPMC) 43

3.3.1. Obtaining alginates 43

3.3.2. Nuclear magnetic resonance of alginates 43

3.3.3. Determination of water desorption isotherms of alginates 45

3.3.4. Water retention capacity (WRC) of corn starch, alginates and HPMC 47

3.3.5. Capillary viscosimetry of alginates and HPMC 49

3.3.6. Rheological characterization of alginates and HPMC 51

3.4. Starch with polyphenols, alginates and HPMC 52

3.4.1. Preparation of starch gels in tube 52

3.4.2. Scanning electron microscopy (SEM) 52

3.4.3. Polyphenols adsorption on corn native starch and gels 53

3.4.4. Rheological characterization of polyphenols, alginates and HPMC with corn starch 54

3.4.4.1. Rheological characterization of starch with polyphenols 54

3.4.4.2. Rheological characterization of starch with alginate 55

3.4.4.3. Rheological characterization of starch with HPMC 56

3.4.5. Starch digestion 56

3.4.5.1. Conventional biochemical method of *in vitro* digestion starch 57

3.4.5.2. Rheometer determining the viscosity drop with time for studying the digestion starch 58

3.4.6. Bread characterization 59

3.4.6.1. Moisture content 59

3.4.6.2. The crumb image analysis 59

3.4.6.3. The crumb texture profile analysis (*TPA*) 60

3.4.6.4. Crumb color 61

4. Publications 62

4.1. Effect of polyphenols from Ascophyllum nodosum seaweeds on the rheology and digestion of corn starch gels and gluten-free bread features 63

4.2. Water sorption isotherms of different sodium alginates: Thermodynamic evaluation and influence of mannuronate-guluronate copolymers 75

4.3. Effect of the addition of different sodium alginates on viscoelastic, structural features and hydrolysis kinetics of corn starch gels 83

4.4. Rheological properties of corn starch gels with the addition of hydroxypropyl methylcellulose of different viscosities 101

5. General discussion 102

5.1. Studies on the polyphenols-native starch interaction 104

5.2. Studies of interaction during starch gelation process 108

5.3. Rheological measurement of starch hydrolysis (preliminary tests): application to α-amylase activity on starch 112

5.4. Effect of polyphenols on corn starch gels rheological properties and enzymatic digestion with α-amylase and amyloglucosidase 117

5.5. Effects of starch gels on bread formulations characteristics 120

5.6. Characterization of alginates employed as texture-modifying applied to starchy foods 122

5.7. Rheological behavior of alginates solutions 127

5.8. Chemical characterization of alginates 133

5.9. Preparation and analysis of starchy systems containing alginates 137

5.10. Preparation and analysis of starchy systems containing cellulose derivate 140

5.11. Comparison of the effects produced by polyphenols, alginates and HPMC on the elastic behaviour of starch gels 143

6. Conclusions 146

References 150

APPENDICES:

Appendix A: Journal publications in which this thesis is based 164

1. INTRODUCTION

1. Introduction

Nowadays the increase of people with celiac disease is increasing drastically. In terms of global incidence, it has increased significantly in the second half of the 20th century and in the 21st century throughout the Western industrialized world (King *et al.,* 2020). Indeed, celiac disease is one of the most common chronic disorders worldwide, with a prevalence mostly ranging between 0.7% and 2.9% in the general population (Gatti *et al.*, 2024). Interestingly, celiac disease is diagnosed 1.5 times more frequently in women than in men and it is approximately twice more common in children than in adults (Singh *et al.,* 2018). Because of this, the global market for gluten-free products is growing rapidly due to the increased demand for healthy gluten-free foods (Knežević *et al.*, 2024). By 2023, this market reached a value of approximately $7.5 billion and is projected to exceed $14 billion by 2032. This growth is driven by the diversification of products such as breads, pastas, and snacks, which are now widely distributed through supermarkets and online channels. Additionally, regions such as Asia-Pacific are showing rapid growth, and gluten-free products are often priced at a premium, making them an attractive and profitable option for manufacturers (https://www.fortunebusinessinsights.com/industry-reports/gluten-free-food-market-100188, by October 2024).

1.1. Celiac disease

Celiac disease is considered as an autoimmune disorder; it is a chronic process that damages the intestine and can damage any organ and tissue. When people with celiac disease eats gluten, even in very low quantity, their immune system responds by damaging the lining of the small intestine. This can lead to various digestive problems, nutrient deficiencies, and other complications (Sharma *et al.*, 2020). Additionally, celiac disease is associated with an increased risk of psychosocial problems, such as depression, anxiety, and eating disorders (Clappison *et al.*, 2020). Currently, the only available solution to improve the quality of life of a person suffering from celiac disease is maintaining a strict compliance with a gluten-free

diet (Caio *et al.*, 2019). Generally, gluten-free bread is considered suitable to the entire population since their consumption is related to healthy eating. Increased gluten-free products consumption has not only been linked to the increasing incidence of gluten-related disorders, but to a consumer demand for gluten-free foods for weight management and digestive health. However, gluten-free products usually have a lower amount of protein and fibre compared to conventional bread, since it usually contains higher fat and carbohydrate content. This characteristic is due to the need for using alternative ingredients to replace gluten (Miranda *et al.*, 2014). There are different types of celiac disease according to different criteria:

Potential celiac disease: It refers to the presence of markers of the disease, such as antibodies, but without evidence of intestinal damage. People with potential celiac disease have a higher risk of developing the disease in the future.

Refractory celiac disease (RCD): It is a rare but serious complication of celiac disease. It is characterized by the persistence of symptoms and damage to the lining of the small intestine, despite following a strict gluten-free diet for a prolonged period, usually for at least 12 months. There are two types of refractory celiac disease (Malamut *et al.*, 2009):

> **RCD type I:** It is characterised by an abnormal proliferation of lymphoid cells in the lining of the small intestine. Although it is a chronic disorder, it generally responds to treatment.
>
> **RCD type II:** This form is more severe and is characterized by the presence of abnormal cells in the lining of the small intestine, which can increase the risk of complications, such as small intestinal T-cell lymphoma. Treatment of refractory type II celiac disease generally involves more intensive therapies, such as immunosuppressants and other specific therapies.

1.2. Diabetes disease

As mentioned above, the unique solution that exists to improve the quality of people suffering from celiac disease is the strict compliance with a gluten-free diet. However, from a nutritional perspective, gluten-free products tend to be high in fat and carbohydrates, but low in protein, which can lead to spikes in the glycemic index during digestion. This problem could lead to the development of diabetes in people who previously did not suffer from this condition due to the higher intake of carbohydrates. Among the several autoimmune diseases related to celiac disease is the diabetes mellitus. This is a chronic disorder in which the body cannot properly regulate blood sugar levels. It may be due to inadequate insulin production or resistance to this hormone. The main result is the high level of glucose in blood, which can cause serious complications. The treatment for diabetes generally involves maintaining a healthy diet, controlling blood sugar levels, and getting regular physical activity (Awuchi *et al.*, 2020). In summary, individuals with celiac disease have been observed to have a higher risk of developing both type 1 and type 2 diabetes.

1.2.1. Type 1 diabetes

Type 1 diabetes is an autoimmune disease in which the body attacks and destroys insulin-producing cells in the pancreas. This leads to a complete lack of insulin, requiring insulin injections to control sugar levels in blood. It is often diagnosed in childhood or adolescence and is not related to lifestyle or obesity. Symptoms include increased thirst, frequent urination, fatigue, and weight loss. Type 1 diabetes has a strong genetic and autoimmune association and is believed to share similar risk factors with celiac disease. Epidemiological studies have shown that the prevalence of celiac disease is significantly higher among patients with type 1 diabetes compared to the general population (Ludvigsson *et al.*, 2006). Additionally, some studies suggest that introducing gluten-containing foods into the diet of babies and children may increase the risk of developing type 1 diabetes in individuals with a genetic predisposition. Therefore, in families with a history of type 1 diabetes,

delaying the introduction of gluten into the baby's diet or following a gluten-free diet may be considered to reduce this risk (Hummel *et al.,* 2011).

1.2.2. Type 2 diabetes

Type 2 diabetes is a chronic disease in which the body does not use insulin effectively or does not produce enough insulin. It is often related to obesity and lifestyle. Symptoms may include increased thirst, frequent urination, fatigue, and blurred vision. Treatment involves changes in diet, exercise, and sometimes medication to control blood sugar levels. Although type 2 diabetes is not classified as an autoimmune disease, an association between celiac disease and an increased risk of developing type 2 diabetes has also been observed. The exact mechanisms behind this association are not yet fully understood but may involve genetic, immunological, and environmental factors (Olokoba *et al.,* 2012).

Therefore, the objective of this Thesis is to study starchy products with antioxidant properties, suitable for people with celiac disease and beneficial for the entire population. The addition of biopolymers (phenolic compounds, alginates and food gums) in gluten-free starch can have a triple beneficial effect since it is expected to increase the antioxidant capacity of the product, act as a cross-linker through interactions with other compounds and, finally, act as a regulator of enzymatic activity in digestive processes to control the glycemic index.

1.3. Gluten-free products

The general concern about health and well-being has led to an increase in demand for safer and healthier food products. Gluten-free products have gained significant relevance due to the increasing prevalence of gluten-related disorders (Cabanillas, 2020). Gluten is found in grains such as wheat, barley and rye. It is composed of two types of proteins: gliadin, which contributes to the elasticity of the doughs, and glutenin, which provides them resistance, cohesion and strength, important for bread making industry (Wieser, 2007). During the kneading process these proteins are hydrated and form bonds with each other, creating an elastic and

cohesive three-dimensional structure. This structure is responsible for gas retention in the dough, contributing to the fluffiness and structure of baked products. The absence of gluten can affect both the texture and flavour of the final products. Gluten-free products tend to have a denser and sandier texture, as well as a flatter and less satisfying flavour (Delcour *et al.*, 2012). Additionally, the lack of gluten can lead to a shorter product shelf-life, since gluten provides stability and high moisture retention.

Starch is commonly used as simplified system of common flours to observe the interactions between selected biopolymers and amylose and amylopectin of the starch. The removal (or absence) of gluten enhances the importance of starch in determining the structure and texture of gluten-free products. Common sources of starch in these products include corn, tapioca, rice, and potato (Aleman, *et al.* 2021). Starch serves as a fundamental storage polymer in numerous plants, comprising two different molecules: branched amylopectin and linear amylose. Both are constituted by α-D-glucopyranose residues, with α-1,4-glycosidic bonds forming the linear structure of amylose, and additional α-1,6-glycosidic branches in amylopectin molecules (Figure 1.1). These structural disparities lead to significant differences in their properties. Amylose tends to more readily undergo crystallization, known as retrogradation, resulting in tough gels and strong films, whereas amylopectin disperses in water and retrogrades at a slower rate, yielding soft gels and weak films (Li *et al.*, 2020b).

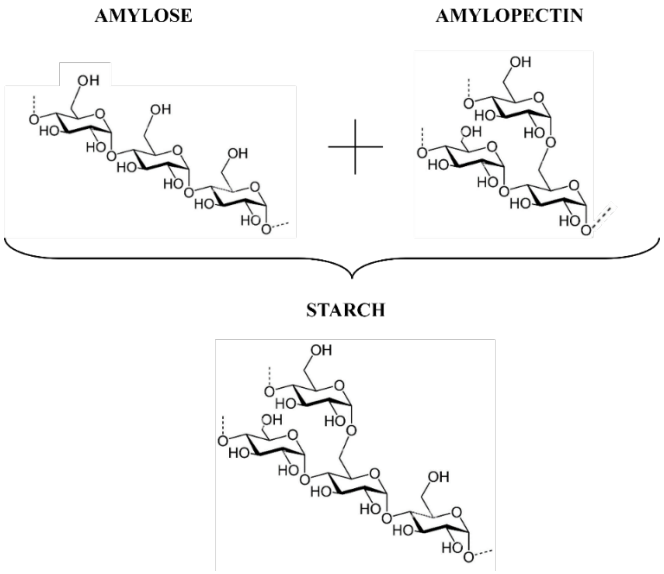

Figure 1.1. Structure of amylose, amylopectin and starch.

1.4. Food biopolymers

Food additives are substances added to food to enhance its flavour, appearance, texture, or preservation. Some of the food additives commonly used in the production of gluten-free products include xanthan gum, guar gum, and hydroxypropylmethylcellulose (HPMC), among others (Anton & Artfield, 2008).

1.4.1. Xanthan gum

Xanthan gum is a natural polysaccharide produced by *Xanthomonas spp.* fermentation with sugars as carbon source (Figure 1.2). This polymer has been widely studied and utilized in the food and cosmetic industry because of its texturing, thickening and gelling properties (Bhat *et al.*, 2022). Xanthan gum is soluble in water and forms viscous gels at very low concentrations. Additionally, it is considered safe for human consumption in the concentrations nowadays authorised in foods in Europe (EFSA) and USA (FDA authorisation 21 CFR 172.695) and is considered a GRAS ingredient ("Generally Recognized as Safe") by US-FDA (obtained from *Xanthomonas campestris* as ethanol precipitate, GRAS Notice GRN 000121).

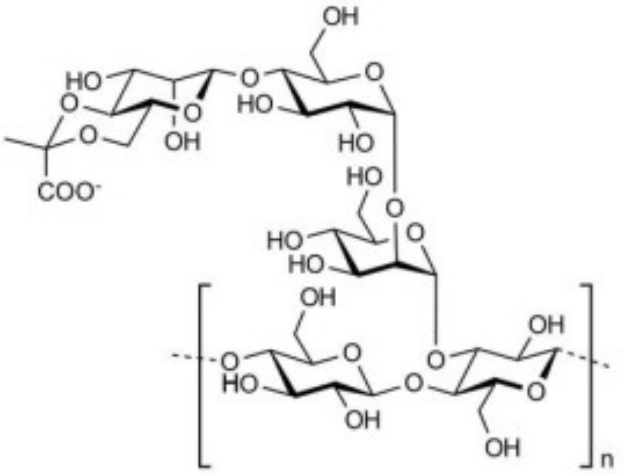

Figure 1.2. Structure of xanthan gum.

1.4.2. Guar gum

Guar gum is a natural polysaccharide extracted from the seeds of the *Cyamopsis tetragonoloba* plant (Figure 1.3). It is obtained as a white powder, which is extensively used in the food industry as a thickener, stabilizer, and gelling agent (Yadav *et al.*, 2018). Like xanthan gum, it is considered safe for human consumption in the quantities used in food.

For example, guar gum and xanthan gum increased the viscosity and viscoelasticity of cationic tapioca starch. Ionic interactions between starch and gums are a key factor: anionic xanthan gum causes rapid aggregation of granules, while non-ionic guar gum wraps the granules more loosely. These interactions result in lower swelling power, solubility index and peak viscosity, but increase the gelatinization temperature and the rheological parameters (Chaisawang & Suphantharika, 2005).

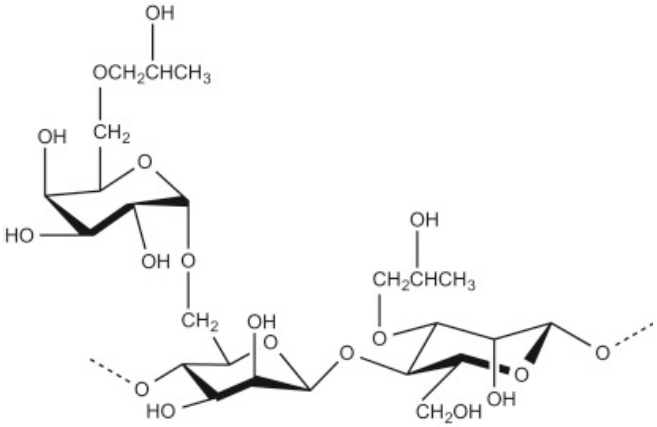

Figure 1.3. Structure of guar gum.

1.4.3. Hydroxypropylmethylcellulose (HPMC)

HPMC is a polymer derived from cellulose and commonly found in plants that belongs to the group of cellulose ethers (Figure 1.4). A white powder, it serves as a thickening, stabilizing, gelling, and water-retention agent. It enhances the texture, viscosity, and stability of foods. It is considered safe for human consumption in the quantities used in foods and is authorised by US-FDA as food additive under the section 21CFR 172.874. In addition, numerous studies demonstrate how incorporating HPMC alters the viscoelasticity of gluten-free systems to replicate the viscoelastic properties of wheat (Ronda *et al.*, 2013; Sun *et al.*, 2016).

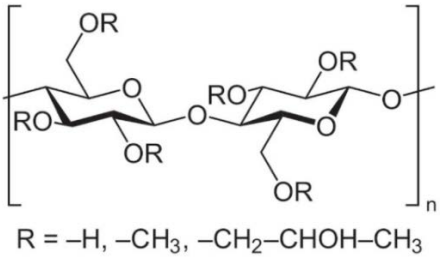

Figure 1.4. Structure of HPMC.

On the other hand, there are many other less-studied additives that could be very interesting to use for the same purposes, among which alginates from the brown alga *Ascophyllum nodosum* stood out. This alga can additionally provide extracts containing compounds polyphenols with antioxidant activity.

1.4.4. Alginates: characteristic carbohydrates in brown seaweeds

Alginates are natural polysaccharides found in the cell walls of brown algae, including those belonging to the order *Fucals*, such is the case of *Ascophyllum nodosum*. This fact is a very important difference with those known as red algae, that belong to the order *Gigartinales*, such is the case of *Chondrus crispus*, which main polysaccharides are known as carrageenan, a type of galactose-derived biopolymers (Ciancia *et al.*, 2020).

Alginates are mainly composed of guluronic acids (*G*) and mannuronic acid (*M*), which are arranged in homopolymer (*GG* and *MM*) and heteropolymer (*MG*) blocks in the polymer chain (Figure 1.5). The proportion and sequence of these blocks determine the physical and chemical properties of the alginate. They are highly studied biopolymers since they are used in industry for various applications in the food, pharmaceutical, cosmetics and tissue engineering industries due to their gelling, thickening and stabilizing properties (Costa *et al.*, 2018).

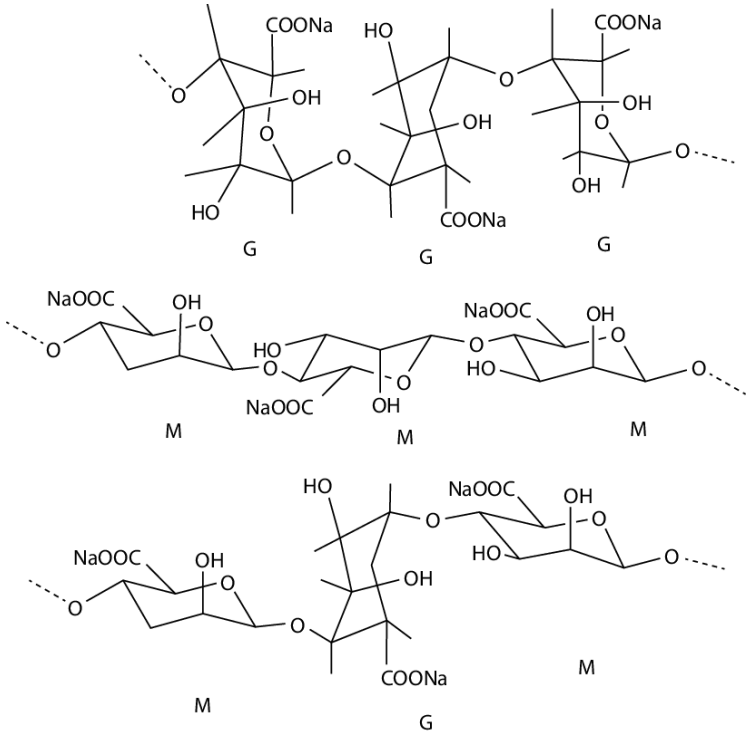

Figure 1.5. Structure of sodium alginate.

Rheological studies are often carried out to analyse the interactions between biopolymers and rheology is widely considered one of the best techniques for the in the study of gelatinization and characterization of starch gels, together with differential scanning calorimetry (DSC). Even some rheological tests can report structural modifications with no relevant thermal effect and that are not detectable by DSC (Jin *et al.*, 2006).

1.4.5. Polyphenols

Polyphenols are secondary metabolites that occur naturally in terrestrial and marine plants. There are several types of polyphenols, flavonoids, phenolic acids, lignans and stilbenes (Figure 1.6). Flavonoids, found in fruits, vegetables, tea, among others, are the most important due to their wide variety of health benefits. In general, polyphenols, thanks to their antioxidant power, have vasodilating, anti-inflammatory

and antithrombotic properties. Because of this, they can help reduce cardiovascular diseases, help reduce the risk of suffering from different metabolic diseases, as well as help people with obesity, diabetes and even cancer (Hazafa *et al.*, 2022). In general, the addition of polyphenols on starch decreases the value of the elastic and viscous modulus, as well as the strength of the gel due to the interference of polyphenols with the crystallization of amylose (Chen *et al.*, 2020). Polyphenols are also recognized as great inhibitors of starch hydrolysis. Some studies have observed that corn starch gels enriched with different polyphenols show a notable influence on their digestibility, which is linked to alterations in the pH and the amount of hydroxyl groups (Aleixandre *et al.*, 2022).

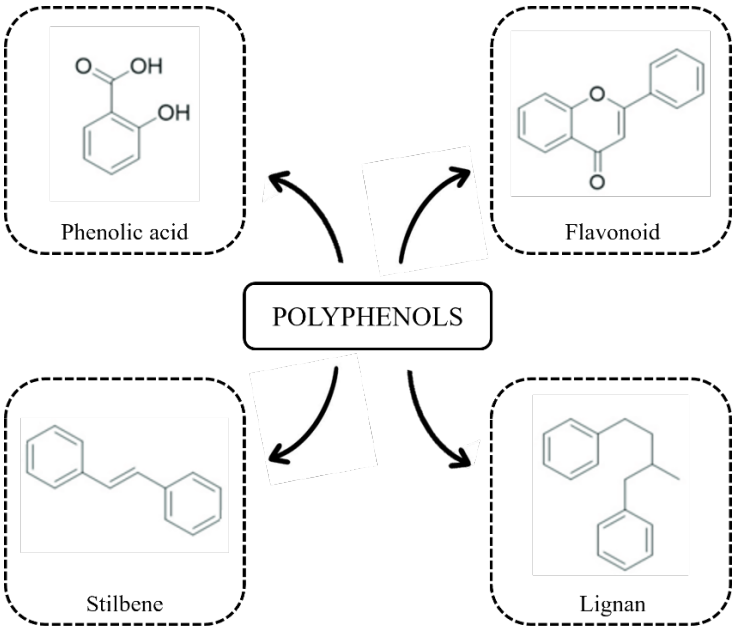

Figure 1.6. Structure of several types of polyphenols.

1.4.6. Phlorotannins: characteristic polyphenols of brown seaweeds

The polyphenols present in brown seaweeds are generally named phlorotannins, because they are polymers which main unit is considered

phloroglucinol (1,3,5 trihydroxybenzene) or tetrahydroxybenzene, similarly to plant tannins, which are derived from the flavanes catechin and its epimer epicatechin. Phlorotannins are named as function of the phenolic ring binding type and the degree of OH substitution on that ring, being the main four classes: fucols, phlorethols, eckols and fuhalols (Figure 1.7). Fucols and phlorethols represent the main phlorotannins found in *Ascophyllum nodosum* (Catarino *et al.*, 2022).

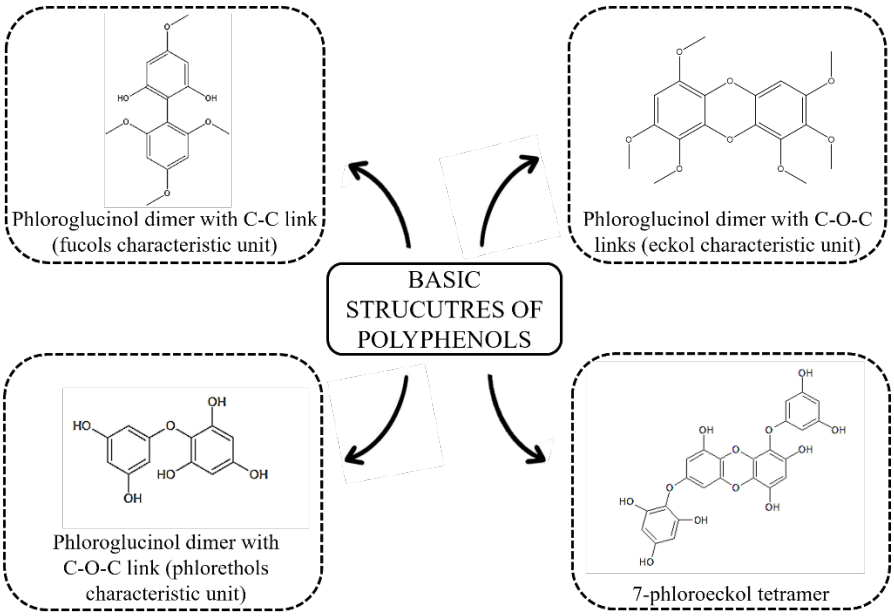

Figure 1.7. Examples of basic structures of polyphenols found in brown seaweeds.

1.5. *Ascophyllum nodosum* seaweed

Ascophyllum nodosum seaweed belongs to the group of brown algae (the only phlorotannin-containing ones) and it is also known as “egg wrack”, “knotted wrack” or, globally, “North Atlantic rockweed”. It belongs to the *Fucaceae* family and lives in rocky areas on the shores of the coasts washed by the North Atlantic Ocean, mainly on the northwest coast of Europe and the northeast coast of North America. It is a slow-growing algae that can grow up to 6 meters in length and can live for

around 14 years. It develops irregularly shaped fronds that contain small nodules like bladders with air inside, which help with its buoyancy. Its fronds, olive green and/or slightly brown (Figure 1.8), reach two meters in length. Unlike other species of brown algae, it withstands periods of marine immersion and periods of exposure to the elements, depending on the tidal cycle, providing a unique biochemical composition, which is why it is rich in polyphenols and alginates, several essential nutrients such as nitrogen, phosphorus and potassium, as well as trace elements such as magnesium, calcium, manganese, zinc and boron (Pereira *et al.*, 2020).

Figure 1.8. Picture of Ascophyllum nodosum seaweed.

1.6. Rheology

Rheology studies the flow and deformation of materials under stress, combining principles of fluid mechanics and deformable solids (Steffe, 1996). It is based on mathematical models that describe how the viscosity and elasticity of a material respond to deformation, distinguishing between Newtonian and non-Newtonian (plastic, dilatant, pseudoplastic) behaviours. The data is obtained using viscometers and rheometers, allowing properties such as viscosity, elasticity and resistance to flow to be analysed.

1.6.1. Capillary viscometry

Even rheometry is a more powerful technique, capillary viscosimetric analysis is one of the reference techniques for determining the molecular weight of biopolymers (known as average viscosimetric molecular weight), as is further explained in methodology section *"3.3.5. Capillary viscosimetry of alginates and HPMC"*.

Viscosity, often denoted as η (Pa s), is a fundamental property of fluids that quantifies their internal resistance to flow when subjected to an external deformation (Steffe, 1996). Understanding viscosity is crucial for characterizing the rheological behaviour of fluids. Rheological testing involves applying different types of deformations and analysing the resulting stresses and flow behaviour. The most studied flow type in rheology is shear flow, where the fluid is considered to consist of multiple layers that slide over each other without mixing, resulting in a linear and unidirectional flow (Kulicke & Clasen, 2004).

1.6.1.1. Dynamic and kinematic viscosities

In shear flow, a velocity profile (v) develops across the fluid, which can be described mathematically by the Eq. (1.1):

$$v = \begin{pmatrix} v_1 \\ v_2 \\ v_3 \end{pmatrix} = \begin{pmatrix} \zeta(t)x_2 \\ 0 \\ 0 \end{pmatrix} \tag{1.1}$$

where ζ(t) represents the rate of deformation (s^{-1}), often referred to as the shear rate $\dot{\gamma}_{21}$ (t), which is a component of the shear velocity tensor.

When a force is applied parallel to the direction of flow, it generates shear stress, σ (Pa), defined as the force, F (N), per unit area, A (m^2) applied, Eq. (1.2):

$$\sigma = \frac{F}{A} \tag{1.2}$$

Shear rate $\dot{\gamma}$ (s^{-1}) is the gradient of velocity across the fluid layers and can be mathematically described as, Eq. (1.3):

$$\gamma = \frac{V}{H} \tag{1.3}$$

where V (m s^{-1}) is the velocity difference between the layers, and H (m) is the distance between them. The dynamic viscosity, η, can then be obtained as the ratio of shear stress to shear rate, Eq. (1.4):

$$\eta = \frac{\sigma}{\dot{\gamma}} \tag{1.4}$$

1.6.1.2. Kinematic viscosity and capillary viscosimetry

Kinematic viscosity v (m^2 s^{-1}) relates dynamic viscosity to the fluid's density ρ (kg m^{-3}) at a specific temperature, Eq. (1.5):

$$v = \frac{\eta}{\rho} \tag{1.5}$$

Capillary viscometry can be employed to measure kinematic viscosity. According to Hagen-Poiseuille's law, the flow rate through a capillary is proportional to both the fluid's viscosity and density. By measuring the time, t (s), it takes for a fluid to pass through a calibrated capillary and applying the Eq. (1.6), the kinematic viscosity can be determined:

$$v = K_{cp}(t - \theta) \tag{1.6}$$

where K_{cp} (m^2 s^{-2}) is the capillary constant (value obtained from manufacturer calibration) and θ (s) is the Hagenbach-Couette correction factor also given by manufacturer.

1.6.1.3. Relative, specific and intrinsic viscosities

The relative viscosity (η_r) is defined as the ratio of the viscosity of a solution (η) to that of the solvent (η_s), Eq. (1.7), and the specific viscosity (η_{sp}) represents the relative increase in viscosity, Eq. (1.8):

$$\eta_r = \frac{\eta}{\eta_s} \tag{1.7}$$

$$\eta_{sp} = \frac{\eta - \eta_s}{\eta_s} = \eta_r - 1 \tag{1.8}$$

Intrinsic viscosity [η] (dL g^{-1}) is a critical parameter extensively applied in the analysis of polymer solutions within the dilute concentration regime. In this regime, the polymer chains are sufficiently spaced apart, minimizing intermolecular interactions. As a result, intrinsic viscosity is governed exclusively by the molecular dimensions and molecular weight of the polymer chains (Khouryieh *et al.*, 2007). Thus, it provides a quantitative measure of the hydrodynamic volume occupied by individual polymer molecules in isolation (Rao, 2007).

1.6.1.4. Models for viscosity estimation

Intrinsic viscosity can be represented as the zero-concentration limit of reduced viscosity (η_{sp}/C), Eq. (1.9), and is obtained by extrapolation of the Huggins, Eq. (1.10), and Kraemer, Eq. (1.11), correlations (Khouryieh *et al.*, 2007).

$$[\eta] = \lim_{C \to 0} \frac{\eta_{sp}}{C} \tag{1.9}$$

$$\frac{\eta_{sp}}{C} = [\eta] + \kappa' [\eta]^2 C \tag{1.10}$$

$$\frac{\ln \eta_r}{C} = [\eta] + \kappa'' [\eta]^2 C \tag{1.11}$$

where C is the polymer concentration (g dL^{-1}) and $k´$ and $k´´$ are the Huggins and Kraemer constants, respectively. These constants provide insights into polymer-polymer and polymer-solvent interactions, indicating the strength of these interactions based on their values.

Intrinsic viscosity is considered valid for extrapolation when relative viscosity has values between 1.2 and 2.0 and specific viscosity is in the range of 0.2 to 1.0. Using the Huggins and Kraemer constants, both the interactions between polymer molecules and the interactions of the polymer with the solvent in which it is found can be studied. If the Huggins constant ($k´$) has values lower than 0.5 and the Kraemer constant ($k´´$) is negative, it can be deduced that the polymer-polymer interactions are very weak while those between polymer and solvent are strong. On the contrary, if the value of $k´$ is higher than 0.50, it indicates that there are significant interactions between the polymer molecules (Khouryieh *et al.*, 2007). Furthermore, to check the goodness of the solvent used once the correlations and the average viscosimetric molecular weight have been obtained, the accomplishment of the rule ($k´ - k´´$) $\approx 0.50 \pm 0.05$ can be checked (Morris *et al.*, 1981).

Another method to obtain the intrinsic viscosity involves using the Fedors equation, Eq. (1.12). This equation can be used when working with polymer solutions in the dilute or semi-dilute range, its use being limited to systems rendering relative viscosity values between 1 and 100 (Fedors, 1979):

$$\frac{1}{2\,(\eta_r{}^{1/2} - 1)} = \frac{1}{C\,[\eta]} - \frac{1}{C_{max}[\eta]} \qquad (1.12)$$

where C_{max} (g/dL) is the theoretical concentration at which the interactions that will occur between the polymer molecules will be very significant.

Yet explained, when working in very dilute regimes, the interaction between polymer molecules can be considered null and the viscosity of the solution is equivalent to the viscosity of the solvent and the small contributions of the loose molecules. Thus, following the Mark-Houwink equation, Eq. (1.13), the average molecular weight, $\bar{M}_v$ (kg mol^{-1}), of high molecular weight polymers can be related to intrinsic viscosity, since this is the measure of the hydrodynamic volume of a polymer molecule in each solvent:

$$[\eta] = K M_v^{\alpha} \qquad (1.13)$$

where K and α are parameters characteristic of a solute-solvent system at a defined temperature, which can be measured by advanced techniques such as osmotic pressure measurements or light scattering and only are valid for a defined range of molecular weights (Steffe, 1996).

1.6.2. Stress-controlled rheology

Several concepts are essential for the comprehension of rheology, between the most important ones are:

- Strain (γ): It is the change in size or shape of a material because of the applied stress. It can be expressed as a fraction of the original length (dimensionless) or as a percentage of the relative change. For example, if a 1-meter object is stretched by 1 cm, the strain would be 0.01 or 1% (Bourne, 2002).
- Shear stress (τ): It is the component of stress that acts tangentially to the plane on which the force is applied. In other words, it is the force attempting to slide one part of the material over another. Like conventional stress, shear stress is measured in Pascals (Pa) (Bourne, 2002).
- Shear rate ($\dot{\gamma}$): It refers to the rate of change of velocity between adjacent layers of a fluid, resulting from the application of shear stress. It is a measure of how quickly one layer of fluid slides past another. The shear rate is measured in reciprocal seconds (s^{-1}), indicating the amount of sliding per second (Bourne, 2002).

1.6.2.1. Elastic behaviour

When a solid material obeys Hooke's law, its stress *vs* strain curve is a straight line through the origin. This indicates a linear relationship, Eq. (1.14), between shear stress and shear strain as:

$$\sigma = G\,\gamma \qquad (1.14)$$

where *G* (Pa) is the shear modulus. Hookean materials are linearly elastic and return to their original shape once the strain is removed, typically for strains less than 0.01. Larger strains may lead to brittle fractures or nonlinear behaviour.

The behaviour of a Hookean solid can be studied through the uniaxial compression of a cylindrical sample (Figure 1.9). By measuring changes in length and radius under compression, normal stress, Eq. (1.15), and strain, Eq. (1.16), can be calculated:

$$\sigma = \frac{F}{A} = \frac{F}{\pi R_0^2} \tag{1.15}$$

$$\varepsilon_0 = \frac{\delta h}{h_0} \tag{1.16}$$

where R_0 (m) and h_0 (m) are the initial radius and height of the cylinder and δh (m) the change in length.

This data is used to determine Young's modulus, *E* (Pa), or the elasticity modulus, which is the slope of the shear stress *vs* strain curve, Eq. (1.17):

$$E = \frac{\sigma}{\varepsilon_o} \tag{1.17}$$

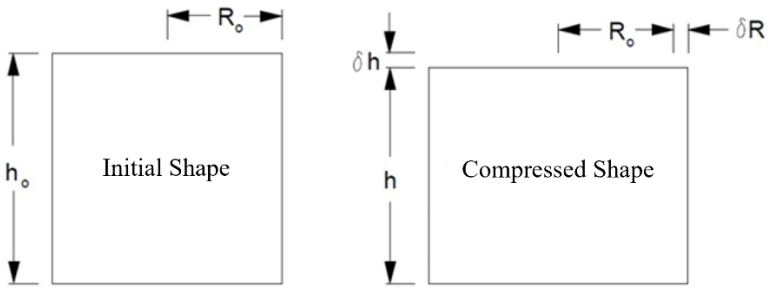

Figure 1.9. Uniaxial compression of a cylindrical sample.

1.6.2.2. Viscous behaviour

In general, the elastic behaviour food-related fluids are generally small or negligible, excepting for gels. Viscosity is related to shear stress and shear rate, being possible to determine their relationship through experimental analysis. This behaviour can be visualized by plotting shear stress against shear rate experimental values. The simplest systems to analyse are Newtonian fluids, for which shear stress is directly proportional to shear rate and is described by Newton's law of viscosity, Eq. (1.18):

$$\sigma = \eta\,\dot{\gamma} \tag{1.18}$$

where η (Pa s) is the proportionality constant, called the dynamic viscosity for Newtonian fluids.

The dynamic viscosity (η) accounts for the fluid's resistance to flow (Barnes *et al.*, 1993). Also, dynamic viscosity represents the internal friction of a fluid or its resistance to flow (Rao, 2007). All Newtonian fluids render a linear relationship between shear stress and shear rate. Fluids that do not exhibit this linear behaviour are known as non-Newtonian fluids (Steffe, 1996). The apparent viscosity (μ) is defined as the ratio of shear stress (σ) to shear rate ($\dot{\gamma}$). For Newtonian fluids, the apparent viscosity is constant and independent of shear rate and therefore, η and μ are the same. However, for non-Newtonian fluids that follow the Ostwald-de Waale law, Eq. (1.19), their apparent viscosity is defined by the following equation:

$$\mu = k\,\dot{\gamma}^{n-1} \tag{1.19}$$

where μ is the apparent viscosity (Pa s), k is the consistency index (Pa s) and *n* the flow index (-).

Or also, the Cross-Williamson model (Eq. 1.20):

$$\mu = \frac{\mu_0}{1 + K\,\dot{\gamma}^{(1-n)}} \tag{1.20}$$

where μ (Pa s) is the apparent viscosity, μ_0 (Pa s) is the viscosity in the Newtonian regime, K is the consistency index, $\dot{\gamma}$ (s^{-1}) is the shear rate and n is the flow index. Non-Newtonian fluids are rheologically complex fluids that exhibit one or more of the following features (Shenoy, 1999):

- Shear rate-dependent viscosities: The viscosity changes depending on the applied shear rate.
- Elastic solid-like behaviour: These fluids may exhibit elastic properties, resisting deformation like a solid before flowing.
- Yield stress: A minimum stress is required for the fluid to start flowing.
- Time-dependent viscosities: The viscosity can change over time under a constant shear rate.

These characteristics differentiate non-Newtonian fluids from Newtonian fluids, which have a constant viscosity regardless of shear rate or time.

1.6.2.3. Viscoelastic behaviour

The term "viscoelastic" refers to a material that exhibits both some elastic properties of an ideal solid and some flow properties of an ideal liquid at the same time. Some authors use "viscoelastic" specifically for materials that are more solid-like than liquid-like and prefer the term "elastic-viscous" for materials that are more liquid-like than solid-like (Bourne, 2002).

The differences between an ideal elastic solid, an ideal liquid, and a viscoelastic material can be understood by considering how each respond to a constant stress applied over three time periods, followed by the removal of that stress:

Ideal Elastic Solid (Hookean Solid):

- *Behaviour under stress:* When a constant stress is applied, the material deforms immediately in proportion to the stress. This deformation is purely elastic, meaning the material stores the applied energy and returns to its original shape once the stress is removed.

- Response after stress removal: The material instantly returns to its original shape without any permanent deformation.

Ideal Liquid (Newtonian Liquid):

- Behaviour under stress: When a constant stress is applied, the material flows continuously at a rate proportional to the applied stress. Unlike the elastic solid, a Newtonian liquid does not store energy but dissipates it as flow occurs.
- Response after stress removal: The liquid stops flowing as soon as the stress is removed, but it does not return to its original form; instead, it remains in the deformed state.

Viscoelastic Material:

- Behaviour under stress: This material exhibits a combination of both solid-like and liquid-like behaviour. When stress is applied, it initially deforms like an elastic solid but continues to flow like a liquid if the stress is maintained over time.
- Response after stress removal: Upon removing the stress, part of the deformation recovers like an elastic solid, but some permanent deformation may remain, like a liquid.

In summary, an ideal elastic solid deforms and recovers instantly, an ideal liquid flows continuously under stress and doesn't recover, whereas a viscoelastic material shows both immediate deformation and gradual flow, with partial recovery when the stress is removed.

Viscoelastic behaviour can be categorized into two main types:

- Linear viscoelastic in which the rheological properties depend solely on time and are not influenced by the magnitude or rate at which the stress is applied. Most foods exhibit linear viscoelasticity when subjected to small strains, typically within a few percentages.

- Non-linear viscoelastic where the mechanical properties depend on the duration of stress application, the magnitude of the stress, and often the rate at which the stress is applied.

1.6.2.4. Small amplitude oscillatory shear rheological analysis

In oscillatory tests, materials are subjected to a deformation (using instruments that control the rate) or stress (using instruments that control the stress) that changes in sinusoidal manner along time. The material is usually placed between a cone and plate or between two parallel plates. The cone or plate oscillates around a central point with a sinusoidal angular velocity at a low amplitude while the shear stress is recorded. This testing method is non-destructive because it involves only small amplitudes inside the linear viscoelastic regime (Steffe, 1996).

Oscillatory tests can be performed for tension, compression, or shear. To accurately describe these tests, several assumptions must be made when developing the mathematical equations: the strain is uniform throughout the sample, the inertia of the sample is negligible and the material behaves as a linear viscoelastic substance (Baltsavias *et al.*, 1997).

The principle behind small amplitude tests in parallel-plate-geometry involves applying a sinusoidal deformation to the sample. According to this setup, the lower plate remains fixed while the upper plate moves back and forth horizontally (Figure 1.10). Now, it can be assumed that the material being tested is placed between the plates (separated by a gap, h (m)) of a controlled rate device. In this scenario, the strain in the material can be defined as a function of time as follows, Eq. (1.21):

$$\gamma = \gamma_0 \sin(\omega\, t) \tag{1.21}$$

where γ_0 is the amplitude of the strain equal to L/h when the motion of the upper plate is $L\ sin(\omega\, t)$, ω is the frequency expressed in rad/s, which is equivalent to $\omega/(2\pi)$ Hertz (Hz).

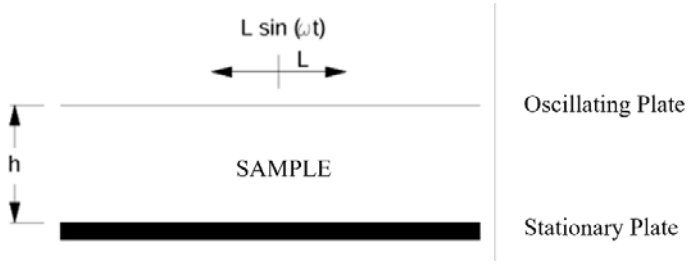

Figure 1.10. Oscillatory strain between rectangular plates.

After a few cycles, the stress within the sample also oscillates sinusoidally at the same frequency as the strain, but it typically lags the strain wave by a phase angle (δ). This concept is fundamental to understand small amplitude tests in parallel-plate-geometry, where a sinusoidal deformation is applied to the sample, and the resulting stress response is measured.

Using the small strain values to remain the conditions of linear viscoelasticity range, the following stress is produced by the strain input, Eq. (1.22):

$$\sigma = \sigma_0 \sin(\omega t + \delta) \tag{1.22}$$

where σ_0 is the amplitude of stress and δ is the phase lag or phase shift relative to the strain.

The mathematical functions for small amplitude oscillatory tests are defined according to the response in shear stress. Using trigonometric functions, the Eqs. (1.23) and (1.24) can be obtained:

$$\sigma = \sigma_0 (\sin\omega t \cos\delta + \sin\delta \cos\omega t) \tag{1.23}$$

$$\sigma = (\sigma_0 \cos\delta) \sin\omega t + (\sigma_0 \sin\delta) \cos\omega t \tag{1.24}$$

Eq. (1.22) presents material functions from small amplitude tests. It shows that part of the stress wave is in phase with the applied deformation $((\sin(\omega t))$, while another part is in phase with the applied strain rate $((\cos(\omega t))$. This agrees with Newton's law, Eq. (1.18), for viscous modulus and Hooke's law, Eq. (1.14), for elastic modulus.

For an ideal elastic solid, shear stress is in phase with strain. For a Newtonian fluid, shear stress is 90 degrees (or $\pi/2$ radians) out of phase with strain. For a viscoelastic fluid, shear stress lags strain by a phase angle between 0 and 90 degrees. This behaviour can be seen in Figure 1.11.

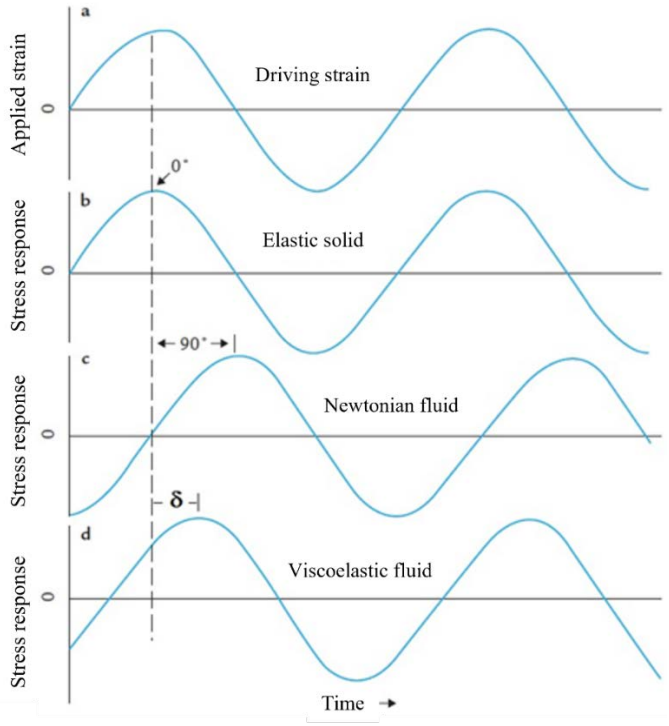

Figure 1.11. Scheme of the fundamentals of oscillatory measurements: applied strain versus time and resultant stress versus time (a) that is measured in an elastic solid (b), Newtonian liquid (c) and viscoelastic liquid (d).

In this context, the shear stress response is typically expanded into its trigonometric components to derive expressions for fundamental material functions, specifically the storage modulus ($G´$) and the loss modulus ($G´´$). These functions are essential for characterizing the material's elastic and viscous properties, Eqs. (1.25) and (1.26), respectively.

$$G' = \frac{\sigma'}{\gamma} \tag{1.25}$$

$$G'' = \frac{\sigma''}{\gamma} \tag{1.26}$$

Eqs. (1.25) and (1.26) can be unified in the expression (Eq. 1.27):

$$\sigma = G'\,\gamma + \frac{G''}{\omega}\,\dot{\gamma} \tag{1.27}$$

These variable definitions are the basis for developing several useful functions (some of them employed in this PhD Thesis). Eqs. (1.28) to (1.35), depending on the frequency, such as the complex modulus (G^*, Pa), complex viscosity (η^*, Pa s), dynamic viscosity (η', Pa s), out of phase component of the complex viscosity (η'', Pa s), tangent of the phase shift (tan δ, -), complex compliance (J^*, Pa^{-1}), storage compliance (J', Pa^{-1}) and the loss compliance (J'', Pa^{-1}) (Villarreal & Iturriaga, 2016):

$$G^* = \frac{\sigma_0}{\gamma_0} = \sqrt{(G')^2 + (G'')^2} \tag{1.28}$$

$$\eta^* = \frac{G^*}{\omega} = \sqrt{(\eta')^2 + (\eta'')^2} \tag{1.29}$$

$$\eta' = \frac{G''}{\omega} \tag{1.30}$$

$$\eta'' = \frac{G'}{\omega} \tag{1.31}$$

$$\tan\delta = \frac{G''}{G'} \tag{1.32}$$

$$J^* = \frac{1}{G^*} \tag{1.33}$$

$$J' = \frac{G'}{(G')^2 + (G'')^2} \tag{1.34}$$

$$J'' = \frac{G''}{(G')^2 + (G'')^2} \tag{1.35}$$

Using Eqs. (1.27) and (1.30), the material behaviour can be clearly represented by (Eq. 1.36):

$$\sigma = G'\,\gamma + \eta'\,\dot{\gamma} \tag{1.36}$$

In qualitative terms, oscillatory curves provide a fingerprint of the microstructure's state by identifying and quantifying various mechanisms based on their position on the frequency axis and the signal amplitude. The most basic form of this spring-damper model is the Maxwell model, which involves connecting a spring and a damper in series. The Kelvin-Voigt model can also be used to describe viscoelastic solids, which also uses springs and dampers, but connects them in parallel. The viscoelastic behaviour of real materials can be described using a combination of the Maxwell and Voigt models, such as the Burgers model. The Maxwell model describes the behaviour at low frequencies and the Voigt model at high frequencies. Figure 1.12 shows the expected viscoelastic spectrum over a range of frequencies (Macosko, 1994).

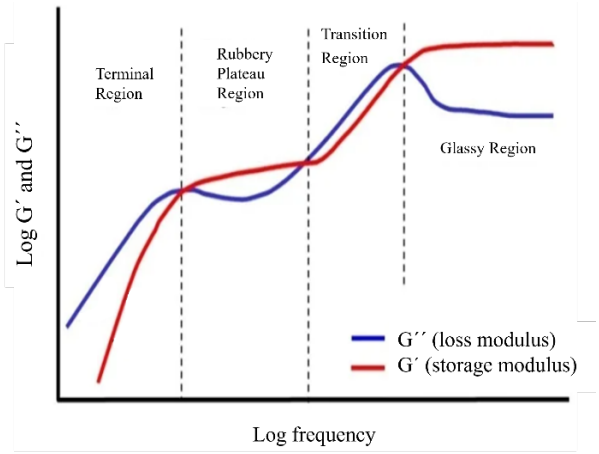

Figure 1.12. Schematic representation of rheological regions.

1.7. Rheology of starchy systems

The rheological study of starch gels provides detailed information about their physical and mechanical behaviour, which is essential for the study of new product formulations, as well as for their application in the food industry. Rheology focuses on understanding how materials change their shape and behaviour in response to these forces, measuring properties such as viscosity, elasticity, plasticity and other aspects related to the fluidity and deformation of materials.

1.7.1. Starch behaviour with temperature

The thermal transitions of starch during heating and cooling are an effective tool for characterizing the gelatinization and retrogradation of starch. These properties are essential for understanding the baking process, as they significantly influence the texture, structure, and overall quality of the final product (Biliaderis, 2009).

Whereas starch is the primary component in most doughs, other ingredients are present, though they typically exhibit fewer or less pronounced thermal transitions under baking conditions. Thermal methods are particularly effective for analysing starch, revealing key transitions that are essential for controlling the baking process. In contrast, other flour components offer limited thermal data, as they often lack significant transitions during baking. This focus on starch transitions is critical, as they play a dominant role in determining the final product characteristics, such as moisture retention, crumb structure, and shelf life (Horstmann *et al.*, 2017).

1.7.1.1. Gelatinization and pasting

Gelatinization and pasting of starch are key processes that occur during heating in the presence of water. Rheology is critical to studying these phenomena, as it measures changes in viscosity and other mechanical properties over time.

Gelatinization is the process by which starch granules absorb water and swell when heated. As seen in Figure 1.13, the pasting temperature is the point where starch grains begin to swell due to water absorption and the starch crystalline structure is

disrupted, reflecting an increase in viscosity. Pasting occurs after gelatinization, when the swollen granules disintegrate, releasing amylose and amylopectin. At this point, the maximum peak viscosity is reached. Afterwards, a drop in viscosity is observed, until reaching a minimum viscosity (holding strength). The difference between the peak viscosity and the drop viscosity is what determines the stability of the gel (breakdown). The viscosity reached at the end of the test (final viscosity) less the minimum viscosity (holding strength) defines the retrogradation (total setback).

In summary, rheology is essential to monitor changes during gelatinization and pasting in real time, identifying critical transition points and quantifying the mechanical properties of starch under different conditions. This helps to predict and control food quality and texture (Ali & Hasnain, 2015).

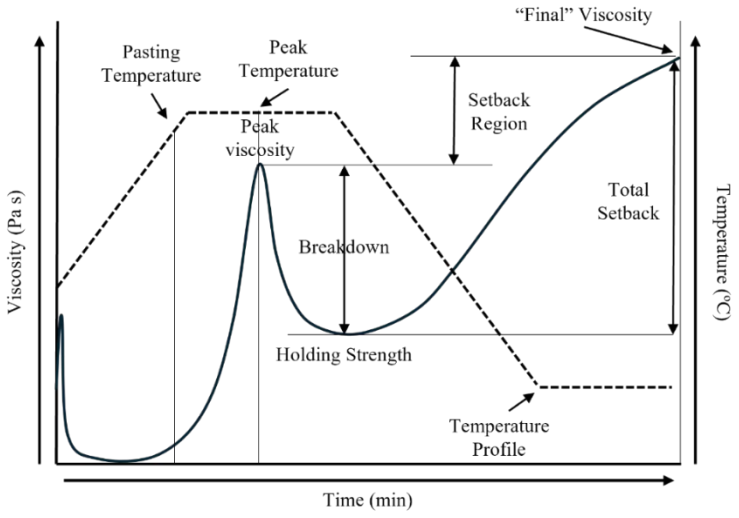

Figure 1.13. Schematic representation of starch gel formation.

1.7.1.2. Retrogradation

Starch retrogradation is a process that occurs after gelatinization, after cooked starches have been cooled and begin to reorganize into more ordered and crystalline structures. This phenomenon involves the formation of additional hydrogen bonds,

which causes a hardening of the gel structure and loss of water-holding capacity (Donmez *et al.,* 2021).

In the early stages of retrogradation, starch chains (particularly amylose) may begin to form simple bonding points, which develop into more ordered regions over time and may eventually form a crystalline structure under favourable conditions. This is especially relevant in baked goods such as bread, where retrogradation is associated with the staling process. Amylose is particularly responsible for the short-term development of the starch gel structure, while amylopectin, with shorter side chains, is more often associated with the long-term development of the gel structure, although to a lesser degree. However, although amylopectin does not associate as rapidly as amylose, its role in retrogradation cannot be considered negligible: short amylopectin chains can also rearrange into helical structures, contributing to gel hardening over time (Karim *et al.,* 2000).

The following Table 1.1 summarizes the current state of the art on how different biopolymers affect different starches. The research is based on the most relevant studies of the last 20 years, focusing on corn starch.

1.8. Starch digestibility

The digestion of starches begins in the mouth with salivary amylase breaking them down into maltose and dextrins. In the stomach, acidity temporarily inactivates this enzyme, but digestion resumes in the small intestine with pancreatic amylase and intestinal enzymes breaking down maltose into glucose, which is absorbed into the bloodstream. Factors such as the proportion of amylose and amylopectin, food processing, and the presence of fiber influence digestibility. Resistant starch reaches the colon, where it is fermented by the microbiota, providing health benefits (Bojarczuk *et al,* 2022; Fuentes-Zaragoza *et al.,* 2011).

Table 1.1. Effect of different additives on different starches.

Type of starch	Additive	Comments	Reference
Potato and corn starch	Xanthan gum HPMC	With these additives a suspension with an increase of viscoelasticity, enthalpy and temperature of starch gel transition was formed. Also, similar thermo-mechanical effects of gluten could be achieved.	Megusar *et al.* (2022)
High-amylose corn starch	Guar gum Xanthan gum	These gums decrease high-amylose starch granule swelling and increase pasting viscosity and the gel strength of high-amylose starch.	Zhang *et al.* (2020)
Corn starch	Xanthan gum and sucrose	Both additives increased the transition temperatures and the enthalpy change (ΔH) of the starch gelatinization and increased the consistency index of the starch pastes.	Zolelmein *et al.* (2019)
Maize starch Sweet potato starch	Guar gum	Rheology showed enhanced pasting characteristics with the addition of guar gum starch.	Zhang *et al.* (2018)
Waxy corn starch	Xanthan gum Guar gum Carrageen gum	These additives decrease onset temperature of gelatinization and give less viscous final gels.	Kowalski *et al.* (2008)
Wheat starch	HPMC Pectin	Hydrocolloids decreased the viscoelastic moduli during heating and cooling, yielding a weakening effect on gluten.	Bárcenas *et al.* (2009)
Wheat starch	Xanthan gum	The addition of xanthan in starch dispersions increases the swelling of granules during heating; furthermore, the gum is concentrates around the swollen granules increasing the shear forces applied to them.	Mandala & Bayas (2004)
Waxy rice starch	HPMC	Higher gelatinization onset, peak temperatures and pasting temperatures were found in samples with HPMC.	Lee & Kim (2019)
Pea starch	Xanthan gum Sodium alginate	Xanthan gum and sodium alginate and increased the viscosity.	Wang *et al.* (2022)

Starch digestion primarily occurs along the oro-gastrointestinal tract through enzymatic action, leading to an increase in blood glucose levels following the ingestion of starchy foods (Santamaria *et al.*, 2021). Two key enzymes are involved in this process: α-amylase and α-glucosidase:

- α-amylase exists in two isoforms in humans: salivary and pancreatic. Salivary α-amylase initiates starch breakdown in the mouth, producing shorter oligomers, which are then further digested by pancreatic α-amylase in the intestine.
- α-glucosidase, which includes the isoforms maltase-glucoamylase (MGAM) and sucrase-isomaltase (SI) located in the small intestine, hydrolyzes the oligomers into glucose.

In vitro starch digestion refers to the analysis of starch breakdown under controlled conditions that simulate the human digestive environment. These simulations primarily focus on intestinal digestion, where most of the starch hydrolysis occurs. Enzymes such as amylase are used under specific pH and temperature conditions to evaluate the conversion of starch into simple sugars like glucose and maltose. *In vitro* studies are essential for investigating the efficiency of starch digestion and the impact of various factors on this process, with significant applications in nutrition, food formulation, and the management of metabolic diseases.

Various *in vitro* methods have been developed to study the rate and extent of starch digestion, aiding in the estimation of glycemic index (*GI*) and the classification of starch based on digestibility:

- Hydrolysis Index (*HI*): Proposed by Granfeldt *et al.* (1992), this method compares the starch digestion rate of a food to that of white bread.
- Starch classification: Englyst *et al.* (1996) classified starch into three types based on its digestion rate: Rapidly Digestible Starch (*RDS*), Slowly Digestible Starch (*SDS*), and Resistant Starch (*RS*).

  - *RDS* is starch that is quickly broken down into glucose within 20-30 minutes in the small intestine, causing a rapid spike in blood sugar levels.
  - *SDS* is starch that is digested more slowly, over 20-120 minutes, leading to a gradual and sustained release of glucose, resulting in a more stable blood sugar level.
  - *RS* is starch that resists digestion in the small intestine and instead ferments in the large intestine, acting like dietary fiber and providing benefits such as improved gut health without raising blood sugar levels significantly.
- Kinetic analysis: Goñi *et al.* (1997) developed a kinetic method to measure the starch digestion rate by fitting hydrolysis curves with a first-order equation, allowing for the calculation of parameters such as the equilibrium concentration (C_∞), kinetic constant (k), and Hydrolysis Index (*HI*) to estimate the *GI*.

Understanding starch digestibility and its relationship with starch properties is crucial for developing starchy foods with desirable glycemic index values. *In vitro* methods provide a powerful tool for exploring compound functionality, hydrolysis mechanisms, and the influence of factors such as food formulation. This knowledge is essential for applications in nutrition, food product development, and the management of metabolic conditions.

The following Table 1.2 summarizes the current state of the art on how different biopolymers affect different starches. The research is based on the most relevant studies of the last 20 years, focusing on corn starch.

Table 1.2. Effect of different additives on digestion starch.

Type of starch	Additive	Comments	Reference
Corn starch	Gum Arabic Xanthan gum Guar gum	The blending hydrocolloids with starch can reduce digestibility, with the most prominent decrease exhibited by the starch-guar gum complex.	Zhou *et al.* (2020)
Corn starch	Locust bean Tara Guar gum	In general, addition of hydrocolloids decreased the rapidly digestible starch and increase de slowly digestible starch and resistant starch.	Chen *et al.* (2018)
Maize starch Sweet potato starch	Guar gum	Addition of guar gum increases the indigestible and antidigestible portion of starch.	Zhang *et al.* (2018)
Chestnut starch	Xanthan gum	Decrease the rapidly digestible starch and increase de slowly digestible starch and resistant starch.	Liu *et al.* (2022)
Potato starch	Calcium alginate	As the concentration of sodium alginate increased, the calcium alginate network became stronger, which could exhibit a strong blocking effect on amylase and thus decreased the digestibility of starch.	Cui *et al.* (2022)
Potato starch	Calcium alginate	As the concentration of sodium alginate increased, the calcium alginate network became stronger, which could exhibit a strong blocking effect on amylase and thus decreased the digestibility of starch.	Cui *et al.* (2022)
Chestnut starch	Xanthan gum	Decrease the rapidly digestible starch and increase de slowly digestible starch and resistant starch.	Liu *et al.* (2022)
High amylose rice starch	Carboxymethyl cellulose (CMC) Guar gum Xanthan gum	The addition of hydrocolloids attenuated rapid increases in blood glucose levels, but xanthan gum was more effective than guar gum or CMC.	Oh *et al.* (2018)
Pea starch	Xanthan gum Sodium alginate	The resistant starch content increased in the presence of xanthan gum and sodium alginate.	Wang *et al.* (2022)

2. OBJECTIVES

2. OBJECTIVES

The primary aim of this Thesis is to investigate simple gluten-free systems with enhanced antioxidant capacity, designed specifically for the celiac population, utilizing biopolymers such as polyphenols and alginates derived from native Galician brown seaweed (*Ascophyllum nodosum*). The research examined the impact of incorporating seaweed extracts rich in polyphenols and alginates, as well as assessed the effects of a semi-synthetic polymer (hydroxypropyl methylcellulose) as a control. Experimental evaluations involved the characterization of the biopolymers and the analysis of their interactions with starch and the modification of the rheological behaviour. Additionally, the study focused on starch gels digestion in the presence of several concentrations of the selected biopolymers. Finally, simplified gluten-free bread systems incorporating polyphenols were developed and evaluated.

To achieve the previous general objectives, the following specific objectives have been established:

1. To study the interaction between polyphenols and native and gelled corn starch.
2. To characterise corn starch gels with the presence of different concentrations of polyphenols by means of rheology.
3. To analyse the digestion of corn starch gels with the presence of polyphenols.
4. To evaluate the effect of polyphenols in simplified bread systems made with corn starch (moisture, colour and texture).
5. To characterise the alginates to be used by means of capillary viscometry (to determine the average viscosimetric molecular weight), rheology (to study the viscoelastic behaviour of alginate solutions) and by means of chemical characterisation (nuclear magnetic resonance and determination of water sorption isotherms).

6. To prepare and analyse corn starch gels with the presence of alginates of different molecular weights and nature as well as different concentrations (water retention capacity, rheology, scanning electron microscopy and digestibility).
7. To characterize hydroxypropyl methylcellulose by capillary viscometry, water retention capacity and rheology.
8. To determine the rheology of corn starch gels with hydroxypropyl methylcellulose of different molecular weights with different polymer concentrations.

3. METHODOLOGY

3. Methodology

This chapter presents the main methodology used in each of the experiments carried out to achieve the objectives set out in the Thesis, which ranges from pages 37 to 39.

3.1. Materials

All chemical reagents used in the treatments and characterizations were analytical grade purchased from Merck[1] (Germany), Panreac[2] (Spain), Megazyme[3] (Ireland), Sigma–Aldrich[4] (USA), EPSA[5] (Valencia, Spain). Reagents used during this Thesis were α–amylase[4] (Type VI–B, EC 3.2.1.1) from porcine pancreatic (8 U/mg), chlorohydric acid[1], corn starch[5], deuterated dimethyl sulfoxide (DMSO–d6), Folin–Ciocalteu reagent[1], glacial acetic acid[1], glucose[4], D–glucose assay kit[3], α–glucosidase[4] (Type I; EC 3.2.1.20) from Saccharomyces cerevisiae (11 U/mg), barium chloride[4], D(+)–guluronic acid[4], D(+)–maltose[2], lithium chloride[4], magnesium chloride[4], Magnesium nitrate[4], methanol[1], phenol[1], phloroglucinol[4], potassium chloride[4], potassium hydroxide[2], resorcinol[4], rice starch[4], sodium acetate[4], sodium alginate (CAS no: 9005–38–3), sodium azide[4], sodium carbonate[2], sodium chloride[4], sodium dihydrogen phosphate[2], sodium hydroxide[4], sodium phosphate[4], sodium tetraborate[4], sulfamic acid[2], sulfuric acid[2], and wheat starch[5].

3.2. Extraction and determination of polyphenols

3.2.1. Extraction of polyphenols

The extraction of polyphenols (*PP*) was performed applying experimental conditions previously optimised in our research group (Gisbert *et al.*, 2021). First, the *Ascophyllum nodosum* seaweed powder is brought into contact with water employing a liquid/solid ratio of 20 during 15 min at room temperature under stirring

(700 rpm). Then, the mixture was centrifuged (8000×*g*, 10 min), and the liquid phase was filtered (2–4 μm of pore), thus obtaining an extract rich in polyphenols.

3.2.2. Determination of the concentration of total polyphenols in the extract of Ascophyllum nodosum seaweed

The quantity of polyphenols presents in the extract obtained from the previous extraction is determined using a common technique known as total polyphenol content (*TPC*). The *TPC* was quantified through calibration against phloroglucinol, following the protocol established by Singleton & Rossi (1965). This method is predicated on the reaction of the Folin-Ciocalteu reagent with hydroxyl groups, with absorbance measured spectrophotometrically at a wavelength of 765 nm. In the procedure, 0.5 mL of aqueous seaweed extract was combined with 2.5 mL of a 10% (v/v) Folin-Ciocalteu reagent solution and 2 mL of a 7.5% (w/w) sodium carbonate solution. *TPC* values were calculated as grams of phloroglucinol equivalents per liter (g*PE*/L), using the calibration curve $C = 135.06\ Abs - 17.35$, where *C* (mg *PE*/L) is de concentration and *Abs* the absorbance (Figure 3.1). For the blank control, seaweed extracts were substituted with double-distilled water. The mixtures were incubated at 40°C for 15 minutes under complete darkness (Figure 3.2).

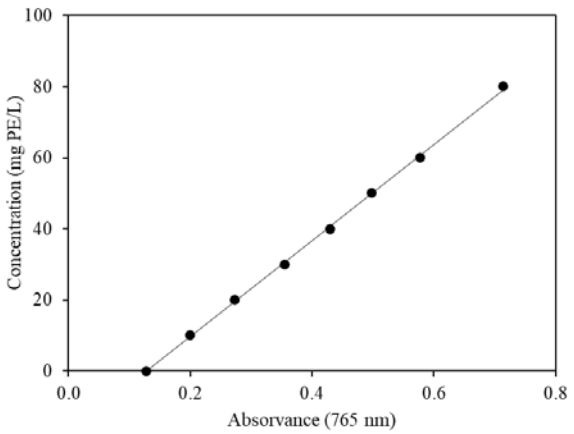

Figure 3.1. TPC calibration curve.

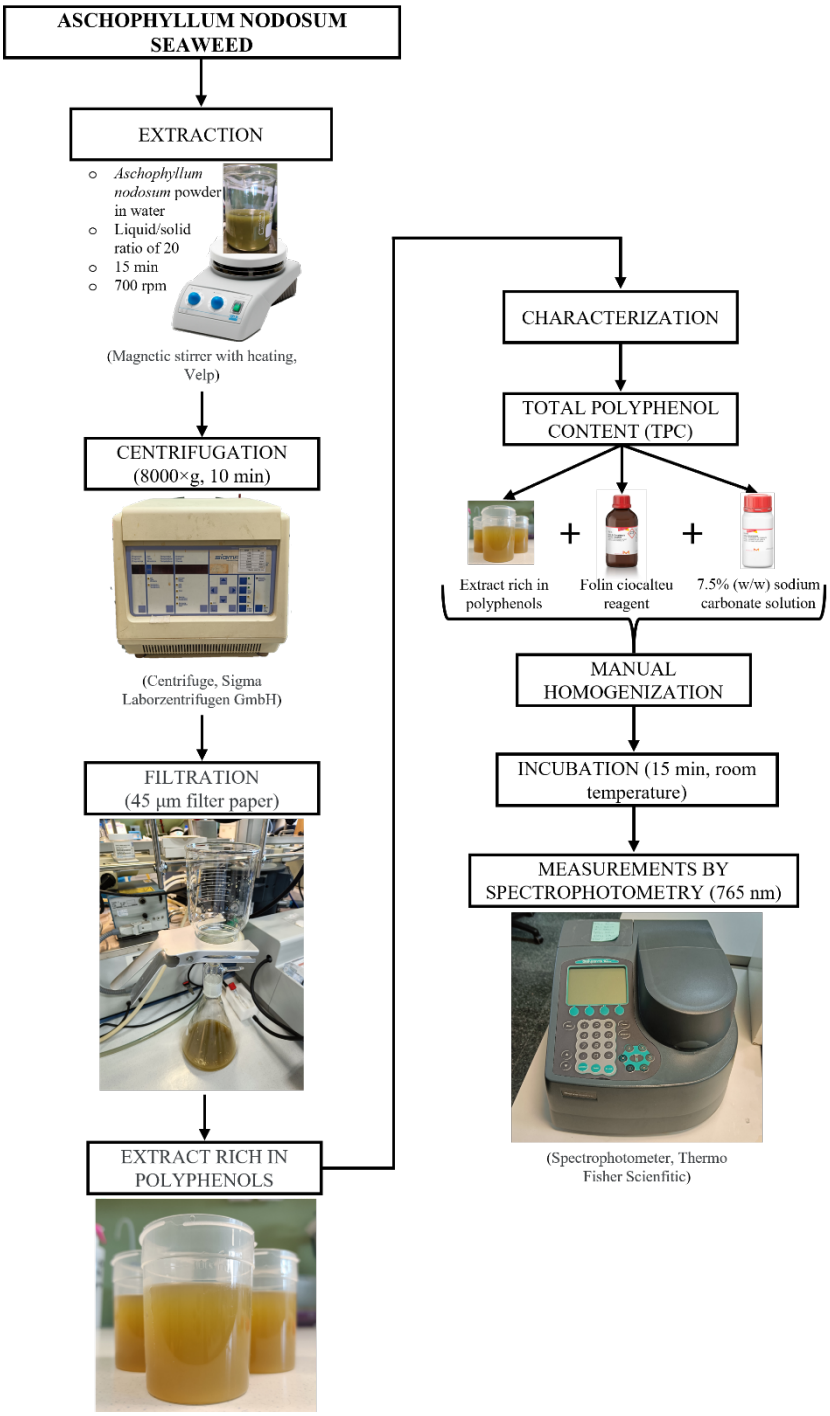

Figure 3.2. Scheme of extraction and characterization of the polyphenols.

3.3. Characterization of alginates and hydroxypropyl methylcellulose (HPMC)

3.3.1. Obtaining alginates

The alginates were obtained in the laboratory by the method followed by Chee *et al.* (2011), who applied a drying step to the pellet obtained at the end of several washing steps. The pellets were air-dried in a convective drier at constant relative humidity (30%) and air velocity (2 m/s) at two different temperatures: 50°C (*50D*) and 90°C (*90D*) for 9.5 and 3 hours, respectively. In all cases, the final moisture content was 10.8 ± 0.4% (dry basis). The dried pellets were stored at room temperature until use for sodium alginate extraction. An additional sample, statically dried over a flat surface and at ambient conditions and not subjected to convective drying into a dryer (*ND*: "not dried by forced convection"), was employed to extract alginates from ultrasound-assisted extraction (*UAE*) wet residue. This *ND* sample was immediately subjected to alginate extraction without additional storage time. Commercial alginate from Sigma Aldrich (*S*) was used as a reference to compare the results with alginates obtained in the laboratory (Montes *et al.*, 2021).

3.3.2. Nuclear magnetic resonance of alginates

Hydrogen nuclear magnetic resonance (^{1}H–NMR) of alginate samples was performed by mixing dried alginates with D_2O. ^{1}H–NMR spectroscopy was used to determine the composition and distribution of mannuronic block (*M*) and guluronic block (*G*) in monads (F_M and F_G), dyads (F_{GG}, F_{MM}, F_{MG}, F_{GM}) and triads (F_{GGG}, F_{MGM}, F_{GGM}), *M*/*G* ratio and mean block length (N_G>1) of sodium alginate samples were also calculated. The monads, dyads, triads, *M/G* ratio and N_G>1 values were evaluated following the equations of ASTM, 2012 (Eqs. (3.1) to (3.16)) where *A*, *B1*, *B2*, *B3*, *B4* and *C* values are peak area values obtained from each spectrum following the schematic representation in Figure 3.3.

$$G = 0.5\left(A + C + 0.5\,(B1 + B2 + B3)\right) \tag{3.1}$$

$$M = B4 + 0.5\,(B1 + B2 + B3) \tag{3.2}$$

$$GG = 0.5\left(A + C - 0.5\,(B1 + B2 + B3)\right) \tag{3.3}$$

$$MG = GM = 0.5\,(B1 + B2 + B3) \tag{3.4}$$

$$MM = B4 \tag{3.5}$$

$$GGM = MGG = (B1)\,0.5\,(B1 + B2 + B3)/(B1 + B2) \tag{3.6}$$

$$MGM = (B2)\,0.5\,(B1 + B2 + B3)/(B1 + B2) \tag{3.7}$$

$$GGG = GG - GGM \tag{3.8}$$

$$F_G = \frac{G}{(M + G)} \tag{3.9}$$

$$F_M = \frac{M}{(M + G)} \tag{3.10}$$

$$F_{GGG} = \frac{GGG}{(M + G)} \tag{3.11}$$

$$F_{MGM} = \frac{MGM}{(M + G)} \tag{3.12}$$

$$F_{GGM} = F_{MGG} = \frac{GGM}{(M + G)} \tag{3.13}$$

$$N_G = \frac{F_G}{F_{GM}} \tag{3.14}$$

$$N_{G>1} = \frac{(F_G - F_{MGM})}{F_{GGM}} \tag{3.15}$$

$$N_M = \frac{F_M}{F_{MG}} \tag{3.16}$$

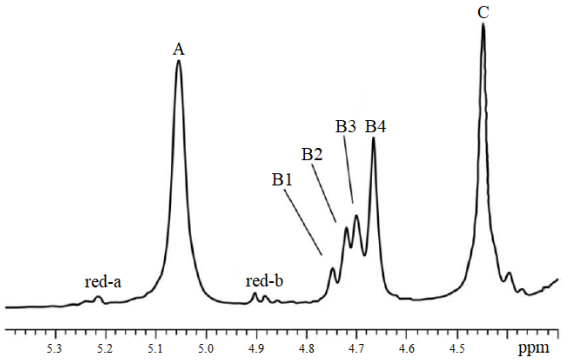

Figure 3.3. Average ^{1}H–NMR spectrum shape of alginate used for quantitative analysis.

3.3.3. Determination of water desorption isotherms of alginates

A gravimetric technique was carried out to determine the equilibrium moisture content of alginate samples. First, samples were hydrated for 3 weeks until constant weight. Then, several jars were prepared with different saturated salt solutions to obtain atmospheres with constant water activity. The salt solutions used were LiCl, $MgCl_2$, $Mg(NO_3)_2$, NaCl, KCl, and $BaCl_2$ which were prepared according to Moreira *et al.* (2008). The samples (0.5 g), previously weighted, were placed in glass jars and introduced in the flasks at three temperatures: 20, 37 and 50ºC (± 0.1ºC). The equilibrium moisture content (X) was measured for all samples and the water sorption isotherms curves were plotted as X versus a_w (water activity). More information is available in Publication 2.

The experimental results of sorption isotherms were fitted by Halsey model, Eq. (3.17):

$$X = \left(\frac{-A}{Tln(a_w)}\right)^{\frac{1}{r}} \tag{3.17}$$

where X is the equilibrium moisture content (kg water/kg dry solid, d. b.), a_w is the water activity, T (K) is the absolute temperature, and A and r are the fitting parameters of Halsey model.

Also, the isosteric heat of sorption, Q_{st} (kJ/mol), (or differential enthalpy) is an indicator of the state of water absorbed by the solid material and is defined by Eq. (3.18):

$$Q_{st} = q_{st} + H_L \tag{3.18}$$

where q_{st} (kJ/mol) is the net isosteric heat of sorption and H_L (kJ/mol) is the heat of vaporization of water at the sorption temperature. Using the Clausius-Clapeyron relationship, q_{st} at constant X can be evaluated from the experimental data by Eq. (3.19):

$$q_{st} = -R\left[\frac{d\ln a_w}{d(1/T)}\right]_X \tag{3.19}$$

The differential entropy, S_d (kJ/mol K), of water adsorption can be calculated from Gibbs-Helmholtz equation and substituting the Gibbs energy by its definition, a linear equation, Eq. (3.20), involving Q_{st}, S_d and a_w is obtained:

$$\ln(a_w)|_X = \frac{Q_{st}}{RT} - \frac{S_d}{R} \tag{3.20}$$

where the S_d value can be calculated from the intercept (S_d/R).

The net integral enthalpy q_{eq}, (kJ/mol) must be evaluated at constant spreading pressure, according to Eq. (3.21):

$$q_{eq} = -R\left[\frac{d\ln(a_w)}{d(1/T)}\right]_{\emptyset} \tag{3.21}$$

The spreading pressure represents the surface excess free energy and provides an indication of the increase in surface tension of bare sorption sites due to adsorbed molecules (Fasina *et al.*, 1999). This property cannot be experimentally measured but can be estimated by Eq. (3.22).

$$\emptyset = \frac{K_B T}{A_m} a^{1/r}\left[\frac{1}{\left(\frac{1}{r}-1\right)\left(-ln(a_w)\right)^{\frac{1}{r}-1}}\right]_{0.05}^{a_w} \tag{3.22}$$

where K_B is the Boltzmann's constant (1.38×10^{-23} J/K), T is the absolute temperature (K), A_m represents the area of a water molecule (1.06×10^{-19} m^2), a is A/T.

Finally, the net integral entropy (S_{eq}, kJ/mol K) is calculated by Eq. (3.23):

$$S_{eq} = \frac{-q_{eq}}{T} - R\ln(a_w) \tag{3.23}$$

where a_w is obtained at constant $\emptyset$ at different T.

3.3.4. Water retention capacity (WRC) of corn starch, alginates and HPMC

First, the moisture content of all the materials used was calculated. For this, a sample quantity between 0.5 and 1.0 g was weighed and dried at 70ºC and under vacuum in a vacuum oven (Thermo Fisher Scientific) until constant weight. Then, the wet weight and dry weight were used to calculate both the dry weight and wet weight moisture content. In addition, the amylose/amylopectin ratio for starch was determined. The amylose/amylopectin ratio was determined following the colorimetric procedure established in the literature (McGrance *et al.* 1998).

Corn starch, alginate-corn starch mixtures and HPMC-corn starch mixtures were characterized by means of water retention capacity (*WRC*). In this case, the *WRC* of alginates and HPMC alone could not be carried out without starch, as a gel was formed. Therefore, the decision was made to use mixtures of starch with alginate and HPMC. The concentrations used for both the alginate and HPMC tests, as well as the specific details of each, are included in Puplications 3 and 4 of this Thesis, respectively. *WRC* was determined following the protocol established by Kassem *et al.* (2022). Briefly, the samples (1.5 g) were weighed and directly added to centrifuge tubes containing 15 mL of distilled water or alginate solutions (previously hydrated overnight). After mixtures equilibration (18 h), samples were centrifuged at 3000 x g (7000 rpm in a 11192 rotor, Model 2-15, Sigma, Germany) at room temperature (22 to 25ºC) for 20 min. The supernatant was decanted, and fresh residue was weighed. Then, samples were dried up to constant weight (dry residue) at 70ºC under vacuum (< 10 kPa). A schematic of this protocol is shown in Figure 3.4. The *WRC* (kg kg-1) was calculated by Eq. (3.24). The equations show how the *WRC* is calculated for alginate, but it is the same for the *WRC* of HPMC.

$$WRC = \frac{Fresh\ residue\ weight - Dry\ residue\ weight}{Dry\ residue\ weight} \qquad (3.24)$$

WRC of alginate-corn starch mixtures was employed to evaluate the *WRC* of alginates, WRC_{SA}, by means of the Eq. (3.25):

$$WRC_{SA} = \frac{WRC_{mixture} - WRC_{CS}\left(1 - \frac{w_{dSA}\,100}{w_{dCS}}\right)}{\frac{w_{dSA}\,100}{w_{dCS}}} \quad (3.25)$$

where WRC_{CS} is the water retention capacity of corn starch, w_{dSA} and w_{dCS} are the dry weights of sodium alginate and starch in the mixture, respectively.

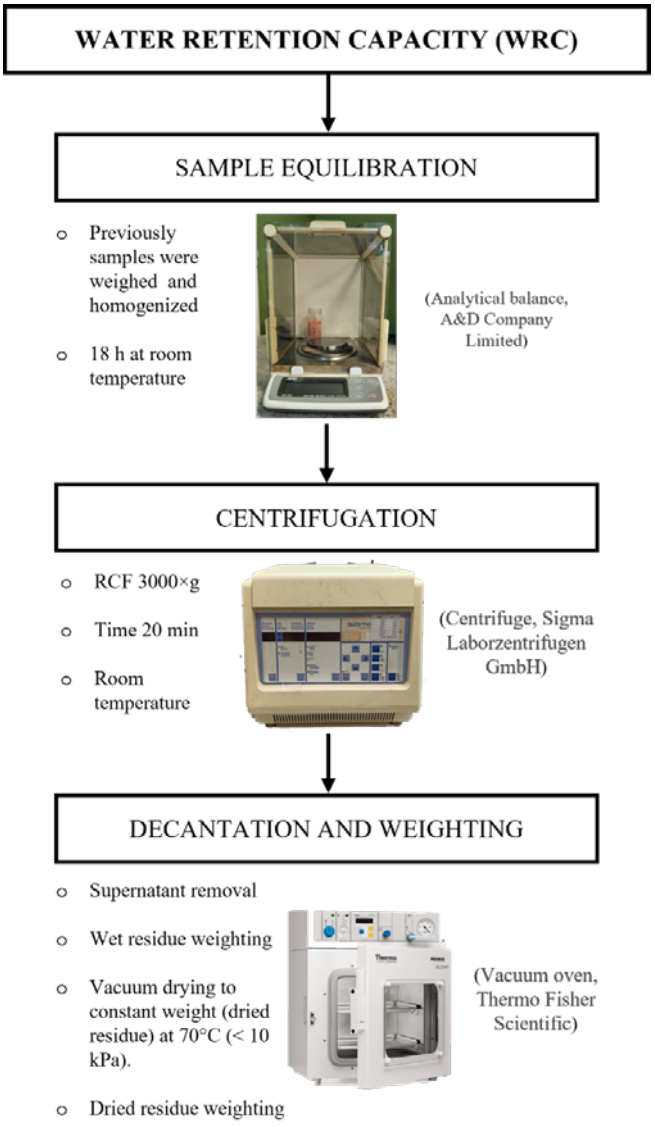

Figure 3.4. Scheme of WRC test.

3.3.5. Capillary viscosimetry of alginates and HPMC

Capillary viscometry was used to determine the average viscosimetric molecular weight of alginates and hydroxypropyl methylcellulose (HPMC). Average viscosimetric molecular weights were determined by viscosity measurements, using a Ubbelohde type viscometer (AVS 350, Schott-Geräte, GmbH, Germany) (Figure 3.5). This method consists of a long, narrow tube (capillary) through which the sample is allowed to flow under the action of a controlled pressure. All measurements (at least 5 replicates) were performed at 25ºC (±0.1ºC). Using intrinsic viscosity $[\mu]$ and the Huggins and Kraemer, and Fedors models, the average viscosimetric molecular weight can be calculated.

Figure 3.5. Ubbelohde type viscometer (AVS 350, Schott-Geräte, GmbH, Germany).

First, with the absolute viscosities of solvent (μ_0) and samples viscosity solutions (μ), the relative viscosity ($\mu_r = \mu/\mu_0$) and the specific viscosity ($\mu_{sp} = \mu_r - 1$) were calculated. Using the values of μ_r and μ_{sp}, the intrinsic viscosity $[\mu]$ was calculated by the Huggins Eq. (3.26) and Kraemer Eq. (3.27) equations:

$$\mu_{red} = [\mu] + K_H\,[\mu]^2\,C \tag{3.26}$$

$$\mu_{inh} = [\mu] + K_K\,[\mu]^2\,C \tag{3.27}$$

where $\mu_{red} = \mu_{sp}/C$, $\mu_{inh} = \ln(\mu_r)/C$ and, K_H and K_K are the Huggins and Kraemer constants, respectively.

On the other hands, the Fedors equation (Eq. 3.28) is valid for polymer solutions in the dilute and semi-dilute ranges and the application range is restricted by the μ_r values (between 1 and 100). The $[\mu]$ is calculated by:

$$\frac{1}{2\,(\mu_r^{\frac{1}{2}} - 1)} = \frac{1}{c\,[\mu]} - \frac{1}{C_{max}[\mu]} \tag{3.28}$$

where C_{max} (g/dL) is the theoretical concentration at which the interactions between polymer molecules are considered very significant.

Finaly, the values of viscosity average molecular weight, $\bar{M}_v$, were determined by the Mark-Houwink equation (Eq. 3.29):

$$[\mu] = K\,M_v^{\alpha} \tag{3.29}$$

where *[μ]* (dL/g) is the intrinsic viscosity and *K* and *α* values depended on the solute-solvent system at constant temperature.

For alginates, several solutions of extracted alginates from 0.025 up to 3% w/v were prepared. Neutral alginate solutions were obtained using an aqueous NaCl 0.1 M solution as solvent. This salt content is above threshold concentration (0.025 mol/L) to assume alginate in a random coil conformation (Dodero *et al.*, 2020b). In this case, density (*ρ*) was determined by pycnometry at 25ºC (± 0.1ºC), enabling the calculation of absolute viscosity values ($\mu = v\,\rho$). A strong linear relationship ($R^2 > 0.99$) was established between density (g/cm^3) and alginate concentration (*C*, g/dL), expressed as $\rho = 1.0038 + 0.0061\,C$ (Montes *et al.*, 2021). While for HPMC solutions were prepared with a concentration of 0.1% (w/w, d. b.) in distilled water. For each HPMC, three dilutions were performed (0.025, 0.050 and 0.075%). At these low

hydrocolloid content, density was constant and equal to density of solvent (water). For more details about HPMC essays read Publication 4.

3.3.6. Rheological characterization of alginates and HPMC

Rheological tests for alginates were performed using an Anton Paar-Physica MCR 301 Rheometer (Graz, Austria) and a solvent trap kit to minimize water evaporation during the tests. Couette geometry (CC24-SN40990) with a 1 mm gap was employed. Flow curves were performed over a wide range of shear rates, from 0.1 to 1000 s^{-1} (upwards) and from 1000 to 0.1 s^{-1} (downwards) to ascertain the presence of thixotropic behaviour at 25ºC. Three concentration values were used for each tested alginate corresponding to 2C^*, 4C^* and 6C^*, where C^* is the overlap concentration from dilute to semi-dilute regime (Montes *et al.*, 2021). On the other hand, only the concentration of 6C^* was used to determine the viscoelastic characteristics of solutions by small amplitude oscillatory shear (*SAOS*) tests. Amplitude sweep tests were performed in the strain range from 0.1 to 10% and at constant frequency (1 Hz) and temperature (25 and 45ºC) to obtain the linear viscoelasticity range (*LVR*). Frequency sweep tests were performed in the range from 0.01 to 10 Hz at a constant strain (1%) and temperature (25 and 45ºC). This protocol was obtained from Montes *et al.*, 2021.

On the other hand, aqueous HPMC solutions (2.0% w/w) were prepared by mixing HPMC and distilled water. These mixtures were kept in agitation until completely dissolved. The rheological characterisation was performed in the rheometer using a plate-plate geometry (diameter, 50 mm). Samples (0.9 mL) were loaded between the parallel plates and compressed up to obtain a gap of 0.3 mm. The measurements were performed at different temperatures (from 25 up to 90ºC (± 0.1ºC)), controlled by a Peltier system. All samples were covered with light paraffin oil to prevent water evaporation. Tests were carried out at least in triplicate. For more details read Publication 4. A diagram of the tests performed is shown in Figure 3.6.

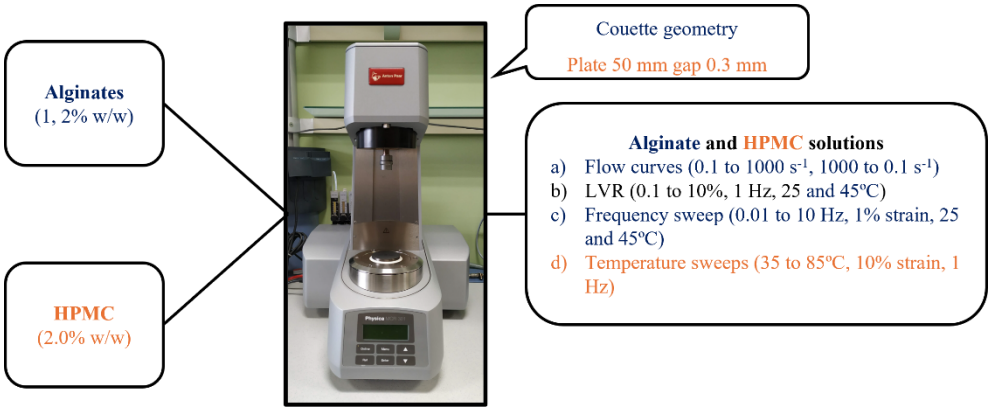

Figure 3.6. Diagram of the tests performed with the rheometer on alginate and HPMC solutions.

3.4. Starch with polyphenols, alginates and HPMC

3.4.1. Preparation of starch gels in tube

Corn starch was weighed and added to the alginate solutions which were dispersed in distilled water and hydrated overnight or polyphenols extract. These mixtures were manually shaken for 60 s to facilitate their homogenization. Then mixtures were heated at 100ºC for 20 min with gentle manual stirring every 5 min during 10 s before gel formation. The starch gels were cooled (for 20 min) up to 37ºC for later analysis. For more information about concentrations see Publication 1 for polyphenol systems or Publication 3 for alginate systems.

3.4.2. Scanning electron microscopy (SEM)

The corn starch gels with alginate were prepared according to the previous section "*3.4.1. Preparation of starch gels in tube*". Alginate-corn starch gels were freeze-dried and observed using the scanning electron microscopy (S-4800, Hitachi, Ibaraki, Japan). Gels were covered with gold by vacuum evaporator (JEE 400; JEOL, Tokyo, Japan) for 5 min. The images were captured using 10 kV of acceleration voltage and 180× magnification.

3.4.3. Polyphenols adsorption on corn native starch and gels

To study the effect of polyphenols on starch gels, studies of polyphenol adsorption were carried out both on native corn starch and on corn starch gel. The corn starch gels were prepared according to the previous section "*3.4.1. Preparation of starch gels in tube"*. On the other hand, the polyphenol extract used was the one obtained in section "*3.2.1. Extraction of polyphenols*" of this chapter. To start the study, from the stock polyphenols solution (2.7 ± 0.1 g/L), several dilutions were prepared to obtain different polyphenol concentrations (0.1, 0.3, 0.5, 1.0, and 2.0 g/L). A 3.0 g/L solution was needed to complete an assay, so the stock solution was slightly concentrated by evaporation of water (Concentrator plus, Eppendorf, Germany). To those solutions, native or gelled corn starch was added at two content (1.95 and 5.00% w/v) and kept stirred in an incubator (New Brunswick, Innova 40, USA) at 25ºC and 200 rpm. These concentrations were chosen to better observe starch-polyphenol interactions. Corn starch gels were prepared at 1.95 and 5.00% w/w. The dispersions were heated at 100ºC for 20 min with gentle stirring during the first 60 s and then every 5 min for 10 s. The starch gels were cooled (20 min) up to 37ºC for later analyses. Polyphenols adsorption kinetics were monitored for 3 h following the total polyphenol content values (*TPC*). This technique is explained in section "3.2.2. Characterization of polyphenols" of this chapter. Equilibrium between solid and liquid phases was achieved when *TPC* was invariant between measures elapsed 30 min. Adsorbed polyphenols on corns starch were evaluated by mass balance. Tests were carried out at least in duplicate. Experimental equilibrium data were fitted by the Langmuir, Eq. (3.30), and the Henry, Eq. (3.31), models.

$$q = q_{max} \frac{[PP]_e \, b}{1 + b \, [PP]_e} \tag{3.30}$$

$$q = K \, [PP]_e \tag{3.31}$$

where q is the amount adsorbed at equilibrium (g polyphenols/g corn starch, g_{PP}/g_{CS}), $[PP]_e$ (g_{PP}/L) is the concentration at equilibrium, q_{max} is the maximum quantity of polyphenols adsorbed and b (L/g_{PP}) and K (L/g_{CS}) are parameters of the models.

3.4.4. Rheological characterization of polyphenols, alginates and HPMC with corn starch

Gel rheology allows the evaluation of aspects such as the hardness or gelatinization of starches, characteristics and properties that help determine the texture of the final product. In this case, the tests were carried out on the same rheometer that was used previously, but for each test different geometries and protocols were used depending on what was to be studied. A diagram of the tests performed is shown in Figure 3.7.

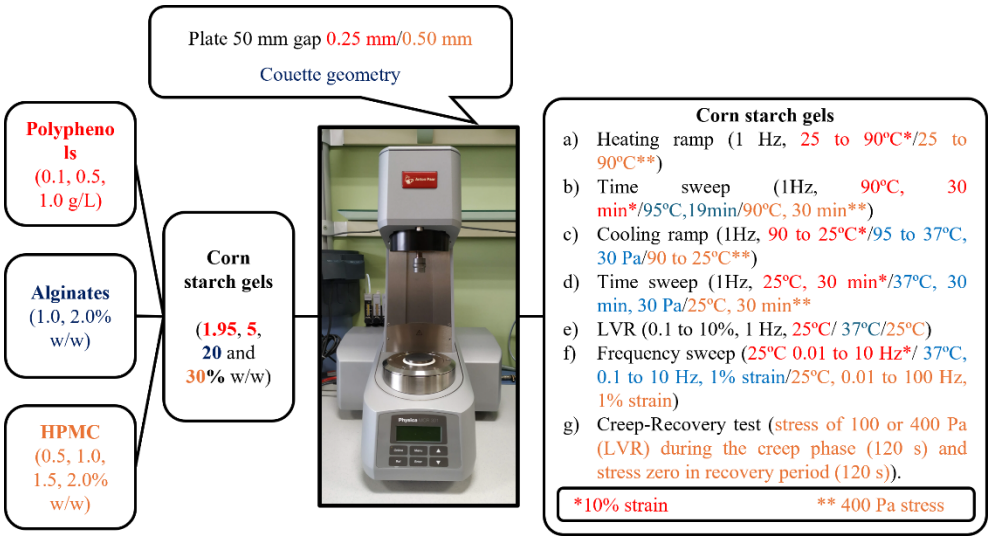

Figure 3.7. Diagram of the tests carried out with the rheometer on starch systems with polyphenols, alginate and HPMC.

3.4.4.1. Rheological characterization of starch with polyphenols

The rheological characterization was performed with plate-plate geometry (50 mm) and a gap of 0.25 mm. Corn starch (*CS*) gels with polyphenols (*PP*) were prepared at 1.95 and 5.00% w/w. For 1.95% w/w samples, the nominal *PP/CS* ratios were: 0.0, 0.5, 2.5 and 5.0; while for gels at 5.00% w/w these ratios were: 0.0, 0.2, 0.9 and 1.9, adding different amounts of PP solutions of 0.0, 0.1, 0.5 and 1.0 g/L.

More specific information on concentrations can be seen in Publication 1. Samples were covered with paraffin oil to prevent water evaporation. A pre-shearing test was made during 75 min at 100 s^{-1} to ensure the complete adsorption of polyphenols on starch. Then, a heating ramp from 25 to 90ºC (at 4ºC/min) was carried out followed by a time sweep at 90ºC (30 min), a cooling ramp from 90 to 25ºC (at 3ºC/min) and a time sweep at 25ºC (30 min) at a constant strain of 10% and a frequency of 1 Hz (inside linear viscoelasticity range, *LVR*). Finally, a frequency sweep from 0.01 to 10 Hz was made at 10% of strain and 25ºC. Tests were carried out at least in triplicate.

3.4.4.2. Rheological characterization of starch with alginate

The rheological characterisation was performed using a starch pasting cell (ST24-2D/2V/2V-30) (gap = 2.460 mm, bob radius = 12.000 mm) with a solvent trap kit to minimize water evaporation during tests. Corn starch (1:4 w/w or 20% w/w) and corn alginate-starch mixtures (0, 1 and 2% w/w, starch basis) were dispersed in distilled water and introduced into the rheometer cuvette at 95ºC. Firstly, a pre-shear of 100 s^{-1} was made for 1 min to homogenize the sample at 95ºC. Secondly, a time sweep was carried out at 95ºC for 19 min and then, a cooling ramp was performed from 95 to 37ºC at 3ºC/min at 30 Pa and 1 Hz in both stages. Then, strain sweep tests (0.1–10%) of gels at 1 Hz and 37ºC to obtain the linear viscoelasticity range (*LVR*) were performed. Finally, a second time sweep (30 Pa, 1 Hz) was carried out at 37ºC for 30 min to observe the maturation of the gel and a frequency sweep was made from 0.1 to 10 Hz at 1% strain and 37ºC. More specific information about protocol can be seen in Publication 3. Complex modulus, G^* (Pa), values evaluated from storage modulus (G') and loss modulus (G'') data obtained through angular frequency (ω, Hz) sweep tests, were correlated to the following power law (Bruno *et al.*, 2021), Eq. (3.32):

$$G^* = \sqrt{(G')^2 + (G'')^2} = A\, w^{1/z} \tag{3.32}$$

where z (-) is the coordination number and measures number of rheological units with one another in the 3-D structure and A (G^* at 1 Hz) is called the proportional coefficient and evaluates the strength of the interaction between units.

3.4.4.3. Rheological characterization of starch with HPMC

The rheological characterisation was performed using a plate-plate geometry (diameter, 50 mm). Dispersions (1.2 mL) were loaded between the parallel plates and compressed up to obtain a gap of 0.5 mm. These dispersions with constant solids content (30% w/w) were prepared by mixing corn starch, and HPMC (by substitution) at different concentrations (0, 0.5, 1.0, 1.5 and 2.0% w/w), and distilled water. More specific information on sample preparation can be found in Publication 4. On this occasion, oscillatory tests and creep-recovery tests were carried out.

First, the oscillatory test consists of determining the linear viscoelastic region (*LVR*) with a strain sweep test from 0.1 to 10% at a constant frequency (1 Hz). Secondly, dispersions were subjected to the next procedure consisting in five steps: (i) temperature sweep (25 to 90ºC at 1ºC min^{-1}, 1 Hz, 100 Pa), to accomplish starch gelatinization; (ii) time sweep (30 min, 1 Hz, 400 Pa, 90ºC); (iii) temperature sweep (90 to 25ºC at 1ºC min-1, 1 Hz, 400 Pa); (iv) time sweep (30 min, 1 Hz, 400 Pa, 25ºC); and finally, (v) frequency sweep (0.01 to 100 Hz, 1% of strain, 25ºC) inside *LVR* of formed gels (preliminary tests were performed to determine the corresponding *LVR*). For more information see Publication 4.

On the other hand, creep-recovery test at 25ºC was performed at a constant stress, σ (Pa), of 100 or 400 Pa within the *LVR* during creep phase. Before the measurements, the gels were rested for 15 min in the rheometer to allow the sample equilibrium. During creep period, the selected constant stress was applied for 120 s and the recovery (stress zero) period lasted 120 s. For more specific information see Publication 4.

3.4.5. Starch digestion

Starch digestion was measured using two different methods: the conventional biochemical method of in vitro digestion and the rheometer, determining the drop in viscosity over time. A diagram of the tests performed is shown in Figure 3.8.

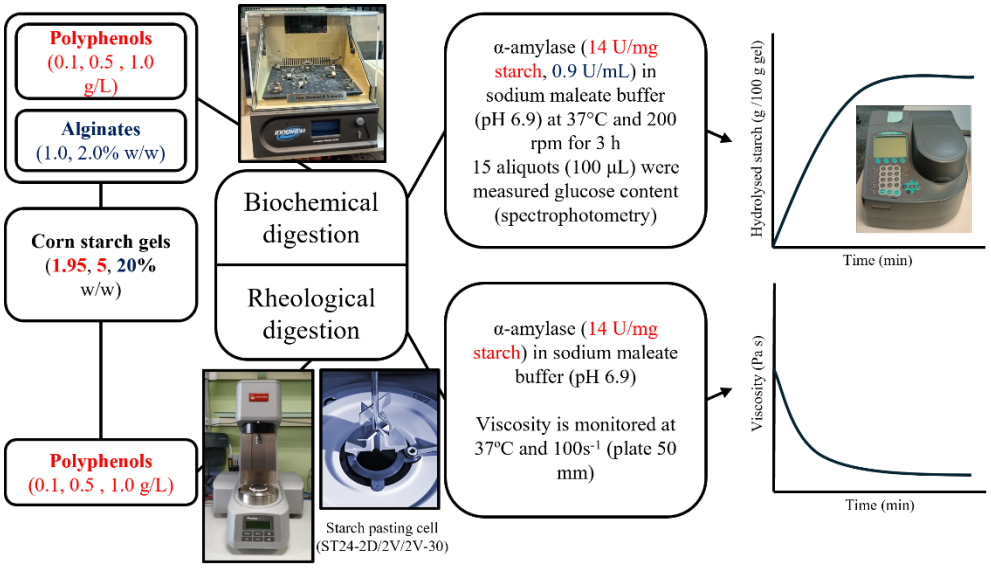

Figure 3.8. Diagram of the tests performed in the in vitro digestion of different starch systems with biopolymers by the biochemical method and in the rheometer.

3.4.5.1. Conventional biochemical method of *in vitro* digestion starch

In vitro digestibility was analysed following the method described by Santamaria *et al.*, (2021) with minor modifications. A quantity of 200 mg of gel was suspended in 4 mL of 0.1 M sodium maleate buffer (pH 6.9) containing porcine pancreatic α-amylase (0.9 U/mL) and incubated in a shaker incubator SKI 4 (ARGO Lab, Carpi, Italy) at 37°C with constant stirring (200 rpm) for 3 h. During incubation, aliquots of 100 µL were taken and mixed with 100 µL cold ethanol (96%) to stop the enzymatic hydrolysis. The samples were centrifuged for 5 min (10,000×g, 4°C) and then, the pellet was suspended in 100 µL of ethanol (50%) and centrifuged again as described before. The supernatants were combined and storage at 4°C. A 100 µL sample of the supernatant was diluted with 885 µL of 0.1 M sodium acetate buffer (pH 4.5) and incubated with 15 µL amyloglucosidase (143 U/mL) at 50°C for 30 min in a shaking incubator, before quantifying glucose content.

Glucose was determined using a glucose oxidase–peroxidase (*GOPOD*) kit (Megazyme, Dublin, Ireland). Starch fractions based on the hydrolysis rate were calculated as glucose (mg)×0.9 and expressed as glucose content (g/100 g gel) using the method of Englyst *et al.*, (1992). The rapidly digestible starch (*RDS*) was determined in the fraction corresponding to the first 20 min of digestion, while the slowly digestible starch (*SDS*) corresponded to the fraction from 20 to 120 min. Tests were carried out at least in duplicate. The *in vitro* digestion kinetics were fitted by first order equation, Eq. (3.33), (Goñi *et al.*, 1997):

$$C = C_{\infty}(1 - e^{-kt}) \tag{3.33}$$

where C is the concentration at t digestion time, C_{∞} the maximum hydrolysis, and k the kinetic constant.

3.4.5.2. Rheometer determining the viscosity drop with time for studying the digestion starch

The rheological experiments to determine the starch digestion in starch systems were carried out using a starch pasting cell (ST24-2D/2V/2V-30) (Figure 3.9) as described previously (Santamaria *et al.*, 2023a). A solvent trap kit was used to minimize water evaporation. First, a pre-shear at 100 rad/s (960 rpm), 50°C for 10 s was applied to achieve sample homogenization, followed by a holding time for 1 min at 50°C and 18 rad/s (160 rpm). This shear rate was kept for the rest of the assay. A temperature sweep was carried out from 50 to 95°C at 10°C/min to form the gel. High temperature of 95°C was maintained for 2.5 min. Then, a temperature sweep was made from 95 to 37°C at 5°C/min to achieve the required temperature to make the enzymatic hydrolysis, followed by holding at 37 °C for 36 s for adding the α-amylase solution (900 U/mL solution). Apparent viscosity, μ, at 37ºC was monitored at shear rate of 10 s^{-1} (~physiological shear rates in the small intestinal (Lentle *et al.*, 2007)). Tests were carried out at least in triplicate.

For the starch digestion tests with polyphenols, the protocol used was the previous one but with some minor modifications. A first step at 200 min^{-1} during 30 min at 37ºC was made for the sample homogenization and to ensure the polyphenols

adsorption on starch. Afterwards, the rest of the protocol is as mentioned above with a minor modification. A stirring period of 10 s at 100 s^{-1} was performed to facilitate the enzyme-starch contact. For more information on this protocol see Publication 1.

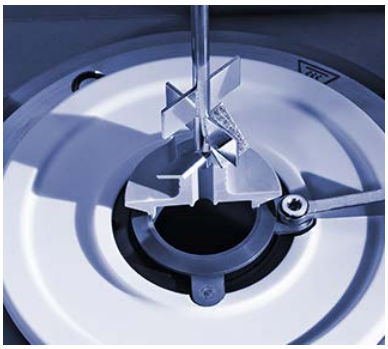

Figure 3.9. Starch pasting cell (ST24-2D/2V/2V-30).

3.4.6. Bread characterization

Bread characterizations were determined as previously reported Matos & Rosell (2013) with moisture content, crumb image analysis, crumb texture profile analysis (*TPA*) and color.

3.4.6.1. Moisture content

The moisture content of gluten-free bread samples was determined according to the International Cereal Chemistry method (ICC 110/1, 1994). The moisture content was expressed as g water/100 g bread crumb. Four replicates were analyzed for each sample.

3.4.6.2. The crumb image analysis

The crumb image analysis was carried out as reported (Espinosa-Ramírez *et al.*, 2018). Bread slices were scanned using a flatbed scanner (Epson V600 Photo, Epson, Japan) in the RGB (Red-Green-Blue) standard format with 1,200 dpi resolution. Image analysis of bread slices was conducted using Fiji Image J software (Schindelin *et al.*, 2012). For image segmentation and determination of crumb grain characteristics, image contrast was improved and then the algorithm “Otsu” was

applied. The crumb grain measurements included: cell density (cell/cm^2), mean cell area (mm^2), surface porosity (total cell area/ total slice area in percentage), and mean cell shape using the circularity factor (0-circle to 1-rectangle). Four slices of bread obtained in two different batches (four breads/batch) were analyzed for each sample.

3.4.6.3. The crumb texture profile analysis (*TPA*)

The crumb texture profile analysis (*TPA*) was carried out using the TA.XT-Plus Texture Analyses (Stable Micro Systems Ltd., Godalming, UK) equipped with a 5 kg load cell and a 25-mm cylindrical probe (Figure 3.10). Slices were double compressed to 50% of their original height at a crosshead speed of 1 mm/s and 30 s gap between compressions, providing insight into how samples behave when chewed (Rosell *et al.*, 2009). The parameters recorded were hardness, cohesiveness, springiness, chewiness, and resilience. All textural parameters were measured at 0 and 48 h, and then the hardening rate was calculated, as the hardness increased regarding the hardness of the fresh bread. The data acquired was the average value of eight replicates.

Figure 3.10. Texture Analyses TA.XT-Plus (Stable Micro Systems Ltd., Godalming, UK).

3.4.6.4. Crumb color

Crumb color was measured using the CIE-*L*a*b** uniform color space using a Minolta colorimeter (Chromameter CR-400/410, Konica Minolta, Tokyo, Japan) (Figure 3.11) after standardization with a white calibration plate. Color parameters: *L** (lightness), *a** (hue on a green to red, *b** (hue on a blue to yellow and ΔE which is used to evaluate perceived color differences between control and samples. Measurements were performed on three slices from each run.

Figure 3.11. Chromameter CR-400/410 (Konica Minolta, Tokyo, Japan).

4.PUBLICATIONS

PUBLICATION 1

Effect of polyphenols from *Ascophyllum nodosum* seaweeds on the rheology and digestion of corn starch gels and gluten-free bread features

Heliyon, 10, e27469 (2024)

Heliyon 10 (2024) e27469

Contents lists available at ScienceDirect

Heliyon

journal homepage: www.cell.com/heliyon

Research article

Effect of polyphenols from *Ascophyllum nodosum* seaweeds on the rheology and digestion of corn starch gels and gluten-free bread features

Leticia Montes [a], Maria Santamaria [b], Raquel Garzon [b], Cristina M. Rosell [b,c], Ramón Moreira [a,*]

[a] Department of Chemical Engineering, Universidade de Santiago de Compostela, rúa Lope Gómez de Marzoa, s/n. 15782, Santiago de Compostela, Spain
[b] Institute of Agrochemistry and Food Technology (IATA-CSIC), C/Agustin Escardino, 7, 46980, Paterna, Spain
[c] Department of Food and Human Nutritional Sciences. University of Manitoba, Winnipeg, Canada

ARTICLE INFO

Keywords:
Corn starch
In vitro digestion
Polyphenols
Rheology
Viscosity

ABSTRACT

The main objective of this work is to study the effect of polyphenols, from the brown seaweed *Ascophyllum nodosum*, on the structure and digestion behaviour of gels at two corn starch concentrations (1.95 and 5.00% w/w) as well as the structure, color and texture features of crumbs from gluten-free breads. Adsorption isotherms of polyphenols on native and gelled starches were carried out and modelled by means of Langmuir and Henry models, respectively. The formation and characteristics of tested gels were rheologically monitored by means of heating ramp, time sweep at high temperature, cooling ramp and frequency sweep at 25 °C. Elastic modulus values decreased with the presence of polyphenols. Additionally, the polyphenols significantly decreased the digestion rate, measured by both chemical and rheological procedures, and the final concentration of digested starch. Finally, the presence of polyphenols in breads increased the hardness and chewiness values and decreased the cohesiveness and resilience values as well as the crumb hardening during storage.

1. Introduction

Gluten-free products are in high demand either due to related pathologies or consumers' choices [1]. However, a high relationship between type 1 diabetes and celiac disease exists because gluten-free diet is richer in carbohydrates and poorer in protein, fiber, minerals, and vitamins [2]. Because of that, there is a growing interest in modulating the starch digestion, particularly in gluten-free starch-based foods.

Polyphenols are secondary metabolites with many reported benefits associated to their antioxidant power, offering protection against development of cancers, cardiovascular diseases, and diabetes among others [3]. Polyphenols have been targeted as great inhibitors of the starch hydrolysis [4]. Other authors observed that corn starch gels enriched with different polyphenols exhibited a notable influence on their digestibility, which was linked to alterations in pH and the quantity of hydroxyl groups [5]. Whether their

* Corresponding author.
E-mail addresses: leticia.montes.martinez@usc.es (L. Montes), masanar@iata.csic.es (M. Santamaria), r.garzon@iata.csic.es (R. Garzon), crosell@iata.csic.es (C.M. Rosell), ramon.moreira@usc.es (R. Moreira).

https://doi.org/10.1016/j.heliyon.2024.e27469
Received 27 December 2023; Received in revised form 19 February 2024; Accepted 29 February 2024
Available online 8 March 2024

effect is due to phenolic compounds interaction with starch [6] or a shared action on starch and enzyme [7,8] is still controversial. Therefore, studies are required to understand the polyphenol action as inhibitors of starch digestibility.

Whatever is the hindering mechanism of the polyphenols, their application in food processing requires to identify any technological impact. It has been reported that polyphenols can generate hydrogen bonds with starch, affecting hydration, gelatinization, and retrogradation properties [9]. In the case of rice starch, the incorporation of tea polyphenols decreases the rheological moduli (storage (G') and loss (G'')), and gel strength, which has been related to the polyphenols interference with amylose crystallization [10]. Even gels can shift from solid-like to liquid-like viscoelastic behavior at high tea polyphenols concentration. Impact on rice starch has been attributed to ferulic acid and gallic acid, that decrease gelatinization temperatures and enthalpies due to hydrogen bonds or van der Waals forces interaction [11]. Likewise, very limited information exists on their impact into final products. The replacement of starch with whole grain red sorghum flour (with high content in phenolics) to improve gluten-free bread was also proposed [12]. A substitution of 30–40% (w/w) of sorghum flour led to increased specific volume and reduced density and texture, which authors associated to an increase in protein. Other authors investigated the incorporation of polyphenol-rich kiwi extract into gluten-free bread formulations and found that bread enriched with the extract was deemed acceptable by a sensory panel, exhibiting a softer and smoother texture compared to regular gluten-free bread, without going into a detailed analysis of the potential effects on the bread's properties [13].

Literature has mainly reported the benefit of phenolic compounds from terrestrial nature, but less information is available about marine polyphenols [14]. It is known that polyphenols from *Ascophyllum nodosum* seaweeds also have many health benefits due to their high antioxidant capacity, offering protection against development diabetes [3], but no information has been provided about their impact on rheology and bread quality. Therefore, the aim of this work is to study the interaction of seaweeds polyphenols with corn starch and resulting gluten-free breads. For this purpose, the adsorption of polyphenols in native and gelled corn starches were studied, as well as the rheology of starch gels with different polyphenol/starch ratios. Low starch concentrations were used to avoid the use high amounts of adsorbate and to observe the polyphenols-starch interactions more easily. In addition, the digestion of these starch gels will be monitored chemically and rheologically. Finally, the polyphenols will be added to a simple starch system for baking and subsequent analysis of the crumb, texture, and colour of the final product. It is worth mentioning that dilutions (1:1) in the mouth, stomach, and intestine, according to the INFOGEST protocol [15], breads with 50% w/w of moisture give rise to low starch content (around 6%) gels to be digested in the intestine.

2. Materials and methods

2.1. Materials

Corn starch (CS) (moisture 11.4 ± 0.2 dry basis (% d. b.), amylose content 20.25 ± 2.4% d. b.) was purchased from EPSA (Valencia, Spain). Fresh *Ascophyllum nodosum* seaweeds from Galicia's coasts (NW of Spain) were supplied by a local company. Dry baker's yeast was provided by Lesaffre Group (Valladolid, Spain). Type VI-B α-amylase from porcine pancreas (E.C. 3.2.1.1) (14 U/mg solid) and amyloglucosidase (143 U/mL) purchased from Sigma Aldrich. The rest of ingredients for breadmaking were acquired from the local market. Solutions and standards were prepared using deionized water.

2.2. Polyphenols extraction

Ascophyllum nodosum seaweeds were air-dried at 50 °C for 180 min. Dried *A. nodosum* (10.0 ± 0.1% d.b.) was ground in an ultra-centrifugal mill and stored at 4 °C. More details about procedure can be found in a previous study [16]. The extraction of polyphenols (PP) from *A. nodosum* was performed with water as solvent employing a liquid/solid ratio of 20 during 15 min at room temperature under stirring (700 rpm). Then, the mixture was centrifuged (8000×g, 10 min), and the liquid phase was filtered (2–4 μm of pore). Total polyphenol content (TPC) of the extract (2.7 ± 0.1 g/L) was determined [17].

2.3. Polyphenols adsorption on corn native starch and gels

From the stock polyphenols solution (2.7 ± 0.1 g/L), several dilutions were prepared to obtain different PP concentrations (0.1; 0.3; 0.5; 1.0, and 2.0 g/L). A 3.0 g/L solution was needed to complete an assay, so the stock solution was slightly concentrated (Concentrator plus, Eppendorf, Germany). To those solutions, native or gelled CS was added at two content (1.95 and 5.00% w/v) and kept stirred in an incubator (New Brunswick, Innova 40, USA) at 25 °C and 200 rpm. CS gels were prepared at 1.95 and 5.00% w/w. The dispersions were heated at 100 °C for 20 min with gentle stirring during the first 60 s and then every 5 min for 10 s. The starch gels were cooled (20 min) up to 37 °C for later analyses. Polyphenols adsorption kinetics were monitored during 3 h following TPC values. Equilibrium between solid and liquid phases was achieved when TPC was invariant between measures elapsed 30 min. Adsorbed polyphenols on CS were evaluated by mass balance. Tests were carried out at least in duplicate. Experimental data were fitted by the Langmuir, Eq. (1), and the Henry, Eq. (2), models.

$$q = q_{max} \frac{[PP]_e \, b}{1 + b \, [PP]_e} \tag{1}$$

$$q = K \, [PP]_e \tag{2}$$

where q is the amount adsorbed at equilibrium (g polyphenols/g corn starch, g_{PP}/g_{CS}), $[PP]_e$ (g_{PP}/L) is the concentration at equilibrium, q_{max} is the maximum amount of polyphenols adsorbed and b (L/g_{PP}) and K (L/g_{CS}) are parameters of the models.

2.4. Rheological properties

CS gels were prepared at 1.95 and 5.00% w/w. For 1.95% w/w samples, the nominal PP/CS ratios were: 0.0, 0.5, 2.5 and 5.0; while for gels at 5.00% w/w these ratios were: 0.0, 0.2, 0.9 and 1.9, adding different amounts of PP solutions of 0.0, 0.1, 0.5 and 1.0 g/L (real values are in Table 1). The rheological characterization was performed with a stress-controlled rheometer (Anton Paar 301, Austria) with plate-plate geometry (50 mm) and a gap of 0.25 mm. Samples were covered with paraffin oil to prevent water evaporation. A pre-shearing test was made during 75 min at 100 s^{-1} to ensure the complete adsorption of polyphenols on starch. Then, a heating ramp from 25 to 90 °C (at 4 °C/min) was carried out followed by a time sweep at 90 °C (30 min), a cooling ramp from 90 to 25 °C (at 3 °C/min) and a time sweep at 25 °C (30 min) at a constant strain of 10% and a frequency of 1 Hz (inside linear viscoelasticity range, LVR). Finally, a frequency sweep from 0.01 to 10 Hz was made at 10% of strain and 25 °C. Temperature was controlled by a Peltier system (±0.01 °C). Tests were carried out at least in triplicate.

2.5. Digestion starch

Starch digestion was measured employing two different methods. With the conventional biochemical method of *in vitro* digestion and with the rheometer determining the viscosity drop with time.

In vitro digestibility was analyzed following the method previously described with minor modifications [18]. The amount of gel for each sample was weighed to maintain a constant enzyme/starch ratio of 14 U/mg starch. The enzymes used were porcine pancreatic α-amylase and amyloglucosidase. Glucose was determined using a glucose oxidase–peroxidase (GOPOD) kit (Megazyme, Dublin, Ireland). Starch fractions based on the hydrolysis rate were calculated as glucose (mg) × 0.9 and expressed as glucose content (g/100 g gel) using the method previously described [19]. The rapidly digestible starch (RDS) was determined in the fraction corresponding to the first 20 min of digestion, while the slowly digestible starch (SDS) corresponded to the fraction from 20 to 120 min. Tests were carried out at least in duplicate. The *in vitro* digestion kinetics were fitted by first order equation, Eq. (3) [20],:

$$C = C_\infty\left(1 - e^{-kt}\right) \tag{3}$$

where C is the concentration at t digestion time, C_∞ the maximum hydrolysis, and k the kinetic constant.

The rheological experiments to determine the starch digestion were carried out using a starch pasting cell (ST24-2D/2V/2V-30) as described previously [18] with some modifications. A solvent trap kit was used to minimize water evaporation. A step at 200 min^{-1} during 30 min at 37 °C was made for the sample homogenization and to ensure the polyphenols adsorption on starch. Then, a temperature sweep was carried out from 37 to 95 °C at 5 °C/min at 100 s^{-1} to gel formation. Afterward, a temperature sweep was made from 95 to 37 °C at 5 °C/min at 10 s^{-1} to achieve the required temperature for the enzymatic hydrolysis. A rest time of 36 s was needed to introduce the α-amylase. A stirring period of 10 s at 100 s^{-1} was performed to facilitate the enzyme-starch contact. Apparent viscosity, μ, at 37 °C was monitored at shear rate of 10 s^{-1} (~physiological shear rates in the small intestinal [21]). Tests were carried out at least in triplicate.

2.6. Breadmaking

Gluten-free bread formulations based on CS (100 g) contained 100% water, 2% dried yeast, 1% salt, and 1% sugar. The tested

Table 1
Experimental data of polyphenols adsorption on native and gelled corn starch: concentration of starch ($[CS]_0$), initial concentration of polyphenols ($[PP]_0$), polyphenols/starch ratio (PP_0/CS_0), equilibrium concentration of polyphenols ($[PP]_e$) and polyphenols adsorbed on starch (q) and initial polyphenols adsorbed (PP_0 adsorbed).

$[CS]_0$ (% w/w)	$[PP]_0$ (g_{PP}/L)	PP_0/CS_0 (%)	Code	$[PP]_e$ (g_{PP}/L)		q, (g_{PP}/g_{CS}) (PP_0 adsorbed, %)	
				Native starch	Gelled starch	Native starch	Gelled starch
1.95	0.09 ± 0.01	0.47 ± 0.01	1.95_0.47	0.00 ± 0.00	0.00 ± 0.00	0.005 ± 0.001 (100 ± 0.0)	0.002 ± 0.001 (100 ± 0.0)
	0.26 ± 0.02	1.33 ± 0.08	1.95_1.33	0.08 ± 0.01	0.04 ± 0.01	0.008 ± 0.001 (70.1 ± 1.8)	0.008 ± 0.001 (83.2 ± 0.4)
	0.49 ± 0.02	2.43 ± 0.09	1.95_2.43	0.25 ± 0.01	0.09 ± 0.01	0.010 ± 0.001 (49.3 ± 1.4)	0.017 ± 0.001 (81.0 ± 0.1)
	0.96 ± 0.02	4.79 ± 0.12	1.95_4.79	0.70 ± 0.01	0.23 ± 0.01	0.011 ± 0.001 (27.1 ± 2.5)	0.033 ± 0.001 (75.9 ± 1.3)
	1.95 ± 0.06	9.79 ± 0.30	1.95_9.79	1.69 ± 0.04	0.47 ± 0.01	0.012 ± 0.001 (13.8 ± 0.5)	0.070 ± 0.001 (75.5 ± 1.1)
5.00	0.09 ± 0.01	0.17 ± 0.01	5.00_0.17	0.00 ± 0.01	0.00 ± 0.00	0.001 ± 0.001 (100 ± 0.0)	0.002 ± 0.001 (100 ± 0.0)
	0.26 ± 0.01	0.49 ± 0.01	5.00_0.49	0.07 ± 0.01	0.07 ± 0.01	0.003 ± 0.001 (74.9 ± 0.8)	0.004 ± 0.001 (72.6 ± 0.1)
	0.44 ± 0.01	0.82 ± 0.01	5.00_0.82	0.11 ± 0.01	0.13 ± 0.01	0.005 ± 0.001 (72.6 ± 0.4)	0.007 ± 0.001 (72.5 ± 0.4)
	0.94 ± 0.01	1.77 ± 0.01	5.00_1.77	0.42 ± 0.01	0.32 ± 0.01	0.009 ± 0.001 (55.1 ± 0.5)	0.013 ± 0.001 (68.5 ± 3.7)
	1.83 ± 0.01	3.44 ± 0.01	5.00_3.44	1.17 ± 0.01	0.49 ± 0.01	0.013 ± 0.002 (35.8 ± 0.8)	0.018 ± 0.001 (65.9 ± 0.3)
	3.17 ± 0.01	5.98 ± 0.01	5.00_5.89	2.55 ± 0.01	–	0.011 ± 0.002 (19.7 ± 0.2)	–

amounts of polyphenol extracts were (0, 0.2, 0.5, and 1.0%). The kneading process was done in the food processor Mambo 10070 (Cecotec, Spain). Half of the water heated at 85 °C was added to the starch and stirred for 10 min at speed 4 promoting its gelatinization. Sugar and salt were added when the gelled mixture was cooled down to 30 °C. The other half of water was separated in two plastic beakers. The yeast was suspended in one and the polyphenols were dissolved in another, and both were added and mixed for 10 min at 500 rpm. Doughs obtained (50 g) were placed into a mold and fermented in a temperature-controlled cabinet (Salva, Guipúzcoa, Spain) for 1 h at 32 °C and 60% relative humidity. After fermentation, the samples were baked at 180 °C for 20 min in a convection oven (Eurofours, Gommegnies, France). Breads were cooled for 30 min at 25 °C before further analysis.

2.7. Bread characterization

Bread characterizations were determined as previously reported with moisture content, crumb image analysis, crumb texture profile analysis (TPA) and color [22].

The moisture content of gluten-free bread samples was determined according to the International Association for Cereal Science and Technology method [23]. Moisture content was expressed as g water/100 g bread crumb. Four replicates were analyzed for each sample.

The crumb image analysis was carried out as reported [24]. Bread slices were scanned using a flatbed scanner (Epson V600 Photo, Epson, Japan) in the RGB (Red-Green-Blue) standard format with 1200 dpi resolution. Image analysis of bread slices was conducted using Fiji Image J software [25]. For image segmentation and determination of crumb grain characteristics, image contrast was improved and then the algorithm "Otsu" was applied. The crumb grain measurements included: cell density (cell/cm^2), mean cell area (mm^2), surface porosity (total cell area/total slice area in percentage), and mean cell shape using the circularity factor (0-circle to 1-rectangle). Four slices of bread obtained in two different batches (four breads/batch) were analyzed for each sample.

The crumb texture profile analysis (TPA) was carried out using the TA.XT-Plus Texture Analyses (Stable Micro Systems Ltd., Godalming, UK) equipped with a 5 kg load cell and a 25-mm cylindrical probe. Slices were double compressed to 50% of their original height at a crosshead speed of 1 mm/s and 30 s gap between compressions, providing insight into how samples behave when chewed [26]. Parameters recorded were hardness, cohesiveness, springiness, chewiness, and resilience. All textural parameters were measured at 0 and 48 h, and then the hardening rate was calculated, as the hardness increase regarding the hardness of the fresh bread. Data acquired were the average value of eight replicates.

Crumb color was measured using the CIE-$L^*a^*b^*$ uniform color space using a Minolta colorimeter (Chromameter CR-400/410,

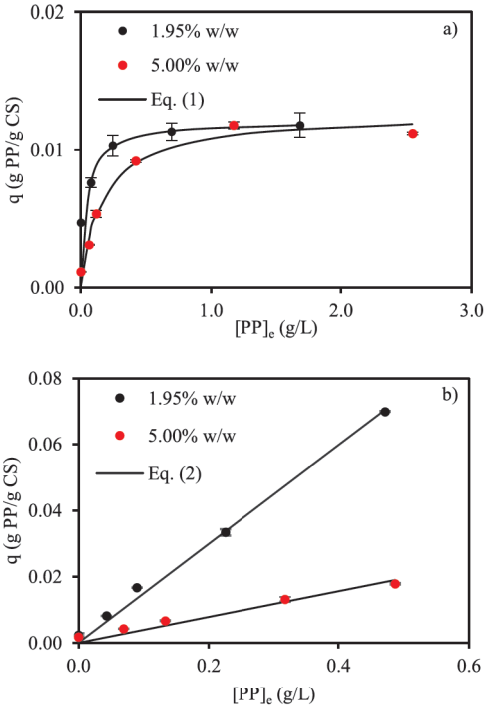

Fig. 1. Adsorption of polyphenols at 25 °C on native corn starch (a) and corn starch gel (b) at different starch content. Eq (1) corresponds to Langmuir model and Eq. (2) to Henry model.

Konica Minolta, Tokyo, Japan) after standardization with a white calibration plate employing diffusion illumination 0° viewing angle geometry. The color parameters were L^* (lightness), a^* (hue on a green to red), b^* (hue on a blue to yellow) and ΔE (total color difference) $= \sqrt{(\Delta L^*)^2 + (\Delta a^*)^2 + (\Delta b^*)^2}$ which was used to evaluate perceived color differences between control and samples. Measurements were performed on three slices from each run.

2.8. Statistical analysis

The results were analyzed through one-factor analysis of variance (ANOVA), followed by the Duncan test, and considering significant p-values <0.05 (IBM SPSS Statistics, New York, United States). Results were expressed as mean ± standard deviation.

3. Results

3.1. Polyphenols adsorption in native and gelled corn starch

Table 1 collects the concentrations used in the experiments carried out to determinate the polyphenols adsorption in native and gelled CS. For samples with 1.95% w/w of starch content, the initial concentration of polyphenols ($[PP]_0$, g/L) varied from 0.09 ± 0.01 to 1.95 ± 0.06, while for samples with 5.00% w/w, $[PP]_0$ reached up to 3.17 ± 0.01 g/L for attaining the saturation point of native starch. PP_0/CS_0 represents the mass polyphenols/starch ratio (w/w %) for each system. Therefore, the code of the samples was "X_Y", where "X" was the starch content and "Y" the corresponding mass polyphenol/starch ratio. Equilibrium polyphenols concentration of solution was $[PP]_e$ (g/L) and the polyphenols adsorbed was evaluated by q (g_{PP}/g_{CS}).

Fig. 1 shows the polyphenols adsorption isotherm for native CS at 1.95% w/w and 5.00% w/w (Fig. 1a) concentrations. In the first case, the maximum q value (0.012 g_{PP}/g_{CS}) was obtained above $[PP]_e$ of 0.6 g/L. Similar ($p > 0.05$) maximum q value (0.013 g_{PP}/g_{CS}) was achieved when higher starch (5.00% w/w) concentration was employed, and was constant above $[PP]_e$ of 1 g/L. Therefore, the greater the amount of starch, the greater the amount of polyphenols needed to saturate the starch surface. Similar maximum q values, independently of starch concentration, allowed to consider that the range of employed starch content was low because the entire surface was available for polyphenols sorption and the contact between starch particles was negligible. The fraction of adsorbed polyphenols, PP_0 adsorbed, Table 1, decreased with increasing the amount of polyphenols initially present since once saturation was reached, adsorption did not occur. Other authors proposed that between starch and phenolic compounds exist interactions through hydrogen bonds and van der Waals forces depending upon the polyphenols chemical structure [27]. For both systems, the shape of the curve corresponded to a Langmuir isotherm ($R^2 > 0.98$) indicating that polyphenols adsorption on the starch surface is physically limited. The parameters (q_{max} and b) obtained of Eq. (1) are in Table 2.

Fig. 1b shows the adsorption isotherms corresponding to CS gels at 1.95 and 5.00% w/w concentrations, respectively. When the highest concentrated solution of polyphenols (2 g/L) was employed the maximum q values were achieved: 0.070 g_{PP}/g_{CS} at low starch content and 0.018 g_{PP}/g_{CS} at high content. Conversely to the behavior described for native starch, a linear relationship was achieved between $[PP]_e$ and q corresponding to Henry's isotherm ($R^2 > 0.99$). Therefore, more polyphenols per gram of starch could be retained employing low concentration starch gels. Independently of starch content, polyphenols sorption of starch gels is far from saturation. The parameter values of Henry equation, Eq. (2), are in Table 2. It is worthy to indicate that polyphenols adsorption was notoriously enhanced (up to almost 7-fold) using the starch gel compared to the native starch at the same PP_0/CS_0. In fact, the minimum fraction of PP_0 adsorbed was higher than 65.9% (5.00_3.44) employing starch gels and decreased dramatically to 13.8% (1.95_9.79) with native starch. The gel state increased considerably the available surface area and interactions between starch and polyphenols were also promoted [28,29].

3.2. Rheological properties

Fig. 2 shows the heating ramps from 25 to 90 °C (at 5 °C/min) for tested samples. An increase in the elastic modulus (G') was observed in the presence of polyphenols in comparison to the controls at both starch concentrations. Likely, the interactions between polyphenol-starch chains contribute to form clusters that strengthen the gels [30]. However, Fig. 2, a threshold concentration of polyphenols existed (less than tested concentrations) promoting the elastic character since in the studied range this effect was constant or even caused a gel softening with the increasing of polyphenols content. A delay in the initial temperature of gelatinization (T_0') promoted ($p < 0.05$) by the polyphenols was observed from 69.2 ± 0.3 up to 71.4 ± 0.5 °C for 1.95_0.00 ($T_0'_{CS}$) and 1.95_4.79, respectively. This effect was also found in 5.00% w/w gels. In fact, a linear relationship ($R^2 > 0.95$) between ΔT_0', defined as T_0' - $T_0'_{CS}$, and adsorbed polyphenols (q) was found.

Table 2
Parameters of Langmuir, Eq. (1), and Henry isotherms, Eq. (2).

	Langmuir isotherm (native corn starch)			Henry isotherm (corn starch gel)	
Starch content (% w/w)	q_{max} (g_{PP}/g_{CS})	b (L/g_{PP})	R^2	k (L/g_{CS})	R^2
1.95	0.012 ± 0.001	21.75 ± 2.07	0.97	0.149 ± 0.003	0.99
5.00	0.013 ± 0.001	6.01 ± 0.22	0.99	0.039 ± 0.001	0.99

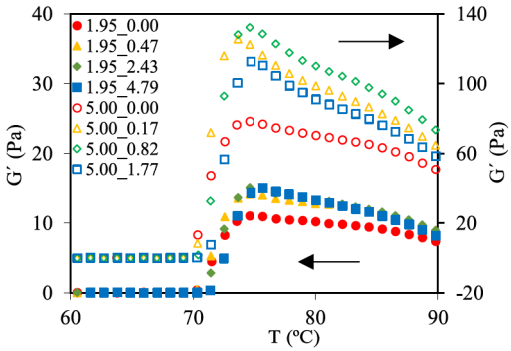

Fig. 2. Temperature sweep (from 25 to 90 °C at 5 °C/min, 1 Hz, and 10% strain) for control (only corn starch at 1.95% and 5.00% w/w) and samples with polyphenols. Error bars are not included to improve the clarity of data shown. Legends: code of samples was "X_Y", where "X" was the starch content and "Y" the corresponding initial mass polyphenol/starch ratio.

During heating ramp, the highest value of G' (corresponding to the peak temperature of gelatinization, T_p) for starch at 1.95% w/w was 11.1 ± 0.3 Pa and increased ($p < 0.05$) with polyphenols content (up to 15.1 ± 0.4 Pa). In starch gels at 5.00% w/w, the highest value of G' without polyphenols was 78.3 ± 5.9 Pa while for the samples with polyphenols increased noticeably from 112.8 ± 2.9 up to 125.4 ± 4.1 Pa. The presence of polyphenols also slightly delayed the corresponding T_p. These results could be related to the decrease in water available for starch gelatinization due to the hydrophilic nature of the polyphenols. This trend agreed with the effect observed during the addition of other biopolymers to starches [31]. Above T_p, G' decreased by the known processes associated to amylopectin crystallites melting and thermal weakening of gel [32], but the polyphenols accelerated this behavior decreasing the differences of G' regarding the samples without polyphenols at 90 °C and consequently the thermostability of gels diminished. This could be related to the filler effect of polyphenols which impaired the aggregation of starch after gelatinization and consequently reduced G' of gels at high temperatures. An attempt was made to relate the increase of T_p, ΔT_p, to q, similarly to ΔT_0', but there was no linear relationship among them. Nevertheless, a linear relationship ($R^2 > 0.98$) was found between ΔT_p and the PP_0 in the samples. This may mean that at the beginning of the gelatinization the adsorbed polyphenols interfered the formation of the gel, but they were desorbed along swelling and subsequent breakage of starch.

After the heating ramp, a time sweep was performed at 90 °C for 30 min. A G' drop was observed ($p < 0.05$) for gels without polyphenols independently of their starch content. The greatest drop occurred during the first 10 min (around 20–25%), reaching a total decrease of approximately 30%. For the samples containing polyphenols, the decrease in G' was lower. In the first 10 min, an average of 15% was achieved, reaching 20–23% on average at the end. This may be related to the crosslinking formed between the polyphenols and the starch, giving a greater elastic character to the gel formed. Evaluating the value of G' in the abrupt change of slope (after 10 min), as $((G'_{10'}-G'_{30'})/G'_0)_{CS}$ - $((G'_{10'}-G'_{30'})/G'_0)_{PP}$ *vs* polyphenols/starch ratio, PP_0/CS_0 of the starch gels, a power relationship, Eq. (4), was obtained ($R^2 > 0.95$):

$$\left(\frac{G'_{10'} - G'_{30'}}{G'_0}\right)_{CS} - \left(\frac{G'_{10'} - G'_{30'}}{G'_0}\right)_{PP} = 0.04\left(\frac{PP_0}{CS_0}\right)^{0.32} \quad (4)$$

where $G'_{10'}$, $G'_{30'}$ and G'_0 are the elastic modulus at 10, 30, and 0 min in the time sweep at 90 °C.

In the cooling ramp from 90 to 25 °C at 3 °C/min (data not shown), starch gels of 1.95% w/w showed similar behavior. At first (90 °C), gels with polyphenols had higher G' values than control (1.95_0.00) but at the end (25 °C) samples with polyphenols showed lower G' values than control. For starch gels at 5.00% w/w with high polyphenols concentration (5.00_1.77), the behavior was like those observed in gels at 1.95% w/w, but samples with lower polyphenols concentration (<5.00_0.82) showed higher G' values at 25 °C. Likely, low polyphenols/starch ratios (<0.82) were insufficient to interrupt the formation of the final gel. The damping factor (tan δ) in this step followed a similar behavior for all gels, with a decrease from 0.10 to 0.04 without polyphenols, and up to 0.01 with polyphenols. Similar results, lower G' values, for corn and wheat starches when apple polyphenols were added to native starch were previously reported [33]. According to these authors, polyphenols molecules might be inserted among starch molecules, avoiding the intermolecular entanglement, and weakening the intermolecular hydrogen bonds between starches.

In the maturation of the gel (25 °C, 30 min), it was observed that the presence of polyphenols increased noticeably ($p < 0.05$) the stability of the gels. In fact, at 1.95% w/w of CS gels, G' values of 1.95_0.00 sample increased from 28.0 ± 1.1 to 35.8 ± 0.4 Pa while for gels with polyphenols the increase was less than 2 Pa. For CS gels at 5.00% w/w, similar behaviour was observed with higher changes (from 179.3 ± 5.4 to 205.9 ± 9.1 Pa) in G' values during maturation in gels without polyphenols regarding those formed with polyphenols (i.e.: 192.1 ± 1.5 to 209.2 ± 0.9 Pa for 5.00_0.82). In this step, the tan δ values were similar for all samples studied at both concentrations.

Fig. 3 shows the frequency sweep from 0.01 to 10 Hz at 10% strain and 25 °C of tested gels. Samples showed a typical behavior of

starch gels. The G' values were higher than G'' values. For gels at 1.95% w/w, a clear effect of polyphenols was observed in the final gel features with lower G' values. However, no significant differences ($p > 0.05$) were observed with the concentration of polyphenols added, confirming that low concentration was required to interfere in the gel structure and weaken it. In the case of 5.00% w/w starch gels without added polyphenols and low polyphenols content (5.00_0.17 and 5.00_0.82 gels) showed similar behavior, but gels with high polyphenols/starch ratio (>5.00_1.77) showed a significant ($p < 0.05$) decrease in G' values. It was reported that G' decreased when polyphenols were added to maize, wheat and rice starches and doughs [33–35].

3.3. Digestion starch

The digestion kinetic constant (k) value for the starch gels without polyphenols (1.95_0.00 and 5.00_0.00) was similar ($p > 0.05$), Table 3, this could be because the gels are so weak that the structure did not influence this parameter. Independently of starch content of gels, the addition of polyphenols decreased the digestion kinetic constant and the final concentration of digested starch (C_∞). Furthermore, the greater the quantity of polyphenols added, the greater the decrease in k. Probably, starch structure changed in the presence of polyphenols, since they could form an "inclusive V-type amylose" complex along α (1 → 4) glycosidic chains with the amylose of the starch [30]. The RDS values corroborated this theory since as polyphenols were added to the gels, less starch was digested. In this way, gels with low starch content without polyphenols (1.95_0.00) a value of 1.62 ± 0.01 g/100 g gel was obtained, while for the gels with the highest polyphenols/starch ratio (1.95_4.79) the value was 0.07 ± 0.01. For the 5.00% w/w gels the same effect was observed. Without polyphenols (5.00_0.00) a value of 2.93 ± 0.13 g/100 g gel was obtained, while for the system with the highest polyphenol/starch ratio (5.00_1.77) decreased up to 0.20 ± 0.02. However, it was observed that SDS values significantly ($p < 0.05$) increased with polyphenols addition. In any case, the extent of starch hydrolysis, C_∞, decreased considerably with the added polyphenols in the gels. This result agreed with those found with the addition of gallic acid to rice starch gels [8].

On the other hand, the study of starch hydrolysis by rheometry was based on the drop in the apparent viscosity with time. Firstly, a calibration of the apparent viscosity (measured at shear rate of 10 s^{-1}) was carried out with gels of starch concentrations from 0.5 to 5.0% w/w dry basis. Eq. (5) was obtained relating the apparent viscosity with starch content ($R^2 > 0.99$):

$$C = 0.637 \ln(\mu_d) + 4.582 \quad (5)$$

where C (% w/w) is the starch concentration and μ_d (Pa s) corresponds to the apparent viscosity of starch gel considering the dilution after maleate buffer addition (without enzyme). The effect of dilution had to be considered in the calibration due to viscosity change considerably with the presence of buffers.

In the digestion study, the enzyme was added to the gel diluted in maleate buffer. Immediately, apparent viscosity data were measured in a time sweep step up to achieve a viscosity plateau meaning that starch digestion was finished. The initial apparent viscosity of starch gels increased with added polyphenols, μ_{dPO}, (at the highest polyphenols/starch ratio (1.95_4.79) the initial viscosity was 9-fold higher starch gel without polyphenols, μ_{dO} (1.95_0.00). For this reason, a correction factor, given by experimental (μ_{dPO}/μ_{dO}) was applied to the experimental values for employing adequately the calibration, Eq. (5), in tested gels. Fig. 4a shows the raw apparent viscosity (log scale) curves obtained during starch digestion, Fig. 4b, the viscosity curve after applying the corresponding conversion factors and, Fig. 4c, the starch concentration curve during digestion.

The digestion curves were treated with the same model, Eq. (3), employed in the biochemical method and kinetic constant, k_v, values are in Table 3. The results obtained by rheology about the effect of polyphenols on digestion were like those reported by biochemical digestion and confirmed that k_v decreased with the presence of polyphenols. Despite the kinetic constant values obtained by biochemical and rheological methods, k and k_v, were numerically different (justified because geometry, scale, stirring, homogenization, etc., were different between both experimental setups), when relative kinetic constant, evaluated as k/k_{oo} or k_v/k_{vo}, (using the

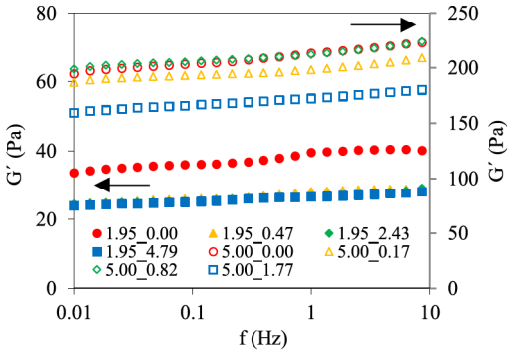

Fig. 3. Frequency sweep (from 0.01 to 1 Hz at 10% strain and 25 °C) for control (only corn starch at 1.95% and 5.00% w/w) and samples with polyphenols. Error bars are not included to improve the clarity of data shown. Legends: code of samples was "X_Y", where "X" was the starch content and "Y" the corresponding initial mass polyphenol/starch ratio.

Table 3
Parameters of *in vitro* starch gels hydrolysis for 1.95% and 5.00% w/w with different ratios polyphenol/starch by biochemical and rheological methods.

	Biochemical Digestion					Rheological Digestion	
Code	RDS (g/100g)	SDS (g/100g)	k (min^{-1})	k/k_{∞}	C_{∞} (g/100g)	k_v (min^{-1})	k_v/k_{vo}
1.95_0.00	1.62 ± 0.01^{a}	0.09 ± 0.01^{d}	0.149 ± 0.002^{a}	1	1.71 ± 0.01^{a}	0.045 ± 0.003^{a}	1
1.95_0.47	0.55 ± 0.09^{b}	0.80 ± 0.01^{a}	0.024 ± 0.004^{b}	0.16 ± 0.03^{a}	1.43 ± 0.07^{b}	0.007 ± 0.002^{b}	0.15 ± 0.02^{b}
1.95_2.43	0.12 ± 0.01^{c}	0.30 ± 0.01^{b}	0.013 ± 0.001^{c}	0.09 ± 0.01^{b}	0.54 ± 0.01^{c}	0.002 ± 0.001^{c}	0.04 ± 0.01^{a}
1.95_4.79	0.07 ± 0.01^{c}	0.21 ± 0.01^{c}	0.008 ± 0.001^{c}	0.05 ± 0.01^{c}	0.44 ± 0.01^{d}	0.0006 ± 0.0001^{d}	0.013 ± 0.001^{c}
5.00_0.00	2.93 ± 0.13^{A}	0.21 ± 0.03^{B}	0.136 ± 0.005^{A}	1	3.14 ± 0.16^{A}	0.195 ± 0.006^{A}	1
5.00_0.17	2.53 ± 0.03^{B}	0.50 ± 0.17^{A}	0.092 ± 0.015^{B}	0.67 ± 0.09^{A}	3.02 ± 0.13^{A}	0.118 ± 0.004^{B}	0.61 ± 0.03^{A}
5.00_0.82	0.19 ± 0.02^{C}	0.54 ± 0.01^{A}	0.012 ± 0.002^{C}	0.09 ± 0.01^{B}	1.05 ± 0.10^{B}	0.006 ± 0.001^{C}	0.03 ± 0.01^{B}
5.00_1.77	0.20 ± 0.02^{C}	0.54 ± 0.01^{A}	0.011 ± 0.002^{C}	0.08 ± 0.01^{C}	1.00 ± 0.02^{B}	0.006 ± 0.001^{C}	0.03 ± 0.01^{B}

Digestion data are reported in g of starch hydrolysed per 100 g of gel. Data are presented as mean ± standard deviation. Data value of each parameter with different superscript letters, in columns, are significantly different ($p < 0.05$).

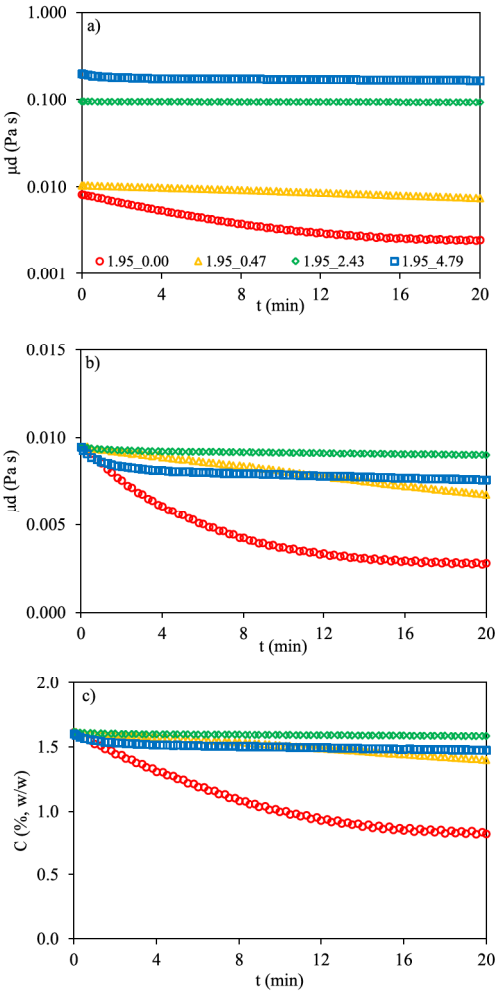

Fig. 4. a) The raw apparent viscosity (log scale), b) viscosity curve after applying the corresponding conversion factors, c) the starch concentration curve during digestion as function of time for control (1.95_0.00) and samples with added polyphenols.

corresponding starch gels without polyphenols as references) were employed a good agreement was found, Table 3. Fig. 5 shows the relationship between k/k_{oo} or k_v/k_{vo} and the polyphenols content for starch gels with 1.95 and 5.00 % w/w. Starch digestions were similarly slowed down following an exponential relationship ($R^2 > 0.991$), Eq. (6), with the polyphenols/starch ratio present independently of the initial starch content of the gels.

$$\frac{k}{k_{00}} \; or \frac{k_v}{k_{v0}} = \frac{0.965}{e^{\left[3.510\left(\frac{PP_0}{CS_0}\right)\right]}} + 0.035 \tag{6}$$

3.4. Bread characterization

The polyphenols addition, in general, affected the analyzed characteristics (Table 4) as well as the appearance of the gluten-free breads (Fig. 6). The moisture content decreased with the addition of polyphenols (Table 4), but significant ($p < 0.05$) differences were only found in the samples with the highest percentage of polyphenols (1.0% w/w starch basis). Likely, less hydroxyl groups were available to link water molecules, which could be indicative of starch-polyphenols interactions [36]. The color of the bread was significantly ($p < 0.05$) affected by the polyphenols added (Table 4). The lightness (L^*) decreased linearly ($R^2 > 0.97$) with the addition of polyphenols. Parameter a^* increased with the addition of polyphenols except for samples with 0.2% w/w starch basis that decreased and b^* values increased significantly with the polyphenols added.

The bread's microstructure was modified ($p < 0.05$) by the addition of polyphenols (Table 4). The bread volume, represented by the 2D slice area (cm^2), decreased with the polyphenols added, but no statistical effect was observed with their concentration. Similar trend was observed in the mean cell area (mm^2), which was lower with added polyphenols. The number of gas cells/cm^2 and the porosity (%) increased with the polyphenol's incorporation. However, the number of cells was higher as the content of polyphenols increased, but the bread with 0.5% displayed more porosity than the other concentrations. It has been reported that the addition of seaweeds or microalgae into bread formulations, led to a reduction in pore size with a simultaneous increase in the number of cells and porosity, and an overall increase in bread volume [37,38]. However, other authors using polyphenols and observed a decrease in yeast activity, which could explain the reduced 2D slice area found here when incorporating seaweed-extracted polyphenols into the formulation [39]. In samples with polyphenols, the 2D slice area exhibited a statistically significant inverse correlation with the kinetic constant ($r = -0.9998$) and the relative kinetic constant ($r = -0.9996$) of the starch gels during the biochemical digestion.

Textural parameters were measured at time 0 and 48 h. In general, the addition of polyphenols to bread increased ($p < 0.05$) the hardness on the fresh bread from 6.7 ± 1.0 to 13.6 ± 4.0 N. The increase in crumb hardness could have been due to the crumb being more compact because of, as previously discussed, the inhibition of yeast activity. For samples at 48 h the hardness was around 30 N without significant differences except for bread with 1% of polyphenols which the hardness value decreased until 17.0 ± 2.2 N. The springiness for fresh bread varied between 0.94 and 0.89 and for bread with 48 h the values varied between 0.91 and 0.83. The chewiness increased from 5.5 ± 0.9 to 9.5 ± 2.4 N with the addition of polyphenols in fresh bread. However, the chewiness decreased from 10.6 ± 4.0 to 3.6 ± 0.1 in the bread at 48 h by polyphenols addition. The resilience values decreased significantly with the addition of polyphenols in fresh and at 48 h breads. The hardening rate (%) decreased greatly with the addition of polyphenols which means that polyphenols delayed the starch retrogradation. Polyphenols contain a significant abundance of free hydroxyl groups, capable of establishing hydrogen bonds with starch molecules, thereby inhibiting the reorganization of starch chains through recrystallization [5,40]. Other researchers reported that when some corn and potato starches were replaced by whole red sorghum flour (up to 40% w/w), the hardness decreased [12]. This may be because these authors carried out the trials by substitution while here the trials were by addition. However, the same effect was observed in the springiness values decreasing with the amount of whole red sorghum flour.

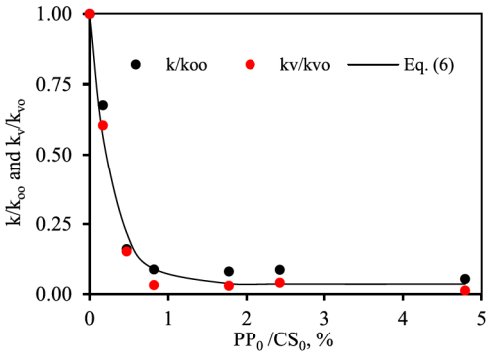

Fig. 5. Experimental relative kinetic constants (by biochemical and rheological methods) as function of polyphenols/starch ratios, PP_0/CS_0, and proposed model, Eq. (6).

Table 4
Bread characterization values: Control (C) and polyphenol-enriched variants at 0.2%, 0.5%, and 1.0% w/w starch basis.

Analysis	Storage (h)	C	0.2%	0.5%	1.0%
Moisture (% w.b.)	0	50.46 ± 0.40^{a}	50.14 ± 0.40^{a}	49.91 ± 0.76^{a}	48.57 ± 0.34^{b}
Crumb color					
*L**-crumb	0	68.10 ± 2.40^{a}	65.40 ± 1.46^{b}	63.71 ± 1.36^{c}	56.37 ± 1.74^{d}
*a**-crumb		-2.80 ± 0.22^{c}	-3.24 ± 0.12^{d}	-2.39 ± 0.21^{b}	-1.11 ± 0.33^{a}
*b**-crumb		7.49 ± 0.70^{d}	17.79 ± 0.86^{c}	25.03 ± 0.56^{b}	29.08 ± 0.75^{a}
ΔE*		–	10.78 ± 0.11^{c}	18.12 ± 0.07^{b}	24.76 ± 0.32^{a}
Slice morphology					
2D slice area (cm^2)	0	2.45 ± 0.07^{a}	2.20 ± 0.13^{b}	2.25 ± 0.17^{b}	2.27 ± 0.09^{b}
Mean cell area (mm^2)		2.48 ± 1.48^{a}	1.46 ± 0.58^{a}	1.57 ± 0.37^{a}	1.48 ± 0.21^{a}
Gas cells/cm2		29 ± 14^{b}	56 ± 24^{a}	65 ± 19^{a}	76 ± 13^{a}
Porosity (%)		10.70 ± 3.07^{b}	14.84 ± 4.17^{b}	23.53 ± 11.36^{a}	14.67 ± 2.67^{b}
Crumb texture profile analysis					
Hardness (N)	0	6.7 ± 1.0^{c}	13.4 ± 2.9^{a}	13.6 ± 4.0^{a}	10.5 ± 0.7^{b}
	48	31.1 ± 5.5^{a}	30.8 ± 13.0^{a}	30.2 ± 8.7^{a}	17.0 ± 2.2^{b}
Hardening rate (%)		464 ± 32^{a}	227 ± 37^{b}	223 ± 1^{b}	162 ± 10^{b}
Springiness	0	0.94 ± 0.02^{a}	0.90 ± 0.04^{b}	0.89 ± 0.01^{b}	0.94 ± 0.05^{a}
	48	0.91 ± 0.06^{a}	0.83 ± 0.07^{b}	0.86 ± 0.01^{b}	0.83 ± 0.03^{b}
Cohesiveness	0	0.87 ± 0.03^{a}	0.79 ± 0.07^{b}	0.77 ± 0.03^{b}	0.80 ± 0.04^{b}
	48	0.37 ± 0.08^{a}	0.28 ± 0.01^{bc}	0.29 ± 0.01^{b}	0.26 ± 0.02^{c}
Chewiness (N)	0	5.5 ± 1.0^{c}	9.5 ± 2.4^{a}	9.2 ± 2.4^{a}	7.9 ± 0.1^{b}
	48	10.6 ± 4.0^{a}	7.2 ± 2.2^{b}	7.5 ± 1.9^{b}	3.6 ± 0.1^{c}
Resilience	0	0.65 ± 0.02^{a}	0.57 ± 0.07^{b}	0.54 ± 0.02^{b}	0.57 ± 0.05^{b}
	48	0.24 ± 0.05^{a}	0.18 ± 0.01^{b}	0.18 ± 0.01^{b}	0.15 ± 0.02^{c}

Data are presented as mean ± standard deviation. Data value of each parameter with different superscript letters, in columns, are significantly different ($p < 0.05$).

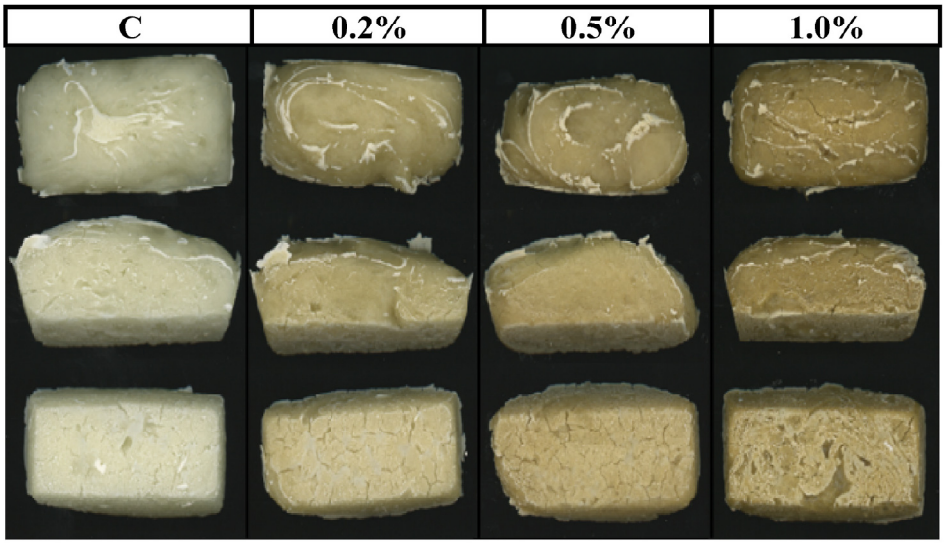

Fig. 6. Images of baked bread for control (C) and with addition of 0.2, 0.5, and 1.0% w/w starch basis of polyphenols.

4. Conclusions

The adsorption of polyphenols on starch was promoted in starch gels regarding native starch because in the gels the available surface area allowing the interactions between starch and polyphenols. On the other hand, the addition of polyphenols in the formation of the starch gel studied by rheology showed a general decrease in the elastic modulus (G') values in the frequency sweep. The results obtained regarding starch digestion indicated that the presence of polyphenols decreased the digestion constant (k) and reduced the final concentration of digested starch (C_∞). The digestion studies were carried out by the biochemical and rheological methods and acceptable agreement between them was found for the evaluation of the relative digestion rate. Finally, polyphenols were added to the starch to make a simplified baking product. The presence of polyphenols increased hardness and chewiness values and decreased the

cohesiveness and resilience values. Nonetheless, the crumb hardening during storage was less noticeable, suggesting its potential integration into gluten-free bread formulations to delay bread aging. This could involve process adaptations aimed at mitigating the impact of polyphenols on slice appearance and texture.

Data availability

Data associated with the study has been deposited into the public Mendeley repository https://doi.org/10.17632/sh8b35h8wm.1.

Ethics declarations

All authors hereby declare that: Review and approval by an ethics committee was not needed for this study because it did not involve any human subjects, patients, animals, or societal groups.

Funding

This research was financed by the Spanish Ministry of Science and Innovation (Project RTI2018-095919-B-C2) and the European Regional Development Fund (FEDER).

CRediT authorship contribution statement

Leticia Montes: Writing – original draft, Investigation. **Maria Santamaria:** Writing – original draft, Investigation. **Raquel Garzon:** Writing – review & editing, Investigation. **Cristina M. Rosell:** Writing – review & editing, Project administration, Funding acquisition, Conceptualization. **Ramón Moreira:** Writing – review & editing, Project administration, Funding acquisition, Conceptualization.

Declaration of competing interest

The authors declare that they have no known competing financial interests or personal relationships that could have appeared to influence the work reported in this paper.

References

[1] P.H. Green, B. Lebwohl, R. Greywoode, Celiac disease, J. Allergy Clin. Immunol. 135 (2015) 1099–1106, https://doi.org/10.1016/j.jaci.2015.01.044.
[2] A.E. Scaramuzza, C. Mantegazza, A. Bosetti, G.V. Zuccotti, Type 1 diabetes and celiac disease: the effects of gluten free diet on metabolic control, World J. Diabetes 4 (2013) 130–134, https://doi.org/10.4239/wjd.v4.i4.130.
[3] J. Poole, A. Diop, L.C. Rainville, S. Barnabé, Bioextracting polyphenols from the brown seaweed *Ascophyllum nodosum* from Québec's north shore coastline, Ind. Biotechnol. 15 (2019) 212–218, https://doi.org/10.1089/ind.2019.0008.
[4] C.Y. Yang, Y.Y. Yen, K.C. Hung, S.W. Hsu, S.J. Lan, H.C. Lin, Inhibitory effects of pu-erh tea on alpha glucosidase and alpha amylase: a systemic review, Nutr. Diabetes 9 (2019) 23, https://doi.org/10.1038/s41387-019-0092-y.
[5] A. Aleixandre, J.V. Gil, J. Sineiro, C.M. Rosell, Understanding phenolic acids inhibition of α-amylase and α-glucosidase and influence of reaction conditions, Food Chem. 372 (2022) 131231, https://doi.org/10.1016/j.foodchem.2021.131231.
[6] F. Barros, J.M. Awika, L.W. Rooney, Interaction of tannins and other sorghum phenolic compounds with starch and effects on in vitro starch digestibility, J. Agric. Food Chem. 60 (2012) 11609–11617, https://doi.org/10.1021/jf3034539.
[7] C. Chi, X. Li, Y. Zhang, L. Chen, L. Li, Z. Wang, Digestibility and supramolecular structural changes of maize starch by non-covalent interactions with gallic acid, Food Funct. 8 (2017) 720–730, https://doi.org/10.1039/c6fo01468b.
[8] C. Chi, X. Li, Y. Zhang, L. Chen, F. Xie, L. Li, G. Bai, Modulating the *in vitro* digestibility and predicted glycemic index of rice starch gels by complexation with gallic acid, Food Hydrocoll 89 (2019) 821–828, https://doi.org/10.1016/j.foodhyd.2018.11.016.
[9] Y.H. Dai, J.R. Wei, X.Q. Chen, Interactions between tea polyphenols and nutrients in food, Compr. Rev. Food Sci. Food Saf. 22 (2023) 3130–3150, https://doi.org/10.1111/1541-4337.13178.
[10] N. Chen, L. Chen, H.X. Gao, W.C. Zeng, Mechanism of bridging and interfering effects of tea polyphenols on starch molecules, J. Food Process. Preserv. 44 (2020) e14576, https://doi.org/10.1111/jfpp.14576.
[11] X. Han, M. Zhang, R. Zhang, L. Huang, X. Jia, F. Huang, L. Liu, Physicochemical interactions between rice starch and different polyphenols and structural characterization of their complexes, LWT–Food Sci. Technol. 125 (2020) 109227, https://doi.org/10.1016/j.lwt.2020.109227.
[12] N. Hryhorenko, U. Krupa-Kozak, N. Baczek, B. Rudnicka, B. Wróblewska, Gluten-free bread enriched with whole-grain red sorghum flour gains favourable technological and functional properties and consumers acceptance, J. Cereal. Sci. 110 (2023) 103646, https://doi.org/10.1016/j.jcs.2023.103646.
[13] D. Sun-Waterhouse, J. Chen, C. Chuah, R. Wibisono, L.D. Melton, W. Laing, L.R. Ferguson, M.A. Skinner, Kiwifruit-based polyphenols and related antioxidants for functional foods: kiwifruit extract-enhanced gluten-free bread, Int. J. Food Sci. Nutr. 60 (2009) 251–264, https://doi.org/10.1080/09637480903012355.
[14] N. Deng, Z. Deng, C. Tang, C. Liu, S. Luo, T. Chen, X. Hu, Formation, structure and properties of the starch-polyphenol inclusion complex: a review, Trends Food Sci. Technol. 112 (2021) 667–675, https://doi.org/10.1016/j.tifs.2021.04.032.
[15] A. Brodkorb, L. Egger, M. Alminger, P. Alvito, R. Assunção, S. Ballance, T. Bohn, C. Bourlieu-Lacanal, R. Boutrou, F. Carrière, A. Clemente, M. Corredig, D. Dupont, C. Dufour, C. Edwards, M. Golding, S. Karakaya, B. Kirkhus, S. Le Feunteun, U. Lesmes, A. Macierzanka, A.R. Mackie, C. Martins, S. Marze, D. J. McClements, O. Ménard, M. Minekus, R. Portmann, C.N. Santos, I. Souchon, R.P. Singh, G.E. Vegarud, M.S.J. Wickham, W. Weitschies, I. Recio, INFOGEST static in vitro simulation of gastrointestinal food digestion, Nat. Protoc. 14 (2019) 991–1014, https://doi.org/10.1038/s41596-018-0119-1.
[16] M. Gisbert, M. Barcala, C.M. Rosell, J. Sineiro, R. Moreira, Aqueous extracts characteristics obtained by ultrasound-assisted extraction from *Ascophyllum nodosum* seaweeds: effect of operation conditions, J. Appl. Phycol. 33 (2021) 3297–3308, https://doi.org/10.1007/s10811-021-02546-5.
[17] V.L. Singleton, J.A. Rossi, Colorimetry of total phenolics with phosphomolybdic-phosphotungstic acid reagent, Am. J. Enol. Vitic. 16 (1965) 144–158, https://doi.org/10.5344/ajev.1965.16.3.144.
[18] M. Santamaria, L. Montes, R. Garzon, R. Moreira, C.M. Rosell, Unravelling the impact of viscosity and starch type on the in vitro starch digestibility of different gels, Food Funct. 13 (2022) 7582–7590, https://doi.org/10.1039/D2FO00697A.
[19] H.N. Englyst, S.M. Kingman, J.H. Cummings, Classification and measurement of nutritionally important starch fractions, Eur. J. Clin. Nutr. 46 (1992) 33–50, https://doi.org/10.1016/0308-8146(96)00056-8.

[20] I. Goñi, A. Garcia-Alonso, F. Saura-Calixto, A starch hydrolysis procedure to estimate glycemic index, Nutr. Res. 17 (1997) 427–437, https://doi.org/10.1016/S0271-5317(97)00010-9.
[21] R.G. Lentle, P.W.M. Janssen, P. Asvarujanon, P. Chambers, K.J. Stafford, Y. Hemar, High-definition mapping of circular and longitudinal motility in the terminal ileum of the brushtail possum *Trichosurus vulpecula* with watery and viscous perfusates, J. Comp. Physiol. B 177 (2007) 543–556, https://doi.org/10.1007/s00360-007-0153-8.
[22] M.E. Matos, C.M. Rosell, Quality indicators of rice-based gluten-free bread-like products: relationships between dough rheology and quality characteristics, Food Bioprocess Techn 6 (2013) 2331–2341, https://doi.org/10.1007/s11947-012-0903-9.
[23] ICC, International Association for Cereal Chemistry (ICC), 1994. Standard No 110/1.
[24] J. Espinosa-Ramírez, R. Garzon, S.O. Serna-Saldivar, C.M. Rosell, Functional and nutritional replacement of gluten in gluten-free yeast-leavened breads by using β-conglycinin concentrate extracted from soybean flour, Food Hydrocoll 84 (2018) 353–360, https://doi.org/10.1016/j.foodhyd.2018.06.021.
[25] J. Schindelin, I. Arganda-Carreras, E. Frise, V. Kaynig, M. Longair, T. Pietzsch, S. Preibisch, C. Rueden, S. Saalfeld, B. Schmid, J.Y. Tinevez, D.J. White, V. Hartenstein, K. Eliceiri, P. Tomancak, A. Cardona, Fiji: an open-source platform for biological-image analysis, Nat. Methods 9 (2012) 676–682, https://doi.org/10.1038/nmeth.2019.
[26] C.M. Rosell, E. Santos, J.M. Sanz Penella, M. Haros, Wholemeal wheat bread: a comparison of different breadmaking processes and fungal phytase addition, J. Cereal. Sci. 50 (2009) 272–277, https://doi.org/10.1016/j.jcs.2009.06.007.
[27] N. Bordenave, B.R. Hamaker, M.G. Ferruzzi, Nature and consequences of non-covalent interactions between flavonoids and macronutrients in foods, Food Funct. 5 (2014) 18–34, https://doi.org/10.1039/c3fo60263j.
[28] M. Gisbert, A. Aleixandre, J. Sineiro, C.M. Rosell, R. Moreira, Interactions between *Ascophyllum nodosum* seaweeds polyphenols and native and gelled corn starches, Foods 11 (2022) 1165, https://doi.org/10.3390/foods11081165.
[29] Y. Wang, S. Li, F. Bai, J. Cao, L. Sun, The physical adsorption of gelatinized starch with tannic acid decreases the inhibitory activity of the polyphenol against α-amylase, Foods 10 (2021) 1233, https://doi.org/10.3390/foods10061233.
[30] M. Li, C. Ndiaye, S. Corbin, E.A. Foegeding, M.G. Ferruzzi, Starch-phenolic complexes are built on physical CH-π interactions and can persist after hydrothermal treatments altering hydrodynamic radius and digestibility of model starch-based food, Food Chem. 308 (2020) 125577, https://doi.org/10.1016/j.foodchem.2019.125577.
[31] V.J. Larrosa, G. Lorenzo, N.E. Zaritzky, A.N. Califano, Effect of the addition of proteins and hydrocolloids on the water mobility in gluten-free pasta formulations, Water 4 (2012) 1–17, https://doi.org/10.14294/WATER.2012.2.
[32] J. Ahmed, H. Attar, Structural properties of high pressure treated chestnut flour dispersions, Int. J. Food Prop. 20 (2017) S766–S778, https://doi.org/10.1080/10942912.2017.1311343.
[33] S. Chou, X. Meng, H. Cui, S. Zhang, H. Wang, B. Li, Rheological and pasting properties of maize, wheat and rice starch as affected by apple polyphenols, Int. J. Food Prop. 22 (2019) 1786–1798, https://doi.org/10.1080/10942912.2019.1671452.
[34] Y. Wu, M. Niu, H. Xu, Pasting behaviors, gel rheological properties, and freeze-thaw stability of rice flour and starch modified by green tea polyphenols, LWT–Food Sci. Technol. 118 (2020) 108796, https://doi.org/10.1016/j.lwt.2019.108796.
[35] A.S. Sivam, D. Sun-Waterhouse, G.I.N. Waterhouse, S. Quek, C.O. Perera, Physicochemical properties of bread dough and finished bread with added pectin fiber and phenolic antioxidants, J. Food Sci. 76 (2011) 97–107, https://doi.org/10.1111/j.1750-3841.2011.02086.x.
[36] N. Chen, H.X. Gao, Q. He, W.C. Zeng, Potato starch-based film incorporated with tea polyphenols and its application in fruit packaging, Polymers 15 (2023) 588, https://doi.org/10.3390/polym15030588.
[37] T. Amoriello, F. Mellara, M. Amoriello, D. Ceccarelli, R. Ciccoritti, Powdered seaweeds as a valuable ingredient for functional breads, Eur. Food Res. Technol. 247 (2021) 2431–2443, https://doi.org/10.1007/s00217-021-03804-z.
[38] R. Garzon, A. Skendi, M.A. Lazo-Velez, M. Papageorgiou, C.M. Rosell, Interaction of dough acidity and microalga level on bread quality and antioxidant properties, Food Chem. 344 (2021) 128710, https://doi.org/10.1016/j.foodchem.2020.128710.
[39] S. Mildner-Szkudlarz, M. Różańska, P. Piechowska, A. Waśkiewicz, R. Zawirska-Wojtasiak, Effects of polyphenols on volatile profile and acrylamide formation in a model wheat bread system, Food Chem. 297 (2019) 125008, https://doi.org/10.1016/j.foodchem.2019.125008.
[40] Z. Fu, J. Chen, S.J. Luo, C.M. Liu, W. Liu, Effect of food additives on starch retrogradation: a review, Stärke 67 (2015) 69–78, https://doi.org/10.1002/star.201300278.

PUBLICATION 2

Water sorption isotherms of different sodium alginates:

Thermodynamic evaluation and influence of mannuronate-guluronate

Journal of Food Processing and Preservation, 46, e17179 (2022)

Received: 27 July 2022 | Revised: 8 September 2022 | Accepted: 14 September 2022

DOI: 10.1111/jfpp.17179

Journal of Food Processing and Preservation

WILEY

ORIGINAL ARTICLE

Water sorption isotherms of different sodium alginates: Thermodynamic evaluation and influence of mannuronate-guluronate copolymers

Leticia Montes | Mauro Gisbert | Ramón Moreira

Chemical Engineering Department, Universidade de Santiago de Compostela, Santiago de Compostela, Spain

Correspondence
Ramón Moreira, Department of Chemical Engineering, Universidade de Santiago de Compostela, rúa Lope Gómez de Marzoa, Santiago de Compostela E-15782, Spain.
Email: ramon.moreira@usc.es

Funding information
Consellería de Cultura, Educación e Ordenación Universitaria, Xunta de Galicia; European Regional Development Fund; Ministerio de Ciencia e Innovación

Abstract

Water desorption isotherms of three alginates with different structural features were determined at 25, 37, and 50°C. The Halsey model was selected to fit the equilibrium water sorption data. Differential and integral enthalpy and entropy were estimated for tested alginates. Optimal storage conditions of tested alginates (moisture content from 0.15 to 0.20 kg water/kg dry solid and relative humidity from 35% to 50%) were determined from the maximum and minimum integral enthalpy and entropy values, respectively. A model was proposed to estimate the water sorption isotherms of alginates based on the alginate monomers (mannuronate, *M*, and guluronate, *G*) at low water activity (<0.4). *M* fraction was mainly responsible for the hygroscopicity of alginates. Alginates with similar *G* fraction showed different hygroscopic features by the presence of more homopolymeric *G* blocks that could form helical structures at low moisture content, decreasing the water affinity.

Practical applications

Determination of water sorption isotherms is fundamental to determine the optimal storage conditions at different temperatures. Their knowledge is essential for designing drying equipment, selecting adequately drying conditions (temperature and relative humidity of air) and drying time. Mathematical models are useful to estimate equilibrium moisture content in wide ranges of water activity and temperature. The thermodynamic study also provides valuable information about energy consumption and consequently operational costs. In this case, high content of mannuronate, *M*, increases the hygroscopic character of alginates, but the optimal moisture content of dried alginates to achieve maximum stability during storing varies in a narrow interval (0.15–0.20 kg water/kg dry solid).

1 | INTRODUCTION

Alginate extraction from brown seaweeds is based on the conversion of the alginic acid from the cell walls into alginate salt forms, followed by its precipitation and purification. Milled seaweeds are soaked in dilute mineral acid to remove fucoidans, laminarins, proteins, and polyphenols that could modify alginate features. Then, alginic acid is transformed into sodium alginate (SA) by employing alkaline solutions, meanwhile solid residues are removed by centrifugation and filtration. Finally, alginate is precipitated with ethanol

to obtain SA (Chee et al., 2011). Recent studies have showed that SA can also be obtained from wasted solids after polyphenols extraction (Montes et al., 2021). SA is a linear polysaccharide composed of β-D-mannuronic acid (M) and α-L-guluronic acid (G) linked by 1–4 glycosidic bonds, and the M/G ratio gives relevant information about the polymer structure (Abka-khajouei et al., 2022). The composition of alginates depends on their natural source, geographical location, and seasonal variations (Fernando et al., 2020). SA is used in cosmetic, pharmaceutical, medical, and textile industries. Particularly, it is widely used in food industry due to its thickening, emulsifying, gelling, stabilizing, and film-forming properties, being one of the most important food additives (Qin et al., 2018).

SA is a hygroscopic material and tends to modify its moisture content as a function of environmental air conditions; hence, adequate storage conditions are very relevant for its correct conservation (Lee & Mooney, 2012). Most biopolymers are sensitive to moisture content, so their properties change with relative humidity and temperature (Kurek et al., 2014). By means of water sorption isotherms, which relate the equilibrium moisture content (X) and water activity (a_w), the optimally hygroscopic conditions can be obtained for its preservation (Shivhare et al., 2004). There are many (empirical, semitheoretical, and theoretical) equations to model the water sorption isotherms. Halsey model can be used to study the multilayer water adsorption (Halsey, 1948). In this model, temperature can be introduced as variable within the model, and one equation is useful to reproduce simultaneously the equilibrium moisture content of a sample over a broad water activity and temperature ranges.

Hygroscopic properties of a food material depend on its chemical composition (Moreira et al., 2009). In this way, the presence of additives such as SA can noticeably modify the equilibrium moisture content of the final product under the same storage conditions. At these circumstances, it is crucial to knowledge the hygroscopic behavior of compounds present in food and non-food formulations. To understand the SA water sorption features and to estimate its optimal storage conditions, some thermodynamic properties can be evaluated such as differential heat of sorption and differential entropy, as well as the integral enthalpy and entropy (Zhang et al., 2016). The differential enthalpy of sorption is an indicator of the water binding strength to the solid, meanwhile the differential entropy is proportional to the number of available sorption site corresponding to a specific energy level (Koksharov et al., 2021). On the other hand, the integral enthalpy provides an indication of the total energy available to do work, and the integral entropy describes the degree of disorder and randomness of motion of water molecules (Moreira et al., 2008).

There are some studies concerning the water sorption isotherms of alginates. For instance, Galus and Lenart (2013) studied the water adsorption isotherms of SA at 25°C, and the experimental data were successfully fitted by Peleg's model. Adamczak et al. (2017) determined water adsorption and desorption isotherms of SA at 25°C, with slightly higher moisture content for desorption in comparison to adsorption process. Xiao and Tong (2013) employed GAB model to fit experimental data of water adsorption of low-viscosity SA in the temperature range from 25 to 45°C.

Previous results indicate discrepancies in the literature regarding hygroscopic properties of SA due to probably the different sources and extraction procedures employed to obtain commercial SA. To the best of our knowledge, no studies relating the sorption isotherms features with the structural features of alginates were found. Therefore, the goals of this study were to: 1. determine water sorption characteristics of SA with different M/G ratios and their modeling using the Halsey model; 2. evaluate some thermodynamic properties to understand sorption phenomena in depth and to assess the optimal storage conditions for dried SA; and 3. establish the relationship between M/G ratio of the different SA and the corresponding water sorption isotherms.

2 | MATERIALS AND METHODS

2.1 | Materials

Processed and commercial sodium alginates (SA) were used. Specifically, processed SA from *Ascophyllum nodosum* brown seaweeds was obtained using a previously reported methodology (Montes et al., 2021), seaweeds pellets dried at 50°C (50D). Commercial sodium alginates (CAS No. 9005-38-3) were purchased from Sigma-Aldrich Chemical Company (S) (Lot MKCJ1280, St. Louis, MO, USA) and PanReac (P) (Lot 0F009964, Barcelona, Spain). Average viscosimetric molecular weights (M_v, kg/mol), P (459 ± 8), S (156 ± 2), and 50D (257 ± 1) and the corresponding average block length, mannuronate-guluronate ratio (M/G), P (1.15), S (0.91) and 50D (1.21), diads (F_{GG}), P(0.23), S (0.35) and 50D (0.20) and triads (F_{GGG}) P(0.13), S (0.30) and 50D (0.10), were previously determined by Montes et al. (2021).

2.2 | Determination of water desorption isotherms

A gravimetric technique was carried out to determine the equilibrium moisture content of SA samples. Firstly, samples were hydrated for 3 weeks until constant weight. Then, several jars were prepared with different saturated salt solutions to obtain atmospheres with constant water activity. The salt solutions used were LiCl, $MgCl_2$, $Mg(NO_3)_2$, NaCl, KCl, and $BaCl_2$, which were prepared according to Moreira et al. (2008). The range of relative humidity of air achieved with these salts was within the interval 11%–90%. The samples (0.5 g), previously weighted, were placed in glass jars and introduced in the flasks at three temperatures: 20, 37, and 50°C (±0.1°C). Thymol was introduced in the jars to inhibit microbial growth at relative humidity higher than 0.6.

An analytical balance (SI-234, Denver Instrument, ±0.0005 g) was used to weight the samples at regular intervals until constant weight. The time required to achieve the equilibrium was about 12 weeks. The moisture content was determined using a vacuum oven (Vacutherm VT650, Heraeus Hanau) at 70°C and 13 kPa until achieve constant weight. The equilibrium moisture content (X) was

measured for all samples, and the water sorption isotherms curves were plotted as X versus a_w. All experiments were done at least in duplicate.

2.3 | Data analysis

2.3.1 | Sorption isotherms models

The experimental results were fitted by Halsey model, Equation (1):

$$X = \left(\frac{-A}{T \ln (a_w)}\right)^{\frac{1}{r}} \quad (1)$$

where X is the equilibrium moisture content (kg water/kg dry solid, d.b.), a_w is the water activity, T (K) is the absolute temperature, and A and r are the fitting parameters of Halsey model.

2.3.2 | Differential and integral enthalpy and entropy

The complete and detailed procedure is explained in Moreira et al. (2008). Briefly, the isosteric heat of sorption, Q_{st} (kJ/mol), (or differential enthalpy) is an indicator of the state of water absorbed by the solid material and is defined by Equation (2):

$$Q_{st} = q_{st} + H_L \quad (2)$$

where q_{st} (kJ/mol) is the net isosteric heat of sorption, and H_L (kJ/mol) is the heat of vaporization of water at the sorption temperature. Using the Clausius–Clapeyron relationship, q_{st} at constant X can be evaluated from the experimental data by Equation (3):

$$q_{st} = -R\left[\frac{d\ln a_w}{d(1/T)}\right]_X \quad (3)$$

where R (kJ/mol K) is the universal constant of gases.

The differential entropy, S_d (kJ/mol K), of water adsorption can be calculated from Gibbs–Helmholtz equation and substituting the Gibbs energy by its definition, a linear equation, Equation (4), involving Q_{st}, S_d, and a_w, is obtained:

$$\ln (a_w)\big|_X = \frac{Q_{st}}{RT} - \frac{S_d}{R} \quad (4)$$

where the S_d value can be calculated from the intercept (S_d/R).

The net integral enthalpy, q_{eq} (kJ/mol), must be evaluated at constant spreading pressure, $\emptyset$ (J/m^2), according to Equation (5):

$$q_{eq} = -R\left[\frac{d \ln (a_w)}{d(1/T)}\right]_{\emptyset} \quad (5)$$

The spreading pressure represents the surface excess free energy and provides an indication of the increase in surface tension of bare sorption sites due to adsorbed molecules (Fasina et al., 1999). This property cannot be experimentally measured but can be estimated by Equation (6).

$$\emptyset = \frac{K_B T}{A_m} a^{1/r}\left[\frac{1}{\left(\frac{1}{r}-1\right)\left(-\ln(a_w)\right)^{\frac{1}{r}-1}}\right]_{0.05}^{a_w} \quad (6)$$

where K_B is the Boltzmann's constant (1.38×10^{-23} J/K), A_m represents the area of a water molecule (1.06×10^{-19} m^2), a is A/T.

Finally, the net integral entropy, S_{eq} (kJ/mol K), is calculated by Equation (7):

$$S_{eq} = \frac{-q_{eq}}{T} - R \ln (a_w) \quad (7)$$

where a_w is obtained at constant $\emptyset$ at different T.

2.4 | Statistical analysis

Experimental data were analyzed through one-factor analysis of variance (ANOVA), followed by the Duncan test, and considering significant p values <0.05 (IBM SPSS Statistics 27, SPSS Inc). All experimental results were expressed as mean ± standard deviation from at least duplicate experiments.

The goodness of fitting of Halsey model was estimated by two statistical indices previously proposed by Moreira et al. (2017), φ (Equation [8]), which is a lumped measure and involves the coefficient of determination (R^2), the root mean squared error (RMSE) and the mean relative deviation (MRD), and χ^2. If φ shows low values, the model shows a poor adequacy to describe the experimental behavior, and if the value of $\chi^2 \geq 5.99$, the model should be rejected with $p > 0.95$.

$$\varphi = \frac{R^2}{(\text{RMSE})(\text{MRD})} \quad (8)$$

3 | RESULTS AND DISCUSSION

3.1 | Experimental water desorption isotherms and modeling

Experimental data of equilibrium water desorption isotherms of different sodium alginates (SA) at 20, 37, and 50°C are depicted in Figure 1. Water sorption isotherms can be classified as type III according to BET classification (Brunauer et al., 1940). All tested SA showed the same temperature trend at constant water activity, X decreased with increasing temperature. In all cases, at a constant temperature, the equilibrium moisture content (X) increased with increasing water activity (a_w). However, two different regions in

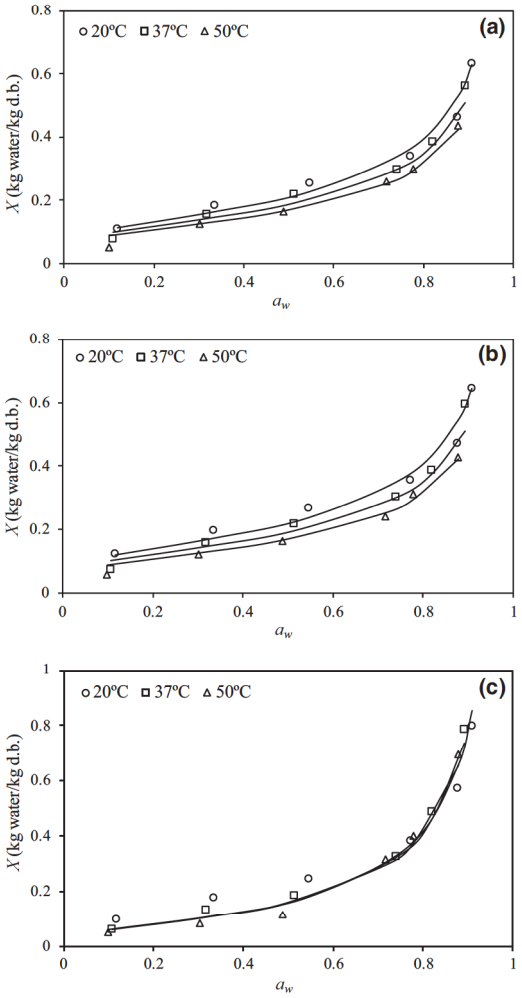

FIGURE 1 Water desorption isotherms of different alginates: (a) from sigma (S), (b) from PanReac (P), and (c) processed (50D) at 20, 37, and 50°C. lines correspond to Halsey model (Equation [1]).

the isotherm curves can be observed. Firstly, a linear trend was observed at low and intermediate a_w values (from 0.1 to 0.5), this region is called multilayer sorption region. Secondly, at higher a_w values, the capillary condensation region can be observed by the pronounced increase of X with increasing a_w. Significant differences were found between tested SA in this last region ($a_w > 0.5$). Particularly, X value at the highest a_w (0.9) was approximately 0.6 (kg/kg d.b.) for S and P alginates (without significant differences between them) and 0.8 (kg/kg d.b.) for 50D. However, below 0.5 of a_w, no significant differences ($p \leq 0.05$) were found between tested SA. These results partly agree with those reported previously by Galus and Lenart (2013) at 25°C, that is, at a_w of 0.5 X was 0.25 (kg/kg d.b.); however, at a_w of 0.9 these authors found higher moisture content value (1.3 kg/kg d.b.) for adsorption process. Also, Adamczak et al. (2017) reported higher X values (up to 1.16 kg/kg d.b. at a_w of 0.9), for the water adsorption stage at 25°C. However, Shimanuki et al. (2020) determined, at the same high a_w value, a moisture content approximately 0.5 kg/kg d.b that agreed with results obtained for S and P alginates tested in the present study. Finally, Xiao and Tong (2013) found for water adsorption of low-viscosity SA at 25°C an equilibrium moisture content of 0.4 kg/kg d.b. at a_w of 0.90.

The Halsey model was employed to fit experimental data, desorption isotherms are plotted in Figure 1 by continuous lines, and the corresponding fitting parameters are presented in Table 1. No significant differences ($p \leq 0.05$) between Halsey parameters (A and r) for S and P alginates at constant temperature. For these alginates, A values decreased (from 12.08 to 8.73 and from 12.46 to 8.42, respectively) with increasing temperature. However, for 50D, A values increased (from 23.21 to 25.28) with temperature. Interestingly, a (A/T) parameter value was invariant with temperature in the case of 50D alginate. In all cases, the r values were invariant with temperature for each alginate, and 50D showed the lowest value (1.187), meaning the highest slope of the isotherm curve, against S and P alginates (around 1.820).

3.2 | Thermodynamic properties

3.2.1 | Differential enthalpy and entropy

Figure 2a shows the variation of the differential enthalpy (q_{st}), evaluated by means of Equation (3), with the moisture content of tested alginates at arithmetic mean temperature (35.7°C). At low moisture content, there are high attractive intermolecular forces between alginate surface and adsorbed water. Afterward, a sharp fall in the q_{st} values is observed when moisture content increases from 0.08 to 0.2 kg/kg d.b., because water molecules are adsorbed in other available sites with lower specific energy (Polachini et al., 2016). Subsequently q_{st} values dramatically decreased and at moisture content above 0.3 kg/kg d.b., water molecules multilayers were formed and progressively approached zero meaning that the adsorption of a water molecule involved an energy equivalent to the heat of vaporization of Xiao and Tong (2013) employing low-viscosity SA observed this effect, but the values obtained (10 kJ/mol at X of 0.1 kg/kg d.b.) were lower than the values of this work (60 kJ/mol at X of 0.1 kg/kg d.b.). The highest q_{st} values found at low X (<0.25 kg/kg d.b.) were for P alginate.

Figure 2b shows the trend of differential entropy (S_d), Equation (4), with moisture content of tested alginates at 35°C. S_d is proportional to the number of available sorption sites at a specific energy level. Negative values are related to the loss of mobility of water molecules during sorption. The S_d values increased continuously at low moisture content (below 0.20 kg/kg d.b.) and above this content remained practically constant. At low moisture content, water molecules were strongly retained (high activation energies) in many available sorption sites, but these sites were progressively occupied with increasing moisture content (Madamba et al., 1996).

TABLE 1 Values of the parameters of Halsey model (Equation 1) and goodness of fitting for water sorption isotherms of commercial S (sigma) and P (PanReac) and processed (50D) alginates

Sample	S			P			50D		
T (K)	293.1	310.1	323.1	293.1	310.1	323.1	293.1	310.1	323.1
A	12.08 ± 0.84^{a,B}	10.18 ± 0.77^{ab,B}	8.73 ± 0.71^{b,B}	12.46 ± 1.03^{a,B}	10.17 ± 0.96^{ab,B}	8.42 ± 0.91^{b,B}	23.21 ± 1.02^{a,A}	24.38 ± 1.48^{ab,A}	25.28 ± 0.84^{b,A}
$a = A/T$	0.041 ± 0.003^{a,B}	0.033 ± 0.003^{b,B}	0.027 ± 0.002^{b,B}	0.043 ± 0.004^{a,B}	0.033 ± 0.003^{ab,B}	0.026 ± 0.003^{b,B}	0.079 ± 0.002^{a,A}	0.079 ± 0.004^{a,A}	0.078 ± 0.005^{a,A}
r	1.815 ± 0.076^{A}			1.847 ± 0.027^{A}			1.187 ± 0.012^{B}		
φ^{*}	347.5	308.1	1287.5	293.8	183.6	261.3	65.7	319.8	152.8
χ^{2**}	4.2	3.3	5.4	3.9	5.6	1.1	1.0	0.6	0.1

Note: Data are presented as mean ± standard deviation. Data value of each parameter with different superscript lowercase letters are significantly different by temperature and capital letters by alginate at constant temperature ($p < 0.05$).

*Low values of φ indicate a poor adequacy of the model; **With value $\chi^2 \geq 5.99$, the model should be rejected ($p > 0.95$).

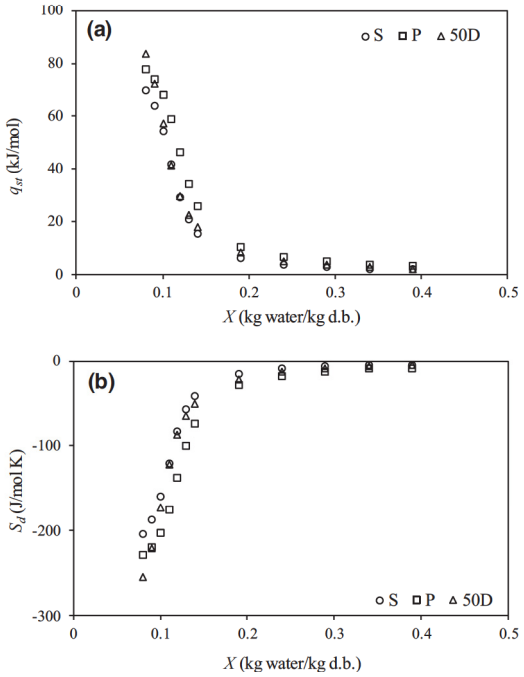

FIGURE 2 Effect of moisture content, X, on the net isosteric heat of sorption, q_{st}, (a) and differential entropy, S_d, (b) for sigma (S), PanReac (P), and processed (50D) alginates.

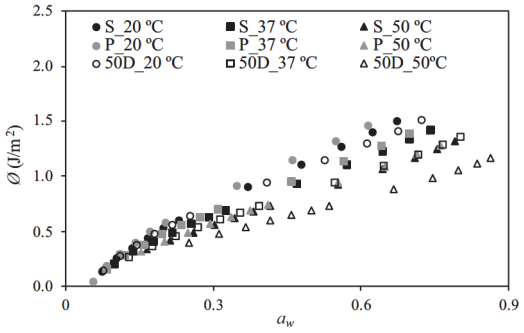

FIGURE 3 Spreading pressure, Ø, versus water activity, a_w, at different temperatures for alginates (a) from sigma (S), (b) from PanReac (P), and (c) processed alginate (50D).

The theory of compensation needs to be applicable that isokinetic (T_i) and harmonic mean (T_h) temperatures are different and, in the range of moisture content studied, the existence of a linear relationship between differential enthalpy and differential entropy (Moreira et al., 2008). The linear relationship was verified by the plotting of q_{st} versus S_d and from the slope T_i values were obtained (340, 337 and 329 K for S, P and 50D, respectively), and T_h was

308 K. As $T_l > T_h$ in all cases, the water sorption of tested alginates can be characterized as enthalpy-driven (Moreira et al., 2016).

3.2.2 | Integral enthalpy and entropy

Figure 3 shows the spreading pressure, calculated by means of Equation (6), as a function of a_w for tested alginates at studied temperatures. The spreading pressure increased (up to 1.50 J/m^2) with increasing a_w and decreased with increasing temperature in all cases. Slight differences were found between spreading pressure values of S and P alginates at constant temperature, and values of 50D alginate were systematically lower. In fact, the ø values for S and P at 50°C were similar to 50D values at 37°C. These trends agreed with results reported for alginates by Xiao and Tong (2013), but with lower values (<0.1 J/m^2).

Figure 4a shows the variation of the net integral enthalpy, q_{eq}, calculated with Equation (5) at constant spreading pressure, with the moisture content. At low X, q_{eq} increased up to achieve maximum values (9.8, 11.0 and 15.2 kJ/mol for S, P, and 50D, respectively) and then continuously decreased with increasing X. On the other hand, the net integral entropy, S_{eq} evaluated with Equation (7), decreased at low X reaching a minimum value (−24.9, −28.7 and −42.2 J/mol K for S, P and 50D, respectively), Figure 4b. Both enthalpy and entropy trends with moisture content reflect the transition from the water molecules occupation of easily accessible sites to localized binding followed by the formation of multi-layers (Moreira et al., 2008).

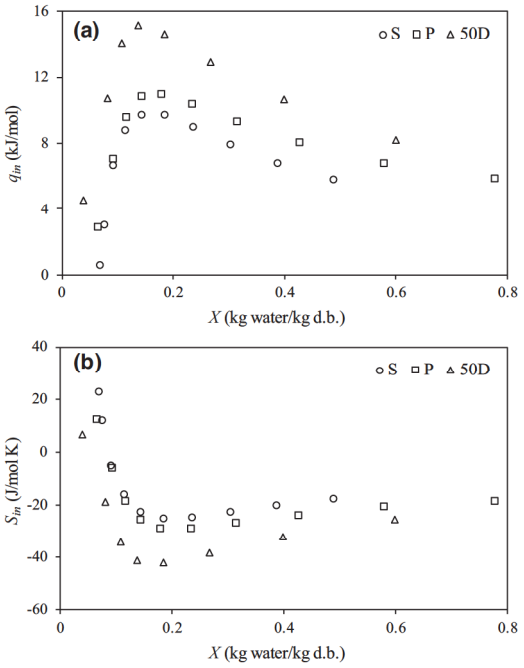

FIGURE 4 Effect of moisture content, X, on the integral enthalpy, q_{in}, (a) and on the integral entropy, S_{in}, (b) for alginates: Alginate from sigma (S), alginate from PanReac (P), and processed alginate (50D).

Regarding the integral enthalpy and entropy curves, the maximum enthalpy and minimum entropy values occurred at the same narrow moisture content range from 0.15 to 0.2 kg/kg d.b., for tested alginates. The minimum integral entropy determines the water activity at which the food product has the highest stability, and additionally, other authors indicated that maximum enthalpy is achieved with the formation of a monolayer of adsorbed water (Kaya & Kahyaoglu, 2007). In this case, it means that maximum stability (optimal water activity) is achieved in the interval from 0.35 to 0.45 for S and P alginates and from 0.40 to 0.50 for 50D alginate.

3.3 | Relationship between equilibrium moisture content and M/G ratio of alginates

To find a relationship between structural features of alginates and water molecules sorption on the sample surface, the water activity range must be restricted to the water activity range in which the water monolayer is formed. In this case, this a_w interval was below 0.4. Parameters of Halsey model (Table 1) were employed to find correlations with M/G ratio of tested alginates. Firstly, a linear regression ($R^2 > 0.9$) was established between guluronate, G, fraction ($G/[M+G]$) values, and the r parameter from Halsey model. Extrapolating this linear regression to guluronate fraction values of zero and one ($G = 0$ and $M = 0$), it could be possible to obtain r values corresponding to hypothetical alginate formed exclusively by M ($r_M = 2.074$) and by G ($r_G = 0.560$), respectively. The water content of alginate can be assumed as the sum of water adsorbed on guluronate (X_G) and mannuronate (X_M) surface (Equations [9] and [10]).

$$X_G = G\left(\frac{-a_G}{\ln a_w}\right)^{\frac{1}{r_G}} \tag{9}$$

$$X_M = (1-G)\left(\frac{-a_M}{\ln a_w}\right)^{\frac{1}{r_M}} \tag{10}$$

where a_G and a_M are the corresponding parameters for G and M of Halsey model.

The a_G and a_M values were obtained by means of a multivariable optimization procedure with the following objective, Equation (11):

$$\min\left[\sum_{a_w=0.1}^{a_w=0.4} X - G\left(\frac{-a_G}{\ln a_w}\right)^{\frac{1}{r_G}} - (1-G)\left(\frac{-a_M}{\ln a_w}\right)^{\frac{1}{r_M}}\right] \tag{11}$$

where X were the moisture content values given by Halsey model. This procedure was applied to each alginate at constant temperature. As chemical characteristics of M and G are independent of the type of alginate, average a_G and a_M values were obtained after individual optimization of each alginate. The a_G and a_M values were 0.30, 0.26, and 0.24 and 0.052, 0.035, and 0.019 at 20, 37, and 50°C, respectively.

These values were linearly correlated ($R^2 > 0.99$) with temperature. Therefore, an equation useful to estimate the equilibrium moisture content of alginate with its guluronate and mannuronate content at different temperatures is given by Equation (12):

$$X = X_G + X_M = G\left(\frac{-0.9616 + 0.002246\,T}{\ln a_w}\right)^{\frac{1}{0.5604}} + (1-G)\left(\frac{-0.3772 + 0.001107\,T}{\ln a_w}\right)^{\frac{1}{2.0742}} \quad (12)$$

Analyzing Equation (12), it was observed that the X value was mainly due to the contribution of X_M meaning that M was more hygroscopic than G. For instance, in S alginate at 20°C and at $a_w = 0.2$, the contribution of X_M to the total adsorbed water was 69.7% and at the same conditions achieved 73.7% and 84.2% in the case of P and 50D alginates. The X_M contribution decreased with increasing a_w (i.e., at $a_w = 0.4$, 59.1, 63.5 and 76.4% for S, P and 50D alginates, respectively). As example, Figure 5 shows the X_M and X_G contributions to the total equilibrium moisture content of 50D alginate at 20 and 50°C. An acceptable agreement can be observed between the water sorption isotherm fitted by Halsey model and the proposed model given by Equation (12).

Shimanuki et al. (2020) demonstrated that, at very low moisture content, helical structures formed by short molecular chains present in alginates are composed exclusively of G blocks. Therefore, under these conditions, the surface of G units was not completely available to adsorb water so easily as M units. The 50D alginate was the tested sample with the highest amount of M units ($M/G = 1.21$) and S the lowest ($M/G = 0.91$), but P showed a M/G (1.15) closer 50D. It seems that exclusively the relative amount of G is not enough to explain these differences. Nevertheless, S alginate contained a greater number of diads F_{GG} (0.35) and triads F_{GGG} (0.30) than P (0.23 and 0.13) and 50D (0.20 and 0.10) alginates. This fact could explain the existence of more helical structures formed by G blocks in S alginate and the contribution of X_G to total adsorbed water consequently decreased. Helical structures were progressively disappearing with water adsorption (higher a_w values) and the contribution of X_G increased with the creation of new available surfaces.

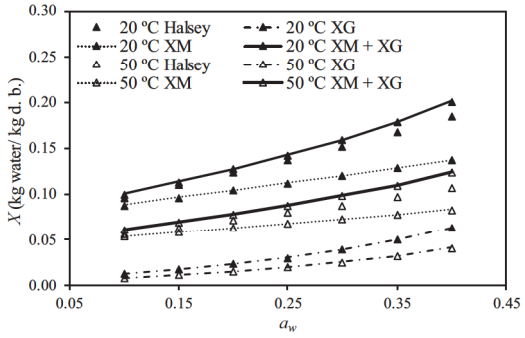

FIGURE 5 Water sorption isotherms of 50D alginate at 20 and 50°C estimated by Halsey model and Equation (12) ($X_M + X_G$) at low water activity, a_w, with the contributions of M (X_M) and G (X_G) fractions.

4 | CONCLUSIONS

No significant differences were found between tested commercial alginates, and processed alginate was the most hygroscopic one. Halsey model was chosen to fit adequately for describing experimental desorption isotherm data for several alginates in the temperature range from 25 to 50°C. The differential enthalpy and entropy of sorption for all samples decreased and increased, respectively, exponentially with increasing moisture content to 0.15–0.20 kg/kg d.b., then decreased slowly to near zero at higher moisture content, due to a decrease of binding energies between water molecules and sorption sites with increasing moisture content. Integral enthalpy and entropy showed respective maximum and minimum values in the interval from 0.15 to 0.20 kg/kg d.b. Alginates must be dried up to this moisture content to achieve optimum stability during storage. A model based on the structural features of alginate was proposed and satisfactorily tested to predict the equilibrium moisture content of alginates at low water activity values (<0.4). Mannuronate, M, was more hygroscopic than guluronate, G, and consequently, a higher amount of M in the alginate increases its hygroscopicity. Nevertheless, the presence of helical structures formed by G blocks must be also considered in a more complex structural model.

AUTHOR CONTRIBUTIONS

Leticia Montes: Conceptualization; Data curation; Formal analysis; Investigation; Validation; Methodology; Writing—original draft. Mauro Gisbert: Formal analysis; Validation; Writing—review & editing. Ramón Moreira: Conceptualization; Methodology; Writing—review & editing; Project administration; Supervision; Funding acquisition.

FUNDING INFORMATION

Authors acknowledge the financial support of the Spanish Ministry of Science and Innovation (Project RTI2018-095919-B-C2) and the European Regional Development Fund (FEDER) and Xunta de Galicia (Consolidation Project ED431B 2019/01).

CONFLICT OF INTEREST

The authors declared no conflicts of interest for this article.

DATA AVAILABILITY STATEMENT

Data available on request due to privacy/ethical restrictions.

ORCID

Leticia Montes https://orcid.org/0000-0001-9758-4142
Mauro Gisbert https://orcid.org/0000-0001-5923-4651
Ramón Moreira https://orcid.org/0000-0002-6388-0063

REFERENCES

Abka-Khajouei, R., Tounsi, L., Shahabi, N., Patel, A. K., Abdelkafi, S., & Michaud, P. (2022). Structures, properties and applications of alginates. *Marine Drugs*, *20*, 364. https://doi.org/10.3390/md20060364

Adamczak, M. I., Martinsen, Ø. G., Smistad, G., & Hiorth, M. (2017). Polymer coated mucoadhesive liposomes intended for the management of xerostomia. *International Journal of Pharmaceutics*, *527*, 72–78. https://doi.org/10.1016/j.ijpharm.2017.05.032

Brunauer, S., Deming, L. S., Deming, W. E., & Teller, E. (1940). On theory of the van der Waals adsorption of glass. *Journal of the American Chemistry Society*, *62*, 1723–1732. https://doi.org/10.1021/ja01864a025

Chee, S. Y., Wong, P. K., & Wong, C. L. (2011). Extraction and characterisation of alginate from brown seaweeds (Fucales, Phaeophyceae) collected from Port Dickson, peninsular Malaysia. *Journal of Applied Phycology*, *23*, 191–196. https://doi.org/10.1007/s10811-010-9533-7

Fasina, O. O., Ajibola, O. O., & Tyler, R. T. (1999). Thermodynamics of moisture sorption in winged bean seed and gari. *Journal of Food Process Engineering*, *22*, 405–418. https://doi.org/10.1111/j.1745-4530.1999.tb00496.x

Fernando, I. P. S., Lee, W., Han, E. J., & Ahn, G. (2020). Alginate-based nanomaterials: Fabrication techniques, properties, and applications. *Chemical Engineering Journal*, *391*, 123823. https://doi.org/10.1016/j.cej.2019.123823

Galus, S., & Lenart, A. (2013). Development and characterization of composite edible films based on sodium alginate and pectin. *Journal of Food Engineering*, *115*, 459–465. https://doi.org/10.1016/j.jfoodeng.2012.03.006

Halsey, G. (1948). Physical adsorption on non-uniform surfaces. *The Journal of Chemical Physics*, *16*, 931–937. https://doi.org/10.1063/1.1746689

Kaya, K., & Kahyaoglu, T. (2007). Moisture sorption and thermodynamic properties of safflower petals and tarragon. *Journal of Food Engineering*, *78*, 413–421. https://doi.org/10.1016/j.jfoodeng.2005.10.009

Koksharov, S. A., Aleeva, S. V., Lepilova, O. V., Krichevskii, G. E., & Fidorovskaya, Y. S. (2021). The properties of sodium alginate hydrocolloids upon sorption binding of papain. *Colloid Journal*, *83*, 722–736. https://doi.org/10.1134/S1061933X21060077

Kurek, M., Guinault, A., Voilley, A., Galic, K., & Debeaufort, F. (2014). Effect of relative humidity on carvacrol release and permeation properties of chitosan based films and coating. *Food Chemistry*, *144*, 9–17. https://doi.org/10.1016/j.foodchem.2012.11.132

Lee, K. Y., & Mooney, D. J. (2012). Alginate: Properties and biomedical applications. *Progress in Polymer Science*, *1*, 106–126. https://doi.org/10.1016/j.progpolymsci.2011.06.003

Madamba, P. S., Driscoll, R. H., & Buckle, K. A. (1996). Enthalpy-entropy compensation models for sorption and browning of garlic. *Journal of Food Engineering*, *28*, 109–119. https://doi.org/10.1016/0260-8774(94)00072-7

Montes, L., Gisbert, M., Hinojosa, I., Sineiro, J., & Moreira, R. (2021). Impact of drying on the sodium alginate obtained after polyphenols ultrasound-assisted extraction from *Ascophyllum nodosum* seaweeds. *Carbohydrate Polymers*, *272*, 118455. https://doi.org/10.1016/j.carbpol.2021.118455

Moreira, R., Chenlo, F., Sineiro, J., Sánchez, M., & Arufe, S. (2016). Water sorption isotherms and air drying kinetics modelling of brown seaweed *Bifurcaria bifurcata*. *Journal of Applied Phycology*, *28*, 609–618. https://doi.org/10.1007/s10811-015-0553-1

Moreira, R., Chenlo, F., & Torres, M. D. (2009). Simplified algorithm for the prediction of water sorption isotherms of fruits, vegetables and legumes based on chemical composition. *Journal of Food Engineering*, *94*, 334–343. https://doi.org/10.1016/j.jfoodeng.2009.03.026

Moreira, R., Chenlo, F., Torres, M. D., & Prieto, D. M. (2017). Statistical criteria for modelling of water desorption isotherms of sugars. Estimation of sucrose hygroscopic properties from glucose and fructose data. *Advances in Food Science and Engineering*, *1*, 18–27. https://doi.org/10.22606/afse.2017.11003

Moreira, R., Chenlo, F., Torres, M. D., & Vallejo, N. (2008). Thermodynamic analysis of experimental sorption isotherms of loquat and quince fruits. *Journal of Food Engineering*, *88*, 514–521. https://doi.org/10.1016/j.jfoodeng.2008.03.011

Polachini, T. C., Betiol, L. F. L., Lopes-Filho, J. F., & Telis-Romero, J. (2016). Water adsorption isotherms and thermodynamic properties of cassava bagasse. *Thermochimica Acta*, *632*, 79–85. https://doi.org/10.1016/j.tca.2016.03.032

Qin, Y., Jiang, J., Zhao, L., Zhang, J., & Wang, F. (2018). Applications of alginate as a functional food ingredient. In A. M. Grumezescu & A. M. Holban (Eds.), *Biopolymers for food design* (pp. 409–429). Academic Press. https://doi.org/10.1016/B978-0-12-811449-0.00013-X

Shimanuki, N., Imai, M., & Nagai, K. (2020). Effects of counter cations on the water vapor sorption properties of alginic acid and alginates. *Journal of Applied Polymer Science*, *137*, 49326. https://doi.org/10.1002/app.49326

Shivhare, U. S., Arora, S., Ahmed, J., & Raghavan, G. S. V. (2004). Moisture adsorption isotherms for mushroom. *LWT-Food Science and Technology*, *37*, 133–137. https://doi.org/10.1016/S0023-6438(03)00135-X

Xiao, Q., & Tong, Q. (2013). Thermodynamic properties of moisture sorption in pullulan-sodium alginate based edible films. *Food Research International*, *54*, 1605–1612. https://doi.org/10.1016/j.foodres.2013.09.019

Zhang, H., Bai, Y., Zhao, X., & Duan, R. (2016). Water desorption isotherm and its thermodynamic analysis of glutinous rice flour. *American Journal of Food Technology*, *11*, 115–124. https://doi.org/10.3923/ajft.2016.115.124

How to cite this article: Montes, L., Gisbert, M., & Moreira, R. (2022). Water sorption isotherms of different sodium alginates: Thermodynamic evaluation and influence of mannuronate-guluronate copolymers. *Journal of Food Processing and Preservation*, *00*, e17179. https://doi.org/10.1111/jfpp.17179

PUBLICATION 3

Effect of the addition of different sodium alginates on viscoelastic, structural features and hydrolysis kinetics of corn starch gels

Food Bioscience, 47, 101628 (2022)

Food Bioscience 47 (2022) 101628

Contents lists available at ScienceDirect

Food Bioscience

journal homepage: www.elsevier.com/locate/fbio

Effect of the addition of different sodium alginates on viscoelastic, structural features and hydrolysis kinetics of corn starch gels

Leticia Montes [a], Maria Santamaria [b], Raquel Garzon [b], Cristina M. Rosell [b], Ramón Moreira [a,*]

[a] Department of Chemical Engineering, Universidade de Santiago de Compostela, rúa Lope Gómez de Marzoa, s/n, 15782, Santiago de Compostela, Spain
[b] Institute of Agrochemistry and Food Technology (IATA-CSIC). C/Agustin Escardino, 7, 46980, Paterna, Spain

ARTICLE INFO

Keywords:
Biopolymers
In vitro digestion
Average molecular weight
Rheology
Scanning electron microscopy (SEM)

ABSTRACT

Corn starch gels (1:4 w:w) were made with the addition (up to 2% w/w starch basis) of sodium alginates of different average molecular sizes and nature. Rheology of the starchy gels were characterized to evaluate their viscoelasticity. Gels were subjected to *in vitro* digestion to estimate the effect of alginates addition on glycemic response. Tested alginates significantly decreased the value of the elastic modulus of gels. The coordination number obtained from complex modulus indicated that in general, less compact structures were obtained in the presence of alginates. These results were confirmed by scanning electron micrographs, where significant differences in the structure of alginate-corn starch gels were observed, but molecular size of alginates was not critical. Hydrolysis rate decreased with the presence of alginates in corn starch gels by interactions of alginates with leached amylose. At high alginate content, slower hydrolysis rates were determined when the most hygroscopic alginates were added.

1. Introduction

Sodium alginate (SA) is a polyuronic saccharide that is isolated from different brown seaweeds species around the world. SA is a copolymer composed of β-D-mannuronic acid (M) and α-L-guluronic acid (G). Alginates have extense industrial uses, like as thickener, in the paper industry, dye in textile industry, and binder in food industry (Kour et al., 2022). Copolymer features (M/G ratio, average block length, etc) depend on natural source, and molecular size is influenced by the process conditions employed during extraction, drying, and isolation, among other operations where alginate depolymerization could be promoted (Montes et al., 2021).

Starch is one of the most important functional food biopolymers. It can be extracted from many natural sources such as cereals, tubers and pulses. Starch is composed of two different glucose polymers: amylose, linear polymer, and amylopectin, branched polymer, joined by glycosidic bounds (Schwartz et al., 2014). Many hydrocolloids have been added to starchy systems to modify some features (texture, control moisture or water mobility) and improve the quality and stability of food products (Rosell et al., 2011). Sodium alginate (Feng et al., 2019), guar gum (Yadav et al., 2018), pectin (Fang et al., 2020), high methoxylated pectin, guar gum, CMC, xanthan gum or HPMC (Gularte & Rosell, 2011) are among the hydrocolloids used in food applications. Particularly, alginate can be used to retard the starch retrogradation during cooling and storage stage. The interaction between alginate and starch displayed a retarding effect on the starch retrogradation, which was correlated with the amylose reaggregation and amylopectin recrystallization (Yu et al., 2018).

Regarding rheological effect of SA addition on starchy systems, several studies were reported. Li et al. (2017) found that the SA addition (0–4% w/w, starch basis) decreased the gel firmness, retrogradation enthalpy, storage modulus (G') and swelling power of corn starch gels obtained after heating at 95 °C for 10 min. Sun et al. (2013) showed that corn starch (10% w/w) with sodium alginate (1% w/w, solids total basis) decreased pasting temperature, peak and final viscosities, break down and setback values. Also, Ji et al. (2017) reported that corn starch (6% w/w) with sodium alginate (1% w/w, starch basis) decreased G', complex viscosity and damping factor (tan δ) values. Same behaviour was reported for other starch sources. In fact, Feng et al. (2019) demonstrated that the addition (0.5% w/w, starch basis) of SA to sweet potato starch (10% w/w) decreased viscoelasticity and starch digestibility. However, Yang et al. (2021) studied rice starch (5% w/v

* Corresponding author. Universidade de Santiago de Compostela, rúa Lope Gómez de Marzoa, s/n, 15782, Santiago de Compostela, Spain.
E-mail addresses: leticia.montes.martinez@usc.es (L. Montes), masanar@iata.csic.es (M. Santamaria), r.garzon@iata.csic.es (R. Garzon), crosell@iata.csic.es (C.M. Rosell), ramon.moreira@usc.es (R. Moreira).

https://doi.org/10.1016/j.fbio.2022.101628
Received 12 October 2021; Received in revised form 1 February 2022; Accepted 17 February 2022
Available online 22 February 2022

water) added with SA (<0.50% w/v, starch basis) and observed a viscoelasticity increase. On the other hand, He et al. (2019) and Fang et al. (2020) showed that rice starch (10% w/w) and waxy potato starch (10% w/w), respectively, in presence of alginate (0.15% w/v and 1% w/w, starch basis) decreased G' and increased tan δ. These results showed that different effect of SA addition on rheological behaviour can be found in the literature and more research is necessary. Obviously, the experimental procedure to gelatinize the starch could partly explain the mentioned differences, but the somewhat the impact of SA characteristics can not be discarded.

The process of digestion involves the breakdown of a complex molecule (i.e., starch) into the simplest form (i.e., glucose). For simulating digestion processes, *in vitro* methods are widely used to study the intestinal behaviour of food (Sensoy, 2021). Most of the studies on the *in vitro* digestion of starch have focused on the intestinal stage. Using *in vitro* protocols, levels of rapidly digestible starch (RDS), slowly digestible starch (SDS), resistant starch (RS) and total starch (TS) of a gel can be calculated (Tuaño et al., 2021). However, the effect of the gel structure on the starch digestion is poorly studied. Food structure can influence in the starch digestion (Zheng et al., 2021), and this fact is also valid for starch gels (Santamaria et al., 2021).

The incorporation of hydrocolloids in the food matrix could decrease the starch digestion due to blocking the interactions between substrate-enzyme or the direct impact on the active site of enzymes (Yemenicioğlu et al., 2020). Hydrocolloid's addition in starch-based food was associated with a decrease in starch digestion and related to a lower glycaemic index (Gularte & Rosell, 2011; Yuris et al., 2019). Furthermore, this impact was also reported with the addition of SA (Feng et al., 2019). This biopolymer could protect starch granules against normal swelling and form a barrier between enzyme-starch reducing the enzymatic activity. Ramírez et al. (2015) associated the effect of viscosity increase and the molecular interactions between alginate-starch with the lower glucose content during *in vitro* digestion. Nevertheless, previous studies on alginate effect on starch digestibility have not focussed on the specific characteristics of alginates and commercial ones have been used.

In this study, several sodium alginates with different average viscosimetric molecular weights isolated in lab from *Ascophylum nodosum* brown seaweeds and commercial alginates were added to corn starch to determine the effects on rheological features during gel formation, structural features of formed gels and, finally, how the digestion kinetics are modified. Firstly, rheological properties and structure were analyzed. Secondly, the digestion kinetics were studied. Finally, relationships between starch gel structure and the digestion were established.

2. Materials and methods

2.1. Materials

Corn starch (CS) (initial moisture content of 12.25 g water · (100 g starch)$^{-1}$ (dry basis, d.b.)) was supplied by EPSA (Valencia, Spain). Commercial and lab-processed alginates were employed. Processed alginates from *Ascophyllum nodosum* seaweeds were obtained using a previously reported methodology (Montes et al., 2021), but drying temperature of seaweeds pellet was modified as follows: not dried (ND), dried at 50 °C (50D) and dried at 90 °C (90D). Furthermore, commercial sodium alginates (CAS No. 9005-38-3) from Sigma-Aldrich Chemical Company (S) (Lot MKCJ1280, St. Louis, MO, USA) and PanReac (P) (Lot 0F009964, Barcelone, Spain) were used as control (without knowledge of seaweeds source nor processing conditions). Average viscosimetric molecular weights (M_v, kg/mol), P (459 ± 8), S (156 ± 2), ND (428 ± 7), 50D (257 ± 1) and 90D (133 ± 1) of tested alginates were previously determined together with the corresponding average block length, mannuronate-guluronate ratio (Montes et al., 2021). The enzymes used were type VI-B α-amylase from porcine pancreas from Sigma-Aldrich Chemical Company (St. Louis, MO, USA) and amyloglucosidase from Novozymes (Bagsvaerd, Denmark). D-Glucose Assay Kit (GOPOD) was purchased to Megazyme (Megazyme International Ireland Ldt., Bray, Ireland). All solutions were prepared using distilled water and standards were prepared using deionized water.

2.2. Preparation of starch gels

Alginates were dispersed in distilled water and hydrated overnight. Then, corn starch was weighed and added to the alginate solutions. These mixtures were manually shaken for 60 s to facilitate their homogenization. Then mixtures were heated at 100 °C for 20 min with gentle manual stirring every 5 min during 10 s before gel formation. The starch gels were cooled (for 20 min) up to 37 °C for later analysis. The gels were prepared at constant corn starch:water ratio (1:4), with different added alginate content (0, 1 and 2% w/w, starch basis).

2.3. Water retention capacity

Corn starch and alginate-corn starch mixtures were characterized by means of water retention capacity (WRC). WRC was determined following the protocol established by Kassem et al. (2022). Briefly, the samples (1.5 g) were weighed and directly added to centrifuge tubes containing 15 mL of distilled water or alginate solutions (previously hydrated overnight). After mixtures equilibration (18 h), samples were centrifuged at 3000×*g* (7000 rpm in a 11192 rotor, Model 2–15, Sigma, Germany) at room temperature (22–25 °C) for 20 min. The supernatant was decanted, and fresh residue was weighed. Then, samples were dried up to constant weight (dry residue) at 70 °C under vacuum (<10 kPa). The WRC (kg kg^{-1}) was calculated by Equation (1).

$$WRC = \frac{Fresh\ residue\ weight - Dry\ residue\ weight}{Dry\ residue\ weight} \quad (1)$$

WRC of alginate-corn starch mixtures was employed to evaluate the WRC of alginates, WRCSA, by means of the Equation (2):

$$WRC_{SA} = \frac{WRC_{mixture} - WRC_{CS}\left(1 - \frac{w_{dSA}\ 100}{w_{dCS}}\right)}{\frac{w_{dSA}\ 100}{w_{dCS}}} \quad (2)$$

where WRC_{CS} is the water retention capacity of corn starch, w_{dSA} and w_{dCS} are the dry weights of sodium alginate and starch in the mixture, respectively.

2.4. Rheological behaviour

The rheological characterisation was performed with a stress-controlled rheometer (MCR 301; Anton Paar Physica, Graz, Austria) using a starch pasting cell (ST24-2D/2V/2V-30) (gap = 2.460 mm, bob radius = 12.000 mm) with a solvent trap kit to minimize water evaporation during tests. The selected protocol was defined to simulate the experimental conditions which were employed during gel preparation (described in section 2.2). Corn starch and corn alginate-starch mixtures were dispersed in distilled water and introduced into the rheometer cuvette at 95 °C. Firstly, a pre-shear of 100 s^{-1} was made for 1 min to homogenize the sample at 95 °C. Secondly, a time sweep was carried out at 95 °C for 19 min and then, a cooling ramp was performed from 95 to 37 °C at 3 °C/min at 30 Pa and 1 Hz in both stages. Then, strain sweep tests (0.1–10%) of gels at 1 Hz and 37 °C to obtain the linear viscoelasticity range (LVR) were performed (random strain sweep tests at 95 °C confirmed the validity of LVR measured at 37 °C in the range of tested temperatures). Finally, a second time sweep (30 Pa, 1 Hz) was carried out at 37 °C for 30 min to observe the maturation of the gel and a frequency sweep was made from 0.1 to 10 Hz at 1% strain and 37 °C. Complex modulus, G* (Pa), values evaluated from G' and G'' data obtained through angular frequency (ω, Hz) sweep tests, were correlated to the following power law (Bruno et al., 2021), Equation (3):

$$G^* = \sqrt{(G')^2 + (G'')^2} = A\, w^{1/z} \quad (3)$$

where z (−) is the coordination number and measures number of rheological units with one another in the 3-D structure and A (G* at 1 Hz) is called the proportional coefficient and evaluates the strength of the interaction between units.

2.5. Scanning electron microscopy (SEM)

Alginate-corn starch gels were freeze-dried and observed using the scanning electron microscopy (S-4800, Hitachi, Ibaraki, Japan). Gels were covered with gold by vacuum evaporator (JEE 400; JEOL, Tokyo, Japan) for 5 min. The images were captured using 10 kV of acceleration voltage and 180× magnification.

2.6. In vitro gel digestibility

Digestibility of alginate-corn starch gels was analyzed following the method described by Santamaria et al. (2021) with minor modifications. The amount of alginate-starch gel, freshly prepared, was modified to 200 mg. The enzymes used were porcine pancreatic α-amylase (0.9 U/mL) and amyloglucosidase (143 U/mL). Glucose was determined using a glucose oxidase–peroxidase (GOPOD) kit (Megazyme, Dublin, Ireland). Starch fractions based on the hydrolysis rate were calculated as glucose (mg) × 0.9 and expressed as glucose content (g/100 g gel) using the method of Kim et al. (2021). Starch fraction hydrolyzed within 20 min of incubation was defined as rapidly digestible starch (RDS), the fraction hydrolyzed within 20 min and 120 min was identified as slowly digestible starch (SDS). Moreover, total digestible starch (DS) and resistant starch (RS) were assessed as hydrolyzed and remnant starch after 24 h of incubation, respectively. The *in vitro* digestion kinetics were fitted by first order equation, Equation (4), based on the method of Ratnaningsih et al. (2017):

$$C = C_\infty\left(1 - e^{-kt}\right) \quad (4)$$

where, C was the concentration at t time, C_∞ was the maximum hydrolysis, k was the kinetic constant and t was the digestion time.

2.7. Statistical analysis

Experimental data were statistically analyzed by IBM SPSS statistics V27 (SPSS Inc., Armonk, NY, USA, 2020) software. Data was subjected to analysis of variance (ANOVA) and values were expressed as a mean ± standard deviation. Duncan test was used to estimate significant differences among experimental mean values with a significance level ($p \leq 0.05$).

3. Results and discussion

3.1. Water retention capacity (WRC)

WRC_{CS} was 0.97 ± 0.04 (g water/g d.b.). To calculate the WRC_{SA}, Equation (2), WRC of starch-alginate mixtures was measured. These WRC values were higher than WRC_{CS}, due to alginates retained relevant amounts of available water in formulations (Hasatsri et al., 2018). The WRC of commercial sodium alginates was 12.09 ± 1.08 and 10.16 ± 2.37 (g water/g d.b.) for P and S. For alginates from the laboratory the WRC values were 7.31 ± 0.61, 5.26 ± 0.88 and 3.77 ± 0.18 (g water/g d.b.) for ND, 50D and 90D, respectively. For these last alginates, a linear relationship ($R^2 > 0.99$) between WRC and M_v was found, meaning that hydrophilic character increases with the length of alginate polymers. However, this trend was lost when commercial alginates were considered, indicating that source, other polymer characteristics (average block length, mannuronate-guluronate ratio, etc.) and extraction procedure can strongly affect the physicochemical alginate features.

3.2. Rheological properties

The rheological properties of the starch gel and alginate-starch gels were studied by small amplitude oscillatory shear tests. All experiments were carried out inside LVR previously determined by strain sweep tests. During the formation of the gels, cooling and maturation, the elastic modulus (G') was greater than viscous modulus (G'') giving evidence of a solid-like behaviour. After 10 min at 95 °C all gels achieved constant G' and G'' values, indicating the presence of fully formed gels at this elapsed time. During cooling a sharp increase of G' (7-fold, from 95 to 37 °C) together with a lower increase of G'' (2-fold) were determined. These results were related to gradual gel strengthening (firmer gels) during temperature decrease. Both moduli slightly raised during the first 20 min during maturation at 37 °C, above this period remained invariant. Fig. 1a, as example, shows the G' changes during 30 min of maturation. In fact, the increases of both moduli were proportional and, consequently, tan δ varied in a narrow range during maturation, Fig. 1b.

In the Fig. 1 it can be also observed the effect of alginates addition on rheological properties of tested corn starch gels. At the beginning and at the end of maturation period, the presence of alginate at 1% w/w decreased significantly ($p > 0.05$) G' values regarding CS. Nevertheless, when higher amount of alginate was added no significant differences ($p > 0.05$) were observed between G' in samples with 1 or 2% w/w of SA, excepting with P alginate where G' was invariant regarding CS. In general, tan δ values were very low (elastic behaviour was very predominant) and slightly varied (0.04 ± 0.01) with the presence of alginates, excepting in the cases of P and S at 1% w/w where higher values (>0.06) were found. These results indicated that former gels were some less structured than the others.

The rheological characteristics of gels formed with alginates from the same seaweeds and with different M_v (ND, 50D, and 90D samples) did not show significant differences between them. These results indicated that M_v of alginate was not critical for the rheological feature of starch gels when alginates had similar nature and extraction procedures. Nevertheless, significant differences were found when alginates from different sources were employed. Fig. 2 shows the frequency sweeps, within the linear viscoelastic region (LVR), performed from 0.1 to 10 Hz at a constant strain of 1% and at 37 °C after maturation period of the tested gels. Gels showed a solid-like behaviour (G' > G'') over the whole frequency range, and both moduli exhibited a slight increase with increasing frequency, typical behaviour of weak gels (Ji et al., 2017). In Fig. 2a, G' values are shown for the CS sample and samples with 1% w/w of alginate. It was observed that, with the addition of alginate, G' decreased over the whole frequencies range, and consequently the gels rigidity. It is worthy to note that two groups of data were clearly visible: those with the addition of commercial alginates (P and S), and those gels formed after the addition of in-house isolated alginates with different M_v. In the former no significant differences between respective trends with angular frequencies were found, but showed lower G' than the gels with commercial alginates within the frequency range. When more amount (2% w/w) of commercial alginate was added, Fig. 2b, G' values were systematically higher than those obtained after alginate addition at 1% w/w. Even with P alginate addition, G' values were similar to those observed with CS gel at low frequencies (<1 Hz) and above G' values were slightly higher. Nevertheless, in-house isolated alginates addition decreased G' dramatically and the drop was practically invariant with the added amount of alginate. This fact could be related to the low WRC values of these alginates in comparison to commercial ones. The addition of alginate at 1% w/w clearly increased tan δ values due to the enhancement of viscous character of these gels, Fig. 2c. In fact, the greatest increase of tan δ was due to the addition of the alginate with the highest M_v. At high (2% w/w) addition of alginates, Fig. 2d, all samples, at low frequencies, showed similar trend, and viscous character increased at high angular frequencies when SA was added. Therefore,

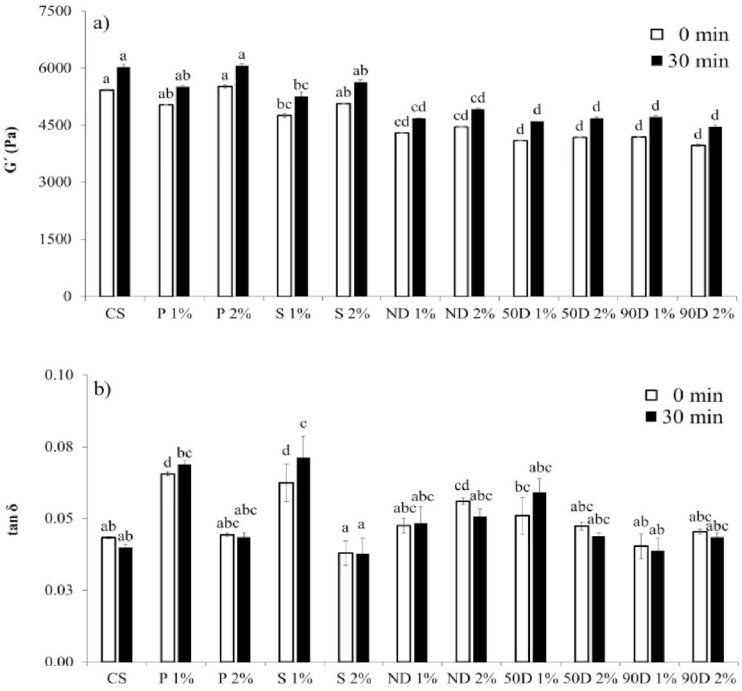

Fig. 1. G'(a) and tan δ (b) values at the beginning (0 min) and at the end (90 min) of maturation period at 37 °C measured at 30 Pa and 1 Hz of corn starch (1:4) gel (CS), CS with commercial alginates: PanReac (P) and Sigma (S), and with processed alginates: not dried (ND), dried at 50 °C (50D), dried at 90 °C (90D) at 1 and 2% (w/w). Different letters on bars denote significant differences ($p < 0.05$).

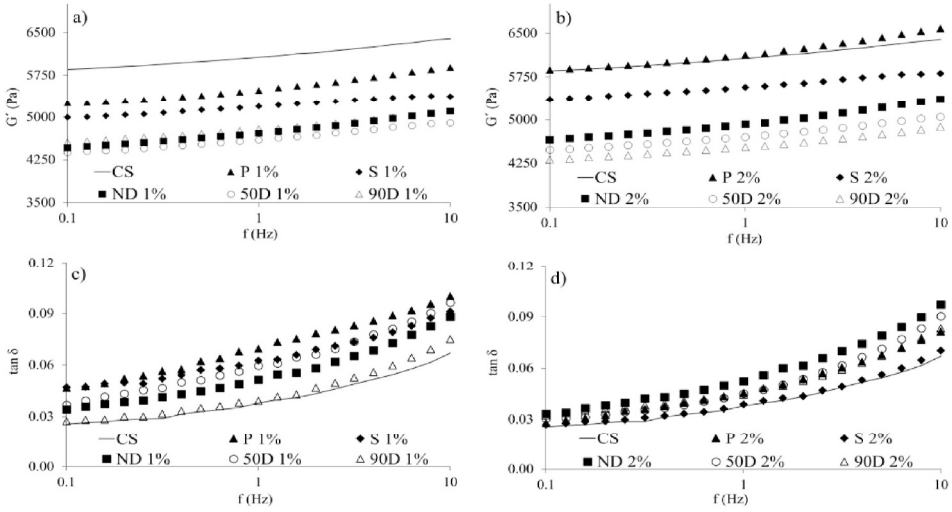

Fig. 2. Frequency sweep tests G' (a, b) and tan δ (c, d) of corn starch (1:4) gel (CS), CS with commercial alginates: PanReac (P) and Sigma (S), and with processed alginates: not dried (ND), dried at 50 °C (50D), dried at 90 °C (90D) at 1% (a, c) and 2% w/w (b, d) alginate content.

alginate addition did not promote the gelation and short time retrogradation of starch by means of additional crosslinking bonds among molecules, and consequently weaker structures were formed, and in turn viscous character was more relevant. In fact, Li et al. (2017) reported that early stage of retrogradation given by the aggregation of amylose was significantly retarded because alginates were associated to leached amylose. Other authors found similar trends (G' decreased and tan δ increased) with SA addition; in example, Fang et al. (2020) added

sodium alginate (1% w/w starch basis) to waxy potato starch gels (10% w/w) and He et al. (2019) studied rice starch (10% w/w) with sodium alginate (5% w/w starch basis). However, Yang et al. (2021) found that both moduli, G' and G'', increased with SA content employing rice starch at lower content (5% w/v) and alginates in the range 0.1–0.5% (w/v).

Complex modulus, G*, of all tested systems was successfully fitted ($R^2 > 0.97$) to Equation (3) and values of parameters are given in Table 1. Coordination number, z, corresponding to CS and S (independently of SA amount added) showed significantly higher values (from 51.52 to 52.76) with respect to samples with other SA (from 31.47 to 38.99). These results indicated that relevant structural changes occurred by the addition of some alginates (P, ND, 50D and 90D) regarding CS gel and the number of rheological units (less compact 3-D network of gel) decreased significantly with the presence of these alginates. Moreover, z was invariant ($p < 0.05$) with the SA content in all cases. No significant differences among alginates with same origin and obtained under the same processing (ND, 50D, and 90D) were observed. In relation to A parameter, a significant decrease ($p > 0.05$) with alginates addition were observed regarding CS. Nevertheless, in this case, some significant increase of A with SA amount could be determined. In fact, like all samples showed a predominant elastic behaviour (G' » G''), the previous discussion about G' trends is also valid here. These results again seemed to indicate that both different source and production process of alginates were more critical than the M_v value to change the starch-gel structure.

On the other hand, the increase of elasticity with increasing alginate concentration could be expected due to lower available water for gel formation by the increase of total dry matter and high WRC of alginates. Interestingly, G' values (measured at 1 Hz and 1% strain) of alginate-starch systems were related to WRC_{SA} values. At high alginate addition (2% w/w), an acceptable positive linear regression was established ($R^2 > 0.98$) between WRC_{SA} and the relative drop of G' for alginate-starch gels regarding pure starch gel, Fig. 3. Curiously, when alginates from AN with different M_v, whose nature and extraction method were controlled, are only considered, $R^2 = 1$ was obtained. Performing the same analysis at low alginate content (1% w/w) a worse linear regression ($R^2 < 0.8$) was achieved. These results could indicate that alginates at low content interacted with leached amylose in different extension as function of their specific molecular characteristics that also determined their water retention. However, at high alginate content the interactions with amylose were less relevant regarding water held by alginates and gel rigidity depended straight on WRC_{SA}.

3.3. Microstructure of alginate-corn starch gels

The impact of alginates addition on the starch gel's structure was analyzed. Fig. 4 shows some micrographs, as example, of tested gels. CS, Fig. 4a, presented uniform and circular structure; but the addition of alginates, Fig. 4b–e, modified clearly the microstructure creating elongated and unequal cavities, described as "honeycomb" network structure. In all cases, the structure of alginate-starch gels was formed by long linear partition walls that configured spatial anisotropic networks. It has been described that the effect of hydrocolloids on starch properties depend on the hydrocolloid structure and concentration, giving weaker structures and less gel-like behaviour due to interactions between starch and hydroxyl groups (Liu et al., 2022). Likely, the interaction with the incorporation of SA was produced at the beginning of starch gelatinization, which could alter the microstructure. Moreover, hydrocolloid concentration could be associated to a phase separation process. Rosell et al. (2011) related this effect to the formation of a network structure with fewer bonds among the starch and more entanglements between the hydrocolloid's chains. This could describe the elongated structures observed after the addition of SA. Fig. 4b and c, for P alginate, as example, show that structure was maintained invariant with increasing SA content. Probably a threshold alginate content (less than 1% w/w) was necessary to create the described structures. Fig. 4d and e shows the micrographs of alginate-starch gels with ND and 90D (high and low M_v) and no significant differences were found between them (independently of SA addition). Nevertheless, in both gels (also with 50D), in comparison to P gels, bigger cavities and more space between partition walls could be observed and this fact could explain their weaker elastic character. Liu et al. (2021) also observed structural changes, employing chestnut starch gels, with fewer and more irregular pores in alginate-starch gels with higher SA amount added. This modification in the microstructure could be also related to water mobility, being this minimized when increasing the amount of SA.

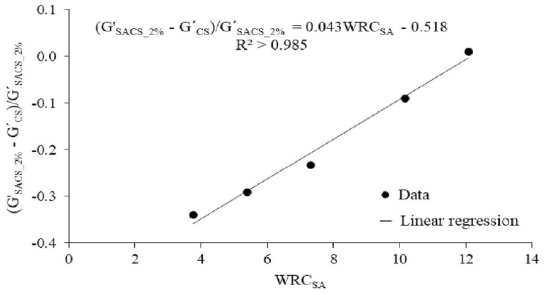

Fig. 3. Linear regression between (G' (alginate 2% w/w) – G' starch)/G' (alginate 2% w/w)) and water retention capacity of alginate (WRC_{SA}).

Table 1
Values of parameters of Equation (4).

Samples	A (kPa)	z
CS	6.07 ± 0.66^{ab}	51.52 ± 1.06^{a}
P 1%	5.52 ± 0.01^{c}	36.96 ± 0.63^{bc}
P 2%	$6.16 \perp 0.53^{ab}$	$38.99 \perp 2.52^{bc}$
S 1%	5.20 ± 0.26^{cd}	52.47 ± 3.56^{a}
S 2%	5.58 ± 0.21^{bc}	52.76 ± 3.93^{a}
ND 1%	4.74 ± 0.51^{de}	33.81 ± 2.36^{c}
ND 2%	4.95 ± 0.39^{de}	31.47 ± 0.79^{c}
50D 1%	4.62 ± 0.37^{e}	37.43 ± 1.16^{bc}
50D 2%	4.73 ± 0.15^{de}	37.22 ± 1.61^{bc}
90D 1%	4.63 ± 0.21^{e}	38.88 ± 3.93^{bc}
90D 2%	4.55 ± 0.10^{e}	37.89 ± 2.88^{bc}

Corn starch (1:4) gel: CS, CS with commercial alginates: PanReac, P, and Sigma, S; and with processed alginates: not dried, ND, dried at 50 °C, 50D, dried at 90 °C, 90D at 1 and 2% (w/w). Values followed by different letters within a column denote significant differences ($p < 0.05$).

3.4. In vitro digestion of starch gels

Typical hydrolysis profiles, Fig. 5a and b, were obtained for commercial and processed alginates, with a sharp increase of hydrolyzed starch during the first 20 min (in the slowest kinetics) up to achieve a stationary content after 60 min (also in the slowest digestion). Hydrolysis plots depended on the type of alginate and their concentration. Globally, the presence of alginates slowed down the hydrolysis rate of starch gels and, in general, increasing alginate content the kinetics rate decreased, Fig. 5a, as example. Fig. 5b shows the same slow hydrolysis kinetics of starch gels with low M_v (S and 90D) alginates at 2% w/w and the clear increase of the hydrolysis extent of corn starch. Other authors also reported that the alginate content was a critical factor affecting starch hydrolysis. Jung et al. (2017) suggested 0.5% as the optimal concentration of hydrocolloids, for affecting the predicted glycemic index. Moreover, Ramírez et al. (2015) reported a significant decrease of potato starch hydrolysis when adding alginate (1.0 and 2.0 g/100 g), which was attributed to change in the viscosity of starch solutions. Hydrolysis parameters extracted from the plots confirmed the impact of alginate addition (Table 2). Starch fractions SDS, DS and RS were

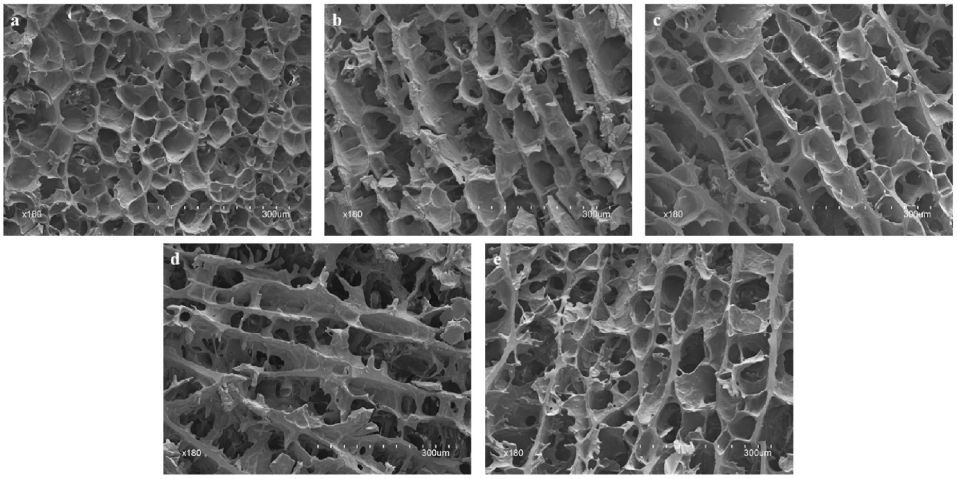

Fig. 4. Micrographs of alginate-corn starch gels. Magnification 180x. (a) Corn starch (CS); (b) and (c) Commercial alginate: PanReac (P) at 1 and 2% w/w starch basis, respectively; (d) processed alginates: not dried (ND) and (e), dried at 50 °C (50D) at 1% w/w, and 90 °C (90D) at 2 w/w.

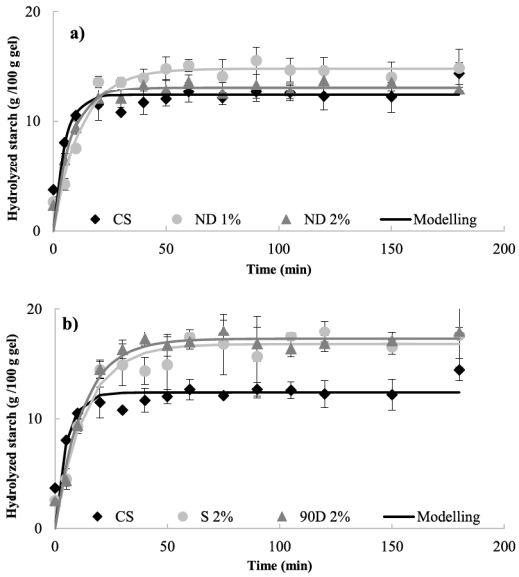

Fig. 5. Enzymatic hydrolysis plots of alginate-corn starch gels. (a) Effect of not dried alginates (ND) at 1 and 2% w/w, (b) Effect of commercial and processed alginates (2% w/w): Sigma (S) and dried at 90 °C (90D). Hydrolysis of corn starch (CS) was included in both graphs. Modelled data by Equation (4).

significantly modified depending on the type of alginate. RDS varied in a narrow interval from 10.65 (S 1%) to 13.80 g/100 g (90 D 2%). RDS was maintained constant or increased significantly with SA content, but no clear trends according to SA type or M_v were observed (Table 2). Conversely, at 1% of SA content, SDS increased significantly ($p > 0.05$) with respect to control (CS) from 0.25 up to 2.85 g/100g (except for 50D addition where no significant differences were observed). SDS significantly increased (up to 3.67 g/100g with S 2%) with added SA amount but decreased with increasing ND and 50D additions. These results could be related to commercial SA might be subjected to thermal processes or solvent extraction that modified their features, facilitating the interaction with the starch chains, behaving like 90D. In opposition, ND and 50D directly extracted by mild physical methods interacted with starch at low concentrations, but higher ones facilitate their inner interactions that led to the phase separation. DS increased in all SA containing gels, except for S 1% and 50D that showed values close to CS. Finally, RS also varied in an interval from 1.36 (50D 2%) up to 2.58 (90D 2%) (g/100 g) with significant differences between alginates employed. These findings were also partly observed by Chung et al. (2007) in cooked rice where SDS content increased, and RS reduced with the SA addition.

Equation (4) was successfully, Fig. 5a and b, employed to hydrolysis kinetics modelling. Hydrolysis kinetic constant (k) decreased with the alginate addition to corn starch gels, except 50D at 2% w/w. Hydrocolloids have been described to act as a barrier between the enzymes and starch molecules, in consequence retarded starch digestion. Feng et al. (2019) observed that the incorporation of xanthan and sodium alginate reduced the starch digestibility of pasta and noodles. When the hydrocolloids were mixed with starch, these interact with leached amylose and amylopectin with low molecular weight developing different network structures. Jung et al. (2017) related the reduced hydrolysis rate with the inhibition of starch swelling, due to the incorporation of arabic gum. In general, this effect was improved at high SA content (2% w/w) and kinetic constant decreased, particularly, with commercial alginates because they increased the rigidity of gels by their high hygroscopic character. With the remaining less hygroscopic alginates this effect was not observed. Maximum hydrolysis (C_∞) increased with SA addition from 12.37 (CS) up to 17.22 (90D 2%) due to mainly the described increase of SDS fraction. No clear trends of C_∞ with the presence of alginates and with added amount of SA were found, but the increase of digestibility could be related to the specific interactions between employed SA with amylose and amylopectin that decreased the starch retrogradation facilitating the access of enzyme during long digestion time and could be responsible of the DS, SDS and C_∞ results obtained with the SA addition. The different interactions of SA with starch might be also responsible of the RS results. However, it was not possible to correlate RS content with the molecular weight or SA content. Additional research is required to understand the entanglements of starch in the presence of different SA. In brief, slower hydrolysis kinetics could be related to the interference of SA molecules in the starch-enzyme interaction and the higher amount of hydrolyzed starch could be

Table 2
Parameters of *in vitro* alginate-corn starch gels digestion: rapidly digestible starch (RDS), slowly digestible starch (SDS), digestible starch (DS), resistant starch (RS), kinetic constant (k) and maximum hydrolysis (C_∞).

Sample	RDS (g/100 g)			SDS (g/100 g)			DS (g/100 g)			RS (g/100 g)			k (min^{-1})			C_∞		
CS	12.13 ±	0.81	abc	0.25 ±	0.16	d	11.85 ±	0.25	c	2.06 ±	0.20	bcd	0.20 ±	0.03	ab	12.37 ±	0.98	a
P 1%	13.47 ±	0.93	a	0.56 ±	0.08	cd	14.73 ±	0.15	a	2.40 ±	0.17	ab	0.16 ±	0.01	bc	14.03 ±	0.85	b
P 2%	13.70 ±	0.77	a	1.28 ±	0.05	bc	13.98 ±	0.38	a	1.77 ±	0.16	cde	0.12 ±	0.00	cd	14.98 ±	0.72	ab
S 1%	10.65 ±	0.23	c	1.79 ±	0.35	b	12.60 ±	0.28	c	1.70 ±	0.16	de	0.10 ±	0.01	d	12.45 ±	0.12	a
S 2%	13.07 ±	0.18	ab	3.67 ±	0.39	a	13.95 ±	1.13	a	1.70 ±	0.27	de	0.08 ±	0.00	d	16.74 ±	0.57	b
ND 1%	11.99 ±	0.35	abc	2.85 ±	0.89	a	14.76 ±	0.55	a	2.11 ±	0.42	bcd	0.08 ±	0.01	d	14.84 ±	1.23	ab
ND 2%	12.13 ±	0.51	abc	0.98 ±	0.22	bcd	14.55 ±	0.52	a	2.25 ±	0.07	ab	0.13 ±	0.01	cd	13.11 ±	0.73	b
50D 1%	13.43 ±	0.05	ab	0.21 ±	0.05	d	12.67 ±	0.04	bc	1.48 ±	0.17	e	0.17 ±	0.01	bc	13.64 ±	0.11	b
50D 2%	13.27 ±	0.54	ab	0.05 ±	0.02	d	12.69 ±	0.74	bc	1.36 ±	0.21	e	0.26 ±	0.07	a	13.32 ±	0.52	b
90D 1%	11.33 ±	2.44	bc	1.41 ±	0.40	bc	13.78 ±	0.17	ab	2.16 ±	0.03	abc	0.11 ±	0.00	cd	12.74 ±	2.83	a
90D 2%	13.80 ±	0.59	a	3.41 ±	1.04	a	14.64 ±	0.58	a	2.58 ±	0.05	a	0.08 ±	0.01	d	17.22 ±	0.45	b
*P-Value**																		
Alginate	0.14			0.01			0.01			0.01			0.01			0.73		
Concentration	0.04			0.21			0.39			0.75			0.98			0.06		

Corn starch (1:4) gel: CS, CS with commercial alginates: PanReac, P, and Sigma, S; and with processed alginates: not dried, ND, dried at 50 °C, 50D, dried at 90 °C, 90D at 1 and 2% (w/w). Values followed by different letters within a column denote significant differences ($p < 0.05$). k and C_∞ were determined by the Equation (3), $C = C_\infty\ (1 - e^{-kt})$. *The significance of the two factors (alginate type and their concentration) after the statistical analysis is indicated.

explained by the structural changes and previously described together with the presence of less retrograded starch amount that promote the accessibility of the enzyme to the starch. This also could be associated with a phase separation process, as mentioned above, with increasing SA content that favours more entanglements between the hydrocolloid's chains (Rosell et al., 2011). SA addition affected significantly enzymatic hydrolysis due to changes among molecular interactions.

4. Conclusions

The addition of sodium alginates caused relevant changes in the viscoelastic characteristics and structural features of the corn starch gels with presence of elongated and unequal cavities and the formation of linear partition walls that configured spatial anisotropic network. These structures were maintained independently of the tested alginate content. The addition of alginates with different origin and production method significantly modified specifically the rheological properties. Weaker gels (lower elastic modulus) were obtained with the addition of alginates and viscous character increased. Stronger gels were obtained increasing alginate content when hydrophilic character of alginates was high. The hydrolysis constant decreased with the addition of any alginate and, in general, with the amount of alginate with high hygroscopicity. At low alginate content, complexes were formed by alginate and leached amylose (and low Mv amylopectin) being hardly hydrolyzed by the enzymes and hindered the enzyme access to the remaining starch for its hydrolysis despite the generation of more open structures. These structures and a less starch retrogradation facilitated the later accessibility of enzymes to starch resulting that both SDS starch fraction and total hydrolyzed starch amount increased. In summary, alginate-corn starch gels can be produced with the same viscoelastic characteristics of corn starch gels, but with different gel structure and lower hydrolysis rates (interesting to decrease glycemic peak). However, in alginate-corn gels with similar structure promoted by the presence of alginates, the increase of the viscoelastic characteristics decreased the hydrolysis rate of starch. That is, the hydrolysis rate depended on rheology and structure of gel.

Contributions of authors

Leticia Montes: Conceptualization; Data curation; Formal analysis; Investigation; Methodology; Writing-original draft; Maria Santamaria: Investigation; Methodology; Writing-original draft; Raquel Garzon: Methodology; Supervision; Data curation; Cristina M Rosell: Conceptualization; Funding acquisition; Supervision; Writing - review & editing; Ramón Moreira: Conceptualization; Formal analysis; Writing-review & editing; Funding acquisition.

Declaration of competing interest

The authors confirm that they have no conflicts of interest with respect to the work described in this manuscript.

Acknowledgements

Authors acknowledge the financial support of the Spanish Ministry of Science and Innovation (Project RTI2018-095919-B-C2) and the European Regional Development Fund (FEDER), Generalitat Valenciana (Project Prometeo 2017/189) and Xunta de Galicia (Consolidation Project ED431B 2019/01).

References

Bruno, E., Lupi, F. R., Martin-Piñero, M. J., Girimonte, R., Baldino, N., Muñoz, J., & Gabriele, D. (2021). Influence of different dispersing systems on rheological and microstructural properties of citrus fiber suspensions. *LWT - Food Science and Technology (Lebensmittel-Wissenschaft und -Technologie), 152*, 112270.

Chung, H. J., Liu, Q., & Lim, S. T. (2007). Texture and in vitro digestibility of white rice cooked with hydrocolloids. *Cereal Chemistry Journal, 84*, 246–249.

Fang, F., Luo, X., BeMiller, J. N., Schaffter, S., Hayes, A. M. R., Woodbury, T. J., Hamaker, B. R., & Campanella, O. H. (2020). Neutral hydrocolloids promote shear-induced elasticity and gel strength of gelatinized waxy potato starch. *Food Hydrocolloids, 107*, 105923.

Feng, Y., Mu, T., Zhang, M., & Ma, M. (2019). Effects of different polysaccharides and proteins on dough rheological properties, texture, structure and in vitro starch digestibility of wet sweet potato vermicelli. *International Journal of Biological Macromolecules, 148*, 1–10.

Gularte, M. A., & Rosell, C. M. (2011). Physicochemical properties and enzymatic hydrolysis of different starches in the presence of hydrocolloids. *Carbohydrate Polymers, 85*, 237–244.

Hasatsri, S., Pitiratanaworanat, A., Swangwit, S., Boochakul, C., & Tragoonsupachai, C. (2018). Comparison of the morphological and physical properties of different absorbent wound dressings. *Dermatology Research and Practice*, 9367034, 2018.

He, X., Xia, W., Chen, R., Dai, T., Luo, S., Chen, J., & Liu, C. (2019). A new pre-gelatinized starch preparing by gelatinization and spray drying of rice starch with hydrocolloids. *Carbohydrate Polymers, 229*, 115485.

Ji, N., Qiu, C., Xu, Y., Xiong, L., & Sun, Q. (2017). Differences in rheological behavior between normal and waxy corn starches modified by dry heating with hydrocolloids. *Starch-Stärcke, 69*, 9–10.

Jung, D. S., Bae, I. Y., Oh, I. K., Han, S. I., Lee, S. J., & Lee, H. G. (2017). Classification of hydrocolloids based on in vitro starch digestibility and rheological properties of Segoami gel. *International Journal of Biological Macromolecules, 104*, 442–448.

Kassem, I., Ablouh, E. H., El Bouchtaoui, F. Z., Kassab, Z., Hannache, H., Sehaqui, H., & El Achaby, M. (2022). Biodegradable all-cellulose composite hydrogel as eco-friendly and efficient coating material for slow-release MAP fertilizer. *Progress in Organic Coatings, 162*, 106575.

Kim, H. R., Hong, J. S., Choi, S. J., & Moon, T. W. (2021). Modeling of in vitro digestion behavior of corn starches of different digestibility using modified log of slope (LOS) method. *Food Research International, 146*, 110436.

Kour, P., Afzal, S., Gani, A., Zargar, M. I., Tak, U. N., Rashid, S., & Dar, A. A. (2022). Effect of nanoemulsion-loaded hybrid biopolymeric hydrogel beads on the release kinetics, antioxidant potential and antibacterial activity of encapsulated curcumin. *Food Chemistry, 376*, 131925.

Liu, W., Wang, R., Li, J., Xiao, W., Rong, L., Yang, J., Wen, H., & Xie, J. (2021). Effects of different hydrocolloids on gelatinization and gels structure of chestnut starch. *Food Hydrocolloids, 120*, 106925.

Liu, W., Zhang, Y., Xu, Z., Pan, W., Shen, M., Han, J., Sun, X., Zhang, Y., Xie, J., Zhang, X., & Yu, L. L. (2022). Cross-linked corn bran arabinoxylan improves the pasting, rheological, gelling properties of corn starch and reduces its in vitro digestibility. *Food Hydrocolloids, 126*, 107440.

Li, Q. Q., Wang, Y. S., Chen, H. H., Liu, S., & Li, M. (2017). Retardant effect of sodium alginate on the retrogradation properties of normal corn starch and anti-retrogradation mechanism. *Food Hydrocolloids, 69*, 1–9.

Montes, L., Gisbert, M., Hinojosa, I., Sineiro, J., & Moreira, R. (2021). Impact of drying on the sodium alginate obtained after polyphenols ultrasound-assisted extraction from *Ascophyllum nodosum* seaweeds. *Carbohydrate Polymers, 272*, 118455.

Ramírez, C., Millon, C., Nuñez, H., Pinto, M., Valencia, P., Acevedo, C., & Simpson, R. (2015). Study of effect of sodium alginate on potato starch digestibility during in vitro digestion. *Food Hydrocolloids, 44*, 328–332.

Ratnaningsih, N., Suparmo, Harmayani, E., & Marsono, Y. (2017). In vitro starch digestibility and estimated glycemic index of Indonesian cowpea starch (Vigna unguiculata). *Pakistan Jounal of Nutrition, 16*, 1–8.

Rosell, C. M., Yokoyama, W., & Shoemaker, C. (2011). Rheology of different hydrocolloids–rice starch blends. Effect of successive heating–cooling cycles. *Carbohydrate Polymers, 84*, 373–382.

Santamaria, M., Garzon, R., Moreira, R., & Rosell, C. M. (2021). Estimation of viscosity and hydrolysis kinetics of corn starch gels based on microstructural features using a simplified model. *Carbohydrate Polymers, 273*, 118549.

Schwartz, J. M., Le Bail, K., Garnier, C., Llamas, G., Queveau, D., Pontoire, B., Srzednicki, G., & Le Bail, P. (2014). Available water in konjac glucomannan–starch mixtures. Influence on the gelatinization, retrogradation and complexation properties of two starches. *Food Hydrocolloids, 41*, 71–78.

Sensoy, I. (2021). A review on the food digestion in the digestive track and the used *in vitro* models. *Current Research in Food Science, 4*, 308–319.

Sun, Q., Si, F., Xiong, L., & Chu, L. (2013). Effect of dry heating with ionic gums on physicochemical properties of starch. *Food Chemistry, 136*, 1421–1425.

Tuaño, A. P. P., Barcellano, E. C. G., & Rodriguez, M. S. (2021). Resistant starch levels and *in vitro* starch digestibility of selected cooked Philippine brown and milled rices varying in apparent amylose content and glycemic index. *Food Chemistry: Molecular Sciences, 2*, 100010.

Yadav, K., Yadav, B. S., Yadav, R. B., & Dangi, N. (2018). Physicochemical, pasting and rheological properties of colocasia starch as influenced by the addition of guar gum and xanthan gum. *Journal of Food Measurement and Characterization, 12*, 2666–2676.

Yang, K., Luo, X., Zhai, Y., Liu, J., Chen, K., Shao, X. W., Li, Y., & Chen, Z. (2021). Influence of sodium alginate on the gelatinization, rheological, and retrogradation properties of rice starch. *International Journal of Biological Macromolecules, 185*, 708–715.

Yemenicioğlu, A., Farris, S., Turkyilmaz, M., & Gulec, S. (2020). A review of current and future food applications of natural hydrocolloids. *International Journal of Food Science and Technology, 55*, 1389–1406.

Yuris, A., Goh, K. K. T., Hardacre, A. K., & Matia-Merino, L. (2019). The effect of gel structure on the in vitro digestibility of wheat starch-Mesona chinensis polysaccharide gels. *Food & Function, 10*, 250–258.

Yu, Z., Wang, Y. S., Chen, H. H., Li, Q. Q., & Wang, Q. (2018). The gelatinization and retrogradation properties of wheat starch with the addition of stearic acid and sodium alginate. *Food Hydrocolloids, 81*, 77–86.

Zheng, M., Ye, A., Singh, H., & Zhang, Y. (2021). The in vitro digestion of differently structured starch gels with different amylose contents. *Food Hydrocolloids, 116*, 106647.

PUBLICATION 4

Rheological properties of corn starch gels with the addition of hydroxypropyl methylcellulose of different viscosities

Frontiers in Nutrition, 9, 866789 (2022)

frontiers in Nutrition

ORIGINAL RESEARCH
published: 22 March 2022
doi: 10.3389/fnut.2022.866789

Rheological Properties of Corn Starch Gels With the Addition of Hydroxypropyl Methylcellulose of Different Viscosities

*Leticia Montes[1], Cristina M. Rosell[2] and Ramón Moreira[1]**

[1] Department of Chemical Engineering, Universidade de Santiago de Compostela, Santiago de Compostela, Spain,
[2] Institute of Agrochemistry and Food Technology (IATA-CSIC), Paterna, Spain

The objective of this study is to determine the effect of the addition of hydroxypropyl methylcellulose (HPMC) (from 0.5 to 2.0% w/w, starch basis) with three different viscosities (40–60, 80–120, and 2,600–5,600 mPa·s) to corn starch (30% w/w, total basis) gels. Average viscosimetric molecular weights (M_v) of tested HPMC were determined (from 27.2 × 10^3 to 82.7 × 10^3 g/mol). Water retention capacity of HPMC varied linearly with M_v. The formation and curation of gels were monitored by rheology employing consecutive steps such as heating ramp (25–90°C), time sweep (90°C), cooling ramp (90–25°C), time sweep (25°C), and frequency sweep. Additionally, creep-recovery tests were performed. HPMC above 1.5% w/w delayed the range of gelatinization temperature of starch up to 2°C. Viscoelasticity and stiffness of corn starch gels with HPMC depend on both the amount of polymer added and M_v of the HPMC. Finally, to achieve corn gels with mimetic viscoelastic properties to wheat gel (with constant total solids), HPMC with relatively low viscosity (low M_v) is necessary to be added at certain content.

Keywords: average viscosimetric weight, creep and recovery, gelatinization, intrinsic viscosity, viscoelasticity

OPEN ACCESS

Edited by:
Carmelo Corsaro,
University of Messina, Italy

Reviewed by:
Ali Rafe,
Research Institute of Food Science and Technology (RIFST), Iran
Luis Arturo Bello Perez,
Instituto Politécnico Nacional (IPN), Mexico

***Correspondence:**
Ramón Moreira
ramon.moreira@usc.es

Specialty section:
This article was submitted to Nutrition and Food Science Technology, a section of the journal Frontiers in Nutrition

Received: *31 January 2022*
Accepted: *22 February 2022*
Published: *22 March 2022*

Citation:
Montes L, Rosell CM and Moreira R (2022) Rheological Properties of Corn Starch Gels With the Addition of Hydroxypropyl Methylcellulose of Different Viscosities. Front. Nutr. 9:866789. doi: 10.3389/fnut.2022.866789

INTRODUCTION

Nowadays, gluten-free products are increasingly in demand due to more people are diagnosed as having celiac disease. Most bakery products are made with wheat flour that contains gluten, but there are flours (some of them underexploited) such as corn, rice, chestnut, and acorn, among others, useful to produce gluten-free starchy food materials (1). However, these flours show some poor performance during kneading, proofing, and baking. For this reason, some additives, such as hydrocolloids or gums, are usually included in recipes of gluten-free products to replace the networking properties of gluten.

Hydrocolloids are capable to control the swelling power, solubility, and rheology of starch aqueous systems, throughout the stabilization of emulsions, suspensions, and foams. In fact, they are widely used in the manufacturing of starchy foodstuffs improving the properties of starch gels (2).

A common hydrocolloid used for cited purposes is the hydroxypropyl methylcellulose (HPMC) that belongs to the group of cellulose ethers and has a wide range of applications in food, cosmetics, adhesives, agriculture, and textiles (3). HPMC is hydrophilic, biodegradable, and their solutions exhibit shear-thinning behavior (4). There are many studies that show how the addition of HPMC modifies the viscoelasticity of gluten-free systems to achieve the viscoelastic characteristics of wheat.

Zhang et al. (5) studied the effect of adding 2% w/w, starch basis (s.b.) of HPMC (166,700 kDa, and its degrees of methoxyl and hydroxypropyl substitution were 27.2 and 6.8%, respectively) to 5 different starches (wheat, corn, tapioca, sweet potato, and potato) on the rheological properties and found that for each source of starch the interactions between starch and HPMC were predominantly physical linkages and showed a different behavior depending on water-binding capacity of the starch. Similar conclusions were previously obtained with the HPMC addition in corn and potato starches (6). Mancebo et al. (7) studied the influence of HPMC (4,000 mPa·s for 2% aqueous solutions at 20°C) (2–4% w/w, by addition, flour basis, f. b.) on rice doughs analyzing the rheological properties and found that elastic modulus (G′) noticeably increased. Sivaramakrishnan et al. (8) studied the addition of HPMC (from 1.5 to 4.5%, w/w, by addition, f. b.) of low viscosity (40–60 mPa·s for 2% aqueous solutions at 20°C) to rice flours and, in general, elastic (G′) and viscous (G″) moduli increased as the amount of HPMC increased. Gujral et al. (9) observed that adding 6% w/w, by addition, f. b., of HPMC (4,000 mPa·s) to rice flour both moduli increased and, dough consistency increased by 120% increasing HPMC content from 2 to 6% w/w. However, Moreira et al. (10) observed that the incorporation of HPMC (2% w/w, by substitution, f. b.) to chestnut flour decreased G′ and tan δ (G″/G′). Bárcenas et al. (11) used HPMC [from 0.002 to 0.013 g of HPMC/g of wheat starch (WS), by substitution] of high viscosity (4,500 mPa·s for 2% aqueous solutions at 20°C) on wheat flour and viscoelastic moduli (G′ and G″) and tan δ decreased with polymer amount. Techawipharat et al. (12) analyzed the effect of adding HPMC (0.8% w/w, by substitution, unspecified viscosity) to rice starch (7.2% w/w) dispersions and observed that both peak viscosity and final viscosity decreased and pasting temperature increased with the HPMC substitution. Moreover, Kim et al. (13) studied the effects of some cellulose derivatives on pea starch. The HPMC used had different viscosities from 45 to 116,640 mPa·s (for 2% aqueous solutions at 20°C) and different ratios of methoxyl and hydroxypropyl substitution. Specifically, regarding HPMC with the same substitution degree, the use of high viscosity HPMC increased G′, G″, tan δ, and complex viscosity. Lee et al. (14) studied the effect of adding HPMC of 3 different viscosities (50, 400, and 4,000 mPa·s) to waxy rice starch at a ratio of 19:1 (w/w) and the total solids content was 25% w/w. These authors observed that the onset gelatinization temperature increased and the final gelatinization temperature decreased for samples with HPMC. Finally, these authors also found that peak and final viscosity decreased with the HPMC addition except for the sample with the addition of the highest viscosity HPMC. These results clearly indicate that, at constant hydration, the procedure of HPMC adjunction of the starchy system by addition (increasing total solids mass) or by substitution (constant total solids mass) and HPMC viscosity are key characteristics to be considered (15) in the gel characteristics. Globally, focusing on gluten-free products, studies have shown that incorporation of hydrocolloids by addition increased the viscosity and viscoelastic moduli of starch pastes by influencing the gelatinization and retrogradation of starch (3). However, lower moduli and viscosity values were found by the addition of hydrocolloids by substitution.

In relation to the effect of the addition of hydrocolloids with different sizes to corn starch (CS), Funami et al. (16) studied the gelatinization behavior of CS (15% w/w) in the presence of guar gum with different molecular weights (from 0.02 to 34.6×10^5 g/mol) and, at constant guar gum content (0.5% w/w, s. b.) the peak viscosity and setback increased with the lowest molecular weight guar gum and the addition of guar gum delayed the pasting temperature from 75.7°C (for CS) up to 79.6°C.

In these previous studies, the effect of the addition of some hydrocolloids, such as xanthan gum, guar gum, and HPMC, among others, was investigated but without considering the effect of molecular size of HPMC. Likewise, considering the specific interaction depending on the starch source, it was hypothesized that the molecular size of HPMC added to CS, commonly used in gluten-free products, might affect starch interactions and in consequence viscoelasticity of CS gels. Therefore, the aim of this study is to determine the effect of the addition of three different HPMC with different molecular weights on CS gels by means of the evaluation of the viscoelastic behavior.

MATERIALS AND METHODS

Materials

Corn starch [moisture content of 11.4 ± 0.2 dry basis (% d. b.), amylose content 28.1 ± 2.4% d. b.] and wheat starch (moisture content of 12.3 ± 0.2% d. b., amylose content 27.6 ± 0.3% d. b.). HPMC, with constant methoxyl and hydroxypropyl content, 28.7 and 9.1%, respectively, of three different apparent viscosities, 40–60 (HPMC L), 80–120 (HPMC M), and 2,600–5,600 cP (HPMC H), at 2% in H_2O at 20°C, [moisture content (d. b.) of 4.0 ± 0.1, 3.0 ± 0.2, and 4.9 ± 0.2, respectively]. All the materials were provided by Sigma Aldrich.

Average Viscosimetric Molecular Weights of Hydroxypropyl Methylcellulose

Average viscosimetric molecular weights were determined by viscosity measurements, using a Ubbelohde type viscometer (AVS 350, Schott-Geräte, GmbH, Germany). Solutions were prepared with a concentration of 0.1% (w/w, d. b.) in distilled water. For each HPMC, three dilutions were performed (0.025, 0.050, and 0.075%). All measurements (at least 5 replicates) were performed at 25°C (± 0.1°C). At these low hydrocolloid content, density was constant and equal to the density of solvent (water). With the absolute viscosities of solvent (μ_0) and HPMC (μ) solutions, the relative viscosity ($\mu_\mu = \mu/_0$) and the specific viscosity ($\mu_{sp} = \mu_r - 1$) were calculated. Using the values of μ_r and μ_{sp}, the intrinsic viscosity (μ) was calculated by the Huggins (Eq. 1) and Kraemer (Eq. 2) Equations (17):

$$\mu_{red} = [\mu] + K_H [\mu]^2 C \quad (1)$$

$$\mu_{inh} = [\mu] + K_K [\mu]^2 C \quad (2)$$

where $\mu_{red} = \mu_{sp}/C$, $\mu_{inh} = \ln(\mu_r)/C$, and K_H and K_K are the Huggins and Kraemer constants, respectively. The values of viscosity average molecular weight, M_v, were determined by the Mark–Houwink Equation (Eq. 3):

$$[\mu] = K M_v^{\alpha} \tag{3}$$

where (μ) (dl/g) is the intrinsic viscosity and K and α values depended on the solute–solvent system at a constant temperature.

Water Retention Capacity

Water retention capacity (WRC) values were determined to characterize the CS and HPMC-CS mixtures. WRC was calculated following the protocol established by Robertson et al. (18). Briefly, samples were weighed and hydrated for 18 h. After the samples were centrifuged, the supernatant was removed and the solid residue was dried to constant weight (dry residue). The WRC (kg^{-1}) was calculated by Eq. (4).

$$WRC = \frac{FRW - DRW}{DRW} \tag{4}$$

where *FRW* is the fresh residue weight and *DRW* is the dry residue weight. WRC of HPMC was not directly determined due to water forms a viscous gel (19), but it was indirectly evaluated by means of HPMC and CS mixtures. WRC_{HPMC} was evaluated by the Eq. (5):

$$WRC_{HPMC} = \frac{WRC_{mixture} - WRC_{CS}\left(1 - \frac{w_{dHPMC}}{(w_{dCS}+w_{dHPMC})}\right)}{\frac{w_{dHPMC}}{(w_{dCS}+w_{dHPMC})}} \tag{5}$$

where WRC_{CS} is the WRC of CS, w_{dHPMC} and w_{dCS} are the dry weights of HPMC and starch in the mixture, respectively.

Rheological Properties

Dispersions with constant solids content (30% w/w) were prepared by mixing CS and HPMC (by substitution) at different concentrations (0, 0.5, 1.0, 1.5, and 2.0% w/w) and distilled water. First, the solids were gently blended and later distilled water was added. The slurry was mildly stirred (100 rpm) using a magnetic stirrer, for 10 min at room temperature. Aqueous HPMC solutions (2.0% w/w) were prepared by mixing HPMC and distilled water. These mixtures were kept in agitation until completely dissolved. The rheological characterization was performed with a stress-controlled rheometer (MCR 301; Anton Paar Physica, Graz, Austria) using a plate–plate geometry (diameter, 50 mm). Samples (1.2 ml) were loaded between the parallel plates and compressed up to obtain a gap of 0.5 mm. In the case of HPMC solutions, the same geometry was used with a smaller gap (0.3 mm) with a volume of sample of 0.9 ml. The measurements were performed at different temperatures [from 25 up to 90°C (± 0.1°C)], controlled by a Peltier system. All the samples were covered with light paraffin oil to prevent water evaporation. Tests were carried out at least in triplicate.

Oscillatory Measurements

Strain sweep tests from 0.1 to 10% at a constant frequency (1 Hz) were made on dispersions and gels to define the corresponding linear viscoelastic regions (LVRs). Second, dispersions were subjected to the procedure previously reported (20) with minor modifications consisting in five steps: (i) temperature sweep (25–90°C at 1°C min^{-1}, 1 Hz, 100 Pa), to accomplish starch gelatinization; (ii) time sweep (30 min, 1 Hz, 400 Pa, 90°C); (iii) temperature sweep (90–25°C at 1°C min^{-1}, 1 Hz, 400 Pa); (iv) time sweep (30 min, 1 Hz, 400 Pa, 25°C); and finally (v) frequency sweep (0.01–100 Hz, 1% of strain, 25°C) inside LVR of formed gels (preliminary tests were performed to determine the corresponding LVR). For HPMC solutions (2.0% w/w in water) a strain sweep from 0.1 to 100% at a constant frequency (1 Hz) was made to analyze the LVR. Then, a temperature sweep was carried out from 35 to 80°C at a constant strain of 10% and a constant frequency of 1 Hz (inside LVR). **Figure 1** shows a general outline of these five steps where viscoelastic properties were evaluated over time.

Creep-Recovery Test

A creep-recovery test at 25°C was performed at constant stress, σ (Pa), of 100 or 400 Pa within the LVR during the creep phase. Before the measurements, the gels were rested for 15 min in the rheometer to allow the sample equilibrium. During the creep period, the selected constant stress was applied for 120 s and the recovery (stress zero) period lasted 120 s (21). The results were analyzed in terms of creep compliance, J(t) (Pa^{-1}) = γ/σ, where γ is the strain experimentally measured. The Burgers model (22) was employed for the creep (Eq. 6) and the recovery phases modeling (Eq. 7):

$$J(t) = J_0 + J_m\left(1 - \left(\exp\left(-\frac{t}{\lambda}\right)\right)\right) + t/\eta_0 \tag{6}$$

$$J(t) = J_{max} - J_0 - J_m\left(1 - \left(\exp\left(-\frac{t}{\lambda}\right)\right)\right) \tag{7}$$

where J_0 (Pa^{-1}) is the instantaneous compliance, J_m (Pa^{-1}) is the viscoelastic compliance, λ (s) is the mean retardation time, t (s) is the phase time, η_0 (Pa·s) is the zero-shear viscosity, and

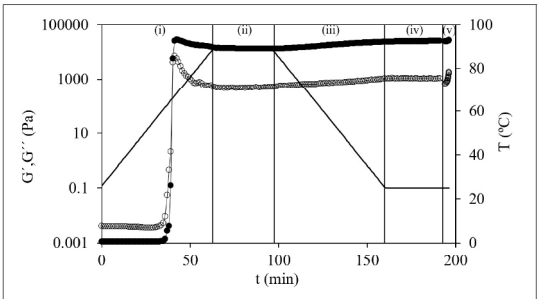

FIGURE 1 | The general outline of the five steps of oscillatory measurements of G′(•) and G″(○) of corn starch and temperature (–) vs. time: (i) temperature sweep (25–90°C at 1°C min^{-1}, 1 Hz, and 100 Pa); (ii) time sweep (30 min, 1 Hz, 400 Pa, and 90°C); (iii) temperature sweep (90–25°C at 1°C min^{-1}, 1 Hz, and 400 Pa); (iv) time sweep (30 min, 1 Hz, 400 Pa, and 25°C); and (v) frequency sweep (0.01–100 Hz, 1% of strain, and 25°C).

J_{max} (Pa^{-1}) is the maximum creep compliance. The goodness of fitting was evaluated by means of the corresponding coefficients of determination [R^2 and the root mean square error (RMSE)].

Statistical Analysis

Experimental data were analyzed through one-factor analysis of variance (ANOVA), followed by the Duncan test and considering significant p-values ≤ 0.05 (IBM SPSS Statistics. New York, NY, United States). All the experimental results were expressed as mean ± SD from at least triplicate experiments.

RESULTS

Average Viscosimetric Molecular Weights of Hydroxypropyl Methylcellulose

Table 1 shows the K_H and K_K constants, intrinsic viscosity (μ) values, and the average viscosimetric molecular weight (M_v) for each HPMC. M_v was calculated by the Mark–Houwink equation, Eq. (3), where the values of K and α parameters were 3.39×10^{-4} dl/g and 0.88, respectively, previously determined by Vázquez et al. (23). Intrinsic viscosity is a measure of the hydrodynamic volume occupied by the individual polymer molecules in isolation (24). The (μ) and M_v values varied from 2.72 to 7.21 dl/g and from 27.2×10^3 to 82.7×10^3 g/mol, respectively. Vázquez et al. (23) studied the (μ) values of HPMC with different nominal viscosity (from 10^2 to 10^5 mPa·s) and obtained values from 3.78 to 14.98 dl/g and M_v values from 39.7×10^3 to 190.0×10^3 g/mol. Bustamante et al. (25) studied the (μ) of HPMC with 28–30% methoxyl and 7–12% hydroxypropyl content and approximate molecular weight of 86 kDa and obtained a value of 8.09 dl/g. These results agree with the results obtained in this study.

The values of K_H and K_K obtained were from 0.21 to 0.63 and from −0.26 to −0.04, respectively. As the nominal viscosity of the HPMC increased, the K_H, K_K, (μ), and M_v significantly ($p < 0.05$) increased as well. HPMC solubility can be related to intrinsic viscosity (25). This behavior shows that an increase in viscosity (and, therefore, an increase in M_v) causes a decrease in the solubility of the biopolymer in water. The values of K_H and K_K could be analyzed to study the interactions between the polymers and solvents. In fact, $K_H < 0.5$ and $K_K < 0$ indicate good solvents (strong interactions polymer–solvent). An additional criterium given by $K_H - K_K$ close to 0.5 based on the solvent goodness (solvent θ), defined a condition in which neither inter- or intramolecular polymer aggregation is produced and particulates behave as non-perturbed units and polymers adopt an extended conformation (flexible coil) in the solvent used (26). Our results indicated that only HPMC H slightly diverged ($K_H = 0.63 > 0.5$ and $K_H - K_K$ close to 0.7) from theoretical considerations for good solvent–polymer interactions and this fact could be tested out in its low water solubility and slow solubilization.

Water Retention Capacity

In order to calculate the WRC of the different HPMC samples, mixtures of starch and HPMC were made. By means of the Eq. (4) the WRC of CS and mixtures were calculated. Then, using Eq. (5) the WRC of HPMC was evaluated. WRC_{CS} was 0.95 ± 0.01 (g water/g d.b.) whereas WRC values of HPMC L, M, and H, were 8.54 ± 0.28, 8.92 ± 0.22, and 12.97 ± 0.45 (g water/g d.b.), respectively. Yılmaz et al. (27) reported the same effect with the addition of HPMC to wheat-rice and wheat-corn flours. The WRC increased in the samples where HPMC was added. Usually, the hydrophilicity depends on the HPMC substitution degree (28). In this case, all samples had a constant substitution degree, therefore, WRC increased with increasing the M_v of HPMC meaning that a high molecular weight of polymer implied high water retention. This fact can be explained because in larger polymers, the hydrophilic groups (hydroxypropyl) are more accessible for water and therefore, more water amount could be retained. Additionally, a linear correlation was found between intrinsic viscosity (μ), of HPMC and WRC_{HPMC} ($R^2 > 0.99$). As (μ) was proportional to M_v, WRC_{HPMC} also varied linearly with M_v of HPMC ($R^2 > 0.99$).

Rheological Characterization

Oscillatory Measurements

Dispersions were subjected to a temperature sweep (step i) where the onset gelatinization temperature (T_0) was evaluated from the first inflection point of elastic modulus (G′) and the final gelatinization temperature (T_f) was determined from the point in which the slope of G′ changes after the peak (29). **Figure 2** shows the curves obtained during the temperature sweep for samples of CS and CS + 2.0% HPMC (L, M, and H). During this stage, G′ values drastically increased 7 decades, approximately, and at the end, G′ > G″. From this point, G′ values remained above G″ throughout the experiment, which means that gels have a solid elastic-like behavior. T_0 obtained for CS gel was 60.7 ± 1.1°C and for gels with HPMC L varied from 61.8 ± 1.1 (for 0.5, 1.0, and 1.5%) to 62.8 ± 1.1°C (for 2.0%), while with HPMC M was 61.8 ± 1.1°C (for 0.5 and 1%) and 62.8 ± 1.1°C (for 1.5 and 2.0%). However, T_0 value for HPMC H hardly changed, 62.8 ± 0.8°C, independently of its content. In addition, the T_f was delayed in a similar way, from 74.2 ± 0.8°C for CS gels to 75.3 and 76.4 ± 0.8°C with the presence of HPMC. This delay of the gelatinization process could be related to the water absorption of the added hydrocolloid (30) that competes with starch for the available water. In fact, the WRC results showed that mixtures of starch with HPMC retained more water than CS without HPMC sample. The same behavior was shown by Moreira et al. (31) in chestnut flour doughs with the addition of 0.5–2% HPMC (viscosity 2,600–5,600 cP, 2% in H_2O at 20°C) by substitution. Moreover, Zhang et al. (32) showed the same trend with other hydrocolloids such as arabic gum, guar gum, and xanthan gum added by substitution. Also, Alamri et al. (33) reported that okra extract delayed the onset temperature in WS.

In the curves of CS and in those of CS + 2.0%, HPMC L and HPMC M both moduli remained constant until reaching T_0 (onset starch gelatinization temperature) (**Figure 2**). For the

TABLE 1 | Parameters obtained from the Eqs (1) to (3).

HPMC	Nominal viscosity (mPa·s)	K_H	K_{HK}	(μ) (dL/g)	M_{Hv} (10^3 g/mol)
L	40–60	0.21 ± 0.11^a	-0.26 ± 0.08^a	2.72 ± 0.15^a	27.2 ± 1.8^a
M	80–120	0.47 ± 0.09^b	-0.08 ± 0.06^b	3.18 ± 0.08^b	32.7 ± 1.0^b
H	2,600–5,600	0.63 ± 0.03^b	-0.04 ± 0.01^b	7.21 ± 0.14^c	82.7 ± 1.8^c

Data are presented as mean ± SD. Data value of each parameter with different superscript letters are significantly different ($p \leq 0.05$).

mixtures of CS with HPMC (M and L), the same behavior was observed at all the HPMC content studied (data not shown). However, for CS + 2.0% HPMC H samples, as the temperature increased, G′ and G″ gently decreased until accomplishing a characteristic temperature (∼57°C) after which a strong decrease is observed. This fact must be related to the thermal behavior of HPMC. To characterize the thermogelation features of HPMC, 2.0% w/w HPMC aqueous solutions were subjected to temperature sweeps (**Figure 3**).

As it can be observed in **Figure 3**, in the HPMC L (and HPMC M, data not shown) solution at temperatures below 60°C, both moduli are almost constant (with G″ > G′) and from this temperature, both moduli started to increase (particularly G′) achieving a gel point (G″ = G′) at 61.0 ± 0.8°C and at higher temperatures G′ sharply increased. However, HPMC H solution showed a different trend, a notorious drop (above 57°C) of both moduli was observed before the gel point achievement. Silva et al. (34) observed this effect (using high viscosity HPMC, 15,000 mPa·s) and concluded that this process is due to the higher hydrophobicity of the polymer chains promoted during heating, suggesting the existence of strong aggregation phenomena. Temperature sweeps seemed to indicate that this fact could be also promoted by the molecular weight of the polymer due to the described behavior before gel point was only observed with tested high molecular weight HPMC. The temperature of the gel point (around 61°C) was the same for all tested HPMC polymers. HPMC gel point depends on methoxyl and hydroxypropyl substitution degree (35) and our results indicate that it is independent of the average molecular weight of HPMC.

Analyzing in detail the results shown in **Figure 2**, it can be observed that CS with HPMC H showed the same drop of both the moduli at the mentioned temperature, so in the aqueous dispersion of starch and HPMC, the interactions between polymers before starch gelatinization are negligible and rheological properties are governed by the individual relationships (affinities) of polymers with water.

A time sweep at 90°C for 30 min (step ii) (**Figure 1**) to evaluate the gel formation rate and to determine the elapsed time until achieve a fully formed gel was carried out. Evaluating

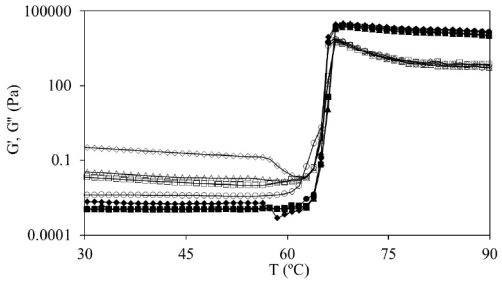

FIGURE 2 | G′ (fully symbols) and G″ (empty symbols) values for temperature sweep (from 30 to 90°C at 1°C min^{-1}, 1 Hz, and 100 Pa) for CS (●) and mixtures CS + 2.0% hydroxypropyl methylcellulose (HPMC) for HPMC L (■), HPMC M (▲), and HPMC H (◆).

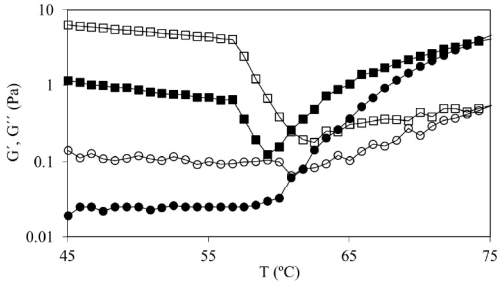

FIGURE 3 | Temperature sweeps from 45 to 75°C of HPMC solutions 2.0% w/w in water for HPMC L (●) and HPMC H (■) where G′ has full symbols and G″ has empty symbols.

TABLE 2 | Data from maturation stage obtained at 400 Pa, 1 Hz, and 25°C during 30 min.

Sample	Polymer dosage (% w/w)	G'_{25i} (Pa·s)	$\Delta G_{25}'$ (Pa·s)
CS	0	$23,955 \pm 431^{ef}$	$1,420 \pm 14^{fg}$
HPMC L	0.5	$21,535 \pm 1039^c$	$1,270 \pm 42^d$
	1.0	$19,880 \pm 283^b$	$1,190 \pm 38^c$
	1.5	$19,630 \pm 724^b$	$1,010 \pm 33^b$
	2.0	$17,490 \pm 919^a$	865 ± 37^a
HPMC M	0.5	$21,900 \pm 212^{cd}$	$1,330 \pm 44^{de}$
	1.0	$21,720 \pm 397^c$	$1,280 \pm 41^d$
	1.5	$19,155 \pm 1308^b$	$1,125 \pm 64^c$
	2.0	$17,450 \pm 933^a$	955 ± 35^b
HPMC H	0.5	$22,430 \pm 14^{cde}$	$1,335 \pm 7^{de}$
	1.0	$23,395 \pm 587^{def}$	$1,275 \pm 7^d$
	1.5	$24,750 \pm 339^f$	$1,360 \pm 12^{ef}$
	2.0	$27,250 \pm 120^g$	$1,460 \pm 15^g$

Data are presented as mean ± SD. Data values in a column with different superscript letters are significantly different at the $p \leq 0.05$ level.

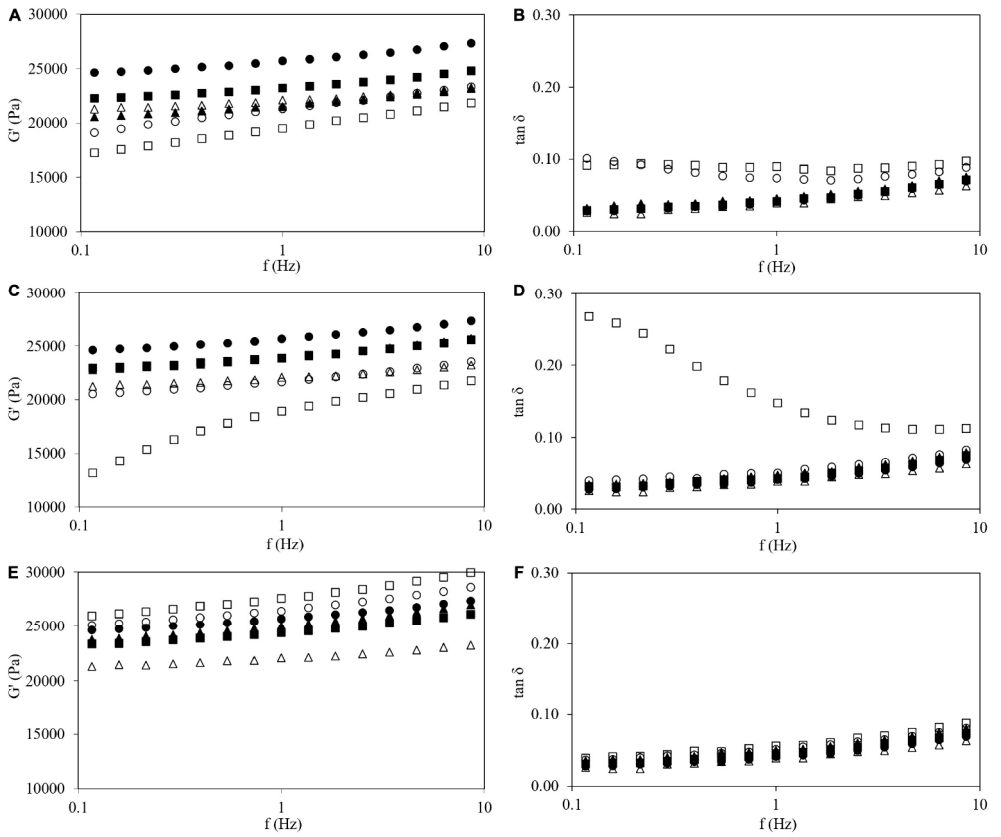

FIGURE 4 | Frequency sweep tests (at 1% of strain, 25°C) of G′ **(A,C,E)** and tan δ **(B,D,F)** of corn starch gel (●), wheat starch (Δ), and corn starch with HPMC L **(A,B)**, M **(C,D)**, and H **(E,F)** gels: 0.5 (●), 1.0 (■), 1,5 (▲), and 2.0% (□).

G′, around 20 min are necessary to reach a constant value in the case of CS gels. However, the HPMC addition substantially shortened the necessary time, around 5 min, to obtain a stable gel. In parallel, G″ values not varied during this time sweep. The fact that corn gels with HPMC needed short times to get the stability could be an industrial advantage by saving time and costs. Moreover, this fact showed that the HPMC gelation promoted and modified the formation of CS gel. During time sweep, the variations of G′ for tested gels, $\Delta G_{90}' = G'_{90f} - G'_{90i}$, were evaluated where G'_{90f} is the G′ after 30 min and G'_{90i} is the initial value. For CS gel, without the addition of HPMC, $\Delta G_{90}'$ was −970 Pa, starch gels with HMPC L and M showed lower changes, but always $G'_{90f} < G'_{90i}$. These variations decreased with the amount of HPMC added. However, with the addition of HPMC H, two different trends were observed depending on the amount of polymer used. Negative values of $\Delta G_{90}'$ were also determined at low content (0.5% w/w), but increasing HPMC H content (>1.0% w/w) positive $\Delta G_{90}'$ values were determined achieving 1,560 Pa at 2.0% w/w. These results showed that M_v of HPMC clearly modifies the formation rate of gels and their final characteristics. In our tests, despite tested polymers had the same substitution degree, when they were added at the same content, the gel features were significantly different. The addition of HPMC, independently of M_v, dampened the decay of G′ observed in CS gels due to the presence of hydroxyl groups that are capable to form additional hydrogen bonds and therefore stronger structures (36). The positive $\Delta G_{90}'$ values found with HPMC H indicated that strengthened gels were formed, confirming that in large polymer molecules the accessibility to the functional groups is facilitated.

In the next stage, the temperature sweep from 90 to 25°C (step iii), **Figure 1**, it was observed that both the moduli gradually increased with decreasing temperature, corresponding to starch retrogradation (37). Afterward, a maturation period (step iv) of 30 min, time sweep at 25°C, stress (400 Pa), and frequency (1 Hz), was carried out to evaluate gel stability at room temperature.

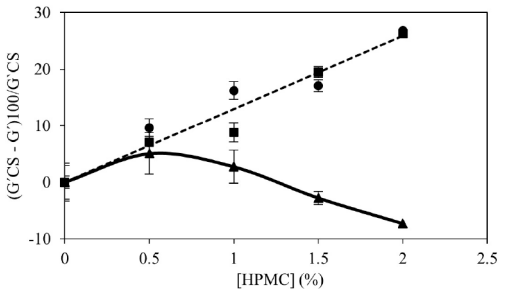

FIGURE 5 | Relationship between the $(G'_{CS} - G')100/G'_{CS}$ values obtained from the mechanical spectrum at 1 Hz and the concentration of HPMC: L (●), M (■), and H (▲).

The evolution of G′ with time during this stage indicated that stationary G′ values were obtained at a short time (less than 2.5 min). In all cases, the presence of HPMC decreased the elapsed time to achieve gel stability until below 1 min for HPMC L at 2.0% w/w. A similar analysis performed in time sweep at 90°C was carried out in this stage by evaluation of $\Delta G_{25}' = G'_{25f} - G'_{25i}$. **Table 2** shows the G'_{25i} and $\Delta G_{25}'$ values for tested gels. Globally, G'_{25i} values decreased with increasing polymer addition of HPMC L and M. This result indicated that short-time starch retrogradation given by the rapid recrystallization of amylose molecules was slowed down by these HPMC additions due to the increase of G′ during cooling (step iii) was significantly lower. However, this decrease of G'_{25i} only was observed at the lowest content of HPMC H (0.5% w/w) because beyond that level G'_{25i} showed a steady increase with the level of HPMC addition (2.0% w/w) maintaining the trend observed at 90°C. In fact, the addition of hydrocolloids can increase, decrease, or have no effect on the extent of (short- and long-time) starch retrogradation, depending on the gel preparation method, temperature, time, added amount of hydrocolloid, and measurement techniques of starch retrogradation (38). The aforementioned effect of HPMC on starch retrogradation was confirmed by the corresponding analysis of the time sweeps at 25°C where positive $\Delta G_{25}'$ values were obtained, meaning that in all cases $G'_{25f} > G'_{25i}$, **Table 2**. Nevertheless, the maximum firming up was observed in CS gels (1,420 Pa) with HPMC H at 2.0 w/w (1,460 Pa). HPMC addition diminished $\Delta G_{25}'$, but different trends with polymer content were found. At higher HPMC L and M content, $\Delta G_{25}'$ values significantly ($p < 0.05$) decreased (up to 865 Pa with HPMC L at 2.0% w/w). No significant differences among $\Delta G_{25}'$ values of gels with different amounts of HPMC H added were observed, and these changes were close to that determined in CS gel ($p > 0.05$).

The previous time sweep (step iv) showed that the gels have reached a stable state and are ready to analyze their structures. For this reason, frequency sweeps (step v) (at constant strain 1%, inside LVR) were carried out to characterize the viscoelastic properties of gels (**Figure 4**). For all samples, G′ increased with increasing frequency, indicating that samples with or without HPMC are typical weak gels (39, 40). In general,

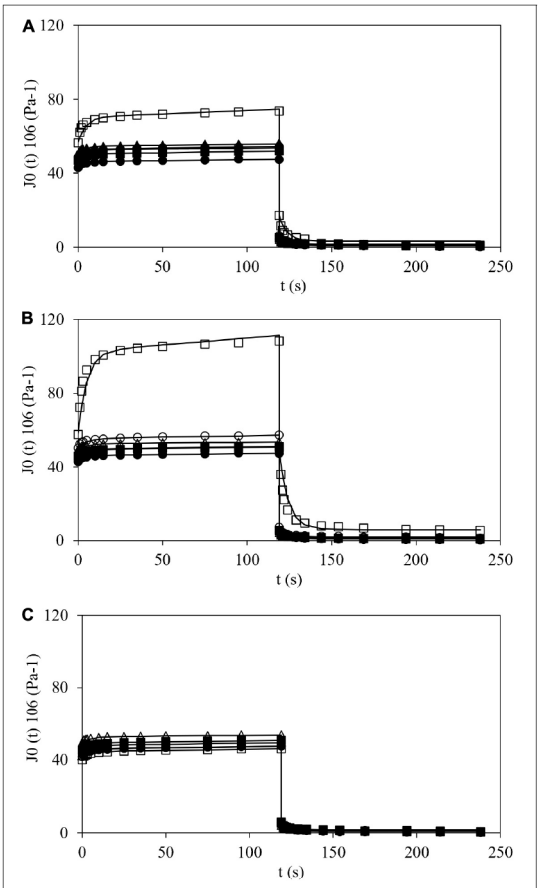

FIGURE 6 | Creep (120 s) and recovery (from 120 to 240 s) plots of corn starch (●), wheat starch (Δ), and corn starch + HPMC L **(A)**, M **(B)**, and H **(C)** at 0.5 (■), 1.0 (▲), 1,5 (○), and 2.0% (□), and modeling (–).

the HPMC L and M addition decreased G′ values. However, the opposite effect was observed when HPMC H was added above 1.0% w/w content. The tan δ (G″/G′) values lower than one indicates a predominance of elastic over viscous properties (5), **Figure 4**. At high concentrations, the addition of HPMC L and M showed higher values of tan δ, particularly at low frequencies. However, both moduli varied proportionally with HPMC H addition and the damping factor was invariant inside the studied frequency range. Lee et al. (14) observed the same trends employing waxy rice starch with the addition of HPMC of different viscosities with a ratio of 19:1 (w/w) and a total solids content of 25% w/w. Low viscosity HPMC (50 mPa·s) addition decreased G′ values in the mechanical spectrum while the addition of high viscosity HPMC (4,000 mPa·s) produced the opposite behavior.

TABLE 3 | Parameters of Burgers model (Eqs. 6 and 7) for creep and recovery tests.

Sample	HPMC(%w/w)	J_0 10^6(Pa^{-1})	J_m 10^6(Pa^{-1})	λ (s)	μ_0(Pa·s)	J_{max} 10^6(Pa^{-1})	R^2	RMSE10^6(Pa^{-1})
WS	0	49.6 ± 0.7^{b}	3.1 ± 0.1^{j}	5.5 ± 0.2^{ab}	391 ± 33^{b}	53.7 ± 0.1^{def}	0.96	0.4
CS	0	43.0 ± 0.7^{de}	3.30 ± 0.2^{ij}	5.5 ± 0.4^{ab}	356 ± 66^{bcd}	47.4 ± 0.8^{hi}	0.95	0.4
HPMC L	0.5	46.8 ± 2.1^{c}	3.6 ± 0.3^{hi}	5.0 ± 0.8^{abcd}	289 ± 58^{cd}	51.9 ± 2.4^{efg}	0.96	0.4
	1.0	50.0 ± 0.1^{b}	4.5 ± 0.1^{d}	4.1 ± 0.4^{d}	395 ± 29^{b}	56.1 ± 0.10^{cd}	0.96	0.5
	1.5	48.6 ± 0.2^{b}	4.3 ± 0.2^{de}	5.3 ± 0.1^{abc}	343 ± 2^{bcd}	54.4 ± 0.3^{cde}	0.96	0.5
	2.0	56.5 ± 0.3^{a}	13.9 ± 1.8^{b}	4.6 ± 0.4^{bcd}	389 ± 24^{bc}	73.6 ± 2.8^{b}	0.95	1.7
HPMC M	0.5	45.8 ± 0.2^{c}	3.7 ± 0.3^{gh}	5.5 ± 0.2^{ab}	329 ± 43^{bcd}	50.9 ± 0.5^{fg}	0.96	0.5
	1.0	45.7 ± 0.3^{c}	4.3 ± 0.1^{def}	5.7 ± 0.2^{a}	349 ± 60^{bcd}	51.3 ± 0.4^{efg}	0.96	0.5
	1.5	50.3 ± 0.1^{b}	5.3 ± 0.4^{c}	5.4 ± 0.4^{ab}	376 ± 56^{bcd}	57.4 ± 0.4^{cd}	0.95	0.7
	2.0	57.7 ± 0.1^{a}	44.7 ± 4.7^{a}	5.3 ± 0.9^{abc}	597 ± 92^{a}	108.4 ± 5.9^{a}	0.96	4.8
HPMC H	0.5	45.4 ± 0.3^{c}	3.9 ± 0.1^{fg}	4.4 ± 0.2^{cd}	323 ± 15^{bcd}	50.7 ± 0.2^{fg}	0.97	0.4
	1.0	43.7 ± 1.1^{d}	4.1 ± 0.2^{ef}	4.8 ± 0.4^{abcd}	286 ± 31^{d}	49.4 ± 1.2^{gh}	0.96	0.5
	1.5	41.8 ± 0.4^{ef}	4.2 ± 0.1^{def}	5.0 ± 0.4^{abc}	332 ± 43^{bcd}	47.6 ± 0.4^{hi}	0.96	0.5
	2.0	40.2 ± 0.2^{f}	4.4 ± 0.2^{d}	5.4 ± 0.5^{ab}	362 ± 12^{bcd}	46.2 ± 0.4^{i}	0.96	0.6

Data are presented as mean ± SD. Data values in a column with different superscript letters are significantly different at the $p \leq 0.05$ level. WS, wheat starch; CS, corn starch.

For comparative purposes, the frequency sweep for a WS gel (also at 30% w/w) formed under the same conditions that tested CS gels included in **Figure 4**. Viscoelastic properties of WS gel nicely agreed with data of wheat gel at the same starch content reported by Sasaki et al. (41). WS gel showed lower G′ and similar tan δ than CS gel. Nevertheless, viscoelastic parameters of WS gel could be obtained with the addition of HPMC L (at 1.0% w/w, **Figures 4A,B**) and HPMC M (at 1.5% w/w, **Figures 4C,D**). Nevertheless, the use of HPMC H was not useful to reproduce the viscoelastic features of CS gels because despite the adequate damping factor, the G′ values are systematically high, independently of the amount added (**Figures 4E,F**). Sivaramakrishnan et al. (8) also found that by adding a specific amount of low viscosity HPMC (around 3% w/w) to rice flour, similar viscoelastic characteristics to wheat flour could be obtained.

To establish some relationships between the rheological properties of fully developed CS gels with HPMC, G′ from frequency sweeps at 25°C were analyzed. **Figure 5** shows the percentage of change of G′ by HPMC addition with respect to the CS gels with values measured at 1 Hz. For gels containing HPMC L and M (low and medium M_v) a positive linear trend was found ($R^2 > 0.98$) with HPMC content. The firmness of gels with HPMC L and M decreased linearly with the amount of polymer added and no significant differences ($p > 0.05$) between both polymers were found. In samples with HPMC H, it was observed that the previous trend is maintained only at the low addition (0.5% w/w) level. At higher content (>1.0% w/w), the opposite effect is observed, and consequently, the change of G′ diminished (negative values meant that G′ values of gels with HPMC were higher than G′ of CS gels) due to the increase of G′ with additional amounts of polymer added. This fact is given by the high viscosity of HPMC in the continuous phase (14).

Creep-Recovery Test

Figure 6 shows creep-recovery curves at 25°C of all the tested samples where typical viscoelastic behavior can be observed. During creep step (120 s) the stress (100 or 400 Pa) was applied and creep compliance, J, was measured. Then, stress was removed, and J was also measured during 120 s (recovery step). For HPMC L and M a similar behavior was shown. In fact, at constant time, during the creep phase, J values increased with HPMC addition. In the case of CS with HPMC H, two different trends were observed. At low addition (0.5% w/w) an increase in J (like the effect observed with HPMC L and H) was displayed, but at higher polymer content (>1.0% w/w) smaller J values than that obtained for CS gels were determined. This is consistent with data obtained and already discussed previously with the oscillatory tests. Additionally, similar curves were obtained by Korus et al. (42) for CS samples.

The Burgers model satisfactorily fitted the experimental creep and recovery data ($R^2 > 0.95$ and RMSE < 4.8 10^{-6} Pa^{-1}). Parameters obtained using the Burgers model (Eqs 6 and 7) are shown in **Table 3**. The J_0 values varied from 43.0 10^{-6} Pa^{-1} for CS gel up to 56.5, 57.7, and 40.2 10^{-6} Pa^{-1} for gels at maximum polymer addition (2.0% w/w) of HPMC L, M and H, respectively. For WS gel, J_0 was 49.6 × 10^{-6} Pa^{-1}. The J_m values obtained varied in a restricted range between 3.3 and 5.3 × 10^{-6} Pa^{-1}, excepting for CS gels with HPMC L and M (at 2.0% w/w) which were noticeably higher, 13.92 and 44.70 × 10^{-6} Pa^{-1}, respectively. In general, λ and μ_0 varied between 4.1 and 5.7 s and 286 and 597 Pa·s, respectively. The J_{max} values varied from 46.2 to 56.1 × 10^{-6} Pa^{-1}, excepting for CS gels with HPMC L and M (at 2.0% w/w), 73.6 and 108.4 × 10^{-6} Pa^{-1}, respectively. These results were also in agreement with the obtained results by oscillatory tests where G′ and tan δ values varied sharply showing lower G′ values and higher tan δ than remaining samples. J_0 varied inversely with respect to G′ (from frequency sweep at 0.1 Hz and 25°C) and a successful linear correlation between both the parameters could be established ($R^2 > 0.96$). Consequently, the trends found for G′ with HPMC amount in the oscillatory tests are also valid here. Similarly, Onyango et al. (43) added HPMC (viscosity not specified) to gluten-free dough at two different concentrations (0.4 and 2.4%

w/w f.b.) and observed that with the lowest concentration, J_0 and J_m increased and, with the highest concentration, J_0 and J_m decreased. J_0 value can be used to analyze the sample rigidity. In general, HPMC addition increased J_0 values and, therefore, decreased the gel stiffness. However, the addition of HPMC H causes a different behavior from the threshold concentration, as previously observed. Moreira et al. (44) observed that the creep compliance (J_0, J_m, and J_{max}) values increased when the HPMC content increased in gluten-free doughs based on chestnut flour.

Analyzing the values of Burgers parameters of wheat and those obtained for CS gels with HPMC, it can be concluded that by adding from 1.0 up to 1.5% of HPMC L or 1.5% of HPMC M, similar values of J_0, λ., μ_0, and J_{max} could be obtained. These results satisfactorily agreed with results from oscillatory tests.

CONCLUSION

Water retention capacity of tested HPMC varied linearly with the average viscosimetric molecular weight (M_v) of HPMC. The temperature of gel point was invariant with M_v (when substitution degree is maintained constant), but HPMC with high M_v showed an aggregation step at temperatures near (below) gel point. The HPMC addition to CS gels causes significant changes in viscoelasticity and stiffness of samples. These effects depend on the amount of polymer added and the M_v of the HPMC.

Based on the viscoelastic response and creep-recovery tests, maintaining constant solid content (30% w/w), CS gels plus HPMC with mimetic features to WS gels can be only obtained under certain circumstances. HPMC with relatively low M_v is recommendable, specifically, from 1.0 up to 1.5% (w/w) of HPMC of $27.2 \cdot 10^3$ g/mol or 1.5% (w/w) of HPMC of $32.7 \cdot 10^3$ g/mol must be added. Nevertheless, the use of HPMC with high M_v is not adequate for this purpose.

DATA AVAILABILITY STATEMENT

The raw data supporting the conclusions of this article will be made available by the authors, without undue reservation.

AUTHOR CONTRIBUTIONS

LM: methodology, data curation, and writing—original draft preparation. CR: supervision, validation, and writing—reviewing, and editing. RM: conceptualization, data curation, supervision, validation, and writing—reviewing and editing. All authors contributed to the article and approved the submitted version.

FUNDING

The authors acknowledged the financial support of the Spanish Ministry of Science and Innovation (Project RTI2018-095919-B-C2) and the European Regional Development Fund (FEDER) and Xunta de Galicia (Consolidation Project ED431B 2019/01).

REFERENCES

1. Monteiro JS, Farage P, Zandonadi RP, Botelho RBA, Oliveira LL, Raposo A, et al. A systematic review on gluten-free bread formulations using specific volume as a quality indicator. *Foods.* (2021) 10:614. doi: 10.3390/foods10030614
2. Dziezak JD. A focus on gums. *Food Technol.* (1991) 45:116–32.
3. BeMiller JN. Hydrocolloids. In: Arendt EK, Dal Bello F editors. *Gluten-Free Cereal Products and Beverages*. San Diego, CA: Academic Press (2008). p. 203–15.
4. Osorio FA, Molina P, Matiacevich S, Enrione J, Skurtys O. Characteristics of hydroxy propyl methyl cellulose (HPMC) based edible film developed for blueberry coatings. *Procedia Food Sci.* (2011) 1:287–93. doi: 10.1016/j.profoo.2011.09.045
5. Zhang D, Mu T, Sun H. Comparative study of the effect of starches from five different sources on the rheological properties of gluten-free model doughs. *Carbohydr Polym.* (2017) 176:345–55. doi: 10.1016/j.carbpol.2017.08.025
6. Gularte MA, Rosell CM. Physicochemical properties and enzymatic hydrolysis of different starches in the presence of hydrocolloids. *Carbohydr Polym.* (2011) 85:237–44. doi: 10.1016/j.carbpol.2011.02.025
7. Mancebo CM, San Miguel MA, Martínez MM, Gómez M. Optimisation of rheological properties of gluten-free doughs with HPMC, psyllium and different levels of water. *J Cereal Sci.* (2015) 61:8–15. doi: 10.1016/j.jcs.2014.10.005
8. Sivaramakrishnan HP, Senge B, Chattopadhyay PK. Rheological properties of rice dough for making rice bread. *J Food Eng.* (2004) 62:37–45. doi: 10.1016/S0260-8774(03)00169-9
9. Gujral HS, Guardiola I, Carbonell JV, Rosell CM. Effect of cyclodextrinase on dough rheology and bread quality from rice flour. *J Agric Food Chem.* (2003) 51:3814–8. doi: 10.1021/jf034112w
10. Moreira R, Chenlo F, Torres MD, Rama B. Fine particle size chestnut flour doughs rheology: influence of additives. *J Food Eng.* (2014) 120:94–9. doi: 10.1016/j.jfoodeng.2013.07.025
11. Bárcenas ME, de la O-Keller J, Rosell CM. Influence of different hydrocolloids on major wheat dough components (gluten and starch). *J Food Eng.* (2009) 94:241–7. doi: 10.1016/j.jfoodeng.2009.03.012
12. Techawipharat J, Suphantharika M, BeMiller JN. Effects of cellulose derivatives and carrageenans on the pasting, paste, and gel properties of rice starches. *Carbohydr Polym.* (2008) 73:417–26. doi: 10.1016/j.carbpol.2007.12.019
13. Kim HS, BeMiller JN. Effects of hydrocolloids on the pasting and paste properties of commercial pea starch. *Carbohydr Polym.* (2012) 88:1164–71. doi: 10.1016/j.carbpol.2012.01.060
14. Lee H, Kim HS. Pasting and paste properties of waxy rice starch as affected by hydroxypropyl methylcellulose and its viscosity. *Int J Biol Macromol.* (2020) 153:1202–10. doi: 10.1016/j.ijbiomac.2019.10.250
15. Morreale F, Garzón R, Rosell CM. Understanding the role of hydrocolloids viscosity and hydration in developing gluten-free bread. *Food Hydrocoll.* (2018) 77:629–35. doi: 10.1016/j.foodhyd.2017.11.004
16. Funami T, Kataoka Y, Omoto T, Goto Y, Asai I, Nishinari K. Food hydrocolloids control the gelatinization and retrogradation behavior of starch. 2a. Functions of guar gums with different molecular weights on the gelatinization behavior of corn starch. *Food Hydrocoll.* (2005) 19:15–24. doi: 10.1016/j.foodhyd.2004.04.008
17. Mirabolhassani SE, Rafe A, Razavi SMA. The influence of temperature, sucrose and lactose on dilute solutionproperties of basil (*Ocimum basilicum*) seed gum. *Int J Biol Macromol.* (2016) 93:623–9. doi: 10.1016/j.ijbiomac.2016.09.021
18. Robertson J, de Monredon FD, Dysseler P, Guillon F, Amado R, Thibault JF. Hydration properties of dietary fibre and resistant starch: a European collaborative study. *LWT Food Sci Technol.* (2000) 33:72–9. doi: 10.1006/fstl.1999.0595

19. Rosell CM, Yokoyama W, Shoemaker C. Rheology of different hydrocolloids-rice starch blends. Effect of successive heating-cooling cycles. *Carbohydr Polym.* (2011) 84:373–82. doi: 10.1016/j.carbpol.2010.11.047
20. Torres MD, Chenlo F, Moreira R. Rheological effect of gelatinisation using different temperature-time conditions on potato starch dispersions: mechanical characterisation of the obtained gels. *Food Bioproc Tech.* (2018) 11:132–40. doi: 10.1007/s11947-017-2000-6
21. Abedfar A, Hosseininezhad M, Rafe A. Effect of microbial exopolysaccharide on wheat bran sourdough: rheological, thermal and microstructural characteristics. *Int J Biol Macromol.* (2020) 154:371–9. doi: 10.1016/j.ijbiomac.2020.03.149
22. Burgers JM. *First Report on Viscosity and Plasticity*. New York, NY: Nordemann Publishing (1935).
23. Vázquez MJ, Casalderrey M, Duro R, Gómez-Amoza JL, Martínez-Pacheco R, Souto C, et al. Atenolol release from hydrophilic matrix tablets with hydroxypropylmehylcellulose (HPMC) mixtures as gelling agent: effects of the viscosity of the HPMC mixture. *Eur J Pharm Sci.* (1996) 4:39–48. doi: 10.1016/0928-0987(95)00030-5
24. Khouryieh HA, Herald TJ, Aramouni F, Alavi S. Intrinsic viscosity and viscoelastic properties of xanthan/guar mixtures in dilute solutions: effect of salt concentration on the polymer interactions. *Food Res Int.* (2007) 40:883–93. doi: 10.1016/j.foodres.2007.03.001
25. Bustamante P, Navarro-Lupión J, Escalera B. A new method to determine the partial solubility parameters of polymers from intrinsic viscosity. *Eur J Pharm Sci.* (2005) 24:229–37. doi: 10.1016/j.ejps.2004.10.012
26. Funami T, Kataoka Y, Hiroe M, Asai I, Takahashi R, Nishinari K. Thermal aggregation of methylcellulose with different molecular weights. *Food Hydrocoll.* (2007) 21:46–58. doi: 10.1016/j.foodhyd.2006.01.008
27. Yılmaz VMB, Süfer Ö, Kumcuoğlu S. Effects of temperature and hydrocolloids on the rheological characteristics of coating batters. *J Food Meas Charact.* (2017) 11:1159–66. doi: 10.1007/s11694-017-9492-7
28. Viridén A, Wittgren B, Larsson A. Investigation of critical polymer properties for polymer release and swelling of HPMC matrix tablets. *Eur J Pharm Sci.* (2009) 36:297–309. doi: 10.1016/j.ejps.2008.10.021
29. Fariña M, Torres MD, Moreira R. Starch hydrogels from discarded chestnuts produced under different temperature-time gelatinisation conditions. *Int J Food Sci Technol.* (2019) 54:1179–86. doi: 10.1111/ijfs.14070
30. Lazaridou A, Duta D, Papageorgiou M, Belc N, Biliaderis CG. Effects of hydrocolloids on dough rheology and bread quality parameters in gluten-free formulations. *J Food Eng.* (2007) 79:1033–47. doi: 10.1016/j.jfoodeng.2006.03.032
31. Moreira R, Chenlo F, Torres MD. Rheology of commercial chestnut flour doughs incorporated with gelling agents. *Food Hydrocoll.* (2011) 25:1361–71. doi: 10.1016/j.foodhyd.2010.12.015
32. Zhang Y, Gu Z, Zhu L, Hong Y. Comparative study on the interaction between native corn starch and different hydrocolloids during gelatinization. *Int J Biol Macromol.* (2018) 116:136–43. doi: 10.1016/j.ijbiomac.2018.05.011
33. Alamri MS, Mohamed AA, Hussain S. Effects of alkaline-soluble okra gum on rheological and thermal properties of systems with wheat or corn starch. *Food Hydrocoll.* (2011) 30:541–51. doi: 10.1016/j.foodhyd.2012.07.003
34. Silva SMC, Pinto FV, Antunes FE, Miguel MG, Sousa JJS, Pais AACC. Aggregation and gelation of hydroxypropylmethyl cellulose aqueous solutions. *J Colloid Interface Sci.* (2008) 327:333–40. doi: 10.1016/j.jcis.2008.08.056
35. Joshi SC. Sol-gel behavior of hydroxypropyl methylcellulose (HPMC) in ionic media including drug release. *Materials.* (2011) 4:1861–905. doi: 10.3390/ma4101861
36. Guarda A, Rosell CM, Benedito C, Galotto MJ. Different hydrocolloids as bread improvers and antistaling agents. *Food Hydrocoll.* (2004) 18:241–7. doi: 10.1016/S0268-005X(03)00080-8
37. Kaur L, Singh J, Singh H, McCarthy OJ. Starch-cassia gum interactions: a microstructure – rheology study. *Food Chem.* (2008) 111:1–10. doi: 10.1016/j.foodchem.2008.03.027
38. Wang S, Li C, Copeland L, Niu Q, Wang S. Starch retrogradation: a comprehensive review. *Compr Rev Food Sci Food Saf.* (2015) 14:568–85. doi: 10.1111/1541-4337.12143
39. Singh A, Gevekea DJ, Yadav MP. Improvement of rheological, thermal and functional propertie of tapioca starch by using gum Arabic. *LWT Food Sci Technol.* (2017) 80:155–62. doi: 10.1016/j.lwt.2016.07.059
40. Ma S, Zhu P, Wang M. Effects of konjac glucomannan on pasting and rheological properties of corn starch. *Food Hydrocoll.* (2019) 89:234–40. doi: 10.1016/j.foodhyd.2018.10.045
41. Sasaki T, Kohyama K, Yasui T. Effect of water-soluble and insoluble non-starch polysaccharides isolated from wheat flour on the rheological properties of wheat starch gel. *Carbohydr Polym.* (2004) 57:451–8. doi: 10.1016/j.carbpol.2004.06.004
42. Korus J, Witczak M, Ziobro R, Juszczak L. The impact of resistant starch on characteristics of gluten-free dough and bread. *Food Hydrocoll.* (2009) 23:988–95. doi: 10.1016/j.foodhyd.2008.07.010
43. Onyango C, Unbehend G, Lindhauer MG. Effect of cellulose-derivatives and emulsifiers on creep-recovery and crumb properties of gluten-free bread prepared from sorghum and gelatinised cassava starch. *Food Res Int.* (2009) 42:949–55. doi: 10.1016/j.foodres.2009.04.011
44. Moreira R, Chenlo F, Torres MD. Effect of chia (*Salvia hispanica* L.) and hydrocolloids on the rheology of gluten-free doughs based on chestnut flour. *LWT Food Sci Technol.* (2012) 50:160–6. doi: 10.1016/j.lwt.2012.06.008

Conflict of Interest: The authors declare that the research was conducted in the absence of any commercial or financial relationships that could be construed as a potential conflict of interest.

Publisher's Note: All claims expressed in this article are solely those of the authors and do not necessarily represent those of their affiliated organizations, or those of the publisher, the editors and the reviewers. Any product that may be evaluated in this article, or claim that may be made by its manufacturer, is not guaranteed or endorsed by the publisher.

5.GENERAL DISCUSSION

5. General discussion

Celiac disease is a chronic digestive and autoimmune disorder that damages the small intestine and impairs the absorption of vitamins, minerals and other nutrients contained in foods and can cause long-lasting digestive problems. This disease is triggered by eating foods that contain gluten, a protein found in wheat, barley, and rye (Mollakhalili *et al.*, 2015). However, the reality of bakeries is that they seek to improve gluten-free bread continuously, but the results obtained do not yet achieve a good final product so far. Gluten-free (*GF*) products show low levels of several nutrients or micronutrients, protein and dietary fibre, and the lack of gluten makes the products worse in quality and consumer acceptance. Furthermore, having a limited shelf-life due to rapid staling is a major issue for gluten-free products (Šmídová & Rysová, 2022). Because the absence of gluten affects the baked products volume, porosity and other quality characteristics, many *GF* products on the market show a lower quality than those equivalent wheat based. Gluten is a protein essential to achieve a high dough elasticity and contributes to the fluffiness and crumb structure of many baked products. The search for compounds to achieve viscoelastic properties like those provided by gluten is currently an important challenge. Several studies have been focused on the use of different hydrocolloids to improve the appearance and structure of the final *GF* products (Bender & Schönlechner, 2020; Espinoza-Herrera *et al.*, 2021). There are studies reporting that a gluten-free diet could influence the risk of developing type-2 diabetes (Romão *et al.*, 2021). This relationship is attributed to many gluten-free products having a higher glycemic index than products containing gluten, because they are often made from refined starches. Additionally, gluten-free products may have less fibre and fewer nutrients content, and a gluten-free diet can also alter the composition of the intestinal microbiota. Taking this into account, the study of this Doctoral Thesis is focused on the research of potential gluten substitutes, which can improve both the nutritional and structural properties of GF products, focusing on the search for natural additives that also reduce their glycemic index. One mode of reducing the glycemic index is the addition of compounds with reported amylase and/or

amyloglucosidase activity inhibition, such is the case of plant or algae polyphenols. Also, obtaining both the texture modifying agent (such as hydrocolloids from algae) and the enzyme-inhibiting molecules from the same raw material is remarkably interesting. For this reason, the study began focusing on a natural compound obtained from a brown alga (*Ascophyllum nodosum*), rich in polyphenols. Polyphenols have a high antioxidant capacity, are slightly hydrophobic secondary metabolites and are one of the most abundant groups in the plant kingdom (Besednova *et al.*, 2021).

5.1. Studies on the polyphenols-native starch interaction

In a first stage of the present Thesis, our research was aimed to know how polyphenols interact with native corn starch and gelatinised corn starch. The generation of the polyphenol extract is described in methodology section "*3.2.1. Extraction of polyphenols*". The total polyphenols (gPP/L) content, expressed as phloroglucinol equivalents, was 2.7 ± 0.1 gPP/L. From this stock solution, several dilutions were made to achieve a range of concentrations from 0.10 to 2.00 gPP/L. To the solutions obtained, a constant amount of starch was added to analyse in equilibrium the fraction of polyphenols adsorbed by the starch. Two corn starch concentration values were used, 1.95 and 5.00% (w/w), for both native and gelatinised starch. The methodology is described in the general methodology in section "*3.4.3. Polyphenols adsorption on corn native starch and gels*" and, in Publication 1. The adsorption kinetics to achieve the equilibrium of these systems can be seen in Figure 5.1, where the concentration values of remaining polyphenols in solution (g_{PP}/L), are plotted against the contact time between the polyphenol solution and native starch. As can be observed, there is a sharp decrease of polyphenols content in liquid phase for all systems during the initial minutes. For instance, in Figure 5.1 (a), with an initial concentration of 0.10 g_{PP}/L, it is evident that after 50 min, complete adsorption (equilibrium) has already taken place. However, given the uncertainty regarding the behaviour of the remaining systems,

all kinetics were extended to a total of 180 min to ensure equilibrium had been reached.

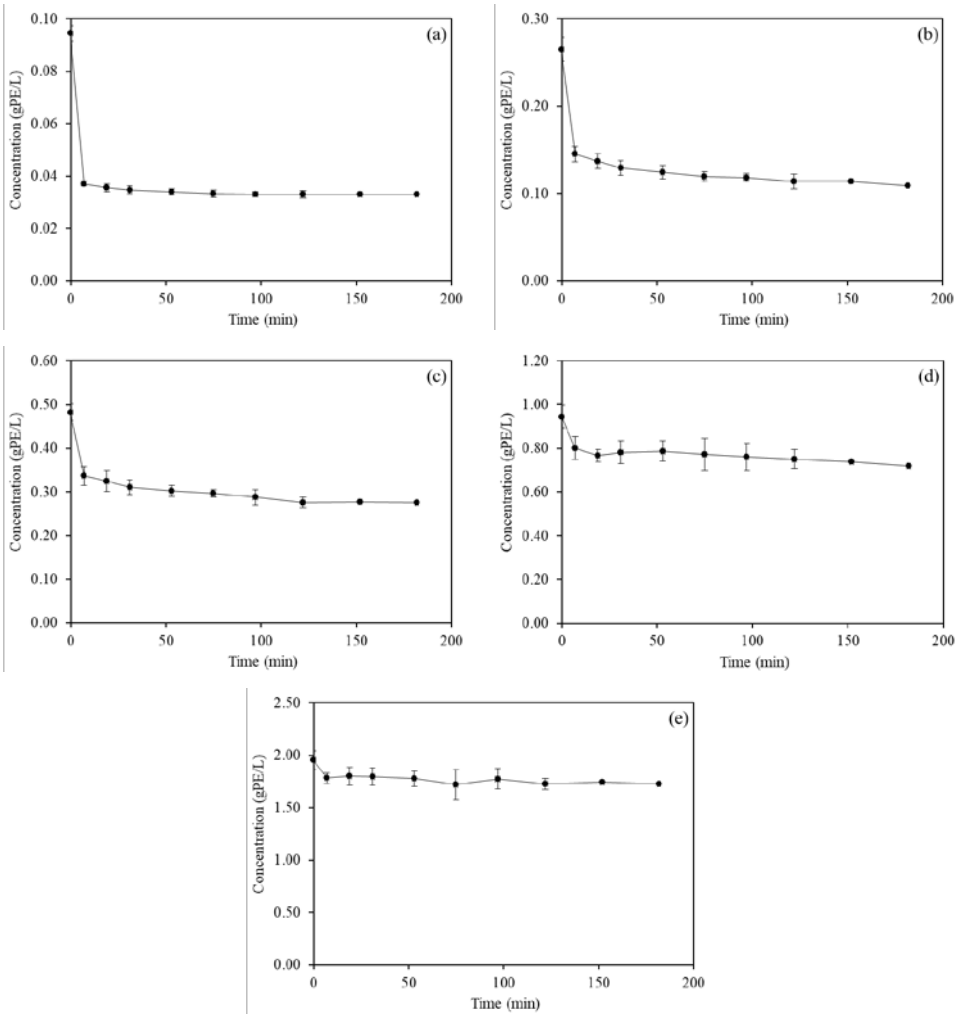

Figure 5.1. Concentration of remaining polyphenols in solution in contact with native starch (1.95% w/w) vs time for different initial concentrations: 0.10 g/L (a), 0.30 g/L (b), 0.50 g/L (c), 1.00 g/L (d), and 2.00 g/L.

When 5.00% w/w starch was employed, a higher polyphenol concentration in the stock solution to analyse the adsorption kinetics was employed. For this, the stock

polyphenol concentration was increased up to 3.00 g_{PP}/L. Adsorption kinetics are shown in Figure 5.2. The results shown in Figure 5.2 (f) were considered for equilibrium analysis and mathematical modelling.

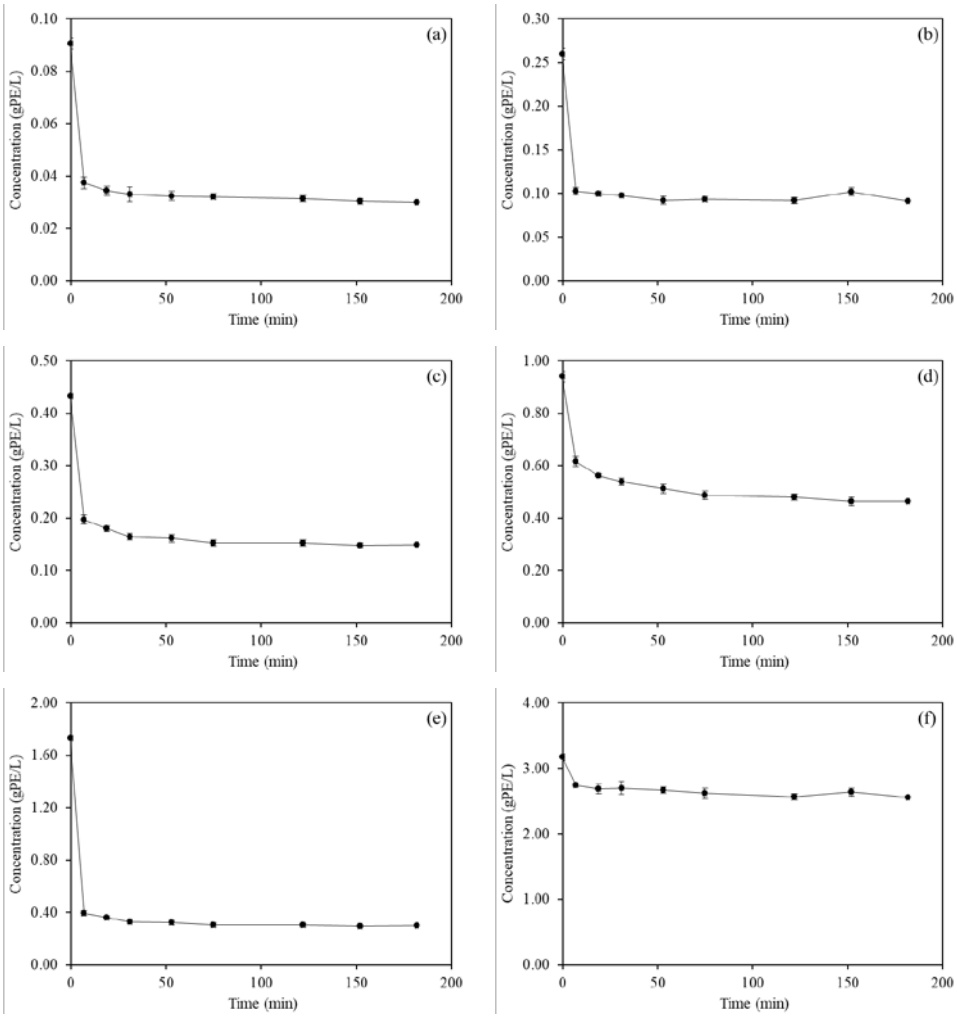

Figure 5.2. Concentration of remaining polyphenols in solution in contact with native starch (5.00% w/w) vs time for different initial concentrations: 0.10 g/L (a), 0.30 g/L (b), 0.50 g/L (c), 1.00 g/L (d), 2.00 g/L (e), and 3.00 g/L (f).

As it was determined from the first the kinetic assay, performed with 1.95% w/w starch content, that an incubation time during 180 min was long enough to achieve equilibrium, this parameter was maintained for further tests.

Once the adsorption tests were completed, the mass of polyphenols adsorbed per mass of starch was calculated from the concentration values of each experiment at equilibrium. These results can be seen in Figure 5.3, where the equilibrium values obtained from the previous assays for the two analysed starch systems are shown: 1.95% w/w (a) and 5.00% w/w (b). Considering the shape of the adsorption curves, the Langmuir isotherm model (Eq. 5.1) was applied to fit experimental data:

$$q = q_{max} \frac{[\mathrm{PP}]_\mathrm{e}\, b}{(1 + b\,[\mathrm{PP}]_\mathrm{e})} \tag{5.1}$$

where q (g polyphenol/g corn starch, g_{PP}/g_{CS}) is the polyphenols mass adsorbed at equilibrium, $[PP]_e$ (g_{PP}/L) is the polyphenol concentration at equilibrium, q_{max}, is the maximum amount of polyphenols adsorbed and b is a parameter of the model.

For 1.95% w/w, the maximum q value was 0.012 ± 0.001 g_{PP}/g_{CS} and it was obtained at $[PP]_e$ above 0.60 g_{PP}/L; in the case of 5.00% w/w, the maximum q value was 0.013 ± 0.002 g_{PP}/g_{CS} and it was obtained with $[PP]_e$ above 1.00 g_{PP}/L. Consequently, the amount polyphenols required to saturate the starch surface increases with the amount of starch. Regardless of the starch concentration, similar maximum q values were obtained, concluding that the range of starch used was in a range adequate to obtain the saturation of starch surface allowing the determination of the corresponding model parameters because the entire surface was available for polyphenol sorption. In both systems, the shape of the curve corresponded to a Langmuir isotherm ($R^2 >$ 0.98) indicating that polyphenols adsorption on the starch surface is physically limited. The parameters b obtained of Eq. (5.1) were 21.75 ± 2.07 and 6.01 ± 0.22 L/g_{PP} for 1.95% and 5.00% w/w starch content, respectively. A more extensive discussion of these results is included in Publication 1.

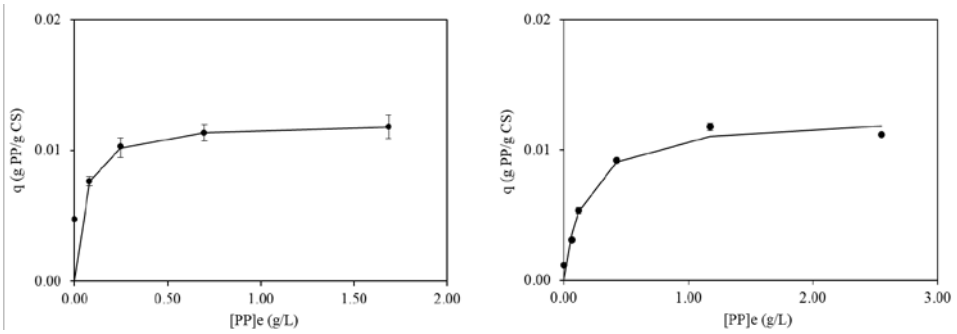

Figure 5.3. Adsorption of polyphenols at 25ºC on native corn starch at 1.95% w/w (a) and 5.00% w/w (b).

5.2. Studies of interaction during starch gelation process

Once the study of polyphenols adsorption on native starch was performed, it was important to study the polyphenols-starch interaction when starch gelation is performed in an environment containing polyphenols and further subjected to thermal processing. This study allows to know the effects on both the gelation conditions and the adsorption/retention of polyphenols onto gel. These conditions are closer to real processing conditions during bread or starchy foods industrial manufacturing. The gelatinised starch was analysed in a similar mode than previous experiments with raw starch and maintaining the same polyphenols/starch mass ratio. Therefore, these studies were carried out for both 1.95 and 5.00% w/w of gel starch. The methodology is described in section "*3.4.3. Polyphenols adsorption on corn native starch and gels*".

First, in Figure 5.4, the plots of polyphenols adsorption on gelatinised starch can be observed for each initial polyphenol solution ranging from 0.10 to 2.00 g_{PP}/L for 1.95% w/w of gelatinised starch. As can be seen, unlike the studies carried out for native starch, the adsorption of gelatinised starch is not only greater but also much faster.

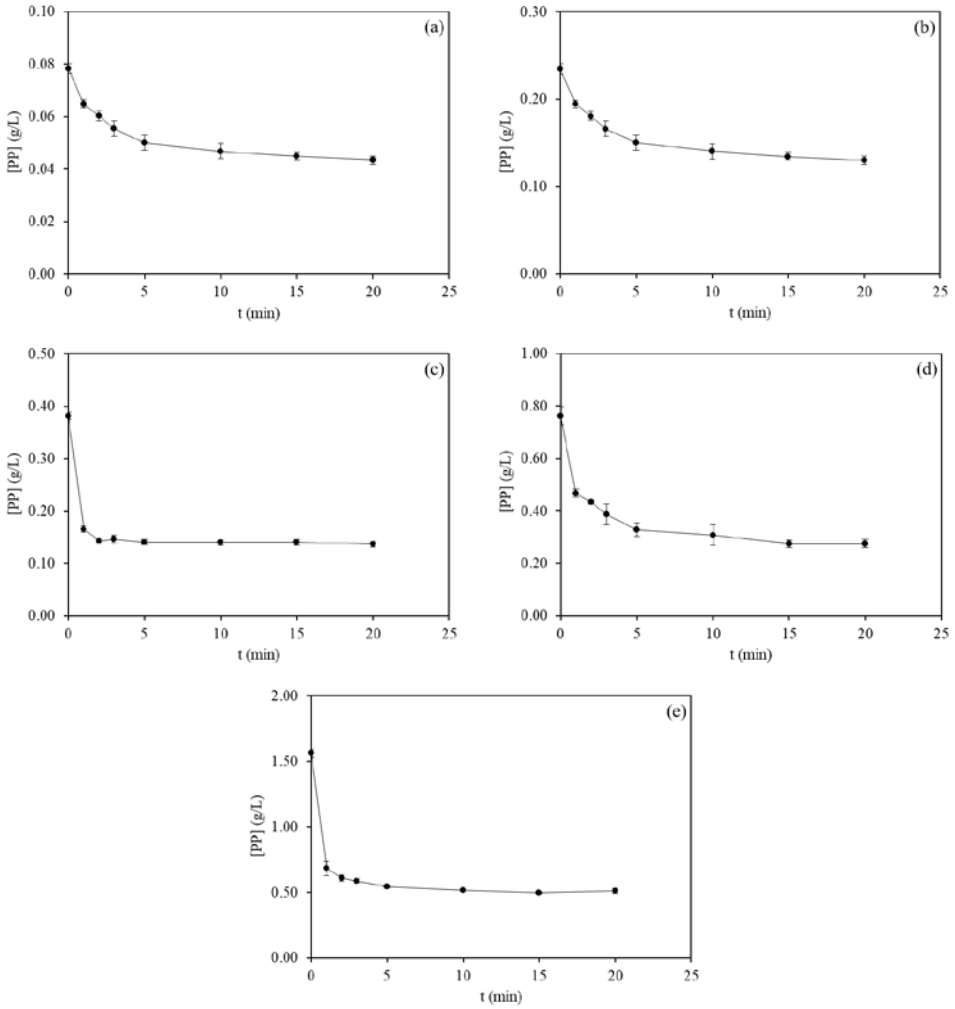

Figure 5.4. Concentration of remaining polyphenols in solution in contact with gelatinised starch (1.95% w/w) vs time for different initial concentrations: 0.10 g/L (a), 0.30 g/L (b), 0.50 g/L (c), 1.00 g/L (d), and 2.00 g/L (e).

For 5.00% w/w starch system, the same solutions with the same concentrations of polyphenols were used as for 1.95% w/w and adsorption kinetics can be observed in Figure 5.5. Also, in this case, the equilibrium was readily achieved (in less than 20 min).

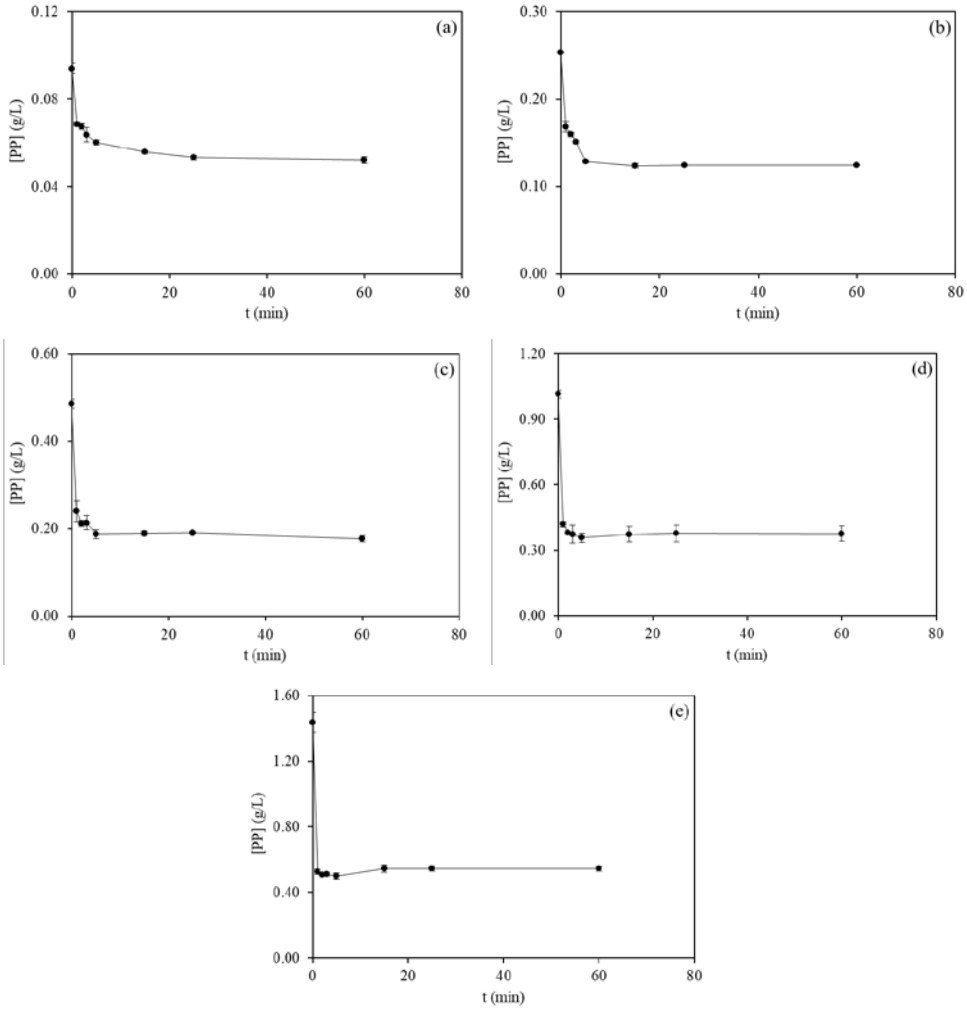

Figure 5.5. Concentration of remaining polyphenols in solution in contact with gelatinised starch (5.00% w/w) vs time for different initial concentrations: 0.10 g/L (a), 0.30 g/L (b), 0.50 g/L (c), 1.00 g/L (d), and 2.00 g/L (e).

The equilibrium polyphenols concentration values obtained from these assays with gelatinised starch can be seen in Figure 5.6, for 1.95% w/w (a) and 5.00% w/w (b). Using 2.0 g/L polyphenol solution, the highest adsorption values, *q*, achieved for 1.95 and 5.00% w/w starch content were 0.070 ± 0.001 and 0.018 ± 0.001 g_{PP}/g_{CS}, respectively. Unlike native starch, a linear relationship ($R^2 > 0.99$) was observed between equilibrium polyphenol concentration of solution and adsorbed

polyphenols. Low concentration starch gels retained more polyphenols per gram of starch. Furthermore, the polyphenol sorption in starchy gels is far from saturation; thus, a different model, Henry's isotherm (Eq. 5.2), was applied to fit experimental data:

$$q = \mathrm{K}\,[\mathrm{PP}]_e \qquad (5.2)$$

where *K* is the parameter of the model, and the corresponding values are collected in Table 5.1.

The polyphenols adsorption increased significantly (almost 7 times) with starch gels compared to native starch. The minimum fraction of polyphenols adsorbed was higher than 65.9% with starch gels, whereas a much lower value of 13.8% was obtained with native starch. These results indicate that gelled starch increased noticeably the available surface area and enhanced interactions between starch and polyphenols (Gisbert *et al.*, 2022). More details can be found in Publication 1.

Table 5.1. Parameters of Langmuir, Eq. (5.1), and Henry isotherms, Eq. (5.2).

	Langmuir isotherm (native corn starch)			Henry isotherm (corn starch gel)	
Starch content (% w/w)	q_{max} (g_{PP}/g_{CS})	b (L/g_{PP})	R^2	k (L/g_{CS})	R^2
1.95	0.012±0.001	21.75±2.07	0.97	0.149±0.003	0.99
5.00	0.013±0.001	6.01±0.22	0.99	0.039±0.001	0.99

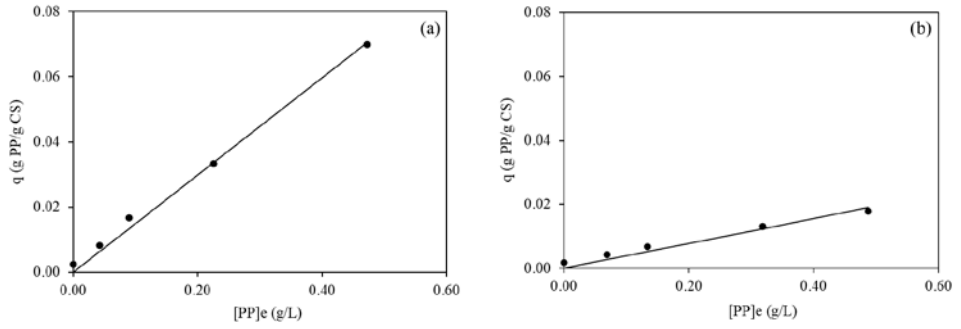

Figure 5.6. Adsorption of polyphenols at 25ºC on native corn starch at 1.95% w/w (a) and 5.00% w/w (b).

The tests carried out to characterise starch and its digestion in the presence of polyphenols were based on previous adsorption tests on native starch. This decision was made with the intention of simulating the production of traditional and industrial bread. However, the effect of the adsorption of polyphenols on starch gel on the structure and digestion of the gels formed was also studied. This procedure is justified by the process for producing gluten-free bread ultimately contained a pre-gelatinisation stage, since after various tests it was the way to obtain doughs with appropriate features.

5.3. Rheological measurement of starch hydrolysis (preliminary tests): application to α-amylase activity on starch

In vitro digestion is usually studied by chemical hydrolysis, but the opportunity arose to do the same study in the decrease of viscosity in a rheometer. In this case, it was decided to perform a study with different starches (corn, wheat and rice) to evaluate the amount of enzyme used in these tests.

To carry out a rapid study of the digestion of different starches, it was decided to perform a rapid gelatinization in the rheometer followed by the subsequent addition of the enzyme. The methodology is described in the section "*3.4.5.2. Rheometer determining the viscosity drop with time for studying the digestion starch*". In Figure 5.7 it can be observed the formation of the gels and then, its maturation (empty symbols) and digestion (filled symbols). During the first 20 min, the gelatinization of the starch can be observed where the viscosity values obtained at the end of this stage were 4975 ± 78, 4520 ± 14, and 2445 ± 134 mPa s for corn, wheat, and rice gels starch, respectively. After gelatinization is completed, the enzyme is added, and starch digestion begins in a simulated medium. The viscosity values recorded over time decrease as starch digestion occurs, reaching values of 1810 ± 42, 323 ± 26, and 94 ± 17 mPa s for corn, wheat, and rice gels starch, respectively. On the other hand, during the maturation period, the increase in apparent viscosity of the starches studied was related to slower cooling due to their higher viscosity which reduces the

cooling rate within the gel structure. In fact, in the case of rice gel, a constant apparent viscosity was observed because its lower viscosity allowed for faster heat transfer within the gel structure (Santamaria *et al.*, 2023a).

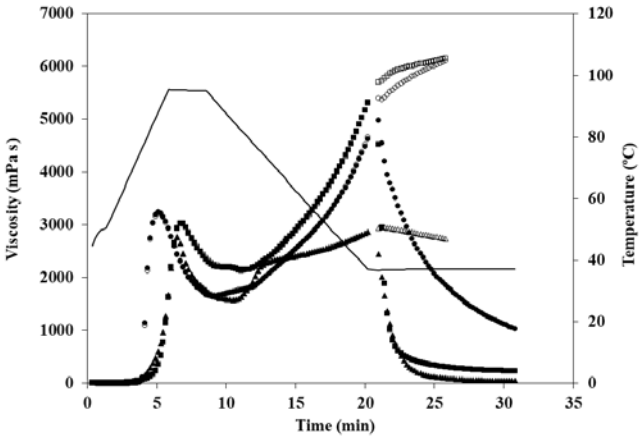

Figure 5.7. The apparent viscosity versus time following the protocol previously described for corn (●), wheat (■), and rice (▲) starches.

It can be seen in Figure 5.8 the decrease of the apparent viscosity for tested starch gels during starch digestion after enzyme addition. The modelling was carried out by adjusting experimental values to Eq. (5.3):

$$\mu = \mu_\infty + (\mu_0 - \mu_\infty)e^{-kt} \tag{5.3}$$

where μ is the apparent viscosity (mPa s), μ_0 is the initial viscosity, μ_∞ is the final viscosity, k (min^{-1}) is the kinetic constant, and t (min) is hydrolysis time.

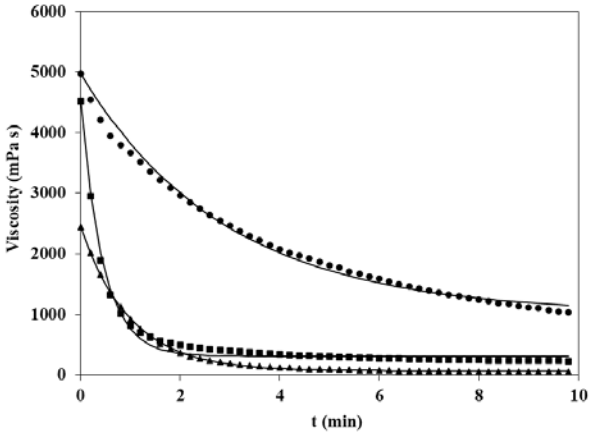

Figure 5.8. The apparent viscosity versus time during gels digestion for corn (●), wheat (■), and rice (▲) starches.

The corresponding parameters of the Eq. (5.3) are summarized in Table 5.2. The lowest kinetic constant, *k*, values were obtained for corn starch, so indicating the slowest starchy gel digestion, whereas the fastest digestion was obtained for the wheat starch gel. These results were also obtained by other authors using a similar protocol but using the *RVA*, where *k* was 0.311 ± 0.020, 1.363 ± 0.172, and 0.764 ± 0.116, for corn, wheat, and rice starch gels, respectively (Santamaria et al, 2023b).

Table 5.2. Gel starch viscosities obtained after adding amylase, the initial viscosity (μ_0), the kinetic constant (k) and the maximum hydrolysis of starch gels (μ_∞).

Gel starch	**μ_0 (mPa·s)**	**μ_∞ (mPa s)**	**k (min^{-1})**
Corn	4975 ± 78^a	1549 ± 68^a	0.46 ± 0.01^c
Wheat	4520 ± 14^b	336 ± 50^b	2.38 ± 0.07^a
Rice	2445 ± 134^c	83 ± 16^c	1.04 ± 0.02^b

Since it was shown that starch digestion can be monitored by rheology, it was proposed to study how the amount of added enzyme affects it. For this study, corn starch was used. The amount of enzyme used was 14 Units/mg starch, being the unit definition given by Minekus *et al.* (2014) as the amount of enzyme able to liberate 1 mg of maltose in 3 min at pH 6.9 and 20ºC. Preliminary, it was decided to consider two points at very low enzyme addition (0.01 and 0.10 U/mg starch) and other two at low range (0.30 and 0.50 U/mg starch) to analyse the linearity at low enzyme concentration and the existence of a plateau due to enzyme saturation by substrate. In these assays, a linear relationship was obtained between the digestion rate kinetic constant and the U/mg starch added, so the reaction was limited by enzyme concentration and excess of substrate is present. After these results, it was decided to add more enzyme and the following values were used: 1.00, 1.50, 2.00, 5.00, 10.00 and 20.00 U/mg starch. For the last two highest values, a maximum digestion rate value was already achieved with the presence of a plateau, so the experiment was not substrate-limited and whole range permits to fit experimental data to a Langmuir-type equation to express the substrate saturation by the enzyme, Eq. (5.4). It is obtained an expression analogue to Michaelis-Menten equation, the simplest model in absence of enzymatic inhibition.

$$k = \frac{k_{max}\,[E/S]}{K_s + [E/S]} \qquad\qquad k = \frac{0.3525\,[E/S]}{0.8710 + [E/S]} \qquad (5.4)$$

where k is the kinetic viscosity constant, k_{max} and K_s are the maximum kinetic constant and saturation constant, respectively, and their values were obtained after non-linear fitting of experimental data, finally, [*E/S*] is the enzyme/substrate ratio (Enzyme units/mg starch).

It can be seen in Figure 5.9 the initial digestion rate values against the enzyme-to-starch ratio, together with the regression curve, Eq. (5.4). At *E/S* ratios lower than 5 U/mg starch the reaction rate is determined by the lack of enzyme, being proportional to enzyme dosage below 3 U/mg of *E/S* ratios. In contrast, the enzyme concentration value reported by Minekus *et al.* (2014) for starch hydrolysis (14 U/mg) accomplished with the region where hydrolysis rate is constant, being this dosage

much higher than K_s parameter value of 0.871 U/mg, determined in this work. Additionally, it is suggested that a [*E/S*] of 10 U/mg starch might be high enough to achieve an initial constat rate for hydrolysis of starch with similar origin and characteristics to those employed in this work. Anyway, it was decided to continue using the same amount of enzyme that was used previously for the subsequent tests, since it was considered better to for comparison with literature, because most researchers follow exactly the Minekus' recipe, applying 14 U/mg starch.

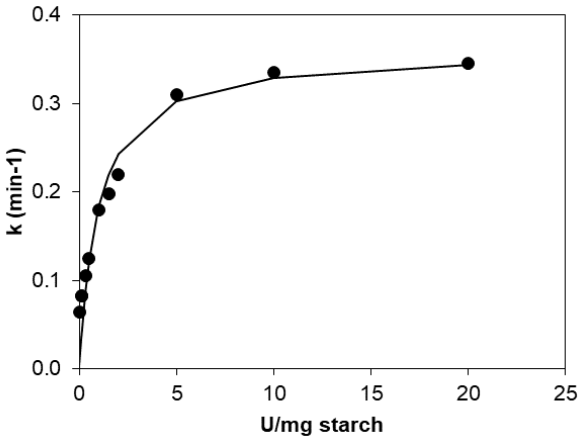

Figure 5.9. Plot (dots) and correlation (continuous line, Eq. (5.4)) of initial hydrolysis rate as a function of increasing enzyme units per mg of starch.

For this reason, after studying the corn starches digestion, it was proposed to study how algae polyphenols affected starch hydrolysis, since these compounds are known to show inhibitory activity upon amylases and alpha glucosidases reactions (Aleixandre *et al.*, 2022) which is that basis for formulation an polyphenols-enriched meal that was able to reduce the gut absorption rate of glucose and maltose from starchy foods, additionally to the important antioxidant activity these polyphenols have demonstrated (Gisbert *et al.*, 2022).

5.4. Effect of polyphenols on corn starch gels rheological properties and enzymatic digestion with α-amylase and amyloglucosidase

In previous section, the interaction between polyphenols and starch was already studied, a further study was carried out with starch gels to investigate how the presence of polyphenols can affect both the viscoelastic characteristics of corn starch gels and their digestion. To achieve this goal, systems of 1.95% and 5.00% w/w of corn starch (*CS*) incubated with polyphenols (*PP*) at different concentration were studied. For 1.95% w/w samples, the nominal *PP/CS* (g_{PP}/g_{CS}) ratios were 0.0, 0.5, 2.5 and 5.0; whereas for gels at 5.00% w/w the ratios were 0.0, 0.2, 0.9 and 1.9, adding different amounts of *PP* solutions of 0.0, 0.1, 0.5 and 1.0 g/L. As discussed in Publication 1, the systems were subjected to a heating stage from 25 to 90ºC, a time sweep at 90ºC, a cooling stage from 90 to 25ºC and a final time sweep at 25ºC. The methodology is described in section "*3.4.4.1. Rheological characterization of starch with polyphenols*". The presence of polyphenols increased the maximum gelatinisation temperature (T_p), which corresponds to the highest value of the elastic modulus ($G´$) during the heating ramp. In the gels without polyphenols, these values were 11.1 ± 0.3 Pa and 78.3 ± 5.9 Pa for 1.95% and 5.00% w/w starch content, respectively, while with the presence of polyphenols the maximum values obtained were 15.1 ± 0.4 Pa and 125.4 ± 4.1 Pa, for 1.95% and 5.00% w/w, respectively. This result may be related to the decrease of water available for starch gelatinisation by the hydrophilic nature of polyphenols. During the time sweep at 90ºC, a relevant decrease of $G´$ value was observed for the systems with added polyphenols; this observation may be related to the cross-linking formed between the polyphenols and the starch during gelatinization, consequently, the elastic character at high temperature is increased. In the cooling sweep, the gels with polyphenols had higher $G´$ values than the systems without polyphenols from the beginning (90ºC), but the samples with polyphenols showed lower $G´$ values than the systems without polyphenols at the end (25ºC). This result seems to indicate that the presence of polyphenols interferes the formation of the final three-dimensional structure of starchy gel. During the gel maturation stage, at 25ºC for 30 min, it was observed

that the presence of polyphenols notably increased the stability of the gels, since the change of *G'* values during this period was much higher for systems without polyphenols. Finally, a frequency sweep was performed in matured gels, and it was observed that the samples had a typical behaviour of starchy gels showing values of *G'* higher than *G''*. For the less concentrated starch gels, 1.95% w/w, a clear effect of polyphenols on the final gel characteristics was observed, giving as result significantly lower *G'* values. Furthermore, no significant differences were observed with the increasing of concentration of added polyphenols concentration confirming that a low concentration was required to interfere with the gel structure and weaken it. For gels with starch content of 5.00% w/w, similar behaviour between gels without added polyphenols and with low polyphenols (below 0.9 *PP/CS* ratio (g_{PP}/g_{CS})) content, was observed, but the gels with a high *PP/CS* ratio showed a significant decrease of *G´* values.

Once the rheological characteristics were analysed, the digestion of these gels was studied. To study digestion, chemical kinetics were carried out and a rapid method was also assessed for the determination of starch depolymerisation degree as measured by apparent viscosity measurements in a shear stress-controlled rheometer Anton Paar-Physica MCR 301 Rheometer (Graz, Austria). Firstly, the starch digestion kinetics were analysed, the methodology is described in section "*3.4.5.1. Conventional biochemical method of in vitro digestion starch*". The values of the digestion kinetic constants (*k*), employing a pseudo-first order model, Eq. (3.33), for corn starch gels without polyphenols, at both concentration values (1.95 and 5.00% w/w) were similar, the obtained values were 0.149 ± 0.002 and 0.136 ± 0.005 min^{-1}, respectively.

This result can be explained because the gels are so weak that the structure did not influence the enzymatic action, not affecting the accessibility of enzymes to starch molecules. Regardless of the gel starch content, the addition of polyphenols decreased both the digestion kinetic constant and the final concentration of digested starch, expressed as the parameter C_∞. Furthermore, the greater the amount of polyphenols added, the greater the decrease of *k*-value. Probably, the structure of

starch changed in the presence of polyphenols, as they could be forming an "inclusive V- type amylose" complex along α (1→4) glycosidic chains with starch amylose, as reported by Li *et al.* (2020a). The rapidly digestible starch (*RDS*) values corroborated this theory, since less starch was rapidly digested when polyphenols were added to the gels. However, it was observed that the slowly digestible starch (*SDS*) values increased significantly with the addition of polyphenols. In any case, the amount of hydrolysed starch decreased considerably with the polyphenols added to the gels. This result agreed with those found with the addition of gallic acid to rice starch gels (Chi *et al.*, 2019).

On the other hand, the study of starch hydrolysis by rheometry developed in this Thesis was based on the decrease of apparent viscosity with time. The methodology is described in the general methodology in section "*3.4.5.2. Rheometer determining the viscosity drop with time for studying the digestion starch*". The gel was formed in the rheometer and the enzyme was added to the gel diluted in maleate buffer. Immediately, apparent viscosity data were measured in a time sweep until a viscosity plateau was achieved, which means the end of starch digestion. The results obtained by rheology on the effect of polyphenols on digestion agreed with those reported by biochemical digestion and confirmed that kinetic constant by viscometry (k_v) was lower in the presence of polyphenols. Although the kinetic constants values obtained by biochemical and rheological methods, k and k_v, were numerically different (because the geometry, scale, agitation, homogenization, etc., were different for both experimental configurations), when the relative kinetic digestion constants, calculated by the ratio between the experimental kinetic constants of gels with polyphenols and the kinetic constant of gels without added polyphenols as reference samples, for both biochemical and rheological methods was determined a similar exponential relationship was found with polyphenols/starch ratio. This result means that the monitoring of starch digestion employing rheological procedure is adequate and can be useful to predict starch digestion kinetics saving labour costs.

5.5. Effects of starch gels on bread formulations characteristics

After studying simple starch systems in the presence of polyphenols and obtaining significant differences in the adsorption of polyphenols on native starch and starch gels, as well as in the rheological tests of these systems, the study continued by evaluating simplified baked samples since other common compounds (yeast, salt and sugar) were added to starchy matrices.

Gluten-free bread formulations based on corn starch (100 g) which contained 100 g water, 2 g dried yeast, 1 g salt, and 1 g sugar were made. Considering the results obtained previously, the tested percentages of polyphenol-containing extracts were 0 (control), 0.2, 0.5, and 1.0% w/w (relative content to mass of corn starch). The incorporation of polyphenols influenced the characteristics and the appearance of gluten-free breads. The methodology employed for the characterization is described in methodology section "*3.4.6. Bread characterization*". Final moisture content (% w.b.) decreased with the addition of polyphenols, although significant differences were only observed at 1.0% w/w starch basis from 50.46 ± 0.40 for control to 48.57 ± 0.34 for 1.0% w/w starch basis of polyphenols. This result might be explained because hydroxyl groups of starch molecules available to hold water molecules slightly decreased by the created interactions between starch and polyphenol molecules resulting in that net hydrophilic character of starch decreased. The bread colour also noticeably changed due to the addition of polyphenols. Luminosity index (L^*) decreased linearly ($R^2 > 0.97$) with the polyphenols content from 68.10 ± 2.40 to 56.37 ± 1.74. Redness index (a^*) increased with the addition of polyphenols from -2.80 ± 0.22 to -1.11 ± 0.33, except for samples with 0.2% w/w starch basis, where it decreased (-3.24 ± 0.12), and the greenness index (b^*) values significantly increased with the addition of polyphenols from 7.49 ± 0.70 to 29.08 ± 0.75. The microstructure of the bread changed significantly with the addition of polyphenols. Bread volume, measured as 2D slice area (cm^2), because depth of samples was 1 cm, was reduced with the addition of polyphenols from 2.45 ± 0.07 cm^2 for control to 2.20 ± 0.13, 2.25 ± 0.17 and 2.27 ± 0.09 cm^2 for 0.2, 0.5, and 1.0% w/w polyphenol

content. A similar trend was observed in the average cell size (mm^2) obtaining values of 2.48 ± 1.48 mm^2 for control and 1.46 ± 0.58, 1.57 ± 0.37 and 1.48 ± 0.21 mm^2 for 0.2, 0.5, and 1.0% w/w polyphenol content. The number of gas cells per cm^2 increased with the addition of polyphenols from 29 ± 14 to 76 ± 13. However, the porosity (%) ranged from 10.70 ± 3.07 to 23.53 ± 11.36 % at 0.50% polyphenol content where a maximum was achieved. It has been reported that the addition of seaweeds or microalgae into bread formulations, led to a reduction in pore size with a simultaneous increase in the number of cells and porosity, and an overall increase in bread volume (Amoriello *et al.*, 2021 and Garzon *et al.*, 2021). However, other authors using polyphenols and observed a decrease in yeast activity, which could explain the reduced 2D slice area found here when incorporating seaweed-extracted polyphenols into the formulation (Mildner-Szkudlarz *et al.*, 2019). For samples containing polyphenols, the 2D slice area had a statistically significant inverse correlation with the digestion kinetic constant (r = - 0.9998) and with the relative kinetic constant (r = -0.9996) of the starch gels during digestion.

Textural parameters of breads were measured at 0 and 48 h. The methodology is described in methodology section "*3.4.6.3. The crumb texture profile analysis (TPA)*". The addition of polyphenols increased the hardness of fresh bread from 6.7 ± 1.0 to 13.6 ± 4.0 N, possibly due to the more compact crumb determined, which likely may be explained by the inhibition of yeast activity. At 48 h, the hardness remained around 30 N, except in the bread with 1% polyphenols, whose hardness decreased to 17.0 ± 2.2 N. The springiness of the fresh bread varied between 0.94 ± 0.02 and 0.89 ± 0.01, and between 0.91 ± 0.06 and 0.83 ± 0.03 at 48 h. The chewiness of fresh bread increased during studied period from 5.5 ± 0.9 to 9.5 ± 2.4 N with the addition of polyphenols but decreased from 10.6 ± 4.0 to 3.6 ± 0.1 N. Resilience of both fresh and 48-h-old breads significantly decreased with the addition of polyphenols from 0.65 ± 0.02 to 0.54 ± 0.02 and from 0.24 ± 0.05 to 0.15 ± 0.02, respectively for fresh and 48-h-old breads. The hardening rate (%) decreased considerably from 464 ± 32 to 162 ± 10, indicating that polyphenols delayed starch retrogradation by interactions (forming hydrogen bonds) with starch molecules.

5.6. Characterization of alginates employed as texture-modifying applied to starchy foods

After obtaining and analysing the effect of the addition polyphenols to starchy materials, it was decided to use the solid residue of seaweeds obtained from the extraction of polyphenols to obtain and characterise alginates to be used as additive that could modify doughs rheological properties and textural properties of gluten-free breads. In this way, a better exploitation of seaweeds as raw material could be achieved. Following the methodology described in section "*3.3.1. Obtaining alginates*", the different alginates were obtained. The pellets were air-dried in a convective drier at two different temperatures: 50°C (*50D*) and 90°C (*90D*), respectively. An additional sample, statically dried over a flat surface and at ambient conditions and not subjected to convective drying into a dryer (*ND*: "not dried by forced convection"). Also, commercial alginate from Sigma Aldrich (*S*) was used as a reference to compare the results with alginates obtained in the laboratory.

The pellets containing alginates dried at different temperatures 50 and 90ºC (*50D* and *90D*) and dried at ambient conditions (*ND*) were studied in this PhD Thesis, because it was previously confirmed in our laboratory that the polymer size of extracted alginates was affected by drying conditions, mainly air temperature. This finding led to carry out an exhaustive study using capillary viscometry, not only obtaining the average viscosimetric molecular weight, but also analysing the specific viscosity complete curves as a function of concentration for several concentration regimes: diluted, semi-diluted, and concentrated. Alginates solutions prepared for alginate concentration ranging from 0.025 up to 3% w/v were tested by capillary viscometry. The methodology is described in the general methodology in section "*3.3.5. Capillary viscometry of alginates and HPMC*". Kinematic viscosity (v) was determined with solvent 0.1 M aqueous NaCl solution, surpassing the threshold concentration (0.025 mol/L) required for assuming that alginate is in a random coil conformation (Dodero *et al.*, 2020a). The absolute viscosity of the solvent (μ_0) and alginate solutions (μ) facilitated the computation of relative viscosity (μ_r) and specific viscosity (μ_{sp}). By representing the specific viscosity against the alginate

concentration, the regime zones in the studied concentration range (diluted, semi-diluted or concentrated) could be determined. Figure 5.10 shows the results obtained for the alginates produced in the laboratory and for the commercial alginate, being possible to distinguish two different regimes for alginates made in the laboratory and three zones for commercial alginates.

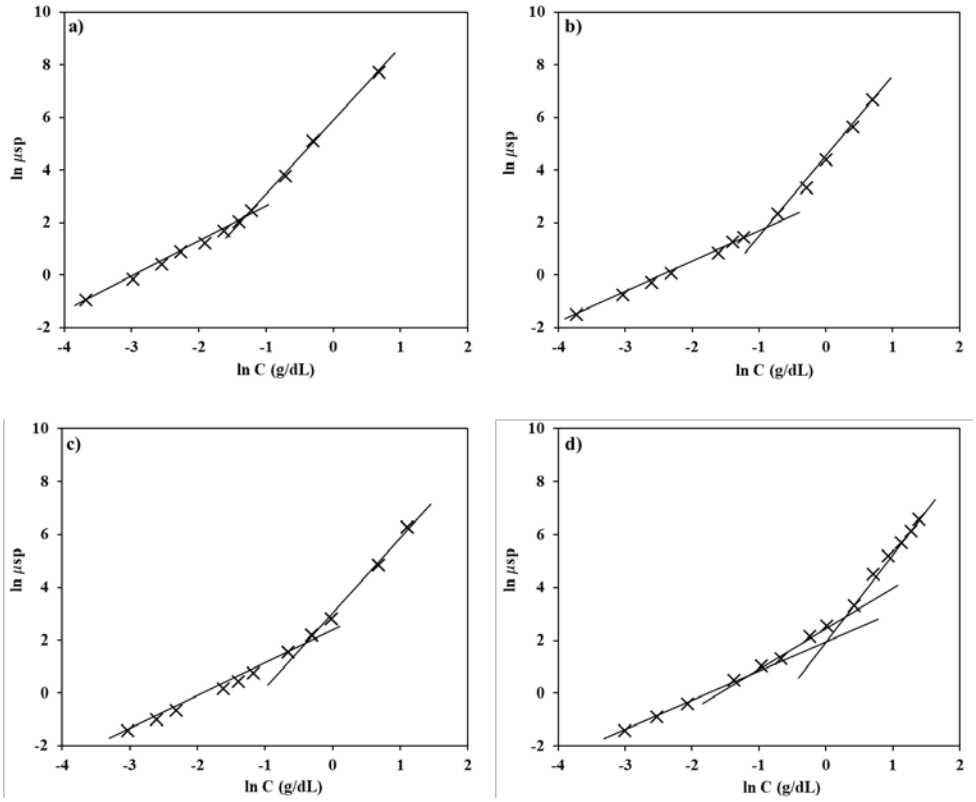

Figure 5.10. Specific viscosity (μ_{sp}) vs concentration (C, g/dL), both in logarithmic scale, for different alginates: a) not dried (*ND*), b) dried at 50ºC (*50D*), c) dried at 90ºC (*90D*) and, d) alginate from Sigma Aldrich (*S*).

By identifying the intersection points of the linear regression lines, the critical overlap concentrations (C^*), which correspond with the transition from dilute to semi-dilute regime, were determined. The calculated C^* values were 0.25 ± 0.01,

0.46 ± 0.02, 0.52 ± 0.03, and 0.52 ± 0.03 g/dL for ND, 50D, 90D, and S, respectively. It is noteworthy that significant differences in *C** values were only observed for ND (not dried solid). In a study by Dodero *et al.* (2020a), *C** values of 0.6 ± 0.1 g/dL were reported for low molecular weight alginates (~100 KDa), falling within the concentration range exhibited by extracted alginates with a convective drying step, studied in the present Thesis. For the commercial alginates S, an additional transition, in this case, from semi-dilute to concentrated regime (*C***) was found at 1.08 ± 0.11 g/dL.

After identifying the regimes to a proper viscosity measurement, the determination of $[\mu]$ using the Huggins and Kraemer method involved calculating the values of reduced viscosity ($\mu_{red} = \mu_{sp}/\mathrm{C}$) and inherent viscosity ($\mu_{inh} = \ln(\mu_r)/\mathrm{C}$). These values were plotted against the alginate concentration (g/dL). Through linear regression analysis of the experimental data and the application of the Huggins (Eq. 3.26) and Kraemer (Eq. 3.27) equations, the *[μ]* values and the Huggins (K_H) and Kraemer (K_K) constants were calculated (Table 5.3). On the other hand, the Fedors equation (Eq. 3.28) is applicable to polymer solutions within the dilute and semi-dilute ranges, with the application range being constrained by the relative viscosity (μ_r) values been between 1 and 100.

After obtaining the intrinsic viscosity values *[μ]* by either the Huggins and Kraemer or the Fedors methods (Dodero *et al.*, 2020b), the average viscosimetric molecular weight ($\bar{M}_v$, kg/mol) can be calculated applying the Mark-Houwink-Sakurada equation, which relates *[μ]* with the $\bar{M}_v$, by Eq. (3.29).

The more adequate *K* and α values for the extracted alginates were considered 4.84 10^{-5} dL/g and 0.97 dL/g, respectively, as previously assessed for *Ascophyllum nodosum* alginate by Stokke *et al.* (2000). For standard commercial *S* alginate, the employed *K* and α values were 7.30 10^{-5} dL/g and 0.92, respectively, based on the study by Martinsen *et al.* (1991). The summarized results can be found in Table 5.3.

Table 5.3. Parameters obtained from the Huggins and Kraemer and Fedors (Eqs. 3.3, 3.4 and 3.5) equations of commercial alginate (*S*) and extracted alginate undried (*ND*), dried at 50 (*50D*) and 90ºC (*90D*).

	Huggins and Kraemer				Fedors		
Sample	K_H	K_K	$[\eta]$ (dL/g)	$\bar{M}_v$ (KDa or kg/mol)	C_{max} (g/dL)	$[\eta]$ (dL/g)	$\bar{M}_v$ (KDa or kg/mol)
ND	0.30±0.02^b	-0.12±0.01^b	14.06±0.16^c	427.8±7.2^d	1.46±0.17^a	14.05±0.18^c	427.7±8.3^d
50D	0.25±0.12^a	-0.14±0.01^a	8.58±0.03^b	257.3±1.2^c	6.21±0.58^b	8.73±0.02^b	262.0±1.1^c
90D	0.36±0.16^a	-0.15±0.01^a	5.03±0.52^a	133.3±1.2^b	5.44±0.81^b	4.65±0.02^a	136.8±1.0^b
CA	0.42±0.12^a	-0.12±0.01^b	4.38±0.02^a	156.1±1.5^a	5.77±0.05^b	4.54±0.36^a	162.9±0.2^a

Data are presented as mean ± standard deviation. Data value of each parameter with different superscript letters are significantly different ($p \leq 0.05$).

The obtained Huggins and Kraemer equations (Eqs. 3.3 and 3.4) parameters, K_H and K_K, varied in a narrow range (from 0.30 to 0.42 and from -0.15 to -0.12, respectively), Table 5.3. Notably, no significant differences ($p > 0.05$) were observed in the K_H values, while statistical differences were identified only in the K_K values among *ND*, *S*, and *50D*, *90D* alginates. Regarding the statistical analysis of C_{max} in the Fedors equation (Eq. 3.5), no significant differences were found between *50D*, *90D*, and *S* alginates, with lower values observed for *ND* alginates. In terms of both methods, similar $[\mu]$ values (similar $\bar{M}_v$) were reported, showing a significant decrease with the presence of a drying step and an increase of drying temperature. Interestingly, no significant differences were found between *90D* and *S*. A wide range of the average viscosimetric molecular weight ($\bar{M}_v$) of the alginates extracted from *Ascophyllum nodosum* was found, in the range 133.3 KDa (*90D*) to 427.8 KDa (*ND*). These results indicated that the molecular size of extracted alginates can be strongly influenced by the methods and conditions employed during drying. The $\bar{M}_v$ determined for standard commercial *S* (156.1 KDa) and *90D* (162.9 KDa) alginates were similar, despite differences in seaweed origin and other factors; this similarity could possibly be attributed to the severe industrial conditions employed during the extraction

process to obtain commercial alginates. Importantly, the molecular weights obtained were within the typical ranges reported for commercial alginates (Dodero *et al.*, 2020b). Correspondingly, Chen *et al.* (2021) determined molecular weights for several brown seaweeds (*Sacharina japonica, Undaria pinnatifida, Sargassum fusiforme, and Sargassum hemiphyllum*), ranging from 171.8 to 663.0 KDa.

The Huggins and Kraemer constants provide insights on the interactions between polymer-polymer and polymer-solvent molecules. The observed k_H values, falling below 0.5 and within the range of 0.25-0.42, were indicative of the alginates behaving as flexible macromolecules. Additionally, the negative K_K values, ranging between -0.15 and -0.12, suggested robust polymer-solvent and weak polymer-polymer interactions, supporting a random coil conformation (Da Costa *et al.*, 2017). These obtained values agreed with those reported by other researchers for carbohydrate polymers (Chenlo *et al.*, 2009).

Obtaining normalised master curve involved plotting (log-log) the μ_{sp} data for each alginate against the dimensionless concentration or Berry number ($C\ [\eta]$). This dimensionless concentration serves as a measure of the polymer's occupancy in the solution (Castelain *et al.*, 1987). At low Berry number μ_{sp} exhibited a linear increase with $[\eta]$ until reaching a critical concentration (C_{cr}), where a sharp increase of slope can be observed. C_{cr} marks the transition from a dilute to a semi-dilute regime, meaning this value the point at which the interactions between polymeric molecules becomes significant. It can be seen in Figure 5.11 the normalized master curve for the tested alginates, with a consistent C_{cr} value of 4.05, aligning with values reported in the literature (Lopez *et al.*, 2020). The slopes obtained were 1.4 and 2.9 in the diluted and semi-diluted concentration range, respectively. These values agreed with those reported by other authors for solutions of several polysaccharides (Hellebois *et al.*, 2020).

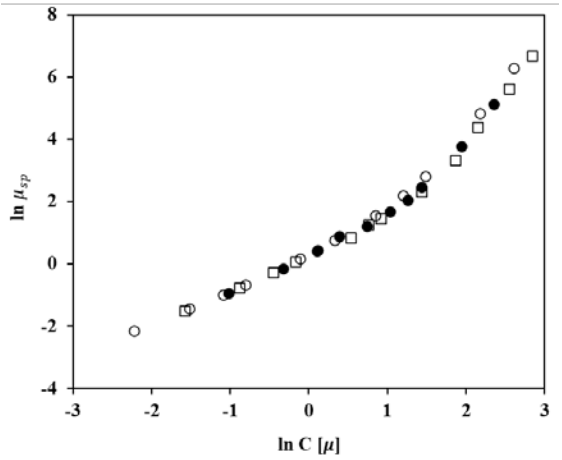

Figure 5.11. Master curve, μ_{sp} vs *C [μ],* for alginates not dried (*ND*) (●), dried at 50ºC (*50D*) (□), and dried at 90ºC (*90D*) (○).

5.7. Rheological behavior of alginates solutions

For a more detailed analysis of the alginates, rheological tests were performed. The methodology is described in the general methodology in section "*3.3.6. Rheological characterization of alginates and HPMC*". Three concentration values were employed for each alginate tested, corresponding to 2*C**, 4*C**, and 6*C**, where *C** represents the overlap concentration from the dilute to the semi-dilute regime. The upward and downward steady-shear flow curves coincided for all cases, indicating that within the tested polymer concentration range, alginate solutions exhibited no time-dependent behaviour, such as thixotropic or rheopectic behaviour. Flow curves revealed two trends concerning shear rate, as can be seen in Figure 5.12. At low shear rates, the apparent viscosity remained constant regardless of the shear rate value, forming a Newtonian plateau. Beyond a specified shear rate, known as critical shear rate ($\dot{\gamma}_c$), the apparent viscosity decreased, indicating shear-thinning behaviour. This behaviour has also been previously reported for alginate solutions (Ma *et al.*, 2014). The range of the plateau tended to increase with the decreasing of average viscosimetric molecular weight ($\bar{M}_v$) or concentration (C) of alginate, impacting the determination of $\dot{\gamma}_c$. Specifically, the alginate with lower $\bar{M}_v$ (*90D*) at

the lowest tested concentration (2*C**) showed Newtonian behaviour. The existence of different ranges for the Newtonian plateau has been attributed to variations in the formation-breakage equilibrium of entanglements between alginate molecules (Doyle *et al.*, 2009). The apparent viscosity of solutions noticeably increased with alginate concentration, resulting in the formation of viscous solutions, which is considered one of the most crucial properties for alginates being used for numerous industrial applications (Draget *et al.*, 2006). To mathematically model the flow curves, the Cross-Williamson model was employed (Eq. 1.20).

The absolute viscosity (μ_0) showed a linear decrease, $\mu_0 = A + B\ T_D$, with the increase of temperature, T_D (K), employed during drying operation, considering the ambient temperature of *ND* samples 293.1 K. *A* and *B* parameters displayed an exponential trend with the *C/C** ratio. Additionally, the parameter *K* (Eq. 1.20) was expressed as a function of drying temperature by an exponential relationship, $K = D\ e^{-E\ T_D}$, where *D* parameter showed a linear correlation with *C/C** ratio. Furthermore, the flow index remained within a narrow range, varying from 0.28 to 0.30, and it was considered constant at 0.29. The Eq. (5.5) reproduced satisfactorily the apparent viscosity within the tested range of alginate concentration and drying temperature, showing a mean relative error of 16% and $R^2 > 0.95$. Goodness of fit can be seen in Figure 5.12 for *50D* and *90D* samples at different alginate concentrations, as example.

$$\mu = \frac{(0.05 - 1.29\ 10^{-4}\ T_D)\ e^{\left(\frac{C}{C^*}\right)}}{1 + \left(4365\ \left(\frac{C}{C^*}\right) - 7494\right)\ e^{-0.04\ T_D \dot{\gamma}^{0.71}}} \tag{5.5}$$

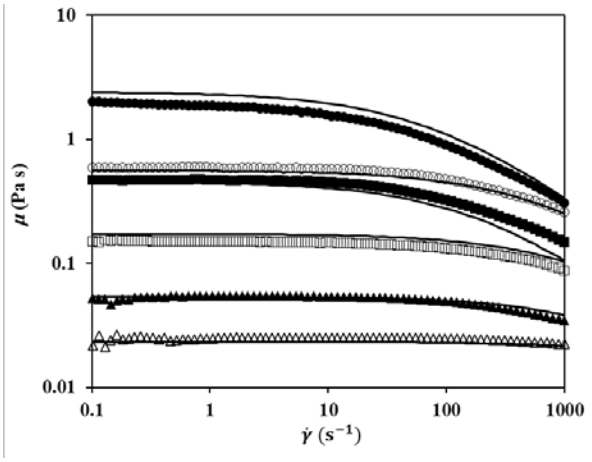

Figure 5.12. Steady-shear flow curves for *50D* (filled markers) and *90D* (hollow markers) alginate solutions, experimental data for 2*C** (●, ○), 4*C** (■, □) and 6*C** (▲, △) and model data. Eq. (5.5) (-).

Conversely, the concentration value noted as 6*C** was used to determine the viscoelastic characteristics of solutions through small amplitude oscillatory shear tests (*SAOS*). A frequency sweep was conducted at a constant strain of 1%, within the linear viscoelasticity range (*LVR*) previously determined through corresponding strain sweeps at high frequency. The frequency varied from 0.1 to 10 Hz and the temperature set at 25 and 45ºC. As illustrated in Figure 5.13, it was found that both elastic (*G´*) and viscous (*G´´*) moduli increased with frequency in all the assays, and consistently, *G´´* exceeded *G´*, thus indicating liquid-like behaviour. Different trends of *G´´* and *G´* slopes with frequency were observed for samples at 25ºC. The *ND* alginate solution exhibited a *G´´* slope higher than the *G´* slope, reaching a tan δ of 1.72 at 10 Hz, approaching to the gel point (*G´* = *G´´*). In the case of the *50D* sample, *G´´* and *G´* slopes were similar, while for *90D* sample, *G´* slope exceeded *G´´* slope. This behaviour agrees with the results reported by Ma *et al.* (2014) for commercial sodium alginate solutions within a similar concentration and molecular weight ranges. Both viscoelastic moduli decreased with temperature as increased from 25 to 45ºC for the *50D* and *90D* alginate solutions. However, the *ND* alginate displayed a different behaviour at 45ºC, where *G´* remained constant with the temperature

increase, and G'' notably increased at low shear rates (below 1 Hz). Notably, at 0.03 Hz, G' value (0.48 Pa) approached to G'' value (0.67 Pa), resulting in a tan δ of 1.39. This observation indicates that higher temperature may potentially lead to the achievement of the gel point for this alginate solution (Steffe, 1996). Such behaviour is typical of semi-dilute polymer solutions exhibiting a high degree of entanglement (Mohammadifar *et al.*, 2006). This outcome suggests that solutions containing high molecular weight alginates have lower gelation temperatures.

The relationship between steady-shear flow and dynamic-shear rheology was examined using the Cox-Merz rule, where the apparent viscosity obtained from rotational tests concurred with the complex viscosity (μ^*) obtained from oscillatory tests. Figure 5.14 illustrates the application of this rule to the tested alginate solutions. In general, the Cox-Merz rule was satisfactorily fulfilled for the *50D* and *90D* solutions, demonstrating a superposition of both viscosity curves regardless of the shear rate range. However, for the *ND* solution, superposition was observed only at high shear rates ($> 10\ s^{-1}$), while at low shear rates ($< 10\ s^{-1}$), the dynamic viscosity was notably higher than the complex viscosity. Despite all tests being conducted at a high polymer concentration ($6C^*$), the concentration of *ND* samples was approximately 1.5 g/dL, which was close to C_{max} as determined by the Fedors equation. At this concentration, polymer interactions became remarkable, indicating a transition to the concentrated regime. In contrast, for the other cases, the employed concentration (3.0 g/dL) was considerably lower than C_{max}, and solutions can be considered within the semi-dilute range. The observed divergence in *ND* solutions, characterized by strong polymer interactions and entanglements due to its high average viscosimetric molecular weights, could explain this behaviour. Similar observations were reported by Ahmad *et al.* (2014) for guar galactomannan solutions and gellan/dextran blends with weak-gel characteristics.

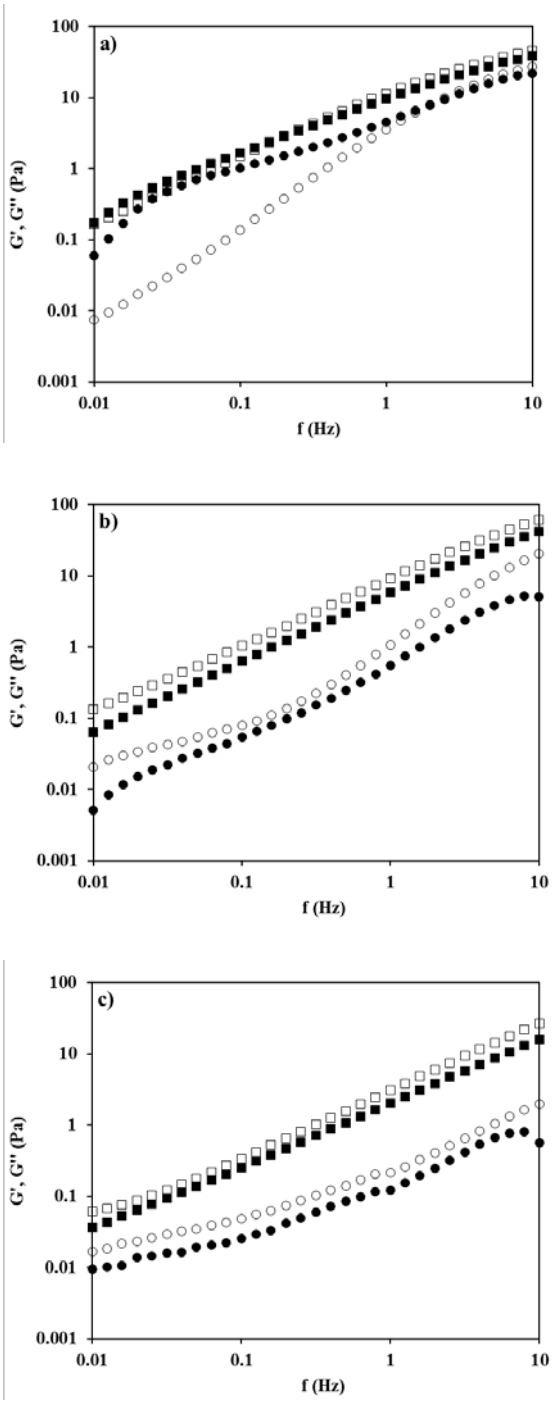

Figure 5.13. Frequency sweeps of alginate solutions at 6C* concentration: experimental data of *G''* (□, ■) and *G'* (○, ●) at 25°C (hollow markers) and 45°C (filled markers)) for different alginates: a) ND, b) 50D and c) 90D.

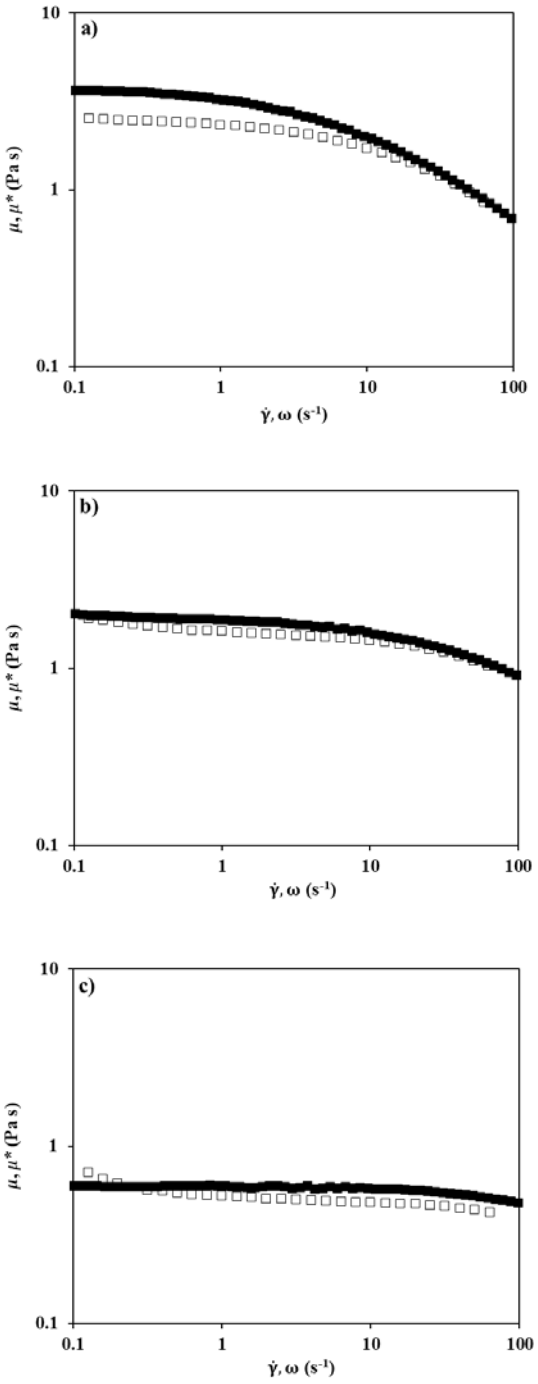

Figure 5.14. Cox-Merz plot: Dynamic viscosity, μ, (■) and complex viscosity, μ^*, (□) at 25ºC of alginate solutions at 6*C** concentration for different alginates: a) *ND*, b) *50D* and c) *90D*.

5.8. Chemical characterization of alginates

As can be deduced from the results shown until now, alginates may show different features depending on the seaweeds source or the thermal conditions employed during processing. Because of these findings, it was decided to perform a deeper study of the structure and chemical composition (D-mannuronic and L-guluronic acids are the monosaccharides monomers that participate, at different ratios, in this biopolymer) of alginates (Montes *et al.*, 2021) and also about the relationships of composition with the hydrophilic character of alginates due to this last property is key to understand the water interaction in starchy matrices in the presence of alginates as additive. For this purpose, water sorption isotherms of different alginates with different structural characteristics were determined at different temperatures (25, 37 and 50ºC). For this study, two commercial alginates from Panreac (hereafter noted as *P*) and Sigma (*S*) were selected in addition to one of those obtained in our laboratory after drying at 50ºC (*50D*) previously described. The average viscosimetric molecular weights of these alginates were 459 ± 8, 156 ± 2, and 257 ± 1 KDa for *P*, *S*, and *50D*, respectively, obtained by means of Huggins and Kraemer equations (using the same methodology). Because alginate is a biopolymer made up of D-mannuronic and L-guluronic monosaccharide units, and the distribution of these units is responsible for solubility, viscosity in liquid solution and gelling properties, it is important to analyse the mannuronic to guluronic ratio (*M/G*), since it provides us with information about its composition. In this case the values of the *M/G* ratios were 1.15, 0.91 and 1.21 for *P*, *S* and *50D*, respectively (Montes *et al.*, 2021). These values were obtained by proton nuclear magnetic resonance (^{1}*H NMR*) spectroscopy following the ASTM F2259-10 standard (*ASTM*, 2012). The methodology is described in section "*3.3.2. Nuclear magnetic resonance of alginates*".

To model the water sorption isotherm data different equations were used: the Brunauer, Emmet and Teller model (*BET*), which is used to mathematically describe the adsorption on homogeneous surfaces; the Guggenheim, Anderson and de Boer (*GAB*) model, an extension of the *BET* model that takes into account the modified

properties of the adsorbed water in the multilayer region and, finally, the Halsey model that focuses on the relationship between the amount of adsorbate and partial pressure of adsorbate at equilibrium. The methodology is described in section "*3.3.3. Determination of water desorption isotherms of alginates*". From these experiments, the Halsey model is recommended to represent the water adsorption behaviour because it was found to be the model that better fit experimental results in the temperature range from 25 to 50ºC, as is shown in Table 5.4. There were no statistically significant differences ($p \leq 0.05$) between Halsey parameters (*A* and *r*) for *S* and *P* alginates at constant temperature. For these alginates, *A* values exhibited a decrease (from 12.08 to 8.73 and from 12.46 to 8.42, respectively) with increasing temperature. However, for *50D*, *A* values showed an increase (from 23.21 to 25.28) with temperature. Notably, $a = A/T$ value remained constant with temperature in the case of *50D* alginate. In all instances, the r-values remained constant with temperature for each alginate, and *50D* displayed the lowest value (1.19), indicating the steepest slope of the isotherm curve compared to *S* and *P* alginates (around 1.82). In general, no significant differences were found between the two commercial alginates, differently from the alginate obtained in our laboratory (*50D*), which was the most hygroscopic alginate. To comprehend the water sorption characteristics of alginates and determine its optimal storage conditions, certain thermodynamic properties can be assessed, including the differential heat of sorption and entropy, as well as the integral enthalpy and entropy (Zhang *et al.*, 2016). The differential enthalpy of sorption indicates the strength of the bond between water and the solid, while the differential entropy of a sample is proportional to the number of available sorption sites at a given energy level. The optimal storage conditions for alginates were found to be conditions of humidity between 0.15 to 0.20 kg of water/kg of dry solid and a under relative humidity in the range 35 to 50%; these values were determined from the integral values of maximum and minimum enthalpy and entropy, respectively. Furthermore, a model based on the structural characteristics of the alginate was obtained to predict the equilibrium moisture content of the alginates at low water activity values. It was concluded that higher amounts of D-

mannuronic monosaccharides lead to an increase of the hygroscopicity of the polysaccharide. A wider explanation regarding this topic and comparison with bibliographic data of other authors can be found in Publication 2, where it is explained and discussed in a broader and more detailed way.

Table 5.4. Values of the parameters of Halsey model and goodness of fitness for water sorption isotherms of commercial *S* (Sigma) and *P* (PanReac) and processed (*50D*) alginates.

Sample	S			P			50D		
T (K)	293.1	310.l	323.1	293.1	310.1	323.1	293.1	310.1	323.1
A	$12.08\pm0.84^{a,B}$	$10.18\pm0.77^{ab,B}$	$8.73\pm0.71^{b,B}$	$12.46\pm1.03^{a,B}$	$10.17\pm0.96^{ab,B}$	$8.42\pm0.91^{b,B}$	$23.21\pm1.02^{a,A}$	$24.38\pm1.48^{ab,A}$	$25.28\pm0.84^{b,A}$
a = A/T	$0.041\pm0.003^{a,B}$	$0.033\pm0.003^{b,B}$	$0.027\pm0.002^{b,B}$	$0.043\pm0.004^{a,B}$	$0.033\pm0.003^{ab,B}$	$0.026\pm0.003^{b,B}$	$0.079\pm0.002^{a,A}$	$0.079\pm0.004^{a,A}$	$0.078\pm0.005^{a,A}$
r	1.815 ± 0.076^{A}			1.847 ± 0.027^{A}			1.187 ± 0.012^{B}		
φ*	347.5	308.1	1287.5	293.8	183.6	261.3	65.7	319.8	152.8
χ^2**	4.2	3.3	5.4	3.9	5.6	1.1	1.0	0.6	0.1

Data are presented as mean ± standard deviation. Data value of each parameter with different superscript lowercase letters are significantly different by temperature and capital letters by alginate at constant temperature ($p \leq 0.05$). *Low φ values indicate a poor adequacy of the model. **With value $\chi^2 \geq 5.99$, the model should be rejected ($p > 0.95$).

5.9. Preparation and analysis of starchy systems containing alginates

After the extensive characterization of the alginates, they were incorporated into the starchy systems that were studied in this Thesis. Several assays were carried out with 1:4 w:w corn starch gels with the addition of up to 2% w/w sodium alginate, in starch basis. The five previously analysed alginates were used for these assays (*S*, *P*, *ND*, *50D* and *90D*). In this case, the water retention capacity (*WRC*) was analysed for the starchy systems with and without alginates (procedure described in methodology section "*3.3.4. Water retention capacity (WRC) of corn starch, alginates and HPMC*"). The *WRC* value for corn starch was 0.97 ± 0.04 (g water/g d.b.). To calculate the *WRC* of alginates, the *WRC* of starch-alginate mixtures was measured. These values were found to be higher than those of starchy system alone, since alginates retain significant amounts of available water in the formulations (Hasatsri *et al.*, 2018).

The *WRC* values of the commercial alginates were 12.09 ± 1.08 and 10.16 ± 2.37 (g water/g d.b.) for *P* and *S*, respectively. For alginates obtained in the laboratory, the *WRC* values were 7.31 ± 0.61, 5.26 ± 0.88 and 3.77 ± 0.18 (g water/ g d.b.) for *ND*, *50D* and *90D*, respectively. For these alginates, a linear relationship ($R^2 > 0.99$) was observed between *WRC* and $\bar{M}_v$, suggesting that the water retention capacity increases with the length of the alginate polymers. However, this relationship did not was observed for commercial alginates, indicating that factors such as the source of the alginate, other polymer characteristics (such as average block length or mannuronic/guluronic acid ratio), and extraction method may significantly affect the physicochemical properties of alginates.

Rheological tests were carried out into the specific rheometer accessory for starch gelatinisation (Couette accessory), into which corn starch gel, either alone or in the presence of alginates, was gelatinised. Once the gel was formed, time sweep tests were performed to study the gel maturation. Linear viscoelastic regions (*LVRs*) determinations and frequency sweeps to achieve a complete rheological gel characterization were performed following the protocol described in methodology

section "*3.4.4.2. Rheological characterization of starch with alginate*". As main result, it was found that the addition of sodium alginates caused important changes in the viscoelastic behaviour. After 10 minutes at 95ºC, the elastic modulus (*G´*) was higher than the viscous modulus (*G´´*), which shows a solid-like behaviour. Furthermore, all gels reached constant values of *G´* and *G´´*, indicating the presence of fully formed gels in this elapsed time. During cooling, a strong increase of *G´* and a smaller increase of *G´´* was obtained, which indicated a great strengthening of the gel. Analysis of the maturation stage at 37ºC gave as result that both moduli increased slightly during the first 20 min. In fact, the increases of both modules were proportional and, consequently, tan δ varied in a narrow range during maturation. On the other hand, it was observed that the effect of the addition of alginates significantly decreased the *G´* values with respect to that of starch alone at the beginning of maturation, although no differences were observed between samples with added alginate above 1% w/w. In fact, the increase of elasticity with increasing alginate concentration could be expected due to lower available water for gel formation by the increase of total dry matter and high *WRC* of alginates. However, at high alginate content the interactions with amylose were less relevant regarding water held by alginates and gel rigidity depended straightly on WRC_{SA}.

However, in the presence of alginate *P*, *G´* had no significant differences with samples containing only starch. In general, the rheological characteristics of the gels formed with alginates from the same seaweed and with different $\bar{M}_v$ (samples *ND*, *50D* and *90D*) did not show significant differences between them. These results indicated that the $\bar{M}_v$ of the alginate was not critical for the rheological characteristics of the starch gels when the alginates had similar nature and extraction procedures. However, significant differences were found when different concentrations and alginates from different sources were used. In the frequency sweeps, carried out within the *LVR* with a constant strain of 1% and at 37ºC from 0.1 to 10 Hz, it was observed a solid-like behaviour of gels (*G´* > *G´´*). In general, it was observed that *G´* decreased and *G´´* increased because of the addition of alginates. This result is different from the results previously obtained with polyphenols, since

the presence of polyphenols decreased both *G´* and *G´´* moduli. Therefore, the viscoelastic characteristic of starch gels can be changed by adding alginate or polyphenols. In both cases, weaker gels are formed, but alginates can be used when a gel with more viscous behaviour is required, whereas the use of polyphenols permits to obtain a less viscous gel.

Additionally, the microstructure of starch gels with and without alginates was also analysed by scanning electron microscopy (*SEM*), either as a raw material and after *in vitro* chemical digestion with a specific enzyme-containing buffer medium.

As main result, it was found that the addition of sodium alginates caused important changes in the viscoelastic behaviour simultaneously to structural features of corn starch gels (the methodology is described in the section "*3.4.2. Scanning electron microscopy (SEM)*"). The presence of alginates created gel structures with elongated and unequal cavities in addition to the formation of linear partition walls, thus forming an anisotropic spatial network, regardless of the alginate used. Furthermore, alginates of different origin and different average viscosimetric molecular weight significantly modified the rheological properties with lower elastic modulus values, meaning weaker gels. Finally, after analysing the results of *in vitro* digestion of the tested systems (protocol is described in methodology section "*3.4.5.1. Conventional biochemical method of in vitro digestion starch*"), it was determined that the presence of alginates in the system gave as result a decrease of the experimental hydrolysis kinetic constant (*k*). However, the addition of alginates resulted in an increase of maximum degree of hydrolysis (C_∞) from 12.37 ± 0.98 (*CS*) to 17.22 ± 0.45 (*90D* 2%), primarily attributed to the observed rise in slowly digestible starch (*SDS*) fraction. No distinct trends in C_∞ were identified concerning the presence of alginates or the added amount of sodium alginate. However, the heightened digestibility could be linked to specific interactions between the specific alginate and amylose and amylopectin molecules. These interactions decreased starch retrogradation, facilitating the access of enzymes during digestion. They may also account for the obtained results for total digestive starch (*DS*), *SDS*, and C_∞ with alginate addition. Finally, resistant starch (*RS*) also varied in an interval from 1.36 ±

0.21 (*50D* 2%) up to 2.58 ± 0.05 (*90D* 2%) (g/100 g) with significant differences between alginates employed. The different interactions of alginate with starch might also contribute to the observed results for resistant starch (*RS*), assessed as the remnant starch after 24 h of incubation. Nevertheless, establishing a correlation between *RS* content and molecular weight or alginate content is still a challenging. In summary, the slower hydrolysis kinetics may result from the interference of alginate molecules in the starch-enzyme interaction. The higher amount of hydrolysed starch may be explained by structural changes and reduced retrograded starch levels, thus increasing the enzyme accessibility. This phenomenon may also be associated with a phase separation phenomenon with increasing alginate content favouring more entanglements among hydrocolloid chains (Rosell *et al.*, 2011).

If the effect of alginates is compared with that observed with the polyphenols addition in corn starch systems, it was observed that both type of compounds delayed the digestion rate. However, the values of *RDS* were influenced by the presence of polyphenols, whereas this value did not show significant differences with the control (starch without alginates) in the presence of alginates. The presence of polyphenols caused a significant decrease of the *RDS*. On the other hand, slowly digestible starch increased with the presence of both alginates and polyphenols. Regarding the results, it can be concluded that the addition of polyphenols is more appropriate for our main objective of reducing the digestion rate and the amount of *RDS*, to avoid peaks of glucose in blood. A more extensive discussion of these results is included in Publication 3.

5.10. Preparation and analysis of starchy systems containing cellulose derivate

A common additive such as hydroxypropyl methylcellulose (HPMC) used in starch-derived foods manufactures at industrial scale, was added to starch to compare its effect with those previously shown for starch gels with additives of marine origin. Considering that the importance of molecular size for alginates was previously revealed, it was decided to study three HPMC with different molecular

weights (characterised by the range of viscosity values developed in aqueous solution at 2% at 20ºC: 40-60, 80-120 and 2600-5600 mPa s). Therefore, the first determination performed was the average viscosimetric molecular weight, employing the same procedure previously described for alginates. As the Huggins and Kraemer and Fedors values obtained for the alginates were coincident, only the Huggins and Kraemer method was used in this case. The obtained values for K_H values were 0.21 ± 0.11, 0.47 ± 0.09 and 0.63 ± 0.03 and the K_K values were -0.26 ± 0.08, -0.08 ± 0.06 and -0.04 ± 0.01, respectively, for the HPMC of 40-60, 80-120 and 2600-5600 mPa s. The K_H and K_K values for the studied alginates were in the same range and varied in a narrow range from 0.25 to 0.42 and -0.15 to -0.12, respectively. The values of both constants could be employed to study the interactions between the polymers and solvent. In fact, $K_H < 0.5$ and $K_K < 0$ indicate good solvents (strong interactions polymer-solvent), as reported by Funami *et al.* 2007. In addition, K_H - K_K values close to 0.5 corroborates the solvent adequacy for a polymer. Our results showed that only high viscosity HPMC slightly diverged ($K_H = 0.63 > 0.5$ and $K_H - K_K$ close to 0.7) from theoretical considerations of good solvent-polymer interactions; this fact could be tested out in its low water solubility and slow solubilization. Intrinsic viscosity $[\mu]$ values were 2.72 ± 0.15, 3.18 ± 0.08 and 7.21 ± 0.14 dL/g and the corresponding resulting average viscosimetric molecular weights, $\bar{M}_v$, values were 27.2 ± 1.8, 32.7 ± 1.0, and 82.7 ± 1.8 KDa, respectively. For alginates the $\bar{M}_v$ obtained were 459 ± 8, 156 ± 2, 428 ± 7, 257 ± 1 and 133 ± 1 KDa, for *P*, *S*, *ND*, *50D* and *90D*, respectively.

The water retention capacity (*WRC*) was also analysed the same mode it was performed on alginates. The value obtained for corn starch was 0.95 ± 0.01 (g water/g d.b.), while the values obtained for the different HPMC increased with molecular weight from 8.54 ± 0.28 up to 12.97 ± 0.45 (g water/g d.b.). The same trend was found between the *WRC* and average molecular weight of tested alginates from 3.77 ± 0.18 up to 12.09 ± 1.08 (g water/g d.b.). In fact, respective linear relationships between $\bar{M}_v$ and *WRC* ($R^2 > 0.99$) were obtained for both alginates and HPMC. For the characterization of the gel structure of starch in the presence of

HPMC, gels stronger, due to higher starch content (30% w/w) was employed than those used to study the alginate addition, were analysed to determine the effect of HPMC with different $\bar{M}_v$ values (labelled as low (*L*), medium (*M*) and high (*H*) viscosity) at several concentrations (0.0, 0.5, 1.0, 1.5 and 2.0% w/w). In all cases, the addition of HPMC increased the initial and final gelatinisation temperatures. The delay in the gelatinisation process could be attributed to the water absorption by the added hydrocolloids, which competes with starch for the available water. This relationship is supported by *WRC* results previously obtained, which indicated that the starch and HPMC mixtures retained more water than corn starch. During the cooling from 90 to 25ºC, the viscoelastic moduli gradually increased with decreasing temperature, indicating starch retrogradation. A maturation period at 25ºC showed that the gel reached stability in less than 2.5 min. The addition of HPMC accelerated this stabilization, especially with HPMC *L* at 2.0% w/w. Interestingly, HPMC slowed down the recrystallization of amylose (responsible of short time retrogradation), decreasing initial $G´$ values at 25ºC when HPMC *H* at 0.5% w/w was added, but an increasing with higher HPMC addition was observed. Maximum firmness was observed with HPMC *H* at 2.0% w/w. Although HPMC generally reduced $\Delta G´$ ($G´_{final} - G´_{initial}$) at 25ºC in the maturation period, variations occurred depending on the type and amount of HPMC used.

In the frequency sweeps of matured gels, it was observed that $G´$ increased with frequency, indicating that the samples, with or without HPMC, are typical weak gels. The addition of low and medium viscosity HPMC (*L* and *M*) decreased $G´$ values; this same behaviour was previously observed with the addition of alginates and polyphenols to starch-water mixtures. However, the addition of high viscosity HPMC (*H*) above 1.0% w/w increased G' values. Also, tan $\delta < 1$ revealed a predominance of elastic properties. High HPMC *L* and *M* concentrations increased tan δ, especially at low frequencies, but both viscoelastic moduli varied proportionally with the frequency when HPMC *H* was added, thus remaining constant the damping factor. A more extensive discussion of these results is included in Publication 4.

5.11. Comparison of the effects produced by polyphenols, alginates and HPMC on the elastic behaviour of starch gels

For the comparison of starch gels with polyphenols, alginates and HPMC, data were normalized with respect to the starch control and the amount of added biopolymer. First, the rheology of the gels was compared by focusing on the frequency sweep test, since it was carried out for all the starch systems containing the biopolymers under study. In addition, this test was considered the most interesting to relate the values obtained from each system, since it is the point where the final gel is obtained. Since the elastic character is predominant in our systems, the values of the *G´* at 1 Hz were chosen for the comparison of the results. In most cases, the addition of biopolymers reduced the elastic modulus (with some exceptions), indicating the formation of a weaker gel. This is explained by the fact that the presence of the added biopolymer interferes with the gel structure in the cross-linking of starch molecules and the formation of a complete network structure within the gel (Wu *et al.*, 2024). In addition, in general, *G´* values obtained for each sample showed a trend according to which the more biopolymer is added, the greater the change. The use of a normalized parameter to evaluate the specific (per mass unit) effect of each biopolymer added to starch, labelled as normalized *G´* value, and evaluated by means of the Eq. (5.6) as a function of the amount of added biopolymer:

$$Normalized\ G´\ value = \frac{\frac{G´_{biopolymer+starch}}{G´_{starch}}}{\frac{m_{biopolymer}}{m_{starch}}} \quad (5.6)$$

where $G´_{biopolymer+starch}$ (Pa) is the elastic modulus at 1 Hz from the frequency sweep test of biopolymer systems, $G´_{starch}$ (Pa) is the elastic modulus at 1 Hz from the frequency sweep test from starch system, $m_{biopolymer}$ (kg) is the mass of biopolymer added and m_{starch} (kg) is the mass of starch added.

Figure 5.15 shows all the values of the tests carried out during this Thesis of the normalized elastic moduli as a function of the added concentration of the three biopolymers used. The normalized *G´* value represents the percentage of change of *G´* value per biopolymer/starch mass ratio. It was observed that, on a double

logarithmic plot, experimental data followed an acceptable linear function (R^2 > 0.90). Therefore, it can be concluded that the elasticity of starch gels, given by the evaluation normalized *G´* parameter, was not depended on the nature of biopolymer used (of those evaluated in this Thesis), but depended on the biopolymer concentration employed.

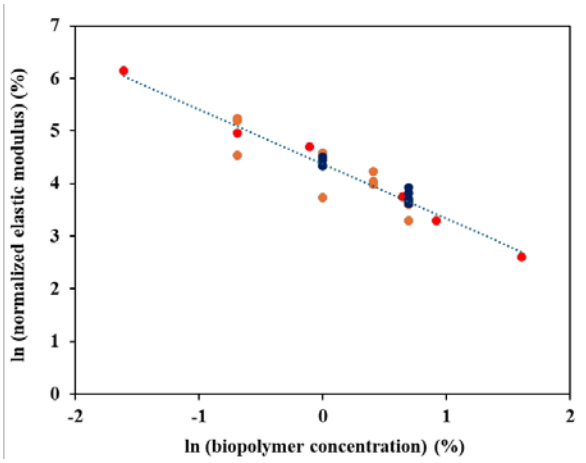

Figure 5.15. Normalized elastic moduli at 1 Hz as a function of the added concentration of the three biopolymers used: polyphenols (red), alginates (blue) and HPMC (orange).

Besides, regarding starch digestion with polyphenols and alginates, both similarities and differences were observed. The addition of polyphenols increased the proportion of slowly digestible starch and decreased the rapidly digestible starch, as well as the rate constant, which resulted in a reduction of the maximum degree of hydrolysis. In contrast, the presence of alginate did not result in significant differences in the rapidly digestible starch between the control and the alginate-containing systems. However, an increase in the slowly digestible starch and the maximum hydrolysis degree was observed, along with a decrease of the rate constant and resistant starch (in some systems). Since both biopolymers decreased the digestion rate constant, data were normalized by Eq. (5.7).

$$RSKR = \frac{\frac{k_{starch} - k_{biopolymer+starch}}{k_{starch}}}{\frac{m_{biopolymer}}{m_{starch}}} \quad (5.7)$$

where *RDKR* is the relative specific (per mass unit) kinetic rate, $k_{biopolymer+starch}$ (min^{-1}) is the kinetic constant of biopolymer systems, k_{starch} (min^{-1}) is the kinetic constant from starch system, $m_{biopolymer}$ (kg) is the mass of biopolymer added and m_{starch} (kg) is the mass of starch added.

Since there are only results of digestion of polyphenols and alginates, the study focused on the common range of concentrations of these biopolymers that were added. Therefore, the evaluated range for both polymers was from 1 to 2% on starch basis. As alginates of different molecular weights were tested, an average value of the effect on digestion rate constant was determined at each concentration. Thus, for the starch gels with 1% alginate the *RDKR* value was 62 ± 19 and for 2% it was 26 ± 7. In the case of starch gels with the polyphenols, at the same concentrations, the *RDKR* values were 10 ± 1 and 4 ± 1, respectively. In both cases, as the biopolymer concentration increased, the enzyme efficiency decreased, since the digestion rate is lower increasing biopolymer content. Analysing jointly the found normalized results of rheology and starch digestion, it can be concluded that the inhibition of digestion with polyphenols or alginates is purely chemical. On the other hand, significant differences on the digestion rate with the use of polyphenols or alginates was observed, since with 1% biopolymer the inhibition effect of polyphenols was 6.3 times greater regarding to the alginates effect and for 2% concentration it is 6.0 higher. In conclusion, the use of alginates or polyphenols modified the elastic behaviour of starch in a similar mode, but the inhibition of enzymatic hydrolysis of starch in the presence of polyphenols is significantly higher.

6. CONCLUSIONS

6. Conclusions

As a result of the proposed objectives and the experimental work carried out throughout this Thesis, as well as the analysis of the results obtained, the most relevant conclusions were:

- ✓ The adsorption of polyphenols on starch was enhanced in starch gels in comparison to native starch because in the gels the available surface area allowing the interactions between starch and polyphenols was considerably increased.
- ✓ The addition of polyphenols in the formation of the starch gels decreased its elastic character.
- ✓ The polyphenols addition significantly modified the starch digestion giving as result a decrease of the digestion rate constant (k) and reduced the final concentration of digested starch (C_∞).
- ✓ The breads with polyphenols showed greater hardness and chewiness and lower cohesiveness and resilience in relation breads without polyphenols. Nonetheless, the crumb hardening during storage was less noticeable, suggesting the potential integration of polyphenols into gluten-free bread formulations to delay the bread aging.
- ✓ The average viscosimetric molecular weight, $\bar{M}_v$ (kg/mol), of alginates extracted from *Ascophyllum nodosum* seaweed varied in a wide range from 133.3 to 427.8 as function of the conditions employed during extraction process (mainly drying temperature). Consequently, the molecular size of the extracted alginates could be modulated by the conditions employed during the drying operation.
- ✓ The rheological properties of sodium alginate solutions extracted and isolated under different conditions were significantly different. Solutions in the semi-dilute regime showed a shear-thinning behaviour and Cross-Williamson model was successfully employed to estimate the apparent viscosity as function of polymer concentration and temperature employed for pellet drying. Liquid-like behaviour was determined by viscoelasticity

tests, but alginate solutions with higher $\bar{M}_v$ showed a trend to achieve a gel point with dissolution temperature. Cox-Merz rule was accomplished for alginate solutions at semi-dilute regime, but at concentrated regime steady shear viscosities were significantly higher than complex viscosities because of its enhanced elastic trend.

- ✓ In relation to hygroscopic character, no significant differences were found between tested commercial alginates, but the alginates processed in the laboratory showed more hygroscopic character. Halsey model was selected to fit successfully the experimental desorption data of alginates from 25 to 50 °C. A model based on the structural features of alginates was proposed and satisfactorily tested to predict the equilibrium moisture content of alginates at low water activity values (< 0.4).
- ✓ The addition of sodium alginates caused relevant changes in the viscoelastic characteristics and structural features of the corn starch gels with the existence of elongated and unequal cavities and the formation of linear partition walls that configured spatial anisotropic network. These structures were formed independently of the tested alginate content.
- ✓ Weaker gels (lower elastic modulus) were obtained with the addition of alginates and their viscous character increased. Stronger gels were obtained increasing alginate content when hydrophilic character of alginates added was high.
- ✓ The hydrolysis rate of starch decreased with the addition of any alginate and, in general, with the amount of alginate with high hygroscopicity. At low alginate content, it was hypothesized that complexes were formed between alginate and leached amylose (and low $\bar{M}_v$ amylopectin). These complexes diminished the enzyme action and hindered the enzyme access to the remaining starch for its hydrolysis, despite the generation of more open structures.

- ✓ In alginate-corn gels with similar structure, the increase of the viscoelastic characteristics decreased the hydrolysis rate of starch. Consequently, the hydrolysis rate depended on rheology and structure of gel.
- ✓ Water retention capacity of tested HPMC varied linearly with $\bar{M}_v$ of HPMC. The temperature of gel point of HPMC solutions was invariant with $\bar{M}_v$ (at constant substitution degree), but when heavy HPMC was employed an aggregation step at temperatures near (below) gel point was observed.
- ✓ The addition of HPMC of low and medium viscosity decreased the $G´$ values, whereas the addition of high viscosity HPMC above 1.0% w/w starch basis increased the $G´$ values. High concentrations of low and medium viscosity HPMC increased the damping factor (tan δ), especially at low frequencies, but both viscoelastic moduli varied proportionally with frequency when high viscosity HPMC was added, so tan δ remained constant.
- ✓ Rheology and digestibility tests of starch gels with polyphenols, alginates and HPMC performed during this Thesis were analysed together. Starch gels elasticity, given by the evaluation of the normalized elastic modulus, did not depend on the nature of the biopolymer, but rather depended on the concentration of biopolymer used. However, in the case of the addition of polyphenols and alginates, as both biopolymers concentration increased, slowed down the corn starch digestion rate. Enzymatic inhibition effects of polyphenols were significantly greater (around 6 times) than those observed with alginates when both polymers were added at the same content (1 or 2%).

References

References

Ahmad, N. H., Ahmed, J., Hashim, D. M., Manap, Y. A., & Mustafa, S. (2014). Oscillatory and steady shear rheology of gellan/dextran blends. *Journal of Food Science and Technology, 52*, 2902–2909. doi:10.1007/s13197-014-1330-x

Aleixandre, A., Gisbert, M., Sineiro, J., & Moreira, R. (2022). In vitro inhibition of starch digestive enzymes by ultrasound-assisted extracted polyphenols from Ascophyllum nodosum seaweeds. *Journal of Food Science*, *87*, 2405–2416. doi:10.1111/1750-3841.16202

Aleman, R. S., Paz, G., Morris, A., Prinyawiwatkul, W., Moncada, M., & King, J. M. (2021). High protein brown rice flour, tapioca starch & potato starch in the development of gluten-free cupcakes. *LWT*, *152*, 112326. doi:10.1016/j.lwt.2021.112326

Ali, T. M., & Hasnain, A. (2015). Physicochemical, morphological, thermal, pasting, and textural properties of starch acetates. *Food Reviews International*, *32*, 161–180. doi:10.1080/87559129.2015.1057842

Amoriello, T., Mellara, F., Amoriello, M., Ceccarelli, D., & Ciccoritti, R. (2021). Powdered seaweeds as a valuable ingredient for functional breads, *European Food Research and Technology*, *247*, 2431–2443. doi:10.1007/s00217-021-03804-z

Anton, A. A., & Artfield, S. D. (2008). Hydrocolloids in gluten-free breads: A review. *International Journal of Food Sciences and Nutrition*, *59*, 11–23. doi:10.1080/09637480701625630

ASTM Standard F2259–10. (2012). Standard test method for determining the chemical composition and sequence in alginate by proton nuclear magnetic resonance (^{1}H–NMR) spectroscopy. Westconshohocken, PA: ASTM International.

Awuchi, C. G., Echeta, C. K., & Igwe, V. S. (2020). Diabetes and the nutrition and diets for its prevention and treatment: a systematic review and dietetic perspective. *Health Sciences Research*, *6*, 5–19.

Bárcenas, M. E., O-Keller, J. D. la, & Rosell, C. M. (2009). Influence of different hydrocolloids on major wheat dough components (gluten and starch). *Journal of Food Engineering*, *94*, 241–247. doi:10.1016/j.jfoodeng.2009.03.012

Barnes, H. A., Hutton, J. F. & Walters, K. (1993). *An Introduction to Rheology*. Amsterdam: Elsevier.

Baltsavias, A., Jurgens, A. & van Vliet, T. (1997). Rheological properties of short doughs at small deformation. *Journal of Cereal Science*, *26*, 289–300. doi:10.1006/jcrs.1997.0133

Bender, D., & Schönlechner, R. (2020). Innovative approaches towards improved gluten-free bread properties. *Journal of Cereal Science*, *91*, 102904. doi:10.1016/j.jcs.2019.102904

Besednova, N. N., Andryukov, B. G., Zaporozhets, T. S., Kryzhanovsky, S. P., Fedyanina, L. N., Kuznetsova, T. A., Zvyagintseva, T. N., & Shchelkanov, M. Y. (2021). Antiviral effects of polyphenols from marine algae. *Biomedicines*, *9*, 200. doi:10.3390/biomedicines9020200

Bhat, I. M., Wani, S. M., Mir, S. A., & Masoodi, F. A. (2022). Advances in xanthan gum production, modifications and its applications. *Biocatalysis and Agricultural Biotechnology*, *42*, 102328. doi:10.1016/j.bcab.2022.102328

Biliaderis, C. G. (2009). Structural Transitions and Related Physical Properties of Starch. *Starch*, *8*, 293–372. doi:10.1016/b978-0-12-746275-2.00008-2

Bojarczuk, A., Skąpska, S., Khaneghah, A. M., & Marszałek, K. (2022). Health benefits of resistant starch: A review of the literature. *Journal of Functional Foods*, *93*, 105094. doi:10.1016/j.jff.2022.105094

Bourne, M. (2002). *Food Texture and Viscosity: Concept and Measurement*. London: Academic Press.

Bruno, E., Lupi, F. R., Martin-Piñero, M. J., Girimonte, R., Baldino, N., Muñoz, J., & Gabriele, D. (2021). Influence of different dispersing systems on rheological and microstructural properties of citrus fiber suspensions. *LWT - Food Science and Technology*, *152*, 112270. doi:10.1016/j.lwt.2021.112270

Cabanillas, B. (2020). Gluten-related disorders: Celiac disease, wheat allergy, and nonceliac gluten sensitivity. *Critical Reviews in Food Science and Nutrition*, *60*, 2606–2621. doi:10.1080/10408398.2019.1651689

Caio, G., Volta, U., Sapone, A., Leffler, D. A. De Giorgio, R., Catassi C., & Fasano, A. (2019). Celiac disease: a comprehensive current review. *BMC Medicine*, *17*, 142. doi:10.1186/s12916-019-1380-z

Castelain, C., Doublier, J., & Lefebvre, J. (1987). A study of the viscosity of cellulose derivatives in aqueous solutions. *Carbohydrate Polymers*, *7*, 1–16. doi:10.1016/0144-8617(87)90037-3

Catarino, M. D., Pires, S. M. G., Silva, S., Costa, F., Braga, S. S., Pinto, D. C. G. A., Silva, A. M. S., & Cardoso, S. M. (2022). Overview of phlorotannins' constituents in fucales. *Marine Drugs*, *20*, 754. doi:10.3390/md20120754

Chaisawang, M., & Suphantharika, M. (2005). Effects of guar gum and xanthan gum additions on physical and rheological properties of cationic tapioca starch. *Carbohydrate Polymers*, *61*, 288–295. doi:10.1016/j.carbpol.2005.04.002

Chee, S. Y., Wong, P. K., & Wong, C. L. (2011). Extraction and characterisation of alginate from brown seaweeds (Fucales, *Phaeophyceae*) collected from Port Dickson, Peninsular Malaysia. *Journal of Applied Phycology*, *23*, 191–196. doi:10.1007/s10811-010-9533-7

Chen, N., Chen, L., Gao, H., & Zeng, W. (2020). Mechanism of bridging and interfering effects of tea polyphenols on starch molecules. *Journal of Food Processing and Preservation*, *44*, 14576. doi:10.1111/jfpp.14576

Chen, S., Sathuvan, M., Zhang, X., Zhang, W., Tang, S., Liu, Y., & Cheong, K. L. (2021). Characterization of polysaccharides from different species of brown seaweed using saccharide mapping and chromatographic analysis. *BMC Chemistry*, *15*, 1. doi:10.1186/s13065-020-00727-w

Chen, Y., Xiong, X., & Gao, Q. (2018). Digestibility and physicochemical properties of starch-galactomannan complexes by heat-moisture treatment. *Food Hydrocolloids*, *77*, 853–862. doi:10.1016/j.foodhyd.2017.11.029

Chenlo, F., Moreira, R., & Silva, C. (2009). Rheological modelling of binary and ternary systems of tragacanth, guar gum and methylcellulose in dilute range of concentration at different temperatures. *LWT - Food Science and Technology*, *42*, 519–524. doi:10.1016/j.lwt.2008.07.011

Chi, C., Li, X., Zhang, Y., Chen, L., Xie, F., Li, L., & Bai, G. (2019). Modulating the in vitro digestibility and predicted glycemic index of rice starch gels by complexation with gallic acid. *Food Hydrocolloids*, *89*, 821–828. doi:10.1016/j.foodhyd.2018.11.016

Ciancia, M., Matulewicz, M. C., & Tuvikene, R. (2020). Structural diversity in galactans from red seaweeds and its influence on rheological properties. *Frontiers in Plant Science*, *11*, 559986. doi:10.3389/fpls.2020.559986

Clappison, E., Hadjivassiliou, M., & Zis, P. (2020). Psychiatric manifestations of coeliac disease, a systematic review and meta-analysis. *Nutrients*, *12*, 142. doi:10.3390/nu12010142.

Costa, M. J., Marques, A. M., Pastrana, L. M., Teixeira, J. A., Sillankorva, S. M., & Cerqueira, M. A. (2018). Physicochemical properties of alginate-based films: Effect of ionic crosslinking and mannuronic and guluronic acid ratio. Food Hydrocolloids, 81, 442–448. doi:10.1016/j.foodhyd.2018.03.014

Cui, C., Jiang, H., Guan, M., Ji, N., Xiong, L., & Sun, Q. (2022). Characterization and in vitro digestibility of potato starch encapsulated in calcium alginate beads. *Food hydrocolloids*, *126*, 107458. doi:10.1016/j.foodhyd.2021.107458

Da Costa, M., Delpech, M., Ferreira, I., Cruz, I., Castanharo, J., & Cruz, J. (2017). Evaluation of single-point equations to determine intrinsic viscosity of sodium alginate and chitosan with high deacetylation degree. *Polymer Testing*, *63*, 427–433. doi:10.1016/j.polymertesting.2017.09.003

Delcour, J. A., Joye, I. J., Pareyt, B., Wilderjans, E., Brijs, K., & Lagrain, B. (2012). Wheat gluten functionality as a quality determinant in cereal-based food products. *Annual Review of Food Science and Technology*, *3*, 469–492. doi:10.1146/annurev-food-022811-101303

Dodero, A., Vicini, S., Alloisio, M., & Castellano, M. (2020a). Rheological properties of sodium alginate solutions in the presence of added salt: An application of Kulicke equation. *Rheologica Acta*, *59*, 365–374. doi:10.1007/s00397-020-01206-8

Dodero, A., Vicini, S. & Castellano, M. (2020b). Depolymerization of sodium alginate in saline solutions via ultrasonic treatments: A rheological characterization. *Food Hydrocolloids*, *109*, 106–120. doi:10.1016/j.foodhyd.2020.106128

Donmez, D., Pinho, L., Patel, B., Desam, P., & Campanella, O. H. (2021). Characterization of starch–water interactions and their effects on two key functional properties: starch gelatinization and retrogradation. *Current Opinion in Food Science*, *39*, 103–109. doi:10.1016/j.cofs.2020.12.018

Doyle, J., Lyons, G., & Morris, E. (2009). New proposals on “hyperentanglement” of galactomannans: Solution viscosity of fenugreek gum under neutral and alkaline conditions. *Food Hydrocolloids*, *23*, 1501–1510. doi:10.1016/j.foodhyd.2008.09.007

Draget, K., Moe, S., Gudmund, S., & Olav, S. (2006). Alginates. In A. Stephen, G. Phillips, & P. Williams (Eds.), *Food polysaccharides and their applications* (pp. 289–334). London: Taylor & Francis.

Englyst, H. N., Veenstra, J., & Hudson, G. J. (1996). Measurement of rapidly available glucose (RAG) in plant foods: a potential *in vitro* predictor of the glycaemic response. *British Journal of Nutrition*, *75*, 327–337. doi:10.1079/bjn19960137

Espinosa-Ramírez, J., Garzon, R., Serna-Saldivar, S. O., & Rosell, C. M. (2018). Functional and nutritional replacement of gluten in gluten-free yeast-leavened breads by using β-conglycinin concentrate extracted from soybean flour. *Food Hydrocolloids*, *84*, 353–360. doi:10.1016/j.foodhyd.2018.06.021.

Espinoza-Herrera, J., Martínez, L. M., Serna-Saldívar, S. O., & Chuck-Hernández, C. (2021). Methods for the modification and evaluation of cereal proteins for the substitution of wheat gluten in dough systems. *Foods*, *10*, 118. doi:10.3390/foods10010118

Fasina, O. O., Ajibola, O. O., & Tyler, R. T. (1999). Thermodynamics of moisture sorption in winged bean seed and gari. *Journal of Food Process Engineering*, *22*, 405–418. doi:10.1111/j.1745-4530.1999.tb004 96.x

Fedors, R. (1979). An equation suitable for describing the viscosity of dilute to moderately concentrated polymer solutions. *Polymer*, *20*, 225–228. doi:10.1016/0032-3861(79)90226-X

Fuentes-Zaragoza, E., Sánchez-Zapata, E., Sendra, E., Sayas, E., Navarro, C., Fernández-López, J., & Pérez-Alvarez, J. A. (2011). Resistant starch as prebiotic: A review. *Starch*, *63*, 406–415. doi:10.1002/star.201000099

Funami, T., Kataoka, Y., Hiroe, M., Asai, I., Takahashi, R., & Nishinari, K. (2007). Thermal aggregation of methylcellulose with different molecular weights. *Food Hydrocolloids*, *21*, 46–58. doi:10.1016/j.foodhyd.2006.01.008

Garzon, R., Skendi, A., Lazo-Velez, M. A., Papageorgiou, M., & Rosell, C. M. (2021). Interaction of dough acidity and microalga level on bread quality and antioxidant properties. *Food Chemistry*, *344*, 128710. doi:10.1016/j.foodchem.2020.128710

Gatti, S., Rubio-Tapia, A., Makharia, G., & Catassi, C. (2024). Patient and community health global burden in a world with more celiac disease. *Gastroenterology*, *167*, 23–33. doi:10.1053/j.gastro.2024.01.035

Gisbert, M., Aleixandre, A., Sineiro, J., Rosell, C. M., & Moreira, M. (2022). Interactions between *Ascophyllum nodosum* seaweeds polyphenols and native and gelled corn starches. *Foods*, *11*, 1165. doi:10.3390/foods11081165

Gisbert, M., Barcala, M., Rosell, C. M., Sineiro, J., & Moreira, R. (2021). Aqueous extracts characteristics obtained by ultrasound-assisted extraction from Ascophyllum nodosum seaweeds: effect of operation conditions. *Journal of Applied Phycology*, *33*, 3297–3308. doi:10.1007/s10811-021-02546-5

Granfeldt, Y., Björck, I., Drews, A., & Tovar, J. (1992). An *in vitro* procedure based on chewing to predict metabolic response to starch in cereal and legume products. *European Journal of Clinical Nutrition*, *46*, 649–660. doi:10.1093/AJCN/59.3.777S

Goñi, I., Garcia-Alonso, A., & Saura-Calixto, F. (1997). A starch hydrolysis procedure to estimate glycemic index. *Nutrition Research*, *17*, 427–437. doi:10.1016/S0271-5317(97)00010-9

Hasatsri, S., Pitiratanaworanat, A., Swangwit, S., Boochakul, C., & Tragoonsupachai, C. (2018). Comparison of the morphological and physical properties of different absorbent wound dressings. *Dermatology Research and Practice*, 9367034. doi:10.1155/2018/9367034

Hazafa, A., Iqbal, M. O., Javaid, U., Tareen, M. B. K., Amna, D., Ramzan, A., Piracha, S., & Naeem M. (2022). Inhibitory effect of polyphenols (phenolic acids, lignans, and stilbenes) on cancer by regulating signal transduction pathways: a review. *Clinical and Translational Oncology*, *24*, 432–445. doi:10.1007/s12094-021-02709-3

Hellebois, T., Soukoulis, C., Xu, X., Hausman, J.-F., Shaplov, A., Taoukis, P. S., & Gaiani, C. (2020). Structure conformational and rheological characterisation of alfalfa seed (*Medicago sativa* L.) galactomannan. *Carbohydrate Polymers*, *256*, 117394. doi:10.1016/j.carbpol.2020.117394

Horstmann, S., Lynch, K., & Arendt, E. (2017). Starch characteristics linked to gluten-free products. *Foods*, *6*, 29. doi:10.3390/foods6040029

Hummel, S., Pfluger, M., Hummel, M., Bonifacio, E., & Ziegler, A. G. (2011). Primary dietary intervention study to reduce the risk of islet autoimmunity in children at increased risk for type 1 diabetes: The BABYDIET study. *Diabetes Care*, *34*, 1301–1305. doi:10.2337/dc10-2456

Jin, Y., Zhang, H., Yin, Y., & Nishinari, K. (2006). Comparison of curdlan and its carboxymethylated derivative by means of Rheology, DSC, and AFM. *Carbohydrate Research*, *341*, 90–99. doi:10.1016/j.carres.2005.11.003

Kassem, I., Ablouh, E. H., El Bouchtaoui, F. Z., Kassab, Z., Hannache, H., Sehaqui, H., & El Achaby, M. (2022). Biodegradable all-cellulose composite hydrogel as ecofriendly and efficient coating material for slow-release MAP fertilizer. *Progress in Organic Coatings*, *162*, 106575. doi:10.1016/j.porgcoat.2021.106575

Karim, A., Norziah, M. H., & Seow, C. C. (2000). Methods for the study of starch retrogradation. Food Chemistry, 71, 9–36. doi:10.1016/s0308-8146(00)00130-8

Khouryieh, H. A., Herald, T. J., Aramouni, F., & Alavi, S. (2007). Intrinsic viscosity and viscoelastic properties of xanthan/guar mixtures in dilute solutions: Effect of salt concentration on the polymer interactions. *Food Research International*, *40*, 883–893. doi:10.1016/j.foodres.2007.03.001

King, J. A., ..., Kaplan. G. G. (2020). Incidence of Celiac Disease Is Increasing Over Time: A Systematic Review and Meta-analysis. The Amerian Journal of Gastroenterology, 115, 507–525. doi:10.14309/ajg.0000000000000523

Knežević, N., Karlović, S., Takács, K., Szűcs, V., Knežević, S., Badanjak Sabolović, M., & Brnčić, S. R. (2024). Consumer Satisfaction with the quality and availability of gluten-free products. *Sustainability*, *16*, 8215. doi:10.3390/su16188215

Kowalski, S., Sikora, M., Tomasik, P., & Krystyjan, M. (2008). Starch polysaccharide hydrocolloid gels. *Polimery*, *14*, 457–464. doi:10.14314/polimery.2008.457

Kulicke, W. M., & Clasen, C. (2004). Basic Concepts. In: Viscosimetry of Polymers and Polyelectrolytes. Springer Laboratory. Springer, Berlin, Heidelberg. doi:10.1007/978-3-662-10796-6_2

Lee, H., & Kim, H. S. (2019). Pasting and paste properties of waxy rice starch as affected by hydroxypropyl methylcellulose and its viscosity. *International Journal of Biological Macromolecules*, *153*, 1202–1210. doi:10.1016/j.ijbiomac.2019.10.250

Lentle, R. G., Janssen, P. W. M., Asvarujanon, P., Chambers, P., Stafford, K. J., & Hemar, Y. (2007). High-definition mapping of circular and longitudinal motility in the terminal ileum of the brushtail possum *Trichosurus vulpecula* with watery and viscous perfusates. *Journal of Comparative Physiology B, 177*, 543–556. doi: 10.1007/s00360-007-0153-8

Li, M., Ndiaye, C., Corbin, S., Foegeding, E. A., & Ferruzzi, M. G. (2020a). Starch-phenolic complexes are built on physical CH-π interactions and can persist after hydrothermal treatments altering hydrodynamic radius and digestibility of model starch-based food. *Food Chemistry*, *308*, 125577. doi:10.1016/j.foodchem.2019.125577

Li, C., Hu, Y., Tao, H., Gong, B., & Yu, W. W. (2020b). A combined action of amylose and amylopectin fine molecular structures in determining the starch pasting and retrogradation property. *International Journal of Biological Macromolecules*, *164*, 2717–2725. doi:10.1016/j.ijbiomac.2020.08.123

Liu, W., Zhang, Y., Wang, R., Li, J., Pan, W., Zhang, X., Xiao, W., Wen, H., & Xie, J. (2022). Chestnut starch modification with dry heat treatment and addition of xanthan gum: Gelatinization, structural and functional properties. *Food hydrocolloids*, *124*, 107205. doi:10.1016/j.foodhyd.2021.107205

Lopez, C. G., Voleske, L., & Richtering, W. (2020). Scaling laws of entangled polysaccharides. *Carbohydrate Polymers, 234*, 115886. doi:10.1016/j.carbpol.2020.115886

Ludvigsson, J. F., Ludvigsson, J., Ekbom, A., & Montgomery, S. M. (2006). Celiac disease and risk of subsequent type 1 diabetes: A general population cohort study of children and adolescents. *Diabetes Care*, *29*, 2483–2488. doi:10.2337/dc06-0794

Ma, J., Lin, Y., Chen, X., Zhao, B., & Zhang, J. (2014). Flow behavior, thixotropy and dynamical viscoelasticity of sodium alginate aqueous solutions. *Food Hydrocolloids, 38*, 119–128. doi:10.1016/j.foodhyd.2013.11.016

Macosko, C.W. (1994) Rheology: Principles, Measurements, and Applications. VCH Publishers, Inc., University of Minnesota, Minneapolis.

Malamut, G., …, Cellier, C. (2009). Presentation and long-term follow-up of refractory celiac disease: comparison of type I with type II. *Gastroenterology*, *136*, 81–91. doi:10.1053/j.gastro.2008.09.069

Mandala, I. G., & Bayas, E. (2004). Xanthan effect on swelling, solubility and viscosity of wheat starch dispersions. *Food Hydrocolloids*, *18*, 191–201. doi:10.1016/s0268-005x(03)00064-x

Martinsen, A., Skjak-Braek, G., Smidsrod, O., & Paoletti, S. (1991). Comparison of different methods for determination of molecular weight and molecular weight distribution of alginates. *Carbohydrate Polymers*, *15*, 171–193. doi:10.1016/0144-8617(91)90031-7

Matos, M. E., & Rosell, C. M. (2013). Quality indicators of rice-based gluten-free bread-like products: relationships between dough rheology and quality characteristics. *Food and Bioprocess Technology*, *6*, 2331–2341. doi:10.1007/s11947-012-0903-9.

McGrance, S. J., Cornell, H. J., & Rix, C. J. (1998). A simple and rapid colorimetric method for the determination of amylose in starch products. *Starch*, *50*, 158–163. doi:10.1002/(SICI)1521-379X(199804)50:4<158::AID-STAR158>3.0.CO;2-7

Megusar, P., Stopar, D., Poklar Ulrih, N., Dogsa, I., & Prislan, I. (2022). Thermal and rheological properties of gluten-free, starch-based model systems modified by hydrocolloids. *Polymers*, *14*, 3242. doi:10.3390/polym14163242

Mildner-Szkudlarz, S., Różańska, M., Piechowska, P., Waśkiewicz, A., & Zawirska-Wojtasiak, R. (2019). Effects of polyphenols on volatile profile and acrylamide formation in a model wheat bread system. *Food Chemistry*, *297*, 125008. doi:10.1016/j.foodchem.2019.125008

Minekus, M., Alminger, M., Alvito, P..., & Brodkorb, A. (2014). A standardised static in vitro digestion method suitable for food – an international consensus. *Food & Function*, *5*, 1113–1124. doi:10.1039/c3fo60702j

Miranda, J., Lasa, A., Bustamante, M. A., Churruca, I., & Simon, E. (2014). Nutritional differences between a gluten-free diet and a diet containing equivalent products with gluten. *Plant Foods for Human Nutrition*, *69*, 182–187. doi:10.1007/s11130-014-0410-4

Mohammadifar, M., Musavi, S., Kiumarsi, A., & Williams, P. (2006). Solution properties of targacanthin (water soluble part of gum tragacanth exudate from *Astragalus gossypinus*).

International Journal of Biological Macromolecules, *38*, 31–39. doi:10.1016/j.ijbiomac.2005.12.015

Mollakhalili Meybodi, N., Mohammadifar, M. A., & Feizollahi, E. (2015). Gluten-free bread quality: A review of the improving factors. *Journal of Food Quality and Hazards Control*, *2*, 81–85.

Moreira, R., Chenlo, F., Chaguri, L., & Fernandes, C. (2008). Water absorption texture, and color kinetics of air–dried chestnuts during rehydration. *Journal of Food Engineering*, *86*, 584–594. doi:10.1016/j.jfoodeng.2007.11.012

Morris, E., Cutler, A., & Ross-Murphy, S. (1981). Concentration and shear rate dependence of viscosity in random coil polysaccharide solutions. *Carbohydrate Polymers*, *1*, 5-21. doi:10.1016/0144-8617(81)90011-4

Montes, L., Gisbert, M., Hinojosa, I., Sineiro, J., & Moreira, R. (2021). Impact of drying on the sodium alginate obtained after polyphenols ultrasound-assisted extraction from Ascophyllum nodosum seaweeds. *Carbohydrate Polymers*, *272*, 118455. doi:10.1016/j.carbpol.2021.118455

Oh, I. K., Bae, I. Y., & Lee, H. G. (2018). Complexation of high amylose rice starch and hydrocolloid through dry heat treatment: Physical property and in vitro starch digestibility. *Journal of Cereal Science*, *79*, 341–347. doi:10.1016/j.jcs.2017.11.017

Olokoba, A. B., Obateru, O. A., & Olokoba, L. B. (2012). Type 2 diabetes mellitus: A review of current trends. *Oman Medical Journal*, *27*, 269–273. doi:10.5001/omj.2012.68

Pereira, L., Morrison, L., Shukla, P. S., & Critchley, A. T. (2020). A concise review of the brown macroalga *Ascophyllum nodosum* (Linnaeus) Le Jolis. *Journal of Applied Phycology*, *32*, 3561–3584. doi:10.1007/s10811-020-02246-6

Rao, M. A. (2007). *Rheology of Fluid and Semisolid Foods: Principles and Applications*. New York: Elsevier Applied Science.

Romão, B. et al. (2021). Glycemic index of gluten-free bread and their main ingredients: A systematic review and meta-analysis. *Foods*, *10*, 506. doi:10.3390/foods10030506

Ronda, F., Pérez-Quirce, S., Angioloni, A., & Collar, C. (2013). Impact of viscous dietary fibres on the viscoelastic behaviour of gluten-free formulated rice doughs: A fundamental

and empirical rheological approach. *Food Hydrocolloids*, *32*, 252–262. doi:10.1016/j.foodhyd.2013.01.014

Rosell, C. M., Santos, E., Sanz Penella, J. M., & Haros, M. (2009). Wholemeal wheat bread: a comparison of different breadmaking processes and fungal phytase addition. *Journal of Cereal Science*, *50*, 272–277. doi:10.1016/j.jcs.2009.06.007

Rosell, C. M., Yokoyama, W., & Shoemaker, C. (2011). Rheology of different hydrocolloids–rice starch blends. Effect of successive heating–cooling cycles. *Carbohydrate Polymers*, *84*, 373–382. doi:10.1016/j.carbpol.2010.11.047

Santamaria, M., Garzon, R., Moreira, R., & Rosell, C. M. (2021). Estimation of viscosity and hydrolysis kinetics of corn starch gels based on microstructural features using a simplified model. *Carbohydrate Polymers*, *273*, 118549. doi:10.1016/j.carbpol.2021.118549

Santamaria, M., Garzon, R., & Rosell, C. M. (2023b). Impact of starch-hydrocolloid interaction on pasting properties and enzymatic hydrolysis. *Food Hydrocolloids*, *142*, 108764. doi:10.1016/j.foodhyd.2023.108764

Santamaria, M., Montes, L., Garzon, R., Moreira, R., & Rosell, C. M. (2023a). Performance of starch gels on in vitro enzymatic hydrolysis assessed by rheological methodologies. *Starch*, *75*, 2200189. doi:10.1002/star.202200189

Schindelin, J., ..., Cardona, A. (2012). Fiji: an open-source platform for biological-image analysis. *Nature Methods*, *9*, 676–682. doi:10.1038/nmeth.2019.

Sharma, N., Bhatia, S., Chunduri, V., Kaur, S., Sharma, S., Kapoor, P., Kumari, A., & Garg, M. (2020). Pathogenesis of celiac disease and other gluten related disorders in wheat and strategies for mitigating them. *Frontiers in Nutrition*, *7*, 6. doi:10.3389/fnut.2020.00006

Singh, P., Arora, A., Strand, T. A., Leffler, D. A., Catassi, C., Green, P. H., Kelly, C. P., Ahuja, V., & Makharia, G. K. (2018). Global prevalence of celiac disease: systematic review and meta-analysis. *Clinical Gastroenterology and Hepatology*, *16*, 823–836. doi:10.1016/j.cgh.2017.06.037

Singleton, V. L., & Rossi, J. A. (1965). Colorimetry of total phenolics with phosphomolybdic-phosphotungstic acid reagent. *American Journal of Enology and Viticulture*, *16*, 144–158. doi:10.5344/ajev.1965.16.3.144

Šmídová, Z., & Rysová, J. (2022). Gluten-free bread and bakery products technology. Foods, 11, 480. doi:10.3390/foods11030480

Steffe, J. F. (1996). *Rheological Methods in Food Process Engineering*. East Lansing, USA: Freeman Press, 2nd ed.

Stokke, B. T., Draget, K. I., Smidsrød, O., Yuguchi, Y., Urakawa, H., & Kajiwara, K. (2000). Small-angle X-ray scattering and rheological characterization of alginate gels. 1. Ca-alginate gels. *Macromolecules, 33*, 1853–1863. doi:10.1021/ma991559q

Sun, J., Zuo, X. B., Fang, S., Xu, H. N., Chen, J., Meng, Y. C., & Chen, T. (2016). Effects of cellulose derivative hydrocolloids on pasting, viscoelastic, and morphological characteristics of rice starch gel. *Journal of Texture Studies*, *48*, 241–248. doi:10.1111/jtxs.12233

Villarreal, M. E., & Iturriaga, L. B. (2016). Viscoelastic properties of amaranth starch gels and pastes. Creep compliance modeling with Maxwell model. *Starch/Stärke*, *68*, 1073–1083. doi:10.1002/star.201600065

Wang, K., Sui, J., Gao, W., Yu, B., Yuan, C., Guo, L., Cui, B., Abd El-Aty, A. M. (2022). Effects of xanthan gum and sodium alginate on gelatinization and gels structure of debranched pea starch by pullulanase. *Food Hydrocolloids*, 130, 107733. doi:10.1016/j.foodhyd.2022.107733

Wieser, H. (2007). Chemistry of gluten proteins. *Food Microbiology*, 24, 115–119. doi:10.1016/j.fm.2006.07.004

Wu, Z., Kong, Y., He, T., Li, Y., Kang, Z., Xie, F., & Liu, T. (2024). Mechanism of interaction between agar and corn starch: Towards improved properties of starch-based cryogel. *Food Hydrocolloids*, *150*, 109672. doi:10.1016/j.foodhyd.2023.109672

Yadav, K., Yadav, B. S., Yadav, R. B., & Dangi, N. (2018). Physicochemical, pasting and rheological properties of colocasia starch as influenced by the addition of guar gum and xanthan gum. *Journal of Food Measurement and Characterization*, *12*, 2666–2676. doi:10.1007/s11694-018-9884-3

Zhang, H., Bai, Y., Zhao, X., & Duan, R. (2016). Water desorption isotherm and its thermodynamic analysis of glutinous rice flour. *American Journal of Food Technology*, *11*, 115–124. doi:10.3923/ajft.2016.115.124

Zhang, Y., Gu, Z., Zhu, L., & Hong, Y. (2018). Comparative study on the interaction between native corn starch and different hydrocolloids during gelatinization. *International Journal of Biological Macromolecules*, *116*, 136–143. doi:10.1016/j.ijbiomac.2018.05.011

Zhang, Y., Li, M., You, X., Fang, F., & Li, B. (2020). Impacts of guar and xanthan gums on pasting and gel properties of high-amylose corn starches. *International Journal of Biological Macromolecules*, *146*, 1060–1068. doi:10.1016/j.ijbiomac.2019.09.231

Zhou, S., Hong, Y., Gu, Z., Cheng, L., Li, Z., & Li, C. (2020). Effect of heat-moisture treatment on the in vitro digestibility and physicochemical properties of starch-hydrocolloid complexes. *Food Hydrocolloids*, *104*, 105736. doi:10.1016/j.foodhyd.2020.105736

Zolelmein, A., Movahhed, S., Azizi, M. H., & Ahmadi Chenarbon, H. (2019). Assessment of simultaneous addition of sucrose and xanthan effects on the thermal, pasting and rheological behavior of corn starch. *Journal of Texture Studies*, *51*, 453–463. doi:10.1111/jtxs.12497

Appendix A:

Journal publications in which this Thesis is based

Effect of polyphenols from *Ascophyllum nodosum* seaweeds on the rheology and digestion of corn starch gels and gluten-free bread features

Leticia Montes[a], Maria Santamaria[b], Raquel Garzon[b], Cristina M. Rosell[bc], Ramón Moreira[a]

[a]Department of Chemical Engineering, Universidade de Santiago de Compostela, rúa Lope Gómez de Marzoa, s/n. 15782, Santiago de Compostela, Spain.

[b]Institute of Agrochemistry and Food Technology (IATA-CSIC). C/Agustin Escardino, 7. 46980 Paterna. Spain.

[c]Department of Food and Human Nutritional Sciences. University of Manitoba, Winnipeg, Canada.

Journal: Heliyon, 10, e27469 (2024).

DOI: 10.1016/j.heliyon.2024.e27469 CITATIONS: 1

Impact factor: 3.4 Q1 Multidisciplinar (28/134, 2023)

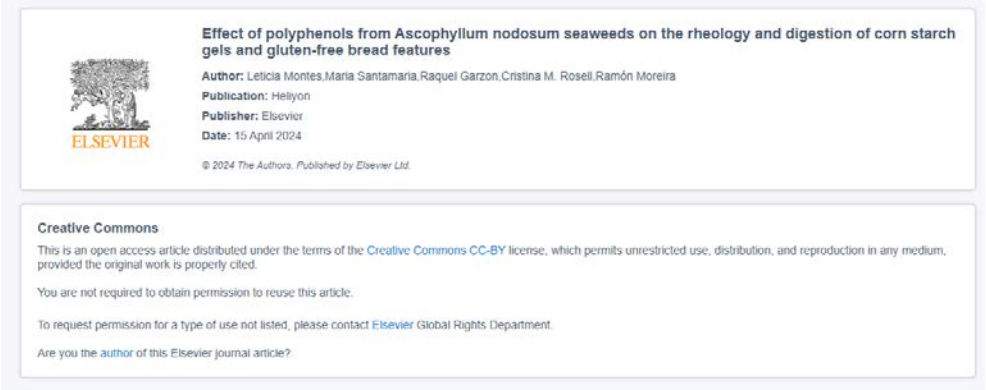

Effect of polyphenols from Ascophyllum nodosum seaweeds on the rheology and digestion of corn starch gels and gluten-free bread features

Author: Leticia Montes,Maria Santamaria,Raquel Garzon,Cristina M. Rosell,Ramón Moreira

Publication: Heliyon

Publisher: Elsevier

Date: 15 April 2024

Author contribution (CRediT taxonomy): Investigation, writing-original draft.

Chapters reproducing the article content: Chapter 4

Water sorption isotherms of different sodium alginates: Thermodynamic evaluation and influence of mannuronate-guluronate copolymers

Leticia Montes, Mauro Gisbert and Ramón Moreira

Chemical Engineering Department, Universidade de Santiago de Compostela, Campus Vida, 15782 Santiago de Compostela, Spain.

Journal: Journal of Food Processing and Preservation, 46, e17179 (2022).

DOI: 10.1111/jfpp.17179 CITATIONS: 1

Impact factor: 2.5 Q3 Food Science and Technology (93/142)

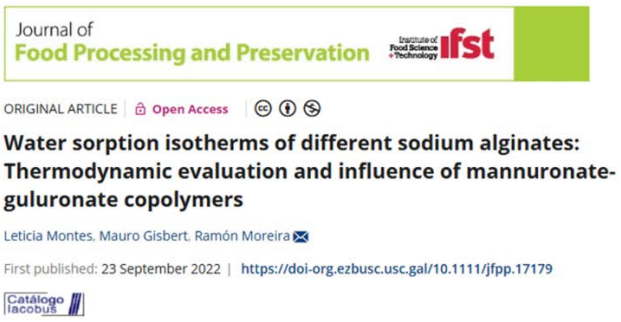

Volume 46, Issue 12
December 2022
e17179

Author contribution (CRediT taxonomy): Conceptualization; Data curation; Formal analysis; Investigation; Validation; Methodology; Writing-original draft.

Chapters reproducing the article content: Chapter 4

Effect of the addition of different sodium alginates on viscoelastic, structural features and hydrolysis kinetics of corn starch gels

Leticia Montes[a], Maria Santamaria[b], Raquel Garzon[b], Cristina M. Rosell[b], Ramón Moreira[a]

[a]Department of Chemical Engineering, Universidade de Santiago de Compostela, rúa Lope Gómez de Marzoa, s/n. 15782, Santiago de Compostela, Spain.

[b]Institute of Agrochemistry and Food Technology (IATA-CSIC). C/Agustin Escardino, 7. 46980 Paterna. Spain.

Journal: Food Bioscience, 47, 101628 (2022).

Impact factor: 5.2 Q1 Food Science and Technology (34/142)

DOI: 10.1016/j.fbio.2022.101628 CITATIONS: 16

Effect of the addition of different sodium alginates on viscoelastic, structural features and hydrolysis kinetics of corn starch gels

Author: Leticia Montes,Maria Santamaria,Raquel Garzon,Cristina M. Rosell,Ramón Moreira

Publication: Food Bioscience

Publisher: Elsevier

Date: June 2022

Author contribution (CRediT taxonomy): Conceptualization; Data curation; Formal analysis; Investigation; Methodology; Writing-original draft.

Chapters reproducing the article content: Chapter 4

Rheological properties of corn starch gels with the addition of hydroxypropyl methylcellulose of different viscosities

Leticia Montes[1], Cristina M. Rosell[2], Ramón Moreira[1]

[1]Department of Chemical Engineering, Universidade de Santiago de Compostela, Santiago de Compostela, Spain.
[2]Institute of Agrochemistry and Food Technology (IATA-CSIC), Paterna, Spain.

Journal: Frontiers in Nutrition, 9, 866789 (2022).

Impact factor: 5.0 Q2 Nutrition and Dietetics (28/88)

DOI: 10.3389/fnut.2022.866789 CITATIONS: 7

ORIGINAL RESEARCH article

Front. Nutr., 22 March 2022
Sec. Nutrition and Food Science Technology
Volume 9 - 2022 |
https://doi.org/10.3389/fnut.2022.866789

This article is part of the Research Topic
Rheological Properties of Plant-Based Food Systems
View all 3 articles >

Rheological Properties of Corn Starch Gels With the Addition of Hydroxypropyl Methylcellulose of Different Viscosities

Leticia Montes[1] Cristina M. Rosell[2] Ramón Moreira[1*]

[1] Department of Chemical Engineering, Universidade de Santiago de Compostela, Santiago de Compostela, Spain
[2] Institute of Agrochemistry and Food Technology (IATA-CSIC), Paterna, Spain

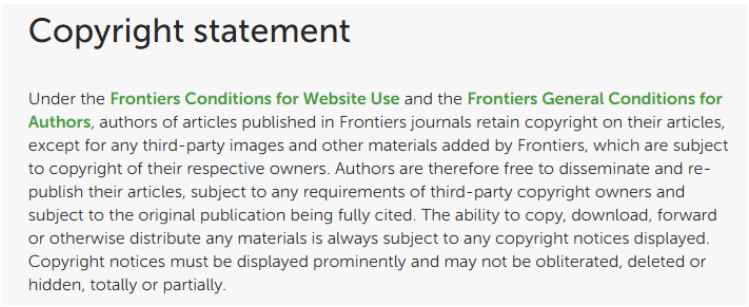

Copyright statement

Under the Frontiers Conditions for Website Use and the Frontiers General Conditions for Authors, authors of articles published in Frontiers journals retain copyright on their articles, except for any third-party images and other materials added by Frontiers, which are subject to copyright of their respective owners. Authors are therefore free to disseminate and re-publish their articles, subject to any requirements of third-party copyright owners and subject to the original publication being fully cited. The ability to copy, download, forward or otherwise distribute any materials is always subject to any copyright notices displayed. Copyright notices must be displayed prominently and may not be obliterated, deleted or hidden, totally or partially.

Author contribution (CRediT taxonomy): Methodology, data curation, and writing—original draft preparation.

Chapters reproducing the article content: Chapter 4

The high demand for gluten-free products has encouraged the interest in improving their nutritional composition, especially due to the relationship between type-1 diabetes and celiac disease, as gluten-free diets are usually rich in carbohydrates and low in protein, ibre and trace elements. This Thesis investigates how polyphenols extracted from brown seaweed (*Ascophyllum nodosum*) can inhibit starch digestion in gluten-free products. It was observed that the elastic characteristics of starch gels and the starch digestibility decreased with polyphenols addition. Also, the addition of alginates and HPMC was evaluated, inding that alginates increased the viscoelastic characteristics and decreased the hydrolysis rate of starch, whereas rheological changes depended on the average molecular weight of HPMC.

GI-1618
Tecnoloxías para o Desenvolvemento de Bioprodutos Industriais